AFOSR-TR- 88-0976

(2)

Motion and Stability Of Saturated Soil Systems Under Dynamic Loading

By
Ranbir S. Sandhu
William E. Wolfe
Harpal S. Chohan

Final Report

Air Force Office of Scientific Research
Grant: AFOSR-83-0055

Geotechnical Engineering Report No. 31

Department of Civil Engineering
The Ohio State University

February 1988

UNCLASSIFIED
SECURITY CLASSIFICATION OF THIS PAGE

REPORT DOCUMENTATION PAGE

Form Approved OMB No. 0704-0188

1a. REPORT SECURITY CLASSIFICATION: UNCLASSIFIED	1b. RESTRICTIVE MARKINGS
2a. SECURITY CLASSIFICATION AUTHORITY	3. DISTRIBUTION / AVAILABILITY OF REPORT: Approved for Public Release; Distribution Unlimited
2b. DECLASSIFICATION / DOWNGRADING SCHEDULE	
4. PERFORMING ORGANIZATION REPORT NUMBER(S): OSURF-717885-88-4	5. MONITORING ORGANIZATION REPORT NUMBER(S): AFOSR-TR- 88 0976
6a. NAME OF PERFORMING ORGANIZATION: The Ohio State University Research Foundation; 6b. OFFICE SYMBOL (If applicable):	7a. NAME OF MONITORING ORGANIZATION: AFOSR/NA
6c. ADDRESS (City, State, and ZIP Code): 1314 Kinnear Road, Columbus, Ohio 43212-1194	7b. ADDRESS (City, State, and ZIP Code): Bldg. 410, Bolling AFB, DC 20332-6448
8a. NAME OF FUNDING / SPONSORING ORGANIZATION: AFOSR; 8b. OFFICE SYMBOL (If applicable): NA	9. PROCUREMENT INSTRUMENT IDENTIFICATION NUMBER: AFOSR-83-0055
8c. ADDRESS (City, State, and ZIP Code): Bldg. 410, Bolling AFB, DC 20332-6448	10. SOURCE OF FUNDING NUMBERS: PROGRAM ELEMENT NO. 6.1102F; PROJECT NO. 2302; TASK NO. C1; WORK UNIT ACCESSION NO.

11. TITLE (Include Security Classification) (U)

Motion and Stability of Saturated Soil Systems Under Dynamic Loading

12. PERSONAL AUTHOR(S)
Ranbir S. Sandhu, William E. Wolfe, and Harpal S. Chohan

13a. TYPE OF REPORT	13b. TIME COVERED	14. DATE OF REPORT (Year, Month, Day)	15. PAGE COUNT
Final	FROM 1/1/83 TO 2/29/88	1988 February 29	238

16. SUPPLEMENTARY NOTATION

17. COSATI CODES		
FIELD	GROUP	SUB-GROUP

18. SUBJECT TERMS (Continue on reverse if necessary and identify by block number)
Dynamic Response; Soil Dynamics; Fluid Saturated Solids; Wave Propagation; Porous Media; Liquefaction

19. ABSTRACT (Continue on reverse if necessary and identify by block number)

Theories of motion and stability of fluid-saturated soils including the commonly used engineering approach to liquefaction analysis as well as theories based on mechanics of mixtures are critically examined. Description of motion, development of equations of balance, constitutive relationships as well as development of solution procedures are reviewed. Limitations of various theories, their similarities as well as inconsistencies are identified. Laboratory investigations into dynamic behavior of saturated soils are reviewed.

A theory of dynamics of saturated soils using a convected coordinate system to describe the motion of soil particles and describing the motion of the fluid as relative to the solid is described. This theory may be regarded as an extension of Gibson's theory of non-linear soil consolidation to three-dimensions and to include inertia effects.

20 DISTRIBUTION / AVAILABILITY OF ABSTRACT	21 ABSTRACT SECURITY CLASSIFICATION
☑ UNCLASSIFIED/UNLIMITED ☐ SAME AS RPT ☐ DTIC USERS	UNCLASSIFIED
22a NAME OF RESPONSIBLE INDIVIDUAL: Major Steven C. Boyce	22b. TELEPHONE (Include Area Code): (202) 767-6963; 22c. OFFICE SYMBOL: AFOSR/NA

DD Form 1473, JUN 86 Previous editions are obsolete.

SECURITY CLASSIFICATION OF THIS PAGE
UNCLASSIFIED

19. ABSTRACT (Cont.)

Solution procedures developed for certain specializations of the equations of motion of saturated soils are described. These include analytical, semi-analytical and numerical solution schemes. The finite element is selected as the numerical procedure for approximate solution. Spatial discretization, time domain solution procedures and alternative formulations of the field equations through a variational formulation are discussed.

Shaking table tests for validation of various theoretical concepts, performed on saturated Ottawa sand are described. These include tests on anisotropically as well as isotropically consolidated samples and tests to study the effect of overburden on a soil system subjected to shaking. Harmonic as well as frequency banded random amplitude excitations were used. Results are compared with previous laboratory investigations.

OSURF-717885-88-4

MOTION AND STABILITY OF SATURATED SOIL SYSTEMS UNDER DYNAMIC LOADING

BY

Ranbir S. Sandhu, William E. Wolfe and Harpal S. Chohan
Department of Civil Engineering

Final Report
to the
AIR FORCE OFFICE OF SCIENTIFIC RESEARCH
Grant: AFOSR-83-0055

Period of Performance: February 1, 1983 to February 29, 1988

Geotechnical Engineering Report No. 31

The Ohio State University Research Foundation
1314 Kinnear Road, Columbus, Ohio 43212

FOREWORD

This report covers research carried out at the Ohio State University under Grant AFOSR-83-0055. Lt. Col. J. J. Allen, Lt. Col. Lawrence D. Hokanson, Dr. Spencer T. Wu, and Major Steven C. Boyce were the Program Managers at different stages of the Project. At the Ohio State University the work was performed under the supervision of Professor Ranbir S. Sandhu from February 1, 1983 till January 31, 1985 and under the joint supervision of Professors Ranbir S. Sandhu and William E. Wolfe from February 1, 1985 till February 29, 1988. Dr. Mahantesh S. Hiremath, Dr. Soon Jo Hong, Mr. Vincent E. Amato, Capt. Dennis L. Jasinski, and Mr. Harpal S. Chohan contributed significantly to the project as Graduate Research Associates. Dr. Leslie W. Morland of the University of East Anglia, United Kingdom, was associated with the project as a Visiting Scientist in 1986. Dr. Baher L. Aboustit was associated with the project briefly during 1983.

ABSTRACT

Theories of motion and stability of fluid-saturated soils, including the commonly used engineering approach to liquefaction analysis as well as theories based on mechanics of mixtures, are critically examined. Description of motion, development of equations of balance, constitutive relationships as well as development of solution procedures are reviewed. Limitations of various theories, their similarities as well as inconsistencies are identified. Laboratory investigations into dynamic behavior of saturated soils are reviewed.

A theory of dynamics of saturated soils using a convected coordinate system to describe the motion of soil particles, and describing the motion of the fluid as relative to the solid, is described. This theory may be regarded as an extension of Gibson's theory of non-linear soil consolidation to three-dimensions and to include inertia effects.

Solution procedures, developed for certain specializations of the equations of motion of saturated soils, are described. These include analytical, semi-analytical and numerical solution schemes. The finite element is selected as the numerical procedure for approximate solution. Spatial discretization, time domain solution procedures and alternative formulations of the field equations through a variational formulation are discussed.

Shaking table tests for validation of various theoretical concepts, performed on saturated Ottawa sand are described. These included tests on anisotropically as well as isotropically consolidated samples and tests to study the effect of overburden on a soil system subjected to shaking. Harmonic as well as frequency banded random amplitude excitations were used. Results are compared with previous laboratory investigations.

TABLE OF CONTENTS

LIST OF TABLES

LIST OF FIGURES

Section I

INTRODUCTION

1.1 THE PROBLEM

Dynamic loading of fluid-saturated geological deposits results in changes in the fluid pressure as well as the stress field in the solid matrix. This phenomenon can, in some cases, lead to instability of the soil matrix resulting in soil liquefaction. Additionally, the energy dissipation associated with the relative oscillatory motion between the fluid and the solid could introduce attenuation of the propagating wave. This effect would be in addition to the energy dissipation due to any inelastic deformation of the soil matrix. Inasmuch as the transmissibility of motion through the soil layer depends upon the soil characteristics, the soil deposit may act as a selective filter/amplifier. For prediction of behavior of saturated soils under dynamic loads due to blast, earthquake or other dynamic event, it is important to develop adequate methodology.

Reliable analysis of saturated soil deposits subjected to dynamic loads involves the following three steps:

1. Correct formulation of the equations of dynamic equilibrium.
2. Correct representation of material behavior.
3. Exact or approximate solution of the problem.

The theoretical model must be validated by laboratory and/or field tests. As exact solutions to the boundary value problems represented by the laboratory and field tests may not be available, it may be necessary to use numerical solution procedures. However, before any computational technique can be used with confidence, it must be veri-

fied against exact solutions to the theoretical model. It may be necessary to construct exact solutions to some simple problems for code verification.

In view of the apparent diversity of opinions, postulates, and assumptions made in setting up various approaches to the problem, there was evident need to develop more realistic models of mechanical behavior of fluid-saturated soils. The research program supported by the Air Force Office of Scientific Research was designed to address all the three components of the problem.

1.2 RESEARCH OBJECTIVES

Figure 1 illustrates the variables involved in the problem of dynamics of fluid-saturated soils. In the absence of water, the dry soil would be modeled as a continuum. Its motion would be defined completely by the components of displacement, velocity and acceleration designated u_i, $\dot{u}_i$, $\ddot{u}_i$, in the figure. These would define strains, and strain-rates, which would be related through constitutive laws to the stresses, and the stress rates. Equilibrium relations would relate the stresses with the applied body and surface forces. Similarly the mechanics of the fluid, in isolation from the solid are well-known. However, when the two occur together, the problem immediately becomes much more complex. The equilibrium equations for each of the two constituents may involve interaction terms; the stresses in each may depend upon the kinematics of both; and there may be other couplings in the behavior. Various theories have been proposed from time to time to explain the mechanical behavior of saturated soils and methodologies have been suggested for analysis of liquefaction.

The objective of the research program, was to critically evaluate the current methods of analysis in the light of recent developments in theories of interacting continua and to develop thermodynamically and physically consistent theoretical or mathe-

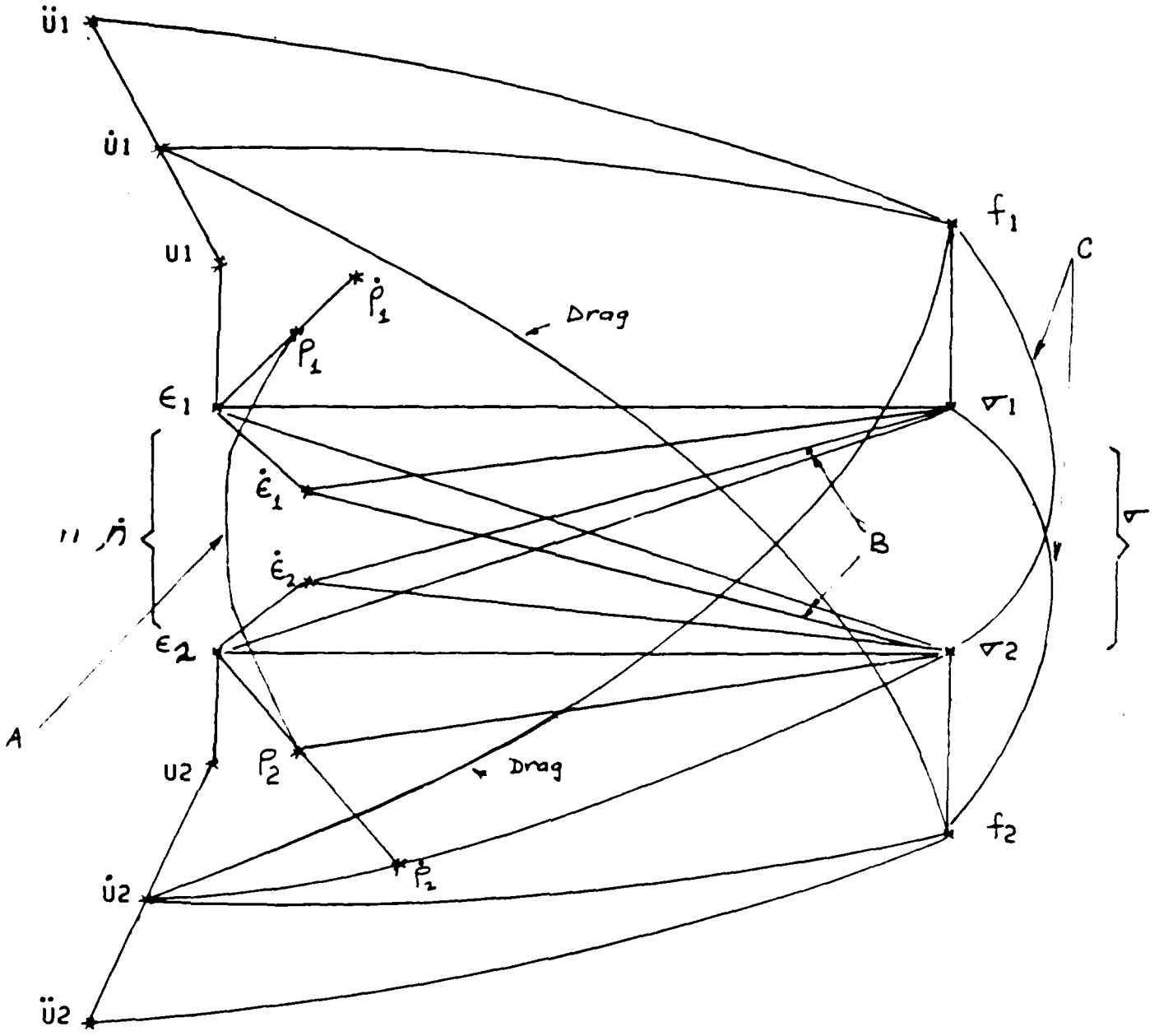

A. INERTIAL COUPLING

B. CONSTITUTIVE COUPLING

C. BALANCE COUPLING
(MASS, MOMENTUM, ENERGY)

Figure 1: Variables Involved in Dynamics of Saturated Soils

matical models of fluid-saturated soil systems. Theories of interacting continua, in general, regard a fluid-saturated soil as a multi-component mixture (superposed continua). This approach had been successfully implemented in the analysis of static and quasi-static response of saturated soils. Several investigators have tried to extend this approach to the dynamic case. However, there have been deficiencies in realistic simulation of behavior of saturated soils. The purpose of the research program was to review the theoretical basis of equations governing behavior of soil-water mixtures under dynamic conditions, including interaction between soil and water. The theoretical development was to be implemented in effective finite element computer programs incorporating recent developments in coding to ensure optimal combination of solution accuracy and economy. The analytical research was to be supplemented by a program of laboratory investigations.

1.3 RESEARCH PLAN.

A two-year program of research was initially approved by the AFOSR starting February 1, 1983. This was later extended to a four year effort ending January 31, 1987 and finally by another one year and one-month to February 29, 1988. The research plan included both theoretical and laboratory investigations.

1.4 ANALYTICAL STUDIES

The first step in the research program was to carefully examine the theoretical underpinnings of various existing theories of motion and stability of fluid-saturated soils. This investigation covered a range of theories and procedures, including the commonly used engineering approach to liquefaction analysis and extending to mathematical theories based on mechanics of mixtures. A theory properly describing the physical phenomena was to be selected/developed and implemented in a solution procedure to predict the liquefaction behavior of the saturated soil under dynamic loading.

1.5 LABORATORY INVESTIGATIONS

To provide a database for validation of various theoretical concepts, shaking table tests were to be performed on saturated Ottawa sand. A program of tests on anisotropically as well as isotropically consolidated samples was to be carried out.

1.6 COMMENTS

The research program essentially followed an evolutionary approach. As the first step in the program, literature on the subject was carefully reviewed. Two approaches were selected for detailed investigation. These were the popular "engineering approach" introduced by Seed and his co-workers [77-80,148] for liquefaction studies, and the theories of mechanics of mixtures including Biot's theory [17-19] which has been the basis of analytic and numerical solutions for the problem. A dynamical theory for dynamics of saturated soil was developed as an extension of Gibson's theory of nonlinear consolidation. For interpretation of test data in terms of predictions from various theories, it was necessary that solutions to boundary value problems defined by the competing theories be available. It was found that solutions to only the simplest configurations were available for Biot's theory. Approximate solution schemes had been proposed by several investigators but these had not been adequately verified. Finite element computer codes were developed for analysis of dynamic response of saturated soils for linear as well as nonlinear material properties for the engineering approach as well as Biot's theory and its appropriate extension. Semi-analytic solution procedures were developed to serve as bench-marks for validation of the time-domain integration schemes. Analytical solutions were developed for certain problems for the purpose of code verification.

Validation of numerical procedures presented a difficulty because of the paucity of exact solutions even for relatively simple problems. Garg's [50] fundamental solution

for Biot's equations specialized one-dimensional wave propagation in fluid-saturated media was integrated to develop solutions for several cases of dynamic loading on the surface of a saturated soil column. Inconsistencies in the solution for 'strong' coupling, for which the drag between the soil and the fluid is high, were removed but it was noticed that, in order to obtain an exact solution to the problem, Garg had made assumptions which reduced the value of his theoretical solutions as bench-marks to verify numerical procedures. To meet the needs of the research program effectively, correct solutions to this problem were developed. It was found that for the materials commonly encountered and for a short period of time after application of a sudden (e.g. blast) load, Garg's approximation is quite good. Analytical solutions for some simple cases were developed for propagation of standing waves by separating the singularity from the smooth diffusive wave motion and using a combination of the method of characteristics and finite element/finite difference procedures. These solutions were extended to some two-dimensional cases. Computer codes were tested against these exact solutions.

To develop alternative finite element approaches, a variational formulation of Biot's theory, along with various extensions and specializations, was developed. It served as the basis for the two-field and the three-field finite element solution procedures. Elements suitable for wave propagation analysis were selected/developed. Singularity elements had to be used near loaded boundaries. For nonlinear problems, an incremental approach was necessary. The equations governing this case along with a variational formulation of the problem were developed. Only material nonlinearity was considered. The theory was implemented in a finite element computer program. A modular structure was used so that a variety of models could be selected. The well-established 'cap model' was implemented to fit the behavior of the sand used in the laboratory experiments. For constitutive equations in incremental form, the corresponding balance equa-

tions too were written in terms of incremental quantities. This introduced incremental changes in porosity and mass density as additional variables. Nonlinear codes were checked against available solutions for wave propagation in single materials.

The experimental component of the research program was completed as envisaged in the proposal. It had the following components:

1. Development of techniques for evaluation of material parameters that appeared in the theoretical models considered.
2. Construction of a uniform, fully saturated sample.
3. Application of motion to the sample on a shaking table.
4. Recording of input acceleration and pore pressures up to liquefaction.
5. Analysis of the experimental data for the purpose of evaluating the theoretical models.

A fine to medium grained sand, Ottawa sand, was chosen as the material to be used in the experimental studies. A program of static tests aimed at identifying basic material parameters that appear in the theoretical models was performed. For liquefaction experiments particular emphasis was placed on laboratory techniques for proper preparation of the necessary sand samples. Suitable methods for saturating the approximately 50 kilograms of sand required to build a sample were developed and samples with a high degree of uniformity were repeatedly achieved. Instrumentation was calibrated under both cyclic and static loading conditions. Different types of pore-pressure gage applications were studied. Initial shaking table tests were designed to identify the most reliable and sensitive instrumentation capable of recording input acceleration and progressive development of pore pressures up to liquefaction. Improvements in collection of data and its processing were implemented. Additional instrumentation was acquired to collect an increased amount of information during tests.

These tests established the capability of the experimental set-up to serve the immediate needs of the program. Both isotropically and anisotropically consolidated samples were tested to liquefaction. Input motions consisted of both harmonic acceleration time histories and random, white noise, accelerations. Further tests were carried out to study the effect of overburden on a soil subjected to shaking. The experimental data obtained were compared with the results of previous laboratory investigations. Shortcomings in these earlier test procedures were identified.

Figure 2 illustrates the scope of the actual work plan and the accomplishments under the research program.

1.7 STRUCTURE OF THE REPORT

Section II contains a review of previous theoretical investigations on the behavior of saturated soils subjected to dynamic loading in order to highlight the basic assumptions of the various approaches. Section III describes a dynamical theory of motion of saturated soils, developed as part of the present research program, based on description of the motion of a given set of soil particles in convected coordinates and regarding the fluid motion as relative to the soil particles. Section IV describes some anlytical, and semi-analytical solution procedures developed to obtain solutions to some simple one-dimensional problems as well as development of finite element techniques for analysis of wave propagation in saturated soils. Section V reviews previous laboratory investigations and summarizes the experimental component of the research program. Section VI summarizes the results of the research and contains recommendations for future work. Appendix A describes some concepts related to the use of convected coordinates to describe the motion of a solid. Appendix B lists the research publications and presentations that resulted from the research effort.

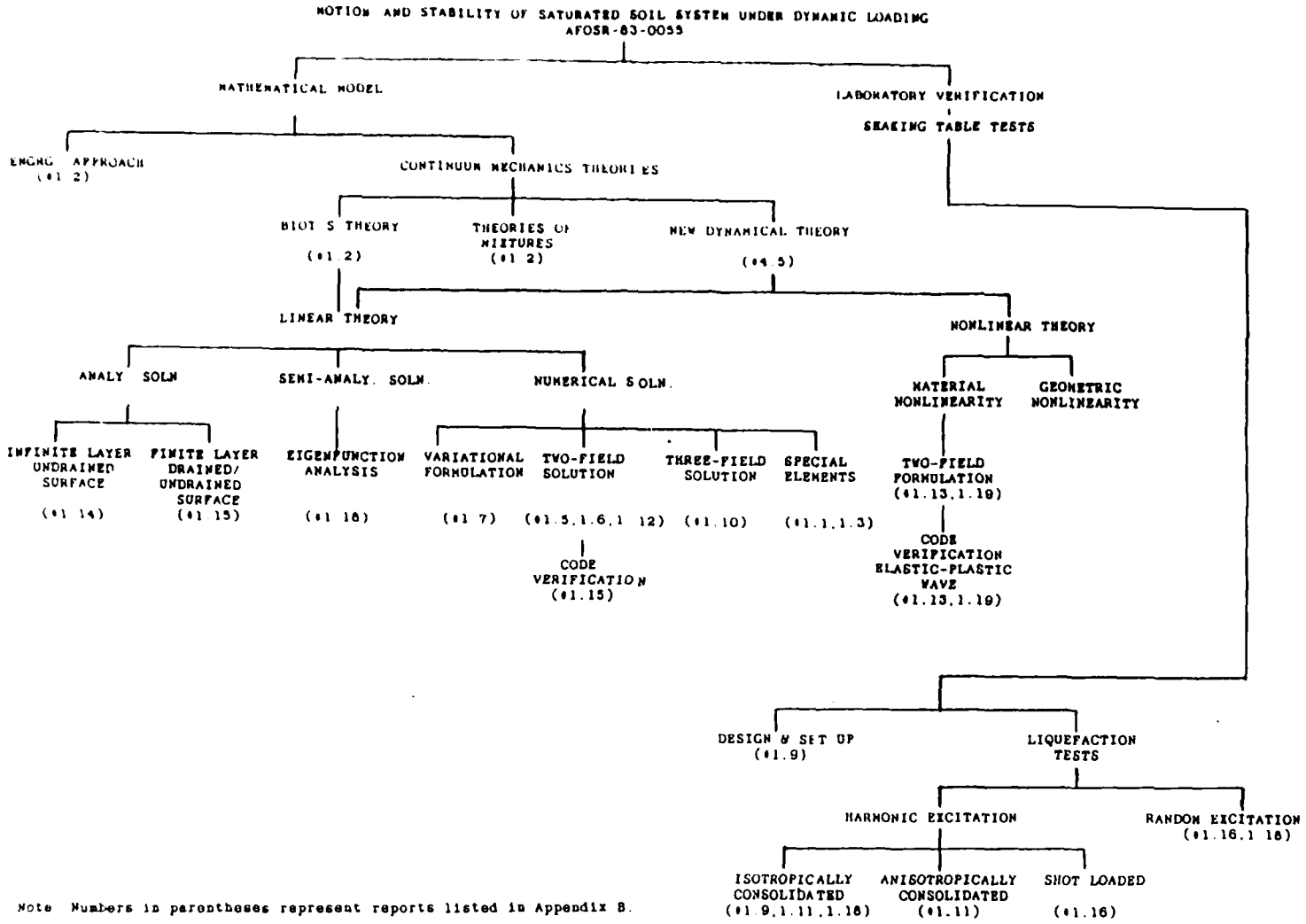

Figure 2: Research Accomplished Under AFOSR Grant 83-0055.

Section II

REVIEW OF PREVIOUS WORK

2.1 INTRODUCTION

Existing theories of dynamics of fluid-saturated soils were reviewed. Limitations of various theories, their similarities as well as inconsistencies were identified. The "engineering approach", described herein and based on methods of structural mechanics, was considered along with the continuum mechanics approaches. Herein we briefly review the salient features of these approaches as the background for the theory developed in the course of this research. Detailed documentation of this review is available in the technical report listed as item 1.2 in Appendix B.

2.2 THE ENGINEERING APPROACH

This approach, introduced by Seed and his co-workers [77-80,148], uses methods of structural dynamics to solve the problem of shear wave propagation in soils. The approach has been successfully applied to several case histories [85,88,128,145-154]. It consists of a finite element analysis of the dynamic system to evaluate the stress history. This is followed by a laboratory study of the material behavior under cyclic stress conditions equivalent to those determined from the finite element analysis. This approach has been extended to include a periodic updating of material behavior to allow for the strain history as well as pore-water pressure build-up and dissipation. The stiffness is assumed to be a function of the volumetric strain and the effective stress in the soil. Generation of pore water pressure is assumed to be related to volume changes in water and soil. Assuming water to be incompressible, an incremental

relationship is proposed between the incremental pore pressure and the volume change in the soil. For one-dimensional idealization of a horizontally layered system subjected to shear wave at the base, dissipation of the pore water pressure is expected to be governed by the equation

$$\dot{\pi} = E_r[\frac{K}{w}\pi_{,z}]_{,z} + E_r\dot{e}_{kk} \tag{2.1}$$

where w is the unit weight of water, K the permeability, E_r the the one-dimensional rebound modulus of the material at the effective stress applicable to the increment, and e_{ij} are components of the strain tensor for the soil. Finn [42] called this the coupled theory of liquefaction. The sequence of occurrences is assumed to be as follows: shearing stresses cause volume changes, volume changes result in pore-water pressure changes, pore-pressure dissipation follows, pore-pressures determine effective stresses and effective stresses along with the cumulative shearing strain define the effective shear modulus to be used for determination of displacements and stresses for the next time step.

Item 1.4 in Appendix B contains details of the methodology of the "engineering approach" to liquefaction as well as its implementation in a computer program. The computer code developed was used to obtain the response of a layered soil system subjected to sinusoidal base acceleration. The problem data were taken from a case study reported by Finn [42]. The surface acceleration and displacement as well as the time to liquefaction reported by Finn and obtained using the code were in good agreement. However, the detailed response history obtained using the implicit and the explicit methods was quite different. With refinement of the time mesh, one would expect the explicit method to yield a sequence of results which would converge to the solution obtained by the implicit method. However, the solution procedure requires experimental data which are dependent upon the frequency of cycling, the natural frequency of the soil system etc. and would have to be generated for each case studied. The

study showed the approach to be cumbersome and based upon several assumptions. The physical properties required as data for the method can only be determined as a function of the complete number of cycles of stress at a certain amplitude. Thus, in an explicit type solution scheme, it is possible to reduce the time interval for updates to only as small as the time period of vibration. For this reason it is not possible to generate a convergent sequence of solutions based upon reducing the size of the time step. Implicit schemes are expected to be more reliable. Post-liquefaction distribution of pore pressures and the extent of the resulting disaplacements in the system cannot be correctly determined in this theory. Furthermore, the approach has only been used for one-dimensional wave propagation, and cannot be readily extended to two and three-dimensional cases. Use of this theory requires considerable experience and "judgement", in addition to extensive laboratory testing program, to get useful results.

2.3 CONTINUUM MECHANICS APPROACHES

2.3.1 Biot's Theory.

Biot's theory, based on concepts of coupled motion of soil and water, has been the most popular alternative to the empirical approaches. This pioneering work was based on certain postulates regarding description of motion, notion of partial stresses, the existence of energy and dissipation functions for the saturated mass and a certain form for the kinetic energy of the mixture. These assumptions led directly to the conclusion that constitutive coupling, inertial coupling and equilibrium couplings exist and are symmetric in form. The equations of momentum balance were written for the mixture as a whole and for fluid motion relative to the solid. Several different forms of Biot's theories exist. The most general form includes body forces, inertia forces and the effects of coupling of the fluid and the soil mass as well as the constitutive coupling between the soil and the water.

Biot [11] wrote the constitutive equations for the flow of a compressible fluid through a porous saturated linearly elastic medium assuming the existence of an energy function quadratic in measures of deformation associated with the saturated soil mass. These included the six components of the soil strain. Change in water content was added as the seventh kinematic variable. While extending the analysis to compressible fluids and anisotropic elastic or viscoelastic solids, Biot [14,15] introduced the volumetric strain of the fluid as the additional strain parameter instead of the change in water content used in the earlier theory and explained later [20] that the two variables were essentially the same. Garg's [50] formulation can be shown to correspond to Biot's. In Garg's theory, the constants are related to the properties of the constituents and their volume fractions. For the dissipative case, a dissipation function, quadratic in relative velocity was introduced. For a statistically isotropic saturated material, Biot [17-19] expected the kinetic energy to be quadratic in the velocities of the fluid and the soil and a coupling term was included. This introduced an inertial coupling between the soil and the fluid. However, it is difficult to assign numerical values to the various quantities that arise as a result of this coupling. As a part of this review, the theory was implemented in a finite element computer program and a parametric study carried out to investigate the efect of this coupling on the dynamic response. Preliminary studies indicated that the effect would be insignificant. However, further study of this particular feature is needed.

While developing finite element solution procedures for the problem, Ghaboussi [53], following Biot [15,18,19], introduced relative volumetric strain in the formulation. The momentum balance and the continuity equations were written in terms of six displacement components viz. the soil displacements and the relative displacements of the fluid. A Rayleigh type viscous damping term was introduced. This intrinsic damping of the soil is in addition to the damping associated with relative motion. Ghaboussi [53]

developed a variational formulation for the problem but for the purpose of finite element analysis he used the Galerkin procedure. Also the boundary conditions were not treated properly.

2.3.2 Theories of Mixtures.

2.3.2.1 Introduction

To apply the principles of continuum mechanics, it is customary to regard a fluid-saturated solid as superposed continua. Averaging of various quantities, kinematic as well as mechanical, associated with the various constituents, is inherent in this assumption. The mixture is defined by the current coincident configuration of the constituents. It is assumed that, in the current configuration, each point of space is occupied by a particle of each of the constituents. This necessitates the introduction of "bulk" description of the material instead of the "intrinsic" description which would apply if the material were the single constituent of a body. In any theory of mixtures, it would be necessary that as the volume fraction of one of the constituents approaches unity, and the remaining constituents disappear, the theory for a single constituent be realized as a limiting case.

In developing a rational theory of mixtures, Truesdell [165] laid down the following principles:

1. All properties of the mixture must be mathematical consequences of properties of the constituents.
2. So as to describe the motion of a constituent, we may in imagination isolate it from the rest of the mixture, provided we allow properly for the actions of the other constituents upon it.
3. The motion of the mixture is governed by the same equations as is a single body.

The third of these "principles" is open to serious objection. This issue is addressed in a later paragraph.

2.3.2.2 Density of Each Constituent and of the Mixture.

The effective (also referred to as partial or bulk) density of the kth constituent, when it is regarded as one of the continua occupying every point in the spatial region of interest, is related to its intrinsic density as

$$\rho^{(k)} = n^{(k)}\rho^{(k)*} \tag{2.2}$$

where $n^{(k)}$ is the volume fraction, superscipted Roman characters enclosed in parentheses identify the constituent in the mixture, and a superscripted asterisk denotes an intrinsic quantity. The density of a mixture of n constituents is defined as the weighted sum of the densities of the constituents i.e.,

$$\rho = \sum_{k=1}^{n} \rho^{(k)} \tag{2.3}$$

Other definitions for partial densities have been used. Terzaghi [161] assumed the effective density of water to have the intrinsic value and regarded the soil as buoyant in the water.

2.3.2.3 Description of Motion.

Several approaches have been used to describe the motion of the constituents of a multicomponent mixture. Often the deformation is referred to an initial configuration for each constituent and motion to the place coordinates. The equations of balance are written for a fixed volume in space. Another approach is to refer the motion of all constituents to the reference configuration of one of them. Yet another is to refer all motion to the current configuration which is the same for all constituents. Superposition of relative diffusive motion of the constituents upon the mean motion of the mixture as a whole is also used. For a binary mixture of a solid and a fluid, some investigators describe the motion of the solid with respect to its reference configuration but the motion of the fluid is described as relative to the solid. Another approach is to refer to a material region consisting of the same set of particles of one of the con-

stituents so that the bounding surface of this constituent varies with time. If the description of the material particles is the same during motion as in the initial configuration, this would be the convected coordinate description for the reference constituent. Gibson's theory of consolidation [55] is a special case of this approach.

Using a fixed rectangular cartesian reference frame, the deformation gradient is defined as the partial derivative of the place coordinates with respect to the reference coordinates. The velocity vectors and the acceleration vectors are defined as the partial time derivatives of the place coordinates for the same material particle. Most investigators, also introduce a barycentric velocity rate for the mixture as a whole as:

$$v_i = \sum_{k=1}^{n} \frac{\rho^{(k)} v_i^{(k)}}{\rho} \tag{2.4}$$

where v_i are components of the velocity vector. A material rate for the mixture is established using the identity:

$$\sum_{k=1}^{n} \rho^{(k)} \frac{D^{(k)}}{Dt} = \rho \frac{D}{Dt} \tag{2.5}$$

The diffusive velocity is defined as the velocity of a constituent relative to that of the mixture, i.e.,

$$u_i^{(k)} = v_i^{(k)} - v_i \tag{2.6}$$

Biot [15,18,19], for the case of binary mixture of a solid and a fluid, introduced a nominal relative velocity

$$w_i = n^{(2)} (v_i^{(2)} - v_i^{(1)}) \tag{2.7}$$

This and its variants were used by Ghaboussi [53], Krause [86] and Kenyon [84], among others.

2.3.2.4 Measures of Deformation.

The deformation gradient and the spatial velocity gradient can be used to completely define rates of deformation. For material objectivity to be satisfied, the vorticity tensors, in binary mixtures, must occur as the difference of the vorticities of the constituents.

For a fluid-saturated porous solid, the deformation gradient can be used to describe the changing configuration of the solid. Garg [48,49], and Morland [103,104] among others, used as measures of deformation of the solid, the quantity

$$e_{ij}^{(1)} = u_{(i,j)}^{(1)} = \frac{1}{2}[u_{i,j}^{(1)} + u_{j,i}^{(1)}] \tag{2.8}$$

where u_i denotes components of the displacement vector. Here, and in the sequel, we use the standard indicial notation. The Roman indices take on values in the range 1, 2, 3. Summation on repeated indices is understood unless stated otherwise. A subscripted comma denotes differentiation with respect to the coordinate represented by the subscript following it. Parentheses around a pair of indices indicate "symmetric part" and square brackets the "antisymmetric part". Superposed dots indicate differentiation with respect to the time parameter. This measure of deformation characterizes the linear theory. For setting up constitutive relations for flow through a porous saturated elastic anisotropic medium, Biot [15,16] used relative volumetric strain defined by the equation

$$\zeta = n^{(2)}(e_{kk}^{(2)} - e_{kk}^{(1)}) \tag{2.9}$$

Other, more general measures of deformation are also used, e.g. [103]. For an initially isotropic solid, it is possible to define as a measure of deformation the quantity

$$2e_{ij} = F_{mi}F_{mj} - \delta_{ij} \tag{2.10}$$

where F_{ij} are components of the deformation gradient tensor. If the only deformation of interest is the volume change the change in density is an adequate measure of deformation. In a binary fluid-solid mixture, for small strain

$$\rho^{(1)} - \rho_0^{(1)} = -\rho^{(1)} e_{ij}^{(1)} \tag{2.11}$$

where the subscript denotes initial value or the value in the reference configuration. For the fluid constituent the deformation is completely represented by its density, i.e.,

$$e_{ij}^{(2)} = \frac{\rho_0^{(2)}}{\rho^{(2)}} - 1 = \frac{n_0^{(2)} \rho_0^{(2)*}}{n^{(2)} \rho^{(2)*}} - 1 \tag{2.12}$$

Introducing an intrinsic measure of deformation [103]

$$F_{ij}^{(2)*} = [n^{(2)} / n_0^{(2)}]^{1/3} F_{ij}^{(2)} \tag{2.13}$$

Morland [104] also proposed, for infinitesimal strain theory,

$$e_{ij}^{(1)*} = e_{ij}^{(1)} - \frac{[n^{(2)} - n_0^{(2)}]}{[1 - n_0^{(2)}]} \tag{2.14}$$

$$-e_{ij}^{(1)*} = \frac{\rho^{(1)}}{\rho_0^{(1)}} - 1 \tag{2.15}$$

$$e_{ij}^{(1)*} - \frac{1}{3} e_{mm}^{(1)*} \delta_{ij} = e_{ij}^{(1)} - \frac{1}{3} e_{mm}^{(1)} \delta_{ij} \tag{2.16}$$

and [106]

$$e_{ij}^{(2)*} = e_{ij}^{(2)} + \frac{[n^{(2)} - n_0^{(2)}]}{n_0^{(2)}} \tag{2.17}$$

In addition to the measures of deformation defined above, the volume fractions of the constituents have been used as state variables. An intrinsic rate of strain of the fluid

$$D_{ij}^{(2)*} = D_{ij}^{(2)} + \frac{1}{3} \left[\frac{n_0^{(2)}}{n_{(2)}} \right] \frac{D^{(2)}}{Dt} \left[\frac{n_0^{(2)}}{n^{(2)}} \right] \delta_{ij} \tag{2.18}$$

was introduced by Morland [104]. Here $\frac{D}{Dt}$ denotes the "material rate". Another measure of relative deformation sometimes used is, (e.g., Krause [86]), the change in fluid content of a fixed volume in space. This amounts to

$$n = \rho^{(2)} - \rho_0^{(2)} = (n^{(2)} - n_0^{(2)}) \rho^{(2)*} \tag{2.19}$$

Carroll [27], considering a fixed volume of the solid in the reference configuration, assumed the total deformation to be the sum of the strains of the solid particles and the change in geometry of the pores. The bulk volume strain was found to be

$$\frac{\Delta V}{V} = \frac{\Delta n^{(2)}}{n^{(1)}} + \frac{\Delta V^{(1)}}{V^{(1)}} \tag{2.20}$$

For the anisotropic case, Caroll [29] wrote

$$e_{ij} = n^{(1)} e_{ij}^{(1)^s} + n^{(2)} e_{ij}^{(2)^s} = e_{ij}^{(1)^s} + n^{(2)} (e_{ij}^{(2)^s} - e_{ij}^{(1)^s}) \tag{2.21}$$

as the strain of the reference material volume of the bulk solid. Carroll [28] assumed the solid intrinsic deformations to be reversible under solid pressure and the pore volume change to be irreversible under effective pressure. This would explain cumulative volume change under cycling of load. Kenyon [84] regarded the specific volume of the solid as a state variable related to the intrinsic pore fluid pressure and the solid deformation gradient.

2.3.2.5 Balance Laws

a). Earlier Theories.

The equation of mass continuity of the fluid, equating the inflow into an elementary volume of a rigid porous one-dimensional solid with the increase in fluid content, is

$$\frac{\partial}{\partial X} (\rho^{(2)} v) + \frac{\partial}{\partial t} (\rho^{(2)} \frac{\partial x}{\partial X}) = 0 \tag{2.22}$$

Here v is the velocity of the fluid relative to the soil and x, X are the coordinates in the current and the reference configurations, respectively, referred to a Cartesian reference frame. Allowing for compressibility of the pore fluid, Gibson [55] used Scheidegger's [140] formulation of d'Arcy's law. The flow equation has the form

$$n^{(2)} \rho^{(2)^s} v \frac{\partial x}{\partial X} = -k [\frac{\partial \pi}{\partial X} + \rho^{(2)^s} \frac{\partial x}{\partial X}] \tag{2.23}$$

Ghaboussi [54] stated Biot's momentum balance equations as

$$t_{ij,j} + \rho b_i = \rho \ddot{u}_i^{(1)} - \rho^{(2)}[\ddot{u}_i^{(1)} - \ddot{u}_i^{(2)}] = \rho^{(1)}\ddot{u}_i^{(1)} + \rho^{(2)}\ddot{u}_i^{(2)} \tag{2.24}$$

and

$$\pi_{,i} + \rho^{(2)} b_i = \rho^{(2)}\ddot{u}_i^{(1)} - \rho^{(2)}[\ddot{u}_i^{(1)} - \ddot{u}_i^{(2)}] - \frac{1}{k}[\dot{u}_i^{(1)} - \dot{u}_i^{(2)}] = \rho^{(2)}\ddot{u}_i^{(2)} - \frac{1}{k}[\dot{u}_i^{(1)} - \dot{u}_i^{(2)}] \tag{2.25}$$

where k is a measure of permeability of the soil and t_{ij} are components of the "total" stress tensor. Garg [50] wrote Biot's equations of motion, in the absence of body forces, in the following form:

$$t_{ij,i}^{(1)} = \rho^{(1)}\ddot{u}_j^{(1)} + b(\dot{u}_j^{(1)} - \dot{u}_j^{(2)}) \tag{2.26}$$

$$\pi_{,j} = \rho^{(2)}\ddot{u}_j^{(2)} - b(\dot{u}_j^{(1)} - \dot{u}_j^{(2)}) \tag{2.27}$$

The second term on the right hand side of these equations represents the viscous coupling between the solid and the fluid.

b). Mechanics of Mixtures.

For each constituent of the mixture, Truesdell [164-166] postulated the balance laws in the point form. Using the notation of [64], these were:

i. *Continuity of Mass.*

$$\frac{\partial}{\partial t}\rho^{(k)} + (\rho^{(k)} v_i^{(k)})_{,i} = \rho c^{(k)} \tag{2.28}$$

where $c^{(k)}$ is the mass production fraction of the kth constituent. An alternative form of the mass continuity equation is

$$\frac{D^{(k)}}{Dt}\rho^{(k)} + \rho^{(k)} v_{i,i}^{(k)} = \rho c^{(k)} \tag{2.29}$$

Bowen [24] wrote the above equation in the form

$$\frac{D}{Dt}(\rho^{(k)} \det F_{ij}^{(k)}) = \rho c^{(k)} \det |F_{ij}^{(k)}| \tag{2.30}$$

ii. *Balance of Linear Momentum.*

$$\frac{\partial}{\partial t}(\rho^{(k)}v_i^{(k)}) + (\rho^{(k)}v_i^{(k)}v_j^{(k)})_{,j} - t_{ji,j}^{(k)} = \rho m_i^{(k)} + \rho^{(k)}b_i^{(k)} \tag{2.31}$$

Here $t_{ji}^{(k)}, \rho b_i^{(k)}, \rho m_i^{(k)}$ are, respectively, components of the partial Cauchy stress tensor, the body force vector per unit mass and the partial momentum supply density for the constituent. An alternative form is:

$$\rho^{(k)}f_i^{(k)} = t_{ji,j}^{(k)} + \rho m_i^{(k)} + \rho^{(k)}b_i^{(k)} - \rho c^{(k)}v_i^{(k)} \tag{2.32}$$

Bowen [24] proposed to replace the momentum supply term $m^{(k)}$ by $m_i^{(k)} + c^{(k)}v_i^{(k)}$ to get

$$\rho^{(k)}f_i^{(k)} = t_{ji,j}^{(k)} + \rho m_i^{(k)} + \rho^{(k)}b_i^{(k)} \tag{2.33}$$

iii. *Balance of Moment of Momentum.*

$$t_{ij}^{(k)} - t_{ji}^{(k)} = \rho M_{ij}^{(k)} \tag{2.34}$$

Here $\rho M_{ij}^{(k)}$ are components of the skew-symmetric tensor describing the partial production density of the moment of momentum of the kth constituent.

iv. Balance of Energy Rates.

$$\rho^{(k)}\frac{D^{(k)}}{Dt}(U^{(k)}) + q_{i,i}^{(k)} - \rho^{(k)}r^{(k)} = t_{ij}^{(k)}v_{(i,j)}^{(k)} + \rho\Delta U^{(k)} \tag{2.35}$$

where

$$\Delta U^{(k)} = e^{(k)} - (U^{(k)} - \frac{1}{2}v_i^{(k)}v_i^{(k)})c^{(k)} - v_i^{(k)}m_i^{(k)} - \frac{1}{2}M_{ij}^{(k)}v_{j,i}^{(k)} \tag{2.36}$$

Here $U^{(k)}$, $q^{(k)}$, $r^{(k)}$, $e^{(k)}$ are, respectively, the specific internal energy, components of the partial heat flux vector, the partial energy supply and the partial energy production density of the kth constituent.

Bowen [24] wrote the energy rate balance equation, for a fixed volume in space of the kth constituent, and derived the point form of the equation of energy balance

$$\rho^{(k)}\frac{D^{(k)}U^{(k)}}{Dt} + q^{(k)}_{j,j} - \rho^{(k)}r^{(k)} = t^{(k)}_{ij}v^{(k)}_{i,j} + \rho e^{(k)} \tag{2.37}$$

Several alternative forms of the above equation have been stated [24,164]. Bowen [24] pointed out that for the case of single temperature mixtures, explicit use of an energy equation for the constituents is not needed.

Truesdell [164,166] postulated balance equations for the mixture as well. These equations can be derived by summing over the equations for the constituents. Truesdell introduced the following quantities to ensure that the resulting equations for the motion of the mixture have the same form as the equations of motion of a single constituent.

i. *Specific internal energy of the mixture*

$$U = \frac{1}{\rho}\sum_{k=1}^{n}\rho^{(k)}\left(U^{(k)} + \frac{1}{2}u^{(k)}_i u^{(k)}_i\right) \tag{2.38}$$

Or, equivalently,

$$\rho\left(U + \frac{1}{2}v_i v_i\right) = \sum_{k=1}^{n}\rho^{(k)}\left(U^{(k)} + \frac{1}{2}v^{(k)}_i v^{(k)}_i\right) \tag{2.39}$$

ii. *Total stress tensor*

$$t_{ij} = \sum_{k=1}^{n}\left(t^{(k)}_{ij} - \rho^{(k)}u^{(k)}_i u^{(k)}_j\right) \tag{2.40}$$

Or, equivalently,

$$t_{ij} - \rho v_i v_j = \sum_{k=1}^{n}\left(t^{(k)}_{ij} - \rho^{(k)}v^{(k)}_i v^{(k)}_j\right) \tag{2.41}$$

iii. *Total heat flux vector*

$$q_i = \sum_{k=1}^{n} (q_i^{(k)} + \rho^{(k)}(U^{(k)} + \frac{1}{2}u_j^{(k)}u_j^{(k)})u_i^{(k)} - t_{ji}^{(k)}u_j^{(k)} \tag{2.42}$$

Or, equivalently,

$$q_i + \rho v_i[U + \frac{1}{2}v_j v_j] - t_{ij}v_j = \sum_{k=1}^{n}[q_i^{(k)} + \rho^{(k)}v_i^{(k)}(U^{(k)} + \frac{1}{2}v_j^{(k)}v_j^{(k)}) - t_{ji}^{(k)}v_j^{(k)}] \tag{2.43}$$

iv. *Specific energy supply.*

$$r = \frac{1}{\rho}\sum_{k=1}^{n}\rho^{(k)}(r^{(k)} + b_i^{(k)}u_i^{(k)}) \tag{2.44}$$

Or, equivalently,

$$\rho(r + b_i v_i) = \sum_{k=1}^{n}\rho^{(k)}(r^{(k)} + b_i^{(k)}v_i^{(k)}) \tag{2.45}$$

Also, thermodynamic isolation of the mixture was assumed, i.e.,

$$\sum_{k=1}^{n} c^{(k)} = 0 \tag{2.46}$$

$$\sum_{k=1}^{n} m_i^{(k)} = 0 \tag{2.47}$$

$$\sum_{k=1}^{n} M_{ij}^{(k)} = 0 \tag{2.48}$$

and

$$\sum_{k=1}^{n} e^{(k)} = 0 \tag{2.49}$$

Kelly [82], Truesdell [164], Green [66] and Bowen [24] wrote the equations of mass, momentum and energy conservation for the mixture contained in a volume V bounded by an arbitrary fixed surface A. The conservation of mass was expressed by

$$\frac{\partial}{\partial t}\int_V \sum_{k=1}^{n}\rho^{(k)}dV + \int_A \sum_{k=1}^{n} n\rho^{(k)}v_j^{(k)}dA = 0 \tag{2.50}$$

Equating the linear change of momentum to the total force exerted on the material, using the divergence theorem, Green [66] obtained

$$\int_V \left(\rho \frac{D}{Dt} v_i + \left[\sum_{k=1}^{n} \rho^{(k)} u_i^{(k)} u_j^{(k)} \right]_{,j} \right] dV = \int_V \sum_{k=1}^{n} (\rho^{(k)} b_i^{(k)} + t_{ji,j}^{(k)}) \, dV \tag{2.51}$$

The point form immediately follows from this integral form of the equation of balance of momentum. Green [66] noted that with the definition of the total stress tensor proposed by Truesdell, their form of the equation is the same as that obtained by Truesdell. However, if the total stress is defined as the sum of the partial stresses, the equation reflects the fact that the total rate of increase of linear momentum is not equal to the barycentric rate of increase of momentum of a continuum of density moving with the barycentric velocity.

The theory for a mixture of two constituents presented by Green [62,64] was generalized by Mills [99] to the case of multicomponent mixtures. Green [62,64] considered the concepts of stress, heat flux, and energy supply, assumed to be primitive to each constituent, to be primitive to the mixture as a whole as well. It was proposed that the total stress and the total heat flux for the mixture should equal the sum of the corresponding quantities for the constituents. Green [66] stated that Truesdell's equations were correct but there was difficulty accepting the interpretations associated with some of the quantities which occur in these equations. For a volume V enclosed by a fixed surface A, following Truesdell's contention that the rate of energy equality has the same form as for a single constituent, Green [66] wrote

$$\frac{\partial}{\partial t} \int_V \rho (U + \frac{1}{2} v_i v_i) dV + \int_A \rho n_j v_j (U + \frac{1}{2} v_i v_i) dA$$

$$= \int_V \sum_{k=1}^{n} \rho^{(k)} (r^{(k)} + b_i^{(k)} v_i^{(k)}) dV + \int_A (t_{ji} v_j - q_i) n_i dA \tag{2.52}$$

Here the left hand side represents the rate of change in energy in volume V bounded by a fixed surface A plus the energy flux for the mixture across the boundary. U is the specific internal energy per unit mass of the mixture and is related to internal energies of the constituents by Truesdell's equation. The equality may be regarded as written for a surface moving with a continuum which has a velocity field equal to the barycentric velocity. Then the left hand side is equal to the material rate, executed on the mixture, of the sum of the internal energy and the kinetic energy of the mixture. However, this line of thought is open to objection. It would assume the existence of mixture particles and the time rates executed on them. This is, in general, not correct as the barycentric velocity is not particle velocity in the ordinary sense. Green [66] accepted the form of (2.52) but not the interpretation associated with some of the quantities occuring in it.

Green [62] proposed a rate of energy equality in the following form:

$$\frac{\partial}{\partial t}\int_V (\rho U + \frac{1}{2}\sum_{k=1}^{n}\rho^{(k)}v_i^{(k)}v_i^{(k)})\,dV + \int_A (U\sum_{k=1}^{n}\rho^{(k)}v_j^{(k)} + \frac{1}{2}\sum_{k=1}^{n}\rho^{(k)}v_i^{(k)}v_i^{(k)}v_j^{(k)})\,n_j\,dA$$

$$= \int_V (\rho r + \sum_{k=1}^{n}\rho^{(k)}b_i^{(k)}v_i^{(k)})\,dV + \int_A \sum_{k=1}^{n}(t_i^{(k)}v_i^{(k)} - q)\,dA \qquad (2.53)$$

Here, the heat fluxes and the energy supply are assumed to be additive. U is the internal energy per unit mass of the mixture allowing for all interactions between the constituents. The $t_i^{(k)}$ are components of tractions associated with the kth constituent and the surface A. In this theory, multipolar stresses and externally supplied multipolar body forces were excluded. Green [62] also made no attempt to define the internal energy and the energy supply for each constituent. It was considered unnecessary for a complete general theory.

Later, [64], the role of interactions between constituents was made explicit by writing, for each constituent, the rate of energy equality

$$\frac{\partial}{\partial t}\int_V \rho^{(k)}\left(U^{(k)}+\frac{1}{2}v_i^{(k)}v_i^{(k)}\right)dV+\int_A \rho^{(k)}n_j v_j^{(k)}\left(U^{(k)}+\frac{1}{2}v_i^{(k)}v_i^{(k)}\right)dA$$

$$=\int_V \rho^{(k)}\left(r^{(k)}+b_i^{(k)}v_i^{(k)}\right)dV+\int_A\left(t_i^{(k)}v_i^{(k)}-q^{(k)}\right)dA$$

$$+\int_V\left[\left(\alpha_i^{(k)}v_i^{(k)}+\lambda_{ij}^{(k)}\Gamma_{ij}^{(k)}\right)+\phi^{(k)}\right]dV-\int_A \bar{q}^{(k)}\,dA \tag{2.54}$$

where $\alpha_i^{(k)}$, $\lambda_{ij}^{(k)}$ are the internal force and couple acting on kth constituent due to interactions and $\phi^{(k)}$, $\bar{q}^{(k)}$ represent volume and surface contributions, respectively, to the balance of energy. Also

$$\sum_{k=1}^{n}\alpha_i^{(k)}=0 \tag{2.55}$$

$$\sum_{k=1}^{n}\lambda_{ij}^{(k)}=0 \tag{2.56}$$

$$\sum_{k=1}^{n}\bar{q}^{(k)}=0 \tag{2.57}$$

Without loss of generality, λ_{ij} can be taken to be [64] antisymmetric as $\Gamma_{ij}^{(k)}$ is antisymmetric. Bowen [24], and Bedford [9] used essentially the same form in writing energy balance equality for each constituent. Assuming the quantities , ρ, U, v_i for the mixture are sufficiently smooth in the space and time variables, it can be shown that:

$$\int_V\left[\rho\frac{DU}{Dt}-\rho r+\sum_{k=1}^{n}\rho^{(k)}v_i^{(k)}\left(f_i^{(k)}-b_i^{(k)}\right)\right]dV+\int_V\sum_{k=1}^{n}\rho c^{(k)}\left(U+\frac{1}{2}v_i^{(k)}v_i^{(k)}\right)dV$$

$$=\int_A\sum_{k=1}^{n}\left(t_i^{(k)}v_i^{(k)}-q\right)dA \tag{2.58}$$

Invariance of the energy equality under superposed uniform translational velocities yields, for arbitrary V,

$$\int_V \sum_{k=1}^{n} \rho c^{(k)} dV = 0 \tag{2.59}$$

i.e., the mass elements of the mixture are conserved. It was also shown that

$$\frac{D\rho}{Dt} + \rho v_{i,i} = 0 \tag{2.60}$$

A generalization of Cauchy's stress principle was derived in the form

$$\sum_{k=1}^{n} t_i^{(k)} = \sum_{k=1}^{n} t_{ji}^{(k)} n_j \tag{2.61}$$

In point form, the equation of balance of linear momentum for the mixture postulated by Truesdell was obtained. Green [62] obtained, for a binary mixture,

$$\int_V \left\{ \rho r - \rho \frac{DU}{Dt} + \frac{1}{2}[\rho^{(1)}(b_i^{(1)} - f_i^{(1)}) - \rho^{(2)}(b_i^{(2)} - f_i^{(2)})](v_i^{(1)} - v_i^{(2)}) + \frac{1}{2} t_{ij}(v_i^{(1)} + v_i^{(2)})_{,j} \right\} dV$$

$$+ \frac{1}{2} \int_A (t_i^{(1)} - t_i^{(2)})(v_i^{(1)} - v_i^{(2)}) dA = \int_A q \, dA \tag{2.62}$$

Defining, following Mills [99]

$$p_i^{(k)} = t_i^{(k)} - t_{ji}^{(k)} n_j \tag{2.63}$$

and applying the rate of energy equality to a tetrahedron bounded by the coordinate planes and a plane with unit normal n_j for heat flow h_j across plane x_p for a binary mixture, Green [62] obtained:

$$q - h_j n_j = \frac{1}{2}(p_i^{(1)} - p_i^{(2)})(v_i^{(1)} - v_i^{(2)}) \tag{2.64}$$

In the special case when $q = h_j n_j$, $p_i^{(1)}$ and $p_i^{(2)}$ vanish except, possibly, in the case of no relative motion between the constituents. Rate of energy equality can also be stated as

$$\int_V \left[\rho \frac{DU}{Dt} - \rho r + h_{j,j} - \sum_{k=1}^{n} \theta_i^{(k)} v_i^{(k)} + \sum_{k=1}^{n} \frac{1}{2} \rho c^{(k)} v_i^{(k)} v_i^{(k)} - \sum_{k=1}^{n} t_{ji}^{(k)} v_{i,j}^{(k)} \right] dV = 0 \tag{2.65}$$

where

$$\theta_i^{(k)} = t_{ji,j}^{(k)} + \rho^{(k)}(b_i^{(k)} - f_i^{(k)}) \tag{2.66}$$

Invariance under a superposed uniform rigid body angular velocity leads to symmetry of the sum of partial stresses. The partial stresses do not have to be symmetric. The rate of energy equality was written in point form as:

$$\rho \frac{DU}{Dt} - \rho r + h_{j,j} - \sum_{k=1}^{n} t_{(ji)}^{(k)} d_{ij}^{(k)} - \sum_{k=1}^{n-1} t_{[ji]}^{(k)} (\Gamma_{ij}^{(k)} - \Gamma_{ij}^{(n)}) - \sum_{k=1}^{n-1} p_i^{(k)} (v_i^{(k)} - v_i^{(n)}) = 0 \qquad (2.67)$$

where

$$p_i^{(k)} = \theta_i^{(k)} - \frac{1}{2} c^{(k)} (v_i^{(k)} - v_i^{(n)}) \qquad (2.68)$$

$$= t_{ji,j}^{(k)} + \rho^{(k)} (b_i^{(k)} - f_i^{(k)}) - \frac{1}{2} c^{(k)} (v_i^{(k)} - v_i^{(n)}) \qquad (2.69)$$

In setting up the rate of energy equality, it was stated that the internal energy per unit mass of the mixture may not be equal to the sum of internal energies of the constituents. Green [66] showed that if the sum of internal energies of the constituents is defined by

$$\rho U^{*} = \sum_{k=1}^{n} \rho^{(k)} U^{(k)} \qquad (2.70)$$

the rate of energy equality in the form of equation (2.58) is realized if the energy of the mixture is defined by the equation

$$\rho \frac{DU}{Dt} = \rho \frac{DU^{*}}{Dt} + K \qquad (2.71)$$

where

$$K = \sum_{k=1}^{n} (\rho^{(k)} u_i^{(k)} U^{(k)})_{,i} \qquad (2.72)$$

c). Other theories.

Several investigators have used the basic concepts introduced by Truesdell and by Green. These efforts aim at simplifying the description of motion for certain special cases. For instance, in granular porous media, the total deformation can be viewed as

made up of two parts; one related to deformation of the solid particles and the other to their rearrangement i.e. changes in pore geometry. For compressible materials, volume fractions have been introduced as additional variables. Herein we outline some of the results.

i. *Mass Continuity Equation Using Relative Velocity*

Krause [86], referring to fixed volumes in space, for continued saturation and no mass production, wrote the mass continuity equation as

$$\dot{n}^{(k)}\rho^{(k)*} + n^{(k)}\dot{\rho}^{(k)*} + (n^{(k)}\rho^{(k)*}v_j^{(k)})_{,j} = 0 \tag{2.73}$$

If the materials are intrinsically incompressible, $\dot{\rho}^{(k)*} = 0$. Hence, if the intrinsic density is also spatially constant,

$$\dot{n}^{(k)} + (n^{(k)}v_j^{(k)})_{,j} = 0 \tag{2.74}$$

For a binary mixture, the above equations lead to

$$[v_j^{(1)} + n^{(2)}(v_j^{(2)} - v_j^{(1)})]_{,j} = 0 \tag{2.75}$$

Hsieh [76] added the equations of continuity of mass for each of the two constituents in a binary mixture and, for no chemical reaction, obtained

$$\dot{\rho} + (\rho v_i^{(1)})_{,i} + (\rho^{(2)}w_i)_{,i} = 0 \tag{2.76}$$

as the mass continuity equation in terms of relative velocity. Assuming small deformations, he also wrote the continuity equation for the fluid volume contained in a fixed volume in space as

$$\frac{\partial}{\partial t}(\rho^{(1)} - \rho_0^{(1)}) + \rho_0 e_{ij}^{(1)} + \left(\rho_0^{(2)}\frac{\partial}{\partial t}(u_i^{(2)} - u_i^{(1)})\right)_{,i} = 0 \tag{2.77}$$

Integrating over time, for compressible fluid of spatially uniform initial density

$$\rho = \rho_0(1 - e_{ij}^{(1)}) + \rho_0^{(2)}\int_0^t w_{i,i}(\tau)\,d\tau \tag{2.78}$$

ii. *Mass Balance in Terms of Porosity*

Fukuo [46] used the equations of mass balance to set up equations in terms of volume fractions of the constituents. Assuming no chemical interaction, using intrinsic densities, he obtained:

$$\dot{n}^{(k)}\rho^{(k)*} + n^{(k)}\dot{\rho}^{(k)*} + (n^{(k)}\rho^{(k)*}v_i^{(k)})_{,i} = 0 \tag{2.79}$$

If the kth constituent is incompressible, $\dot{\rho}^{(k)*} = 0$, and $\rho_{,i}^{(k)*} = 0$. Hence,

$$\dot{n}^{(k)} + (n^{(k)}v_i^{(k)})_{,i} = 0 \tag{2.80}$$

Hsieh [76] considered a porous solid saturated with an incompressible fluid and undergoing small deformations. For this condition, considering a unit volume in the undeformed state, they showed that the fluid content change is

$$n = -(n^{(2)} - n_0^{(2)}) - n^{(2)}e_{ij}^{(1)} \tag{2.81}$$

They also showed that

$$\frac{\partial}{\partial t}(n^{(2)} - n_0^{(2)}) + n_0^{(2)}\frac{\partial}{\partial t}e_{ij}^{(1)} + w_{i,i} = \dot{0} \tag{2.82}$$

This is a relationship between rate of porosity change, the rate of volumetric strain and the relative velocity vector. These quantities, in a theory for incompressible fluids and no thermal or chemical effects cannot, therefore, be treated as independently variable. For compressible fluids, Morland [103] proposed constitutive equations for porosity.

iii. *Alternative Form of Linear Momentum Balance.*

Considering balance of momentum of fixed volumes in space, Hsieh [76] derived the local form of the momentum balance equation, for no body forces, as:

$$\frac{\partial}{\partial t}\sum_{k=1}^{n}\rho^{(k)}v_i^{(k)} + \sum_{k=1}^{n}(\rho^{(k)}v_i^{(k)}v_j^{(k)})_{,j} = \sum_{k=1}^{n}t_{ji,j}^{(k)} \tag{2.83}$$

Assuming additivity of stresses, for a binary mixture, he obtained

$$\rho \frac{D}{Dt} v_i^{(1)} + \rho^{(2)} \left[\frac{\partial}{\partial t} v_i + v_j^{(2)} v_{i,j} + v_j v_{i,j} \right] = t_{ji,j} \tag{2.84}$$

where $v_i = v_i^{(2)} - v_i^{(1)}$ is the relative velocity.

iv. *Energy Balance in Terms of Porosity.*

Goodman [57] postulated the equation of energy balance for a porous material with porosity n as

$$\frac{D}{Dt} \int_V n\rho^* \left(U + \frac{1}{2} v_i v_i + \frac{1}{2} K \left(\frac{\partial n}{\partial t} \right)^2 \right) - b_i v_i - l \frac{\partial n}{\partial t} - r \Big| dV$$

$$= \int_A (t_{ji} v_j + s_i \frac{\partial n}{\partial t} - q_i) n_i \, dA \tag{2.85}$$

Here K, s_j, l are, respectively, the equilibrated inertia, components of the equilibrated stress vector, and the external equilibrated body force. This equation admits an additional degree of freedom, viz., the volume fraction. A kinetic energy term was associated with the rate of change of n. Similarly, rate of work terms were associated with the rate of change of n over volumes and surfaces using generalized forces s_j and l. Invariance of this equality, as in Green theory, leads to the equations of linear momentum and angular momentum balance. Goodman [57] also postulated an equation of motion, called the equation of balance of equilibrated forces, for the variable n, as

$$\frac{D}{Dt} \int_V n\rho^* \left[K \frac{\partial n}{\partial t} + l + g \right] dV = \int_A s_j n_j \, dA \tag{2.86}$$

Here g is the intrinsic equilibrated body force. They also wrote the local form of this equation.

v. *Other Form of Energy Balance Equation* Bowen [24] postulated the point form of the rate of energy equality as

$$\rho \frac{\partial}{\partial t} \left[U + \frac{1}{2} v_i v_i \right] = (t_{ji} v_j - q_i)_{,i} + \rho r + \sum_{k=1}^{n} \rho^{(k)} v_i^{(k)} b_i^{(k)} \tag{2.87}$$

Using an interaction force vector, Green [67] wrote the energy balance equation in point form as

$$\rho \frac{DU}{Dt} = \rho r - q_{i,i} - \phi + \sum_{k=1}^{n} (\mu_i^{(k)} v_i^{(k)} + t_{ji}^{(k)} v_{i,j}^{(k)} + \frac{1}{2} \rho c^{(k)} u_i^{(k)} u_i^{(k)}) \tag{2.88}$$

where

$$\phi = \sum_{k=1}^{n} (\rho^{(k)} u_i^{(k)} U^{(k)})_{,j} \tag{2.89}$$

$$\rho U = \sum_{k=1}^{n} \rho^{(k)} U^{(k)} \tag{2.90}$$

and

$$\mu_i^{(k)} = t_{ji,j}^{(k)} + \rho^{(k)} (b_i^{(k)} - f_i^{(k)}) - \rho c^{(k)} u_i^{(k)} \tag{2.91}$$

Mokadam [101] considered the total internal energy for the mixture to consist of three components,

$$E = U + T + L \tag{2.92}$$

where U, T, L, are respectively, the molecular, the kinetic, and the potential energies per unit mass of the mixture. Identifying the diffusive force as the body force causing mass flow, Mokadam postulated equations of balance of energy in the form

$$\frac{\partial \rho E}{\partial t} = -(\rho U v_j + q_j - t_{ij} v_i)_{,j} + D_j v_j \tag{2.93}$$

where D_j are components of the diffusive force. Also

$$\frac{\partial \rho L}{\partial t} = -(\rho L v_j)_{,j} - \rho f_j v_j \tag{2.94}$$

For no chemical reaction, the above equation along with mass conservation implies

$$\frac{DL}{Dt} = f_i v_i \tag{2.95}$$

Mokadam wrote, for no chemical reaction

$$\frac{\partial \rho U}{\partial t} = (t_{ij} v_i)_{,j} - (\rho T v_i + q_i)_{,i} \tag{2.96}$$

2.3.2.6 Constitutive Relations

In order to set up constitutive equations, it is necessary first to define the mechanical quantities for which such relationships are desired and to identify the kinematic or state variables on which these quantities might depend. For a mixture of several constituents, the stresses in the constituents are obviously the primary mechanical variables. Truesdell [163] following Maxwell [97], recognized diffusive resistance as another mechanical variable reflecting the interaction between the constituents. The rate of energy equality contains scalar products of "corresponding" quantities. This indicates the need for postulating constitutive relations for components of the symmetric and the antisymmetric parts of the partial stress tensors and an interaction quantity. Again, if the equations of mass, linear momentum, angular momentum, and energy balance for constituents be regarded as equations for certain quantities, constitutive equations are required for the other quantities appearing in those equations and also for the partial entropy of each constituent. These constitutive equations are subject to the balance equations for the mixture and to an appropriate entropy production inequality.

There has been some difficulty in defining components of the partial stress tensors. For fluid-saturated solids, the isotropic fluid stress is generally considered to be the stress variable in addition to the stresses in the solid. Biot [11] regarded the total stress and the fluid stress as the mechanical variables. The definition of pore-fluid pressure used by various investigators differs considerably. Traditionally, for a water-saturated soil, the pressure recorded by piezometers inserted into the water-filled pores has been assumed to be the fluid pressure acting over 100 percent of the area of internal surfaces [5,26,74,81,90,162,175]. Biot [17] pointed out that the generalized forces defined by divergence of the stresses are correctly defined by the virtual work of microscopic stresses per unit value of the displacements of the constituents and not as the average of the microscopic stresses. Mokadam [100] following Guggenheim [68] regarded the fluid pressure to be the thermodynamic property such that

$$\pi\, dV = dW \tag{2.97}$$

where dV is the differential change in the intrinsic fluid volume and dW the reversible work of the fluid phase.

Garg [49], Morland [103-105] Pecker [119] and Carroll [27] among others, introduced the notion of intrinsic stresses for each constituent leading to

$$t_{ij}^{(k)} = n^{(k)} t_{ij}^{(k)*} \tag{2.98}$$

Tsien [166] divided the total stress into stress deviation and a hydrostatic component. The hydrostatic stress was expected to be distributed over the solid and the fluid in proportion to their volume fractions and the solid was expected to take the entire stress deviation. Terzaghi [161,162], as well as Green [61-67] assumed the partial stresses to act over the entire area of any surface element. Further, assuming partial stresses to be additive, the total stress in a saturated soil, assuming isotropic fluid stress, is

$$t_{ij} = t_{ij}^{(1)} + t_{ij}^{(2)} \tag{2.99}$$

Biot regarded the partial soil stress to be the bulk stress acting over the entire area of internal surfaces. In his earlier work [11], there was no reference to the area over which the fluid pressure acts. Later [12], Biot assumed the fluid pressure to act only over the pore area. This corresponds to the notion of the fluid pressure being an intrinsic quantity. Thus

$$t_{ij} = t_{ij}^{(1)} + n^{(2)} t_{ij}^{(2)*} \tag{2.100}$$

a). Diffusive Resistance.

Diffusive force, identified as the interaction force by Truesdell [163,164] was called "diffusive resistance" by Green [62-67] and Crochet [37]. Biot [18] described it as "disequilibrium force". The words "friction" and "drag" have also been used. Max-

well [97] defined it as a pair of equal and opposite forces acting on the two constituents in a binary mixture. For non-chemically reacting continua, in the absence of inertia effects, the equilibrium equations for the fluid-saturated solid can be re-written as

$$t^{(1)}_{ij,i} + \rho^{(1)} b^{(1)}_i = -t^{(2)}_{ji,i} - \rho^{(2)} b^{(2)}_i \tag{2.101}$$

Each side of the equality represents interaction between the constituents and is set equal to components of the diffusive resistance vector. A set of single-constituent stresses in equilibrium can be added to the stresses on either side without affecting the definition of diffusive resistance. For hydrostatic fluid stress, the diffusive resistance is

$$D_i = -(\pi_{,i} + \rho^{(2)} b^{(2)}_i) - \bar{t}^{(2)}_{ji,j} \tag{2.102}$$

where

$$(\bar{t}^{(1)}_{ji} + \bar{t}^{(2)}_{ji})_{,j} = 0 \tag{2.103}$$

the superposed bar indicating a set of stresses in equilibrium. Maxwell assumed the interaction force to be proportional to the densities of the constituents and to the relative velocity. This is easily seen to be a special case of the more general relationship indicated by the above definition of diffusive resistance.

If inertia effects are included, for a binary mixture, $p^{(\alpha)}_i$ the quantity conjugate to the relative velocity in the energy equality is

$$-p_i = \rho^{(2)}(f^{(2)}_i - b^{(2)}_i) + \rho c^{(2)} v^{(2)}_i - t^{(2)}_{ji,j} - \bar{t}^{(2)}_{ji,j} \tag{2.104}$$

This definition is somewhat more general than the one used by Green [64,65] where the term involving mass supply was ignored. In [66], however, following Mills [99], a general form was stated for a mixture of n-1 fluids and a solid.

Truesdell [164] proposed a mechanical theory of diffusion and showed that the kinetic theory, the hydrodynamical theory and the thermodynamical theory were all specializations of his general theory. According to Truesdell: "diffusion, being a change

of motion, arises from forces; the motions produced by these forces must conform to the principle of linear momentum applied to each constituent and to the whole mixture". The sum of supplies of partial momenta to the constituents must vanish. The simplest constitutive equation for supply of momentum would be a linear dependence of the partial momentum upon the quantity "corresponding" to it in the energy balance equation. viz., the relative velocity of the constituent with respect to the others. The restriction that the sum of partial moment supplies must vanish places a restriction upon the coefficients. Truesdell showed that this restriction leads to the necessary and sufficient condition

$$\sum_{j=1}^{n} (L_{ji}^{(k)} - L_{ki}^{(j)}) = 0 \tag{2.105}$$

where the scalar coefficients $L_{ji}^{(k)}$ relating velocity of the kth constituent with its partial momentum are uniquely defined for $k \neq j$ and must vanish for $k = j$. For a binary mixture, this implies symmetry with respect to j and k.

Mokadam [100] proposed that constitutive equations for the diffusive force have the form

$$p_i = -\frac{a}{T} v_i - \frac{b}{T^2} T_{,i} \tag{2.106}$$

Crochet [37], assuming the existence of an energy function for the mixture, showed that under isothermal conditions and in the absence of chemical reactions, the constitutive relations will involve deformation gradients, deformation rates, velocities, and relative vorticities. For the linear theory of irrotational relative motion, in the absence of chemical reaction and inertia effects, and non-Newtonian behavior in a binary mixture of a fluid and a solid this immediately leads to an expression of the type

$$p_i = \pi_{,i} + \rho^{(2)} b_i^{(2)} = -C_{ji} v_j \tag{2.107}$$

The inverse form of this equation is the well-known d'Arcy flow rule [120,141]. Biot [11,14-21] and earlier investigators had used this rule as the starting point for their theories. The observation of linear dependence of one-dimensional water flow and the potential gradient has been extended to two and three-dimensional flow. The constant of proportionality was enlarged to have the nature of a second rank tensor transforming the potential gradient to the flux vector. The permeability tensor is generally assumed to be symmetric correponding to Biot's assumption of the existence of a dissipation function. Nonhomogeneity of the solid and spatial variations in fluid properties have been allowed for by assuming the components of the permeability tensor to be spatially varying. The tensorial character has been used to admit hydraulic anisotropy. In case where the solid as well as the fluid are in motion, d'Arcy's law has been applied to the relative velocity of the fluid with respect to the solid matrix (e.g. [14,55]).

Schiffman [144] wrote the following equations for coupled mass and heat flow

$$\begin{Bmatrix} h_i \\ \dfrac{v_i}{T} \end{Bmatrix} = \begin{pmatrix} -C_{ji} & -D_{ji} \\ -J_{ji} & -K_{ji} \end{pmatrix} \begin{Bmatrix} \dfrac{1}{T^2} T_{,j} \\ D_j \end{Bmatrix} \tag{2.108}$$

where T is the temperature.

Mokadam [100-102] studied the thermodynamics of d'Arcy's law under multicomponent flow. Setting up an expression for rate of increase of entropy, he wrote, for the flow of n fluids through a rigid solid:

$$\begin{Bmatrix} h_i \\ m_i \\ \dfrac{v_i}{T} \end{Bmatrix} = \begin{pmatrix} -C_{ji} & -A^m_{ji} & -D_{ji} \\ -B_{ji} & -E^m_{ji} & -F_{ji} \\ -J_{ji} & -G^m_{ji} & -K_{ji} \end{pmatrix} \begin{Bmatrix} \dfrac{1}{T^2} T_{,j} \\ \dfrac{\mu^m_{,j}}{T} \\ D_j \end{Bmatrix} \tag{2.109}$$

where h_i, m_i, v_i, D_i, denote, respectively, components of the heat flux, the diffusive flux,the mass velocity, and the diffusive force vector. μ^m is the chemical potential of the mth constituent. For isothermal flow, in the absence of chemical reactions, this equation merely indicates the temperature dependence of the permeability tensor.

The d'Arcy fluid flow equation has been generalized still further [58,59], and indeed forms part of the general phenomenological equations given by Onsager [118] These express the effect of simultaneous presence of fields of mechanical pressure, electric potential, temperature and chemical concentration. The general relationship is expressed as

$$J_i = L_{ji} F_j \tag{2.110}$$

where J_i are the fluxes viz., mass flow, heat flow, electric current, chemical diffusion. F_j are the Prigogine forces [59,118]. L_{ji} are components of a positive definite symmetric tensor. The components L_{ji} have to satisfy the Curie-Prigogine principle and in some cases of system symmetry, L_{ji} would vanish where the tensorial rank of the "forces" F_j and the "fluxes" J_i are not the same. Onsager [118] expected the relationship to be symmetric i.e., $L_{ij} = L_{ji}$. Evidently, the Onsager equation, proposed originally for small perturbations on an equilibrium state, is a restricted type of relationship, assuming a quadratic form for the entropy rate function. In general, J_i can be treated as functionals, and may depend linearly or nonlinearly on the spatial gradients, of all orders, of the potential fields and their history. This has been discussed by Coleman [36] in the case of heat conduction. The same type of reasoning would apply to other flux phenomena, and the only thermodynamic restriction is that the scalar product of flux and force be non-negative [164].

Ghaboussi [54] pointed out that Biot's [17,18] formulation for momentum balance may be regarded as a generalization of (2.107) to include inertia effects in the body

force term giving, for no chemical reaction and isotropic fluid stress, a specialization of the more general relationship,

$$p_i = \pi_{,i} + \rho^{(2)}(b_i^{(2)} - f_i^{(2)}) = -C_{ji}v_j \tag{2.111}$$

Using the definition of p_i, (2.69), a general relationship based on the correspondence of $p_i^{(k)}$ and the relative velocity $v_i^{(1)} - v_i^{(2)}$ is

$$p_i = \pi_{,i} + \rho^{(2)}(b_i^{(2)} - f_i^{(2)}) - \frac{1}{2}\rho c^{(2)}v_i = -C_{ji}v_j \tag{2.112}$$

b). Stresses

It has been difficult to define the dependence of components of the partial stress tensors upon the kinematic variables and densities of the constituents of a mixture. In his earlier work, Adkins [1,2] assumed that the stress in each constituent depended upon the density and the kinematic quantities associated with that constituent only. Green [60] admitted interdependence of partial stresses of each constituent upon the kinematics of all. This was in line with the principle of equipresence. However, to make the independent variables distinct for various constituents, Green [60] stipulated that the partial stresses for any constituent would depend upon the densities, velocities and antisymmetric deformation of all constituents but only on the symmetric part of the deformation gradient of the constituent itself. Invariance of stress under superposed rigid body motions and under superposed uniform rigid body angular velocities of the mixture as a whole showed that, for a binary mixture, the velocities and the rotation tensors must occur as difference terms in the set of independent variables. Mokadam [100] assumed the stress tensor to be a linear function of velocity gradients. Carroll [27] and Morland [103-106], among others, also assumed that the shear traction is carried by the bulk solid and is related to changes in pore geometry. The hydrostatic stress components in the solid and the fluid were expected to cause intrinsic volume changes in the constituents.

Bedford [9] pointed out that fluid-saturated porous media fall in the class of immiscible mixtures. The constituents of such mixtures remain physically separate on a scale which is large in comparison with molecular dimensions. This immiscibility has two important consequences. Because of physical separation, in some local sense, each constituent will obey the constitutive relations for that constituent alone. Also, the constituents intrinsically have microstructure defined by the inter-faces which separate the constituents. To set up macroscopic constitutive relations, one approach would be to postulate these relations directly as described above. Another alternative would be to relate macroscopic behavior to intrinsic properties of the constituents. The simplest theories involve the volume fraction of the constituents in addition to the usual variables. Morland [103] pointed out the meaning of deformation and stress associated with the continuum model of each constituent. In particular, the partial density variation is not the density variation of the constituent since the mixture postulate eliminates reference to the actual volume occupied by each constituent in an immiscible mixture.

Terzaghi [161] introduced the concept of effective stress. This was defined to be the stress component causing deformations of the soil. For hydrostatic pore-water pressure acting on incompressible soil grains, the entire deformation of the soil was assumed to be due to changes in the pore volume and pore geometry. For this case, Terzaghi [161] called the partial solid stress the effective stress related to deformation of the solid. Biot [11] regarded the total stress and the fluid pressure as the mechanical variables. It was found (e.g. [113]) that the fluid pressure did in fact influence the effective stress-strain relationship when the solid grains had compressibility comparable to that of the matrix as a whole and the fluid was not incompressible. To allow for this the effective stress related to deformation was defined as

$$t'_{ij} = t_{ij} - c\pi\delta_{ij} \tag{2.113}$$

$$= t^{(1)}_{ij} + (1-c)\pi\delta_{ij} \tag{2.114}$$

where c = 1 implies Terzaghi's definition and c = 0 would correspond to total stress being regarded as effective. Suklje [160] discussed selection of appropriate values of c. Schiffman [143] expected c to be between the value of porosity and 1. This was based on the assumption that the pore fluid pressure may not act over the entire area of surface elements but only over a part. This fractional area of action of the fluid pressure would be bounded below by the porosity and above by 1. Several investigators confuse the effective stress with the partial stress. This is due to the dual definition originally given by Terzaghi. The term "effective stress" used in this report is the stress component causing deformations of the solid and is thus defined completely by these deformations. The partial stress in the solid could conceivably be related to quantities other than the deformations of the solid. Verruijt [167,168] used the term "intergranular stress" for the difference between the total stress and the intrinsic pore-water pressure assumed to act over 100 percent area. The relationship of "intergranular stress" and the "effective sress" with the partial stress which appears in equations of balance of momentum needs to be established. Considering the solid grains to be compressible, Nur [113] derived the equation

$$c = 1 - K/K_s \tag{2.115}$$

where K, K_s are, respectively, the bulk and the intrinsic compressibility of the solid, For incompressible grains and highly deformable pore space, $K/K_s=0$, and Terzaghi's two definitions coincide. Suklje [160] suggested, without proof,

$$c = 1 - n^{(1)}\frac{K}{K_s} \tag{2.116}$$

Schiffman [143] gave a more general form allowing fluid pressure to be a second rank tensor and c a fourth rank tensor, i.e.,

$$t'_{ij} = t_{ij} - A_{klij}t^{(2)}_{kl} \tag{2.117}$$

Carroll [27] carried out a similar development. These approaches were based on superposition of effects of the hydrostatic stress and the stress deviation. Carroll [27] determined, for the linear case, the relation

$$t'_{ij} = t_{ij} - E_{klij} C^{(s)}_{klmn} \pi \delta_{mn} \tag{2.118}$$

where E_{klij} are components of the elasticity tensor for the dry solid material and $C^{(s)}_{ijkl}$ those of the intrinsic compliance under hydrostatic stress. Biot [18] defined effective stress as

$$t'_{ij} = t_{ij} - \alpha \pi^* \delta_{ij} \tag{2.119}$$

and assumed t'_{ij} to be the quantity related to solid deformation. This coincides with Terzaghi's concept of effective stress for $\alpha = 1$.

Garg [49], following Haimson [73], proposed a dual definition for effective stress. For strength of rock, he would set $c \approx 1$ but for constitutive relations another value of c would be used.

Carroll [28] introduced intrinsic solid stress on the solid particles and an effective stress influencing deformation of the pore space. Kenyon [83,84] also considered the effect of grain and fluid compressibilities and introduced material parameters to characterize this dependence. Contact stress in the solid and the bulk stress independent of K_s were used.

For large deformation, an incremental form of the stress tensor was introduced by Biot [20]. Carter [30] and Prevost [121] used the Jaumann stress-rate to ensure frame indifference.

Form of the Stress-Strain Relations.

Gibson [55] expected the effective stress to depend upon the deformation or the rate and history of deformation of the solid skeleton. The fluid pressure was expected to depend upon the fluid density in an isothermal system.

Tsien [167] proposed a linear elastic isotropic relation for the partial soil stress in terms of the soil strain using Terzaghi's definition i.e. $c = 1$ in (2.113). Biot [11] assumed a quadratic energy function in the change in water content per unit volume of the solid, and the soil strains leading, for isotropic linear elastic soil and incompressible fluid, to

$$\pi = Me_{kk} + N\theta \tag{2.120}$$

and

$$t_{ij} = 2\mu e_{ij} + \lambda e_{kk}\delta_{ij} + M\theta\delta_{ij} \tag{2.121}$$

In later work, [17], the total stress was replaced by the partial solid stress. In extension to anisotropic elastic [15,16] solid and compressible fluid the relationships for the total stress and the intrinsic pore-water prssure were stated as

$$t_{ij}^{(1)} = E_{klij}e_{kl}^{(1)} + M_{ij}\zeta \tag{2.122}$$

$$\pi^{*} = M_{ij}e_{ij}^{(1)} + M\zeta \tag{2.123}$$

An alternative form of the above relationships, assuming $M_{ij} = \alpha M\delta_{ij}$ and $t_{ij} = t'_{ij} + \alpha\pi\delta_{ij}$ [16,18,19], is

$$t_{ij} = E_{klij}e_{kl}^{(1)} + \alpha M\delta_{ij}(\alpha e_{kk}^{(1)} + \zeta) \tag{2.124}$$

and

$$\pi^{*} = \alpha Me_{kk}^{(1)} + M\zeta \tag{2.125}$$

Here α is a measure of compressibility of the solid particles. This form was used by Ghaboussi [53,54] for development of finite element solution procedures. Garg [50] wrote the constitutive relations for an isotropic system in the form

$$t_{ij}^{(1)} = a\, e_{kk}^{(1)}\delta_{ij} + c\, e_{kk}^{(2)}\delta_{ij} + 2\mu(e_{ij}^{(1)} - \frac{1}{3}\delta_{ij}e_{kk}^{(1)})$$

$$\pi = n^{(2)}\pi^{*} = c\, e_{kk}^{(1)} + b\, e_{kk}^{(2)} \tag{2.126}$$

Here μ is the bulk shear modulus of the porous solid and a,b,c are functions of the volume fractions of the constituents, the bulk modulus of the porous solid, and the intrinsic bulk moduli of the fluid and the solid. The constants, for isotropic elasticity have been shown to correspond to Biot's and to depend upon the properties of the constituents and their volume fractions.

Similar construction was used for viscoelastic soils [12]. In [20] the fluid strain was again replaced by the change in water content. The same concept was extended to the case of finite elastic deformation [21].

Lubinski [93] assumed that the total strain of a bulk porous solid can be expressed as a summation of the strains due to pore-water pressure and strains due to stress acting on the solid skeleton. He proposed relations of the type

$$t_{ij}^{(1)} = E_{klij}e_{kl}^{(1)} + (n^{(1)} - \gamma)\pi\delta_{ij} \tag{2.127}$$

$$\pi^{*} = Me_{ij}^{(1)} + N(n^{(2)} - n_0^{(2)}) \tag{2.128}$$

where γ, M, N, are material constants. Krause [86] added terms to the right side of (2.120) to reflect linear dependence of the fluid pressure on the deformation rate of the fluid. This assumes a viscous component for fluid flow. Adkins, in his earlier theory [1,2], assumed that the stress in each constituent depended only on the density and the kinematic quantities associated with only that constituent. Nur [113] assumed the effective stress, given by (2.113) along with (2.115), to be related to the soil strains. This admitted a certain dependence of the partial soil stress upon the fluid pressure. Explicitly,

$$t'_{ij} = t^{(1)}_{ij} + (1-c)\pi\delta_{ij} = C_{klij}e^{(1)}_{kl} \tag{2.129}$$

Hence

$$t^{(1)}_{ij} = C_{klij}e^{(1)}_{kl} - (1-c)\pi\delta_{ij} \tag{2.130}$$

These approaches were based on the superposition of effects of the hydrostatic stress and the shear stress. Carroll [27] determined, that for the linear case, (2.130) would be

$$t^{(1)}_{ij} = E_{klij}e^{(1)}_{kl} - E_{klij}C^{(1)*}_{klmn}\pi^{*} \tag{2.131}$$

where E_{klij} are components of the elasticity tensor for the dry solid material and $C^{(1)*}_{ijkl}$ are those of the intrinsic compliance under hydrostatic stress. This formulation was specialized to allow for the presence of internal symmetries. For isotropy, the formulation reduces to Nur's [113]. Schiffman [143] proposed a more general form of (2.131) viz.,

$$t^{(1)}_{ij} = E_{klij}e^{(1)}_{ij} - (\delta_{ik}\delta_{jl} - A_{klij})t^{(2)}_{kl} \tag{2.132}$$

The quantity A_{ijkl} was termed the soil-water interaction tensor. Garg [49] obtained a relationship between the intrinsic and the bulk behavior of rocks under hydrostatic stress.

In extending the theory to the nonlinear case, Westmann [170] assumed the partial solid stress to be a function of the deformation tensor for the solid and the rate of deformation (Eulerian description) of the fluid. The fluid stress was expected to consist of a hydrostatic component and another component depending upon the same quantities as the partial solid stress. It was noted that in this formulation it would be difficult to design experiments to evaluate the parameters. A simplification proposed assumed the fluid pressure to be hydrostatic and related to the velocity field through d'Arcy's law. This is similar to Sandhu's [131-133] argument that the constitutive equation for diffusive resistance is a sufficient relationship between the fluid partial stress and kinematics of the mixture. Westmann [170] wrote relative velocity as a function

of the partial fluid stress, the diffusive resistance and the Cauchy deformation tensor for the solid. This would reflect, among other factors, the dependence of permeability on the porosity of the solid.

Morland [103] and Garg [49] assumed the intrinsic stress in each component to be a function of the deformation of that constituent only and having the same form as for a single material. Thus

$$t_{ij}^{(k)*} = f[e_{mm}^{(k)*}] \tag{2.133}$$

The bulk stresses and deformations were expected to be related to the corresponding intrinsic quantities through scaling functions. Thus, the bulk stress in the kth constituent is

$$t_{ij}^{(k)} = n^{(k)} t_{ij}^{(k)*} \tag{2.134}$$

For linear isotropic elastic rock

$$t_{ij}^{(1)} = n^{(1)} K_D^{(1)*} e_{ij}^{(1)*} \tag{2.135}$$

where the subscript D denotes "dry" rock. The bulk deformation gradient was related to the effective deformation gradient as:

$$F_{ij}^{*} = [n^{(1)}/n_0^{(1)}]^{1/3} F_{ij}^{(1)} \tag{2.136}$$

The relation between the deformation gradient and the partial soil stress was expected to be the same function f as for the intrinsic quantities. The isotropic pressures in the fluid and the solid were assumed to depend upon the volumetric strain of both the constituents, i.e.

$$t_{ij} = a e_{mm}^{(1)} + b e_{mm}^{(2)} \tag{2.137}$$

$$\pi = c e_{mm}^{(1)} + d e_{mm}^{(2)} \tag{2.138}$$

However, unlike Biot, the existence of an energy function was not postulated so that the constants b and c in (2.137) and (2.138) do not have to be equal. Morland

expressed the coefficients in terms of compressibilities of the fluid and the solid, and the bulk shear modulus of the mixture.

Carroll [29] postulated the following relations for a fluid-saturated solid:

i. Relation between stress in the mixture and stresses in the constituents:

$$\frac{1}{3} t_{ij} = \frac{1}{3} n^{(1)} t_{ij}^{(1)} + n^{(2)} \pi^* \tag{2.139}$$

ii. Solid stress-strain law

$$\frac{1}{3} t_{ij}^{(1)} = -K_s \frac{\Delta V^{(1)}}{V^{(1)}} \tag{2.140}$$

where the symbol Δ indicates change in the quantity following it.

iii. Effective stress-strain law:

$$\frac{1}{3} t'_{ij} = \frac{1}{3} t_{ij} - \pi^* = -K^* \frac{\Delta n^{(2)}}{n^{(1)}} \tag{2.141}$$

Combining these relationships they obtained the bulk relations for the mixture.

Thermodynamic considerations.

Adkins [3] and Green [60] admitted interdependence of stress of each constituent upon the kinematics of all. This was in line with the principle of equipresence stated by Truesdell [164]. In application to elastic materials, the existence of an energy function for the mixture was assumed by Biot [11,14-16,19-21]. This has been consistently followed by numerous investigators (e.g. [6,7,25,37,39,62-67,159]). Sandhu [131-134] pointed out that as the mixture could not be regarded as a continuum in motion, it was inappropriate to assume energy functions for it in the form that has been popular.

Sandhu [131-134], Westmann [171] and Morland [103-105] followed Adkins' [2] original idea that the stresses in each constituent depend upon the kinematics of only

that constituent. However, Morland [103-105] used this for the intrinsic rather than the bulk stresses. This brings back some dependence of the partial solid stress upon the fluid pressure because the porosity was postulated to be a linear function of the partial stresses.

Seeking constitutive equations for internal energy, entropy, heat flux vector, partial stresses and diffusive resistance vectors p_i and the quantity $q-h_j n_j$ in the case of mixture of two Newtonian fluids, Green [62] assumed these to depend upon the densities of the constituents, the velocities, the gradients of velocities, and the temperature. For the heat flux vector, the temperature gradient replaced the deformation gradients.

Discussing thermodynamics of fluid flow in a rigid porous medium, Mokadam [101,102] pointed out that d'Arcy's law is valid only for isothermal flow in which the inertial and viscous effects are negligible. Also that the rate of entropy production must be non-negative separately for terms involving quantities of different tensorial ranks. Crochet [37] applied thermodynmic considerations to the flow of a fluid through an elastic solid. Atkin [6] explicitly stated the form of these constitutive assumptions for flow of a fluid through an elastic solid. He also presented an alternative method of deriving the linearized theory of elastic solid-viscous fluid mixtures and the thermodynamic restrictions imposed on this theory by the entropy production inequality. In later work, Green [67] based the thermodynamic restrictions on the behavior of each constituent on the requirement that suitable combinations of the equations for individual constituents should yield a single entropy production inequality for the mixture as a whole. Bowen [23] noted that these formulations lead to the result that, in equilibrium, the partial free energy density of a given constituent is independent of the deformations of the other constituents. Also that such independence fails to be confirmed by experiments on fluid mixtures. Muller [108] showed that if gradients of densities of

the constituents were included among the constitutive variables, this difficulty would not arise. Some investigators have proposed use of an entropy production inequality for each constituent. Bowen [23] considers this to be too special.

Morland [103-105] did not assume the existence of an energy function for the mixture but still admitted interdependence. This implies admitting a possibly nonsymmetric constitutive relationship of the type proposed earlier by Schiffman [143]. For c = porosity, the constitutive equations for stresses become uncoupled.

Crochet [37] started by admitting fairly general constituive assumptions in line with Truesdell's [163] principle of equipresence, and then determined the restrictions placed upon these general constitutive relations by thermodynamic considerations. This approach is similar to that used by Noll [111] and Coleman [36]. Crochet [37] showed that the restriction of nonnegative entropy production requires that the entropy and the internal energy be independent of the deformation rates, relative velocity and the temperature gradient. Green [66] extended Crochet's [37] work to anisotropic solids and to include initial stresses.

d. Constitutive Relations for Porosity.

Gibson [55] treated porosity as a function of effective stress and proposed compliance relationships in the form

$$n^{(2)} = f(t_{ij}, X_j, t) \tag{2.142}$$

Walsh [169] regarded the pore space or the volume fraction of the pores to be a function of the solid stress. This leads to the relationship:

$$\frac{d\,n^{(2)}}{d\,t_{ij}^{(1)}} = \frac{1}{V}\frac{dV^{(2)}}{d\,t_{ij}^{(1)}} - \frac{n^{(2)}}{V}\frac{d\,V}{d\,t_{ij}^{(1)}} = \frac{1}{V}\frac{d\,V^{(2)}}{d\,t_{ij}^{(1)}} - \frac{V^{(2)}}{V^2}\frac{d\,V}{d\,t_{ij}^{(1)}} \tag{2.143}$$

Garg [49] pointed out that Walsh's analysis was acceptable for very dense rock. For the general case, they introduced bulk and intrinsic solid compressibilities and set up more general expressions. They proposed constitutive equations for porosity based on the existence of an energy function.

Aifantis [4] assumed effects of changes in fluid pressure and the solid stress to be additive and proposed a compliance relationship

$$\Delta n^{(2)} = a\Delta\pi + b\Delta t_{kk}^{(1)} \tag{2.144}$$

Assuming the intrinsic properties of any constituent are not affected by the presence of the other constituents, Morland [103] proposed a constitutive equation for porosity in the form

$$n^{(2)} = n_0^{(2)}(1 + at_{ij}^{(1)} + b\pi) \tag{2.145}$$

To include dilatancy, the relationship was generalized further to

$$n^{(2)} = n_0^{(2)}(1 + a_{ij}t_{ij}^{(1)} + b\pi) \tag{2.146}$$

2.3.2.7 Comments.

Various approaches to description of the constituents and the mixture as well as description of their motion, formulation of the equations of balance of mass, linear momentum, angular momentum, and rate of energy, and the constitutive relations have been discussed. In most theories of mixtures, deformation is referred to an initial configuration for each constituent and motion to the place coordinates. Also the equations of balance are written for a fixed volume in space. This approach may not be convenient for soil-water mixtures.

Truesdell [164,166] postulated equations of balance of mass, linear momentum, moment of momentum and energy such that the form of the equations was the same for each constituent and for the mixture. The notion of motion of a mixture as a

whole was introduced. Indeed, Truesdell would require the form of the equations of balance for the mixture to be the same as for a single material. To accomplish this identity of form, the total stress tensor, the total heat flux vector, and the specific energy supply had to be specially defined and did not equal the sum of the corresponding quantities for the constituents. The specific energy (internal plus kinetic) of the mixture was, however, equal to the sum of the corresponding quantities associated with the constituents. The existence of the mixture as a continuum in motion with acceleration derived from the barycentric velocity is implied in this line of thought. The analysis was founded on the so-called fundamental identity involving "material derivatives of the mean value". Whereas these can be accepted as hypothetical entities for simplification of analysis, it is difficult to assign a physical meaning to them. This material rate has, in Atkin's [7] words, "no particular physical significance". This is so because the rate is executed not on a material particle but on a center of mass. The mixture, at any instant of time, has been constructed by superposition of constituent particles, is not a set of particles, consists only of centers of mass, and is defined only for the particular instant of time. It cannot be regarded as a continuum, consisting of a set of non-penetrating particles, in motion. Atkin [7] pointed out that the mixture density cannot be associated with a material in the physical sense. Sandhu [133,134] pointed out that the mixture defined above has a physical existence only in the case of no relative motion between constituents. For this special case the mixture will have motion and deformation as a material body and the development of equations of motion for the mixture is meaningful, for example, in the post-liquefaction stage. However, in study of wave propagation leading to liquefaction of soils, it is of little interest. If relative motion is present, the mixture does not satisfy the axiom of continuity and its corollary, the principle of impenetrability. Accordingly, the mixture density, momentum, moment of momentum and energy defined by Truesdell are only mathe-

matical entities without any physical interpretation. These quantities cannot be regarded as functions of time associated with a set of physical particles. Truesdell's third postulate, therefore, appears to be irrelevant to the development of a general theory.

Chao [34] noted that combining the balance equations of constituents to obtain the balance equations of the mixture can lead to errors. As an example, the absence of inertial coupling forces in the momentum equations of the constituents was cited. This is contrary to Biot's "mass coupling" assumption.

On the other hand, Green [62] considered the concepts of stress, heat flux, and energy supply to be primitive to each constituent and to the mixture as a whole as well. The additive property of stress, heat flux, and the energy supply was postulated and the balance laws derived from the frame invariance of a rate of energy equality. The energy density of the mixture was seen to be different from the sum of energy densities of the constituents. This was attributed to interaction between the constituents. Green [66] established a relationship between these quantities.

The balance equations due to Truesdell [164,166] and to Green [66] have similar form and are essentially equivalent but the quantities appearing in the two sets have different interpretations based upon the relationships postulated between the quantities associated with the constituents and with the mixture. Gurtin [69,70] and Morland [103] support the additivity of partial stresses on the ground that tractions are additive and Cauchy's stress principle should hold for total stress and total traction as well as for the constituents. In Green's theory, the equations of mass and momentum balance are derived from the material frame invariance of a rate of energy equality. In another discussion the heat fluxes and the energy supply were assumed to be additive. In another, more recent version of the theory, Green [64] made the role of interactions between constituents explicit by writing the rate of energy equality for each constituent.

Bowen [24] postulated the point form of the rate of energy equality and pointed out the effect of certain approximations. He claimed that Green's theory is a special case of Truesdell's. This is not true. The interpretation of quantities appearing in Truesdell's equations is quite different from that of similar quantities in Green's theory because the two formulations are based on different definitions for the quantities associated with the mixture in terms of those for the constituents rather than due to any approximation.

Westman [170] noted that while writing mass continuity relations care must be exercised because the volume of each continuum phase is not the same as the true volume of each material. For the case of initial stresses, equilibrium must be satisfied in the initial as well as the deformed configuration realized after incrementation of stress.

In recent work by Gurtin [69,70] Oliver [116,117], Williams [171], and Sampaio [129,130] the equations of balance of momentum and energy differ from those of Truesdell [163,165] and Kelly [82] They showed that extension of the traditional theory for single materials to mixtures by simply replacing the forces by "total force" is inadequate to express balance of forces for other than pure constituents. In addition to the partial stress for each constituent, they obtained embedding stresses governed by additional balance of force equations.

Several investigators have introduced volume fractions as additional variables in theories for compressible materials. The balance equations have been written in terms of relative motion and porosity, which is essentially a measure of relative deformation. Fukuo's [46] equations of mass balance may be regarded as an extension of Gibson's [55] approach of referring to the fixed set of particles in the reference configuration.

In Gibson's theory of one-dimensional nonlinear consolidation, the equation of equilibrium of vertical forces associated with reference volume of the solid in the reference configuration were written for the current configuration. The density was related to the densities of the constituents in the current configuration which in turn depended upon the volume fractions of the constituents. Beacause, in this representation, the description of the solid phase is unaffected by deformation, the equation of mass continuity for the solid is simply the equation relating the current density to the reference density of the solid.

The definition of diffusive resistance or the interaction force, given by Green [62-67] appears to be appropriate. as also writing constitutive relations for it in terms of relative velocities of the constituents. For the simple case of a binary mixture, e.g. a saturated soil, the linear dependence of the diffusive resistance upon the relative velocity is essentially a statement of the phenomological observation by d'Arcy. Biot assumed the existence of a dissipation function, quadratic in relative velocity. This corresponds to the assumption of a linear dependence of velocity upon the pressure gradients. Mokadam [100] pointed out that d'Arcy's law is valid only for isothermal flow in which the inertial and viscous effects are negligible. Generalizations of d'Arcy's law to thermomechanical mixtures and simultaneous mechanical and chemical diffusion along Onsager's principle form a part of the general theory of mechanical diffusion presented by Truesdell [165].

For stresses in the constituents, several descriptions have been used. Constitutive equations need to be written for the partial stresses that appear in the equilibrium equations. Biot [18,19] wrote the equations of momentum equilibrium for the mixture using the total stress. In soil mechanics, it is well known that constitutive equations for the total stress are very sensitive to the pore-water pressures and the effective

stress is preferred for the purpose. Terzaghi [161] used a dual definition for effective stress. It appears reasonable to define it as the component of soil skeleton stress which is related to the kinematics of the soil alone. According to the other definition the effective stress is the difference between the total stress and the intrinsic pore-water pressure. Verruijt [167,168] calls it intergranular stress. This definition appears to be unnecessary except in the case of the so-called double-porosity soils in which the soil grain compressibility is taken care of separately from the deformation of the soil as a whole. The relationship between the deformations of the grains and the voids on the one hand and the total soil mass on the other has been established for the double-porosity materials by several investigators [e.g. Carroll].

Biot's [18] and Crochet's [37] assumption of the existence of an energy function for the soil-water mixture is open to objection. The mixture consists of centers of mass and not non- penetrating material particles. As such it does not satisfy the axiom of impenetrability and it is not correct to assign deformation, material rates, energy etc. to this entity. Thus the stress-strain relationships for the fluid and the solid may not be derived from an energy function. Biot's [18,19] theory based upon the existence of an energy function quadratic in the strains of the soil and the water content or the density or the isotropic strain in the fluid is thus arbitrary and restrictive. Garg's [48,49] formulation also is similar and the constants can be shown to correspond to Biot's. Garg related these to the properties of the constituents and the volume fractions.

The argument over whether the stresses in any constituent depend upon the kinematics of that constituent only or that of all the constituents is easily resolved noting that the partial stress need not coincide with the effective stress. The difference would depend upon the compressibility of the fluid and the soil as well as upon the connectivity of the pore space. We find Bedford's [9] argument that, in some local

sense, each constituent will obey the constitutive relations for that constituent alone quite appealing. To set up macroscopic constitutive relations, one approach would be to postulate these relations directly and the other would be to relate macroscopic behavior to intrinsic properties of the constituents. Apparently, the thermodynamic restrictions on entropy production as well as the notion of energy density are applicable to each constituent. Bowen's [24] comments regarding mixtures of fluids need further careful investigation.

Morland [103-105] did not assume the existence of an energy function for the mixture but still admitted interdependence in constitutive relationships. This implies admitting constitutive relationships with possibly nonsymmetric coupling effects of the type proposed earlier by Schiffman [143].

Some theories involve the volume fraction of the constituents in addition to the usual variables. Morland pointed out that the partial density variation is not the density variation of the constituent since the mixture postulate eliminates reference to the actual volume occupied by each constituent in an immiscible mixture. A correct theory would ensure that deformation be associated with a set of particles rather than with a fixed volume in space.

For a statistically isotropic saturated material, Biot expected the kinetic energy of the saturated soil to be quadratic in the velocities of the fluid and the soil and a coupling term was included. This introduced an inertial coupling between the soil and the fluid. It is difficult to assign numerical values to the various quantities that arise as a result of this coupling. Implementation of this theory in a finite element computer program, and a preliminary parametric study to investigate the efect of this coupling on the dynamic response, indicated that the effect would be insignificant. However, further study of this particular feature is needed.

It appears that a theory of dynamics of saturated soils should use a convected coordinate system to define the motion of the soil so that the same set of particles constitute the reference volume. The flow of the fluid should be considered as relative to this reference set of soil particles. Stress would be defined in terms of these convected coordinates and the balance equations would then be written for the reference set of particles. This would represent a generalization of Gibson's theory of nonlinear soil consolidation to three-dimensions and also to include inertia effects. For slow flow and small deformation, certain simplifying assumptions would lead to Biot's theory. The soil and water have relative motion prior to liquefaction. At liquefaction, the relative velocity reduces to zero and the soil-water mixture would move as a single fluid. Development of constitutive equations would involve the thermodynamics of the constituents including their interaction but it would not include assigning physical meaning to a "mixture in motion". Constitutive and inertial couplings might exist. However, symmetry of these couplings cannot be apriori claimed on the basis of the existence of energy functions for the mixture. The next section describes such a theory developed by Hiremath [75].

Section III

A DYNAMICAL THEORY OF SATURATED SOILS

3.1 INTRODUCTION

In existing theories of mixtures the multicomponent mixture has been regarded as a set of superposed continua in motion. The mixture, at any instant of time, has been defined as a set of particles constructed by superposition of constituent particles. In reviewing theories of mixtures, including their possible relationship with mechanics of saturated soils and liquefaction phenomena, an important finding was that the notion of the mixture as a continuum in motion is inadmissible except in the case of no relative motion between the constituents. Liquefaction is primarily caused by the relative motion of soil and water and, therefore, a correct theory of liquefaction cannot be derived from the assumption of the saturated soil being a mixture in motion as a continuum.

Because the mixture cannot be viewed as a continuum in motion, it appears inappropriate to define energy functions on the "mixture" consisiting of centers of mass. This implies that in setting up constitutive relationships for the mixture, one cannot invoke the existence of an energy function.

Some investigators (e.g., [46,76,86]) considering the special problem of flow through deformable porous solids, have attempted to write the balance equations in terms of relative motion and porosity, which is essentially a measure of relative deformation. It would appear that a theory based on balance equations written for a reference set of particles of the porous solid would be the most appropriate for this case. Gibson [55] developed such a theory for the quasi-static problem.

Hiremath developed a [75] theory of dynamics of saturated soils based on use of convected coordinate system to describe the motion of a fixed set of soil particles in a reference volume and regarded the flow of water to be relative to this volume of the soil (Item 4.5 in Appendix B). This theory may be regarded as an extension of the concepts presented by Gibson [55] for the case of one-dimensional quasi-static deformation of soils, to three dimensions and to include inertia. In the remainder of the section we summarize the salient features of this theory.

3.2 KINEMATICS

Description of motion, deformation and stress in a single continuum using convected coordinates is well known [112] and is summarized in Appendix A. Here we describe the simultaneous motion of a compressible solid and a fluid with low compressibility. A material volume V_0 in the reference state C_0, upon motion and deformation, occupies a volume V in state C. The material volume throughout its motion encompasses the same set of particles. The convected coordinate frame, assumed for convenience to be rectangular cartesian in the reference configuration C_0, is, in general, curvilinear in any other state. The strain in the solid, $\gamma^{(1)}_{ij}$, is defined as (A.108)

$$\gamma^{(1)}_{ij} = E^{(1)}_{ij} = \frac{1}{2}\left[u^{(1)}_{i,j} + u^{(1)}_{j,i} + u^{(1)}_{m,i}\, u^{(1)}_{m,j}\right] \tag{3.1}$$

Here $E^{(1)}_{ij}$ are components of the Green's strain tensor and $u^{(1)}_i$ are components of the solid displacement referred to the cartesian system in C_0. The fluid is assumed to be isotropic and, in view of its low compressibility, the components of the strain tensor for the fluid, $\gamma^{(2)}_{kk}$, referred to a cartesian system in C_0 are

$$\gamma^{(2)}_{kk} = e^{(2)}_{kk} = u^{(2)}_{k,k} \tag{3.2}$$

3.3 BALANCE LAWS

3.3.1 Mass Balance of the Solid

If $\rho_0^{(1)}$ and $\rho^{(1)}$ denote the mass densities in the configurations C_0 and C respectively, of a volume element containing the same set of solid particles,

$$\rho_0^{(1)} = n_0^{(1)} \rho_0^{(1)*} \tag{3.3}$$

and

$$\rho^{(1)} = n^{(1)} \rho^{(1)*} \tag{3.4}$$

in which $n_0^{(1)}$ and $n^{(1)}$ are the solid volume fractions in the initial and the current configurations, respectively, and a superposed asterisk denotes an intrinsic quantity. This leads to an equation of mass balance in the form,

$$\int_{V_0} \rho_0^{(1)*} n_0^{(1)} dV_0 = \int_V \rho^{(1)*} n^{(1)} dV \tag{3.5}$$

V_0 and V denote volume of the same set of particles in C_0 and C, respectively. Using (A.126),

$$\int_{V_0} [\rho_0^{(1)*} n_0^{(1)} - \sqrt{G}\, \rho^{(1)*} n^{(1)}] \; dV_0 = 0 \tag{3.6}$$

The point form of this equation is

$$\rho_0^{(1)*} n_0^{(1)} = \sqrt{G}\, \rho^{(1)*} n^{(1)} \tag{3.7}$$

If the solid is incompressible, $\rho_0^{(1)*} = \rho^{(1)*}$ and

$$n_0^{(1)} = \sqrt{G}\, n^{(1)} \tag{3.8}$$

3.3.2 Mass Balance of the Fluid

The motion of the fluid is relative to the solid and the fluid itself does not have a reference state. Mass continuity of the fluid constituent is described for a solid volume in the current configuration.

Consider a rectangular parallelopiped of the solid at point P_0 in the reference configuration C_0, which corresponds to a skew parallelopiped at point P in the current configuration C. The parallelopiped in C_0 is made up of surfaces x_i = constant and $x_i + dx_i$ = constant (Figure 3), and during motion, encloses the same solid particles.

Recalling (A.110) and (A.112), the velocities of the solid and the fluid in terms of the base vectors $\mathbf{e}_i$ and $\mathbf{G}_i$ (or $\mathbf{G}^i$) are

$$\mathbf{v}^{(1)} = v^{(1)m}\mathbf{G}_m = v_m^{(1)}\mathbf{G}^m = \dot{u}_m^{(1)}\mathbf{e}_m \tag{3.9}$$

and

$$\mathbf{v}^{(2)} = v^{(2)m}\mathbf{G}_m = v_m^{(2)}\mathbf{G}^m = \dot{u}_m^{(2)}\mathbf{e}_m \tag{3.10}$$

The components $\dot{u}_m^{(k)}$ $(k = 1, 2)$ are quantities associated with the reference state. The face of the parallelopiped formed by the sides dx^2 and dx^3 in the reference state becomes an area formed by the vectors $\mathbf{G}_2 dx^2$ and $\mathbf{G}_3 dx^3$ in the deformed state. Thus, the mass flux per unit time entering this face is

$$n^{(2)}\rho^{(2)*}[\dot{u}_1^{(2)} - \dot{u}_1^{(1)}]dx^2 dx^3 \tag{3.11}$$

The mass flux leaving the opposite face is

$$n^{(2)}\rho^{(2)*}[\dot{u}_1^{(2)} - \dot{u}_1^{(1)}]dx^2 dx^3 + \frac{\partial}{\partial x^1}\{n^{(2)}\rho^{(2)*}[\dot{u}_1^{(2)} - \dot{u}_1^{(1)}]dx^1\}dx^2 dx^3 \tag{3.12}$$

The net rate of gain including the fluid flow in all the three-directions is,

$$\frac{\partial}{\partial x^1}\{n^{(2)}\rho^{(2)*}[\dot{u}_i^{(2)} - \dot{u}_i^{(1)}]\}dx^1 dx^2 dx^3 \tag{3.13}$$

The rate of increase of fluid within the deformed parallolepiped is

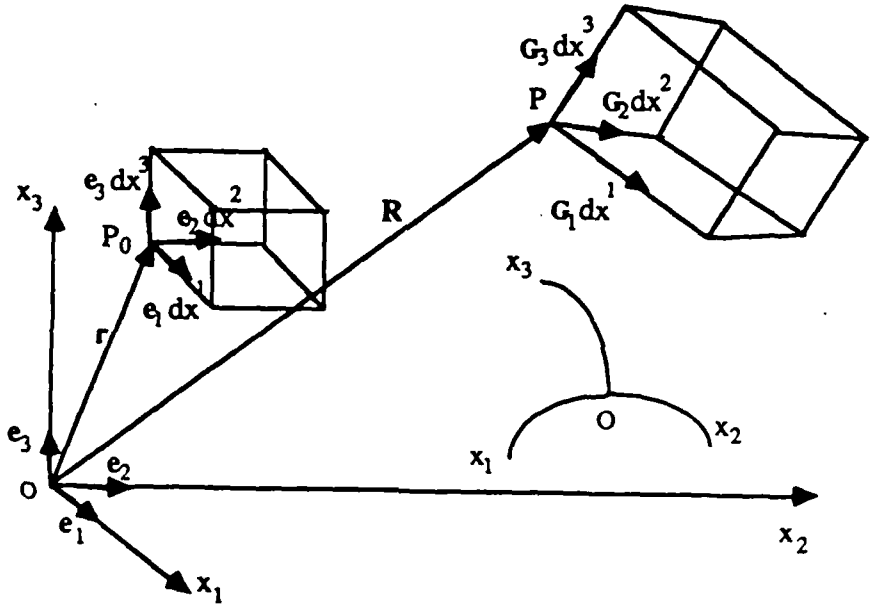

Figure 3: Geometry of an Infinitesimal Parallelepiped

$$\frac{\partial}{\partial t}[n^{(2)}\rho^{(2)*}\sqrt{G}\,dx^1\,dx^2\,dx^3] \tag{3.14}$$

Adding (3.13) and (3.14) and cancelling $dx^1\,dx^2\,dx^3$, the equation of fluid mass continuity is

$$\frac{\partial}{\partial t}[n^{(2)}\rho^{(2)*}\sqrt{G}] + \frac{\partial}{\partial x^i}\{n^{(2)}\rho^{(2)*}[\dot{u}_i^{(2)} - \dot{u}_i^{(1)}]\} = 0 \tag{3.15}$$

3.3.3 Balance of Momentum of the Fluid Phase

Consider the elementary parallelopiped that is rectangular in the reference configuration and is transformed into a skew parallelopiped in the current configuration (Figure 4).

Let $-t_1^{(2)}$ denote the stress vector of the fluid phase acting normal to the surface formed by the vectors $G_2\,dx^2$ and $G_3\,dx^3$. The net force due to this stress across the surface is, noting (A.132) and (A.142);

$$-t_1^{(2)}\sqrt{GG^{11}}\,dx^2\,dx^3 = T_1^{(2)}\,dx^2\,dx^3 \tag{3.16}$$

The internal forces on the six faces of the parallelopiped then are;

$$\begin{aligned}
&-T_1^{(2)}\,dx^2\,dx^3, \quad T_1^{(2)}\,dx^2\,dx^3 + \frac{\partial}{\partial x^1}T_1^{(2)}\,dx^1\,dx^2\,dx^3 \\
&-T_2^{(2)}\,dx^1\,dx^3, \quad T_2^{(2)}\,dx^1\,dx^3 + \frac{\partial}{\partial x^2}T_2^{(2)}\,dx^1\,dx^2\,dx^3 \\
&-T_3^{(2)}\,dx^1\,dx^2, \quad T_3^{(2)}\,dx^1\,dx^2 + \frac{\partial}{\partial x^3}T_3^{(2)}\,dx^1\,dx^2\,dx^3
\end{aligned} \tag{3.17}$$

Similarly the net body forces, inertial forces and viscous coupling forces, respectively, acting over the deformed volume $\sqrt{G}\,dx^1\,dx^2\,dx^3$ are;

$$[\rho^{(2)}F_1^{(2)},\ \rho^{(2)}F_2^{(2)},\ \rho^{(2)}F_3^{(2)}]\ \sqrt{G}\,dx^1\,dx^2\,dx^3 \tag{3.18}$$

$$[-\rho^{(2)}f_1^{(2)},\ -\rho^{(2)}f_2^{(2)},\ -\rho^{(2)}f_3^{(2)}]\ \sqrt{G}\,dx^1\,dx^2\,dx^3 \tag{3.19}$$

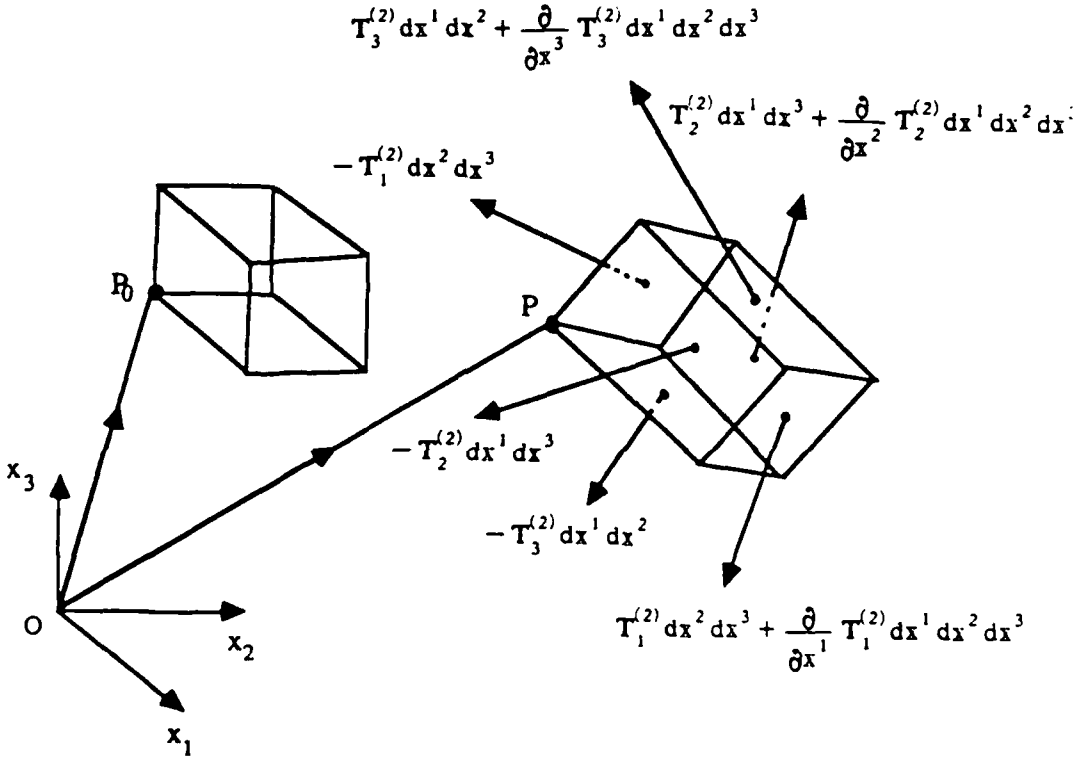

Figure 4: Fluid Equilibrium in the Deformed State

$$\{-D(v_1^{(2)}-v_1^{(1)}),\ -D(v_2^{(2)}-v_2^{(1)}),\ -D(v_3^{(2)}-v_3^{(1)})\}\ \sqrt{G}\,dx^1\,dx^2\,dx^3 \tag{3.20}$$

Summing up the forces and setting the total equal to zero for equilibrium,

$$\frac{\partial}{\partial x^i}T_i^{(2)}+\sqrt{G}\,\rho^{(2)}F^{(2)}-\sqrt{G}\,\rho^{(2)}f^{(2)}-\sqrt{G}\,D[v^{(2)}-v^{(1)}]=0 \tag{3.21}$$

Upon use of (A.141), and rearranging

$$\frac{1}{\sqrt{G}}\frac{\partial}{\partial x^i}[\sqrt{G}\,\tau^{(2)ij}G_j]+\rho^{(2)}F^{(2)}=\rho^{(2)}f^{(2)}+D(v^{(2)}-v^{(1)}) \tag{3.22}$$

Recalling (A.110), (A.111), (A.112) and (A.113) along with (A.143) gives

$$\tau^{(2)ij}{}_{|i}+\rho^{(2)}F^{(2)j}=\rho^{(2)}f^{(2)j}+D[v^{(2)j}-v^{(1)j}] \tag{3.23}$$

Alternatively, using (A.114) one can refer the quantities in (3.22) to the reference state C_ψ and write

$$\frac{\partial}{\partial x^i}[\sqrt{G}\,\tau^{(2)ij}z_{m,j}e_m]+\sqrt{G}\,\rho^{(2)}F_m^{(2)}e_m=\sqrt{G}\,\rho^{(2)}\ddot{u}_m^{(2)}e_m+\sqrt{G}\,D(\dot{u}_m^{(2)}-\dot{u}_m^{(1)})e_m \tag{3.24}$$

which gives, by (A.150) and (A.151),

$$[s^{(2)ij}z_{m,j}]_{,i}+\sqrt{G}\,\rho^{(2)}F_m^{(2)}=\sqrt{G}\,\rho^{(2)}\ddot{u}_m^{(2)}+\sqrt{G}\,D(\dot{u}_m^{(2)}-\dot{u}_m^{(1)}) \tag{3.25}$$

or

$$[S_m^{(2)i}]_{,i}+\sqrt{G}\,\rho^{(2)}F_m^{(2)}=\sqrt{G}\,\rho^{(2)}\ddot{u}_m^{(2)}+\sqrt{G}\,D(\dot{u}_m^{(2)}-\dot{u}_m^{(1)}) \tag{3.26}$$

For isotropic fluid,

$$S_m^{(2)i}=\pi\,\delta_m^i \tag{3.27}$$

Then (3.26) gives,

$$\pi_{,m}+\sqrt{G}\,\rho^{(2)}F_m^{(2)}=\sqrt{G}\,\rho^{(2)}\ddot{u}_m^{(2)}+\sqrt{G}\,D(\dot{u}_m^{(2)}-\dot{u}_m^{(1)}) \tag{3.28}$$

3.3.4 Balance of Momentum of the Fluid-Saturated Solid

Considering the reference set of solid particles in the current configuration of the deformed parallelopiped Figure 5, let $-\mathbf{t}_1$ denote the total stress vector acting on the strained body per unit area formed by the vectors $\mathbf{G}_2 dx^2$ and $\mathbf{G}_3 dx^3$. The net force across this surface using (A.142) is,

$$-\mathbf{T}_1 dx^2 dx^3 = -t_1 \sqrt{GG^{11}}\, dx^2 dx^3 \tag{3.29}$$

The other quantities viz. $\mathbf{T}_2$ and $\mathbf{T}_3$ are defined likewise by cyclic permutation and are shown in Figure 5. The forces on the six bounding surfaces are:

$$\begin{aligned}
&-\mathbf{T}_1 dx^2 dx^3, \quad \mathbf{T}_1 dx^2 dx^3 + \frac{\partial}{\partial x^1}\mathbf{T}_1 dx^1 dx^2 dx^3 \\
&-\mathbf{T}_2 dx^1 dx^3, \quad \mathbf{T}_2 dx^1 dx^3 + \frac{\partial}{\partial x^2}\mathbf{T}_2 dx^1 dx^2 dx^3 \\
&-\mathbf{T}_3 dx^1 dx^2, \quad \mathbf{T}_3 dx^1 dx^2 + \frac{\partial}{\partial x^3}\mathbf{T}_3 dx^1 dx^2 dx^3
\end{aligned} \tag{3.30}$$

For $\mathbf{F}^{(1)} = \mathbf{F}^{(2)} = \mathbf{F}$ the body forces and inertial forces acting over the deformed volume $\sqrt{G}\, dx^1 dx^2 dx^3$ can be expressed as,

$$[\rho \mathbf{F}_1,\ \rho \mathbf{F}_2,\ \rho \mathbf{F}_3]\ \sqrt{G}\, dx^1 dx^2 dx^3 \tag{3.31}$$

and

$$[-\{\rho^{(1)}\mathbf{f}_1^{(1)} + \rho^{(2)}\mathbf{f}_1^{(2)}\},\ -\{\rho^{(1)}\mathbf{f}_2^{(1)} + \rho^{(2)}\mathbf{f}_2^{(2)}\},\ -\{\rho^{(1)}\mathbf{f}_3^{(1)} + \rho^{(2)}\mathbf{f}_3^{(2)}\}]\sqrt{G}\, dx^1 dx^2 dx^3 \tag{3.32}$$

Summing up the forces, we have,

$$\frac{\partial}{\partial x^i}\mathbf{T}_i + \sqrt{G}\,\rho \mathbf{F} = \sqrt{G}[\rho^{(1)}\mathbf{f}^{(1)} + \rho^{(2)}\mathbf{f}^{(2)}] \tag{3.33}$$

Using (A.141) in (3.33)

$$\frac{1}{\sqrt{G}}\frac{\partial}{\partial x^i}[\sqrt{G}\,\tau^{ij}\mathbf{G}_j] + \rho \mathbf{F} = \rho^{(1)}\mathbf{f}^{(1)} + \rho^{(2)}\mathbf{f}^{(2)} \tag{3.34}$$

Recalling (A.62), and (A.110) through (A.113),

$$\tau^{ij}|_i + \rho F^j = \rho^{(1)} f^{(1)j} + \rho^{(2)} f^{(2)j} \tag{3.35}$$

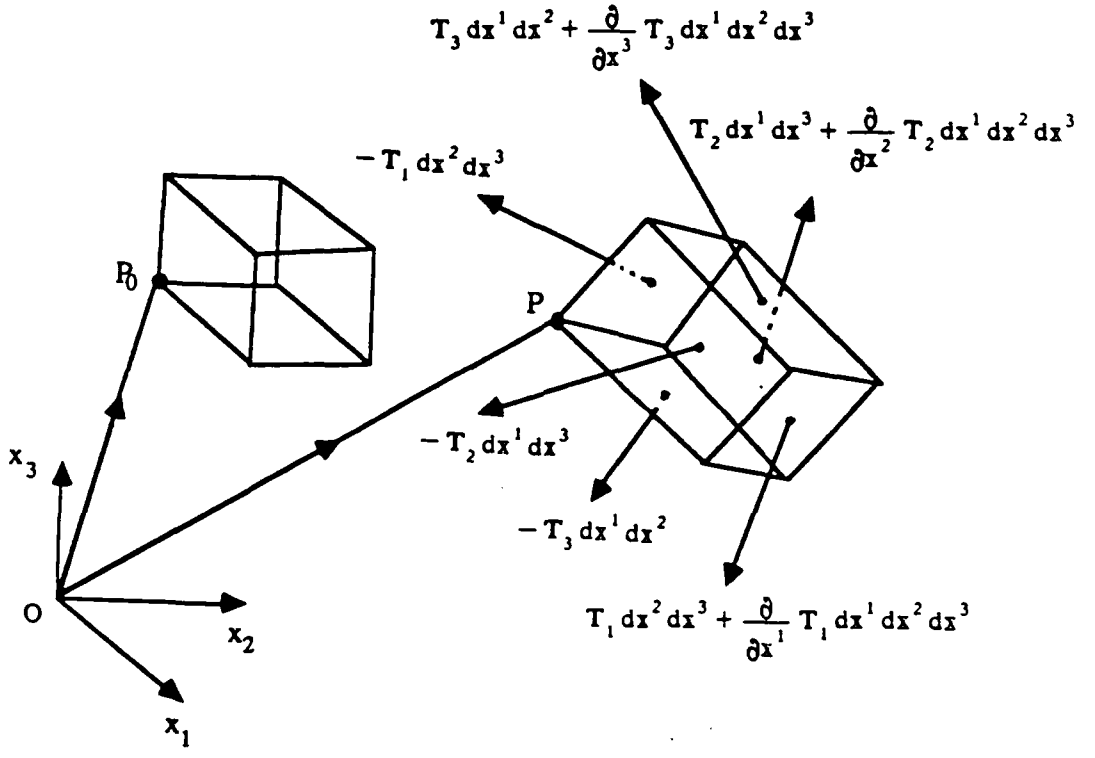

Figure 5: Equilibrium of the Fluid-Saturated Reference Volume in the Current Configuration

Referring quantities in (3.34) to the reference state C_0 and using (A.150) and (A.151), two alternative forms of (3.34) are,

$$[s^{ij} z_{m,j}]_{,i} + \sqrt{G}\,\rho\,\hat{F}_m = \sqrt{G}\,\rho^{(1)} \overset{\cdot\cdot}{u}{}_m^{(1)} + \sqrt{G}\,\rho^{(2)} \overset{\cdot\cdot}{u}{}_m^{(2)} \tag{3.36}$$

and

$$[S^i_m]_{,i} + \sqrt{G}\,\rho\,\hat{F}_m = \sqrt{G}\,\rho^{(1)} \overset{\cdot\cdot}{u}{}_m^{(1)} + \sqrt{G}\,\rho^{(2)} \overset{\cdot\cdot}{u}{}_m^{(2)} \tag{3.37}$$

3.3.5 Balance of Angular Momentum of the Fluid Saturated Solid

In absence of body couples, the angular moments of these forces with respect to the deformed axes along G_i are given by,

$$\begin{aligned}
&-(T_1 \times R)\,dx^2\,dx^3, \quad (T_1 \times R)\,dx^2\,dx^3 + \frac{\partial}{\partial x^1}(T_1 \times R)\,dx^1\,dx^2\,dx^3 \\
&-(T_2 \times R)\,dx^1\,dx^3, \quad (T_2 \times R)\,dx^1\,dx^3 + \frac{\partial}{\partial x^2}(T_2 \times R)\,dx^1\,dx^2\,dx^3 \\
&-(T_3 \times R)\,dx^1\,dx^2, \quad (T_3 \times R)\,dx^1\,dx^2 + \frac{\partial}{\partial x^3}(T_3 \times R)\,dx^1\,dx^2\,dx^3
\end{aligned} \tag{3.38}$$

For body forces and inertial forces the angular moments are, respectively,

$$[\rho F_1 \times R,\ \rho F_2 \times R,\ \rho F_3 \times R]\ \sqrt{G}\,dx^1\,dx^2\,dx^3 \tag{3.39}$$

and

$$\begin{aligned}
&[-\{\rho^{(1)} f_1^{(1)} + \rho^{(2)} f_1^{(2)}\},\ -\{\rho^{(1)} f_2^{(1)} + \rho^{(2)} f_2^{(2)}\},\ -\{\rho^{(1)} f_3^{(1)} + \rho^{(2)} f_3^{(2)}\}] \\
&\qquad \times R\ \sqrt{G}\,dx^1\,dx^2\,dx^3
\end{aligned} \tag{3.40}$$

Summing up the moments,

$$\frac{\partial}{\partial x^i}(T_i \times R) + (\rho F \times R)\sqrt{G} - \{\rho^{(1)} f^{(1)} + \rho^{(2)} f^{(2)}\} \times R\ \sqrt{G} = 0 \tag{3.41}$$

or, by (A.38) and rearrangement of terms

$$\left[\frac{\partial T_i}{\partial x^i} + \sqrt{G}\,\rho F - \sqrt{G}\{\rho^{(1)} f^{(1)} + \rho^{(2)} f^{(2)}\}\right] \times R + T_i \times G_i = 0 \tag{3.42}$$

Noting (3.33) and (3.42)

$$\mathbf{T}_i \times \mathbf{G}_i = 0 \tag{3.43}$$

Using (A.141), this gives

$$\sqrt{G}\,\tau^{ij}\mathbf{G}_j \times \mathbf{G}_i = 0 \tag{3.44}$$

or, equivalently;

$$\epsilon_{ijk}\,\tau^{ij} = 0 \tag{3.45}$$

which is same as

$$\tau^{ij} = \tau^{ji} \tag{3.46}$$

Further, in view of (A.103),

$$s^{ij} = s^{ji} \tag{3.47}$$

The bulk stress tensors, τ^{ij} and s^{ij}, are symmetric. This is in line with Green's [64] assertion that the partial stresses need not be symmetric but the total (bulk) stress is symmetric.

3.4 SOME SPECIALIZATIONS

3.4.1 Specialization to One-Dimensional Problem

The direction x_1 is referred to simply as x and the associated quantities are denoted by a super- or sub-script x.

a). Kinematical Quantities

From (A.86) and (A.87),

$$z = z(x, \tau) \tag{3.48}$$

and

$$x(\tau = 0) = a \tag{3.49}$$

For the motion to be possible, from (A.5),

$$|\frac{\partial z}{\partial x}| > 0 \tag{3.50}$$

The position vectors of points P_0 in C_0 and P in C are, respectively, ((A.77) and (A.78))

$$\mathbf{r} = x\,\mathbf{e} = a\,\mathbf{e} \tag{3.51}$$

$$\mathbf{R} = z\,\mathbf{e} \tag{3.52}$$

The displacement vector, $\mathbf{u}$, is (A.79)

$$\mathbf{u} = \mathbf{R} - \mathbf{r} = u\,\mathbf{e} \tag{3.53}$$

$$u = z - x = z - a \tag{3.54}$$

The base vectors, G_x, G^x and metric tensors G_{xx}, G^{xx} may be defined for the system x in the body at time t. From (A.97) through (A.99), we have in one-dimension,

$$G_x = \mathbf{R}_{,x} = \frac{\partial z}{\partial x}\,\mathbf{e} = (1 + \frac{\partial u}{\partial x})\,\mathbf{e} \tag{3.55}$$

$$G^x = \frac{\partial x}{\partial z}\,e \tag{3.56}$$

$$G_{xx} = G_x \cdot G_x = \frac{\partial z}{\partial x}\,\frac{\partial z}{\partial x} = (1 + \frac{\partial u}{\partial x})^2 = 1 + 2\,\frac{\partial u}{\partial x} + (\frac{\partial u}{\partial x})^2 \tag{3.57}$$

$$G^{xx} = \frac{\partial x}{\partial z}\,\frac{\partial x}{\partial z} \tag{3.58}$$

The line elements are given by (A.101) and (A.102),

$$ds^2 = G_{xx}\,dx\,dx \tag{3.59}$$

$$ds_0^2 = dx\,dx \tag{3.60}$$

The strain tensor, using (A.100) is,

$$\gamma_{xx} = \frac{1}{2}(G_{xx} - 1) = \frac{\partial u}{\partial x} + \frac{1}{2}\,\frac{\partial u}{\partial x}\,\frac{\partial u}{\partial x} \tag{3.61}$$

The changes in volume are obtained from (A.123) and (A.126) as,

$$dV_0 = dx \tag{3.62}$$

$$dV = \sqrt{G}\,dV_0 \tag{3.63}$$

where,

$$G = |G_{xx}| = |(1+\frac{\partial u}{\partial x})^2| = (1 + \frac{\partial u}{\partial x})^2 = (\frac{\partial z}{\partial x})^2 \tag{3.64}$$

(3.63) and (3.64) give

$$dV = (1+\frac{\partial u}{\partial x})\,dx \tag{3.65}$$

The expressions for velocity and acceleration derived from (A.110) through (A.123) for one-dimension are,

$$\mathbf{v} = \dot{u}\,\mathbf{e} = v^x G_x = v_x G^x \tag{3.66}$$

$$\mathbf{f} = \ddot{u}\,\mathbf{e} = f^x G_x = f_x G^x \tag{3.67}$$

b). Mass continuity of the solid.

From (3.7)

$$\rho_0^{(1)*} n_0^{(1)} = \sqrt{G}\,\rho^{(1)*} n^{(1)} \tag{3.68}$$

Using (3.64), mass continuity in one-dimension

$$\rho_0^{(1)*} n_0^{(1)} = \frac{\partial z}{\partial x}\,\rho^{(1)*} n^{(1)} \tag{3.69}$$

This expression is the same as Gibson's [55]

c). Mass continuity of the fluid.

From (3.15)

$$\frac{\partial}{\partial t}[n^{(2)}\rho^{(2)*}\sqrt{G}] + \frac{\partial}{\partial x}\{n^{(2)}\rho^{(2)*}[\dot{u}^{(2)} - \dot{u}^{(1)}]\} = 0 \tag{3.70}$$

which, upon use of (3.64), is

$$\frac{\partial}{\partial t}[n^{(2)}\rho^{(2)*}\frac{\partial z}{\partial x}] + \frac{\partial}{\partial x}\{n^{(2)}\rho^{(2)*}[\dot{u}^{(2)} - \dot{u}^{(1)}]\} = 0 \tag{3.71}$$

This is the same as Gibson's equation [55].

d). Momentum balance of the fluid.

(3.28), for one-dimensional analysis, using (3.64) is;

$$\frac{\partial \pi^{*}}{\partial x} + \frac{\partial z}{\partial x}\rho^{(2)*}\hat{F}_{x}^{(2)} = \frac{\partial z}{\partial x}\rho^{(2)*}\ddot{u}^{(2)} + \frac{\partial z}{\partial x}\frac{\mu}{\kappa}n^{(2)}(\dot{u}^{(2)} - \dot{u}^{(1)}) \tag{3.72}$$

If the inertia term is neglected, Gibson's [55] equation for quasi-static analysis is recovered viz.

$$\frac{\partial \pi^{*}}{\partial x} + \frac{\partial z}{\partial x}\rho^{(2)*}\hat{F}_{x}^{(2)} = \frac{\partial z}{\partial x}\frac{\mu}{\kappa}n^{(2)}(\dot{u}^{(2)} - \dot{u}^{(1)}) \tag{3.73}$$

e). Momentum balance of the fluid-saturated solid.

Recalling (3.64), for one-dimension, (3.37) is

$$[S^{x}_{x}]_{,x} + \frac{\partial z}{\partial x}\rho\hat{F}_{x} = \frac{\partial z}{\partial x}\rho^{(1)*}\ddot{u}^{(1)} + \frac{\partial z}{\partial x}\rho^{(2)}\ddot{u}^{(2)} \tag{3.74}$$

Ignoring the inertial term, we recover Gibson's [55]. equation of motion for the bulk viz.,

$$\frac{\partial S^{x}_{x}}{\partial x} + \rho\hat{F}_{x}\frac{\partial z}{\partial x} = 0 \tag{3.75}$$

3.4.2 Small deformation Theory

Biot's [17,19] equations for small deformation theory are embedded in the general theory presented in this work as a specialization. Assuming small strain, explicit forms of continuity equations are not required as the changes in density are small. All quantities are referred to the initial state with rectangular cartesian system as a frame of reference. In that case, the distinction between the contravariant and covariant components dispppears. The kinematical relations in (3.1) and (3.2) reduce to

$$\gamma_{ij}^{(1)} = E_{ij}^{(1)} = \frac{1}{2}[u_{i,j}^{(1)} + u_{j,i}^{(2)}] \tag{3.76}$$

The momentum balance equations in terms of the bulk stress t_{ij} and the partial pressure π are obtained from (3.37) and (3.26), respectively, as

$$t_{ij,j} + \rho F_i = \rho^{(1)} \ddot{u}_i^{(1)} + \rho^{(2)} \ddot{u}_i^{(2)} \tag{3.77}$$

$$\pi_{,i} + \rho^{(2)} F_i = \rho^{(2)} \ddot{u}_i^{(2)} + D[\dot{u}_i^{(2)} - \dot{u}_i^{(1)}] \tag{3.78}$$

which is often also written in the form;

$$\pi^*_{,i} + \rho^{(2)*} F_i = \rho^{(2)*} \ddot{u}_i^{(2)} + \frac{\mu}{\kappa} n^{(2)} [\dot{u}_i^{(2)} - \dot{u}_i^{(1)}] \tag{3.79}$$

The above equations are the same as in one formulaion of Biot's theory. Subtracting (3.78) from (3.77), an equilibrium equation in terms of the partial solid stress is obtained viz.

$$t^{(1)}_{ij,j} + \rho^{(1)} F_i = \rho^{(1)*} \ddot{u}_i^{(1)} - \frac{\mu}{\kappa} n^{(2)} n^{(2)} [\dot{u}_i^{(2)} - \dot{u}_i^{(1)}] \tag{3.80}$$

Comparing with Biot's [17,18] equations, (3.79) and (3.80) do not have the mass coupling terms.

3.5 CONSTITUTIVE RELATIONS

The issue of defining mechanical quantities for which constitutive relationships need to be defined has been discussed in Section II and in the technical report listed as item 1.2 in Appendix B. The dynamical theory summarized in this section is based on studying the movement of a connected set of non-interpenetrating particles. In this theory, the constitutive equations are required only for the partial stresses and the diffusive resistance. Porosity is a quantity directly related to the deformation of the set and need not be treated as an additional variable. The relative movement between the pore-water and the reference set of soil particles would apparently be the principal kinematical variable related to the interaction force. For linear theory this relationship would reduce to d'Arcy's rule. The stresses in the reference set of particles must be described in convected coordinates just as the deformation and defromation rates are.

For the case of rate-independent materials, a theory for a single elastic-plastic material was presented by Ayoub [8]. He used the Cauchy stress as the mechanical variable. He showed that, for large deformations, the difference between the conventional description of stress/strain relaions using quantities referred to the original configuration and the correct description proposed by him would be quite significant. The procedures and descriptions suggested by Ayoub can be easily generalized to admit possible coupling between the partial soil stresses and the fluid pressures. There is apparent need for the development of data on the behavior of saturated soils under large deformations to define the nature of the constitutive relations. Morland's [103] proposal that the constitutive equations for effective stresses in the porous material be assumed to have the same form as that for the intrinsic material appears to be attractive but needs verification. The distinction between the partial stress and the effective stress would allow for the possible coupling between the constitutive equations for the soil and the pore-water.

Section IV

SOLUTION PROCEDURES

4.1 INTRODUCTION

The solution procedures for the initial value problem of dynamic response of soil masses can be classed into the following groups.

1. Exact Solutions
2. Semi-Discrete Solution Procedures
3. Finite Element Solutions

Exact solutions were developed for the linearized version neglecting mass and constitutive couplings and assuming that the water was completely free to move relative to the soil. This essentially implied a specialization to Biot's theory. The exact solutions described in items 1.14, 1.15, 2.7, 2.8, 3.5 in Appendix B and the semi-discrete methods described in items 1.8 and 4.2 of the same Appendix were based on this theory. For the purpose of numerical solution (items 1.5, 1.6, 1.10, 1.12, 1.13, 1.17, 2.3, 2.4, 3.3, 3.4, 4.1 in Appendix B), nonlinearity and couplings could be accomodated to a certain extent. In this section we describe briefly the results of the research under each of the three headings.

4.2 EXACT SOLUTIONS

4.2.1 Introduction

Exact solutions to Biot's equations of dynamics of fluid-saturated porous media were obtained by Biot [17-19]. Later Deresiewicz [40], Chakraborty [33], and Garg [50] obtained solutions for various boundary conditions. In the present research the work was extended and computer codes for numerical solution were tested against these exact solutions. Items 1.14, 1.17, 2.7, 2.8, and 3.5 in Appendix B contain details of this development. The specific items of research included the following:

a). Garg's fundamental solution for the problem of one-dimensional wave propagation in fluid-saturated media was integrated to develop solutions for several cases of surface loading of a saturated soil column of infinite extent. [Items 1.14 and 2.7, Appendix B].

b). In order to obtain a solution to the problems of "strong coupling" "weak coupling" Garg had made certain assumptions. These assumptions were carefully investigated. [Item 3.5, Appendix B].

c). Solutions to Biot's equations of wave propagation involving sudden changes in excitation were developed by separating the propagation of the singularity from the diffusive process. These solutions were extended to some two-dimensional cases. [Item 1.15 and 2.8, Appendix B].

In the following paragraphs we summarize some of the results of these investigations.

4.2.2 Garg's Solution

Figure 6(b) shows the load for which Garg obtained an exact solution and the four load cases for which additional solutions were obtained as part of the present research. Garg [13] wrote Biot's equations, for the one-dimensional problem, without inertial mass coupling in the form;

$$\rho^{(1)}\ddot{u} = a u_{,11} + c U_{,11} - D(\dot{u} - \dot{U}) \tag{4.1}$$

$$\rho^{(2)}\ddot{U} = c u_{,11} + b U_{,11} + D(\dot{u} - \dot{U}) \tag{4.2}$$

where u, U are the displacements of the solid and fluid respectively. Garg [50] assumed the displacements of the constituents to be specified on the end $x = 0$ as

$$\left.\begin{aligned} u(0,t) &= f(t) \\ U(0,t) &= g(t) \end{aligned}\right\} \tag{4.3}$$

Only the conditions at $x = 0$ were needed as the column was assumed to be of infinite extent. The initial conditions were;

$$\begin{aligned} u(x,0) &= u_0(x) \\ U(x,0) &= U_0(x) \\ \dot{u}(x,,0) &= \dot{u}_0(x) \\ \dot{U}(x,0) &= \dot{U}_0(x) \end{aligned} \tag{4.4}$$

In order to solve the wave equations, (4.1) and (4.2) were differentiated with respect to the time variable. For homogeneous initial conditions, the boundary conditions on the velocities of the constituents, assuming they move together at this point, were

$$\dot{u}(0,t) = \dot{U}(0,t) = \phi(t) \tag{4.5}$$

Applying the Laplace transform to the time derivatives of (4.1) and (4.2), and denoting the velocities of the solid and the fluid by v, V,

$$\rho^{(1)} p^2 \bar{v} = a \frac{\partial^2 \bar{v}}{\partial x^2} + c \frac{\partial^2 \bar{V}}{\partial x^2} + D p (\bar{V} - \bar{v}) \tag{4.6}$$

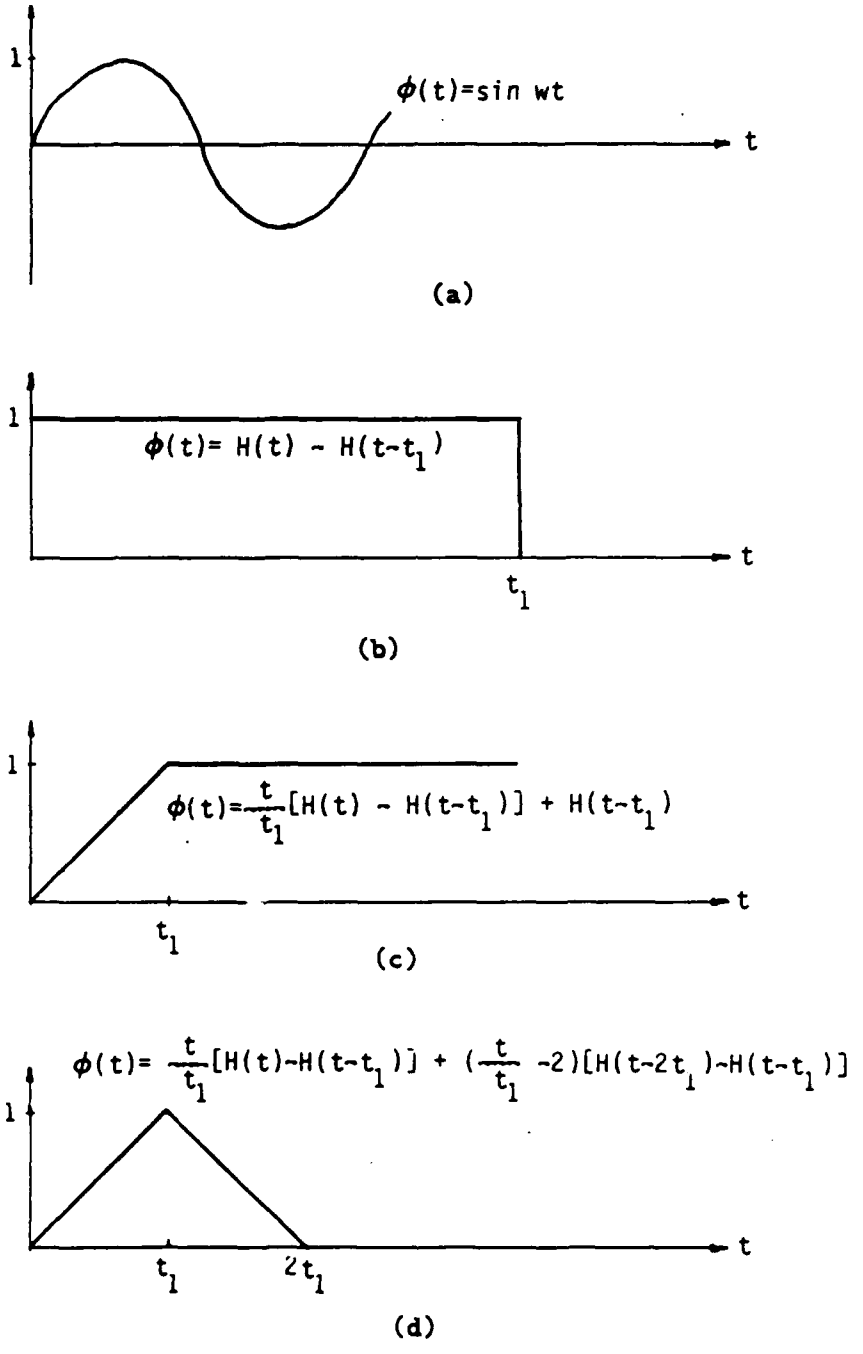

Figure 6: Velocity Excitations Applied at the Boundary

$$\rho^{(2)} p^2 \bar{V} = c \frac{\partial^2 \bar{v}}{\partial x^2} + b \frac{\partial^2 \bar{V}}{\partial x^2} - Dp(\bar{V} - \bar{v}) \tag{4.7}$$

where

$$L[\dot{u}(x,t), \dot{U}(x,t)] = [\bar{v}(x,p), \bar{V}(x,p)] \tag{4.8}$$

indicates Laplace transformation, and p is the transform parameter. Assuming the solution to have the form

$$\begin{Bmatrix} v \\ V \end{Bmatrix} = \begin{Bmatrix} A \\ B \end{Bmatrix} \exp(-\gamma x) \tag{4.9}$$

the characteristic equation is:

$$\nu p(C_0^2 \gamma^2 - p^2) - (C_+^2 \gamma^2 - p^2)(C_-^2 \gamma^2 - p^2) = 0 \tag{4.10}$$

where:

$$\begin{aligned} C_0^2 &= \frac{a + b + 2c}{\rho} \\ 2C_\pm^2 &= C_1^2 + C_2^2 \pm [(C_1^2 - C_2^2)^2 + 4C_{12}^2 C_{21}^2]^{1/2} \\ C_1^2 &= a/\rho^{(1)} \\ C_2^2 &= b/\rho^{(2)} \\ C_{12}^2 &= c/\rho^{(1)} \\ C_{21}^2 &= c/\rho^{(2)} \\ \nu &= \frac{D\rho}{\rho^{(1)}\rho^{(2)}} \end{aligned} \tag{4.11}$$

C_0 is the wave velocity when the saturated medium acts as a single material and $C_\pm$ are the wave velocities when no viscous coupling exists. (4.10) has four roots, viz.,

$$\gamma_{1,2}^2 = M_1(p) \pm [M_1^2(p) - M_2(p)]^{1/2} \tag{4.12}$$

where

$$2M_1(p) = (1/C_-^2 + 1/C_+^2)p^2 + \nu p C_0^2/(C_-^2 C_+^2)$$

$$M_2(p) = \frac{p^3(p+\nu)}{C_+^2 C_-^2}$$

Thus, the general solution can be written as

$$\left.\begin{aligned} \bar{v}(x,p) &= A_1 \exp(-\gamma_1 x) + A_2 \exp(-\gamma_2 x) \\ \bar{V}(x,p) &= B_1 \exp(-\gamma_1 x) + B_2 \exp(-\gamma_2 x) \end{aligned}\right\} \quad (4.13)$$

Here A_1, A_2, B_1 and B_2 are functions of p and must be determined by the following boundary conditions and compatibility equations.

$$\begin{aligned} A_1 + A_2 &= \bar{\phi}(p) \\ B_1 + B_2 &= \bar{\phi}(p) \\ [p^2 - C_1^2\gamma_1^2 + Dp/\rho^{(1)}]A_1 &= [C_{12}^2\gamma_1^2 + Dp/\rho^{(1)}]B_1 \\ [p^2 - C_1^2\gamma_2^2 + Dp/\rho^{(1)}]A_2 &= [C_{12}^2\gamma_2^2 + Dp/\rho^{(1)}]B_2 \end{aligned} \quad (4.14)$$

Hence,

$$\left.\begin{aligned} A_1 &= \bar{\phi}(p)(1-S_2)/(S_1-S_2) \\ A_2 &= \bar{\phi}(p)(S_1-1)/(S_1-S_2) \\ B_1 &= S_1 A_1 \\ B_2 &= S_2 A_2 \end{aligned}\right\} \quad (4.15)$$

where

$$\begin{aligned} S_1 &= (p^2 - C_1^2\gamma_1^2 + Q)/(C_{12}^2\gamma_1^2 + Q) \\ S_2 &= (p^2 - C_1^2\gamma_2^2 + Q)/(C_{12}^2\gamma_2^2 + Q) \\ Q &= \frac{Dp}{\rho^{(1)}} \end{aligned}$$

A general solution based on inverse transformation of (4.13) is not available. Two special cases were solved by Garg [50] For relatively small value of D, Garg approximated

the solutions of the characteristic equation (4.10) to the first order in D to get:

$$\gamma_1^2 = \frac{1}{C_+^2}(p^2 + 2\eta_1 p) = \frac{1}{C_+^2}[(p+\eta_1)^2 - \eta_1^2] \tag{4.16}$$

$$\gamma_2^2 = \frac{1}{C_-^2}(p^2 + 2\eta_2 p) = \frac{1}{C_-^2}[(p+\eta_2)^2 - \eta_2^2] \tag{4.17}$$

where

$$\eta_1 = \frac{\nu}{2}(C_+^2 - C_0^2)/(C_+^2 - C_-^2) \tag{4.18}$$

$$\eta_2 = \frac{\nu}{2}(C_0^2 - C_-^2)/(C_+^2 - C_-^2) \tag{4.19}$$

As D approaches zero, η_1, η_2 vanish, and the expressions for amplitudes in (4.15) reduce to;

$$\begin{aligned} A_1 &= A^* \bar{\phi}(p) \\ A_2 &= A_2^* \bar{\phi}(p) \\ B_1 &= B_1^* \bar{\phi}(p) \\ B_2 &= B_2^* \bar{\phi}(p) \end{aligned} \tag{4.20}$$

where

$$A_1^* = (C_1^2 - C_-^2 + C_{12}^2)/(C_+^2 - C_-^2)$$

$$B_1^* = (C_+^2 - C_1^2 + C_{21}^2)/(C_+^2 - C_-^2)$$

$$A_2^* = 1 - A_1^*, \qquad B_2^* = 1 - B_1^*$$

Garg termed this special case "weak" coupling. In evaluating A_1^*, B_1^*, he set $D = 0$, i.e., no coupling to get $\gamma_1 = p/C_+$ and $\gamma_2 = p/C_-$. This assumption to avoid dependence of the amplitudes on the transform parameter p made inversion of the solution possible, but is inconsistent with the approximation to get equations (4.15) and (4.16). Substituting these results into (4.13), the transformed solution for weak coupling was written as;

$$\begin{Bmatrix}\bar{v}(p)\\ \bar{V}(p)\end{Bmatrix} = \begin{Bmatrix}A_1^*\\ B_1^*\end{Bmatrix} \bar{\phi}(p) \exp[-(x/C_+)F_1] + \begin{Bmatrix}A_2^*\\ B_2^*\end{Bmatrix} \bar{\phi}(p) \exp[-(x/C_-)F_2] \tag{4.21}$$

where

$$F_1 = [(p+\eta_1)^2 - \eta_1^2]^{1/2}$$

$$F_2 = [(p+\eta_2)^2 - \eta_2^2]^{1/2}$$

Inversion of (4.21) gave

$$\begin{Bmatrix}\dot{u}(x,t)\\ \dot{U}(x,t)\end{Bmatrix} = \begin{Bmatrix}A_1^*\\ B_1^*\end{Bmatrix} [\exp(-\eta_1 t)\, \delta(t-\frac{x}{C_+}) + \frac{\eta_1 x}{C_+} \exp(-\eta_1 t)\, f_1(t) H(t-\frac{x}{C_+})] * \phi(t)$$

$$+ \begin{Bmatrix}A_2^*\\ B_2^*\end{Bmatrix} [\exp(-\eta_2 t)\, \delta(t-\frac{x}{C_-}) + \frac{\eta_2 x}{C_-} \exp(-\eta_2 t)\, f_2(t)\, H(t-\frac{x}{C_-})] * \phi(t) \tag{4.22}$$

where

$$f_1(t) = \frac{I_1[\eta_1 (t^2 - x^2/C_+^2)^{1/2}]}{(t^2 - x^2/C_+^2)^{1/2}}$$

$$f_2(t) = \frac{I_1[\eta_2 (t^2 - x^2/C_-^2)^{1/2}]}{(t^2 - x^2/C_-^2)^{1/2}}$$

Here, $H(t)$ is the Heaviside step function, $\delta(t)$ is the Dirac delta and I_1 is the modified Bessel function of first kind of order one. The symbol * denotes convolution product. In evaluating the amplitudes no viscous coupling was assumed while effect of viscous coupling approximated to the first order was retained in the exponentially decaying terms. If, for consistency, we set $D=0$ in the exponential decay terms, the transformed solution (4.21) would reduce to:

$$\begin{Bmatrix}\bar{v}(p)\\ \bar{V}(p)\end{Bmatrix} = \begin{Bmatrix}A_1^*\\ B_1^*\end{Bmatrix} \bar{\phi}(p) \exp[-(x\,p/C_+)] + \begin{Bmatrix}A_2^*\\ B_2^*\end{Bmatrix} \bar{\phi}(p) \exp[-(x\,p/C_-)] \tag{4.23}$$

The inverse is:

$$\begin{Bmatrix}\dot{u}(x,t)\\ \dot{U}(x,t)\end{Bmatrix} = \begin{Bmatrix}A_1^*\\ B_1^*\end{Bmatrix} \delta(t-x/C_+) * \phi(t) + \begin{Bmatrix}A_2^*\\ B_2^*\end{Bmatrix} \delta(t-x/C_-) * \phi(t) \tag{4.24}$$

This is the solution for no viscous coupling in which the solid and the fluid particles move independently.

As D goes to infinity, the characteristic equation (4.10) yields a single root:

$$\gamma = \frac{p}{C_0} \tag{4.25}$$

which corresponds to wave propagation with speed C_0 i.e., the mixture moves as a single material. For moderately large value of D, i.e, "strong" coupling, Garg [50] wrote the first order approximation of the characteristic root in 1/D as:

$$\gamma = \frac{p}{C_0}\left[\frac{1}{1+\theta p}\right] \tag{4.26}$$

where

$$\theta = -\frac{1}{2\nu}[C_+^2/C_0^2 - 1][C_-^2/C_0^2 - 1] \tag{4.27}$$

The expression for θ given in [50] is in error. (4.27) is the corrected form given by Garg [51]. (4.26) describes the motion of the mixture in which $\bar{v}$ and $\bar{V}$ are different in order 1/D. Hence, Garg [50] assumed:

$$\bar{v} = \bar{V} \tag{4.28}$$

Based on this approximation, the transformed solution was obtained, using equations (4.26) and (4.28) as:

$$\bar{v}(p) = \bar{\phi}(p)\left[\frac{xp}{C_0(1+\theta p)}\right] \tag{4.29}$$

or, equivalently:

$$\bar{v}(p) = \bar{\phi}(p)\exp\left[-\frac{x}{C_0\theta}\right]\exp\left[\frac{x}{C_0\theta^2(p+1/\theta)}\right] \tag{4.30}$$

The inverse is:

$$\dot{u}(x,t) = \exp\left[-\frac{x}{C_0\theta}\right]\phi(t)*$$

$$\left\{\frac{1}{\theta}\left(\frac{x}{C_0 t}\right)^{1/2} I_1\left[\frac{2}{\theta}\left(\frac{xt}{C_0}\right)^{1/2}\right] + \delta(t)\right\}\exp\left[-\frac{t}{\theta}\right] \tag{4.31}$$

4.2.3 Integration of Garg's Solution

Garg's solution (4.24), for "weak coupling", was integrated to obtain explicit solutions for four different velocity boundary conditions shown in Figure 6. These solutions are listed below. Details are given in item 1.14. of Appendix B.

a). Unit Box Function

The applied velocity boundary condition at $x = 0$ is

$$\phi(t) = H(t) - H(t-t_1) \tag{4.32}$$

where t_1 is the time at which the excitation is reduced to zero. Substitution into (4.21) gives

$$\begin{Bmatrix} \dot{u} \\ \dot{U} \end{Bmatrix} = \begin{Bmatrix} A_1^* \\ B_1^* \end{Bmatrix} \{ \exp[-\frac{\eta_1 x}{C_+}] + \frac{\eta_1 x}{C_+} \int_{x/C_+}^{t} \exp[-\eta_1 \tau] f_1(\tau) d\tau \}$$

$$\times H(t-\frac{x}{C_+}) - H(t-t_1-\frac{x}{C_+})$$

$$+ \begin{Bmatrix} A_2^* \\ B_2^* \end{Bmatrix} \{ \exp[-\frac{\eta_2 x}{C_-}] - \frac{\eta_2 x}{C_-} \int_{x/C_-}^{t} \exp[-\eta_2 \tau] f_2(\tau) d\tau \}$$

$$\times H(t-\frac{x}{C_-}) - H(t-t_1-\frac{x}{C_-}) \tag{4.33}$$

b). Sine Function

Assuming that the velocity specified on the boundary is harmonic; i.e.,

$$\phi(t) = \sin(\omega t) \tag{4.34}$$

where ω is the frequency, the corresponding solution is given by

$$\begin{Bmatrix} \dot{u} \\ \dot{U} \end{Bmatrix} = \begin{Bmatrix} A_1^* \\ B_1^* \end{Bmatrix} \{ \sin\omega(t-\frac{x}{C_+}) \exp[-\frac{\eta_1 x}{C_+}] + \frac{\eta_1 x}{C_+} [\sin\omega t \int_{x/C_+}^{t} f_1(\tau) \cos\omega t \, d\tau$$

$$- \cos\omega t \int_{x/C_+}^{t} f_1(\tau) \sin\omega t \, d\tau] \} H(t - x/C_+)$$

$$+ \begin{Bmatrix} A_2^* \\ B_2^* \end{Bmatrix} \{ \sin\omega(t-\frac{x}{C_-}) \exp[-\frac{\eta_2 x}{C_-}] + \frac{\eta_2 x}{C_-} [\sin\omega t \int_{x/C_-}^{t} f_2(\tau) \cos\omega t \, d\tau$$

$$- \cos\omega t \int_{x/C_-}^{t} f_2(\tau) \sin\omega t \, d\tau] \} H(t-x/C_-) \qquad (4.35)$$

c). Ramp Function

Velocity function specified as acting on the boundary is

$$\phi(t) = \frac{t}{t_1} [H(t) - H(t-t_1)] + H(t-t_1) \qquad (4.36)$$

The solution for this case is:

$$\begin{Bmatrix} \dot{u} \\ \dot{U} \end{Bmatrix} = \begin{Bmatrix} A_1^* \\ B_1^* \end{Bmatrix} \{ [\frac{1}{t_1} (t-\frac{x}{C_+}) \exp[-\frac{\eta_1 x}{C_+}]$$

$$+ \frac{\eta_1 x}{C_+} \int_{x/C_+}^{t} f_1(\tau) \frac{(t-\tau)}{t_1} \exp[-\eta_1 \tau] \, d\tau] H(t-x/C_+)$$

$$+ [\frac{1}{t_1} (t_1 - t + \frac{x}{C_+}) \exp[-\frac{\eta_1 x}{C_+}]$$

$$+ \frac{\eta_1 x}{C_+} \int_{x/C_+}^{t} f_1(\tau) (1 - \frac{t-\tau}{t_1} \exp[-\eta_1 \tau] \, d\tau] H(t-t_1-x/C_+) \}$$

$$+ \begin{Bmatrix} A_2^* \\ B_2^* \end{Bmatrix} \{ [\frac{1}{t_1} (t-\frac{x}{C_-}) \exp[-\frac{\eta_2 x}{C_-}]$$

$$+ \frac{\eta_2 x}{C_-} \int_{x/C_-}^{t} f_2(\tau) \frac{(t-\tau)}{t_1} \exp[-\eta_2 \tau] \, d\tau] H(t-x/C_-)$$

$$+ [\frac{1}{t_1} (t_1 - t + \frac{x}{C_-}) \exp[-\frac{\eta_2 x}{C_-}]$$

$$+ \frac{\eta_2 x}{C_-} \int_{x/C_-}^{t} f_2(\tau) (1 - \frac{t-\tau}{t_1} \exp[-\eta_1 \tau] \, d\tau] H(t-t_1-x/C_-) \} \qquad (4.37)$$

d). Spike Function

The excitation in this case may be expressed as

$$\phi(t) = \frac{t}{t_1}[H(t) - H(t-t_1)] + (\frac{t}{t_1} - 2)[H(t-2t_1) - H(t-t_1)] \qquad (4.38)$$

The solution for velocity is:

$$\begin{Bmatrix}\dot{u}\\ \dot{U}\end{Bmatrix} = \begin{Bmatrix}A_1^*\\ B_1^*\end{Bmatrix}\{[\frac{1}{t_1}(t-\frac{x}{C_+})\exp[-\frac{\eta_1 x}{C_+}] + \frac{\eta_1 x}{C_+}\int_{x/C_+}^{t} f_1(\tau)\frac{(t-\tau)}{t_1}\exp[-\eta_1\tau]\,d\tau]$$

$$\times [H(t-x/C_+) - H(t-t_1-x/C_+)] + [\frac{1}{t_1}(t-\frac{x}{C_+}-2t_1)\exp[-\frac{\eta_1 x}{C_+}]$$

$$+ \frac{\eta_1 x}{C_+}\int_{x/C_+}^{t} f_1(\tau)\frac{(t-\tau)}{t_1} - 2)\exp[-\eta_1\tau]\,d\tau]$$

$$\times [H(t-2t_1-x/C_+) - H(t-t_1-x/C_+)]\}$$

$$+ \begin{Bmatrix}A_2^*\\ B_2^*\end{Bmatrix}\{[\frac{1}{t_1}(t-\frac{x}{C_-})\exp[-\frac{\eta_2 x}{C_-}] + \frac{\eta_2 x}{C_-}\int_{x/C_-}^{t} f_2(\tau)\frac{(t-\tau)}{t_1}\exp[-\eta_2\tau]\,d\tau]$$

$$\times [H(t-x/C_-) - H(t-t_1-x/C_-)] + [\frac{1}{t_1}(t-\frac{x}{C_-}-2t_1)\exp[-\frac{\eta_2 x}{C_-}]$$

$$+ \frac{\eta_2 x}{C_-}\int_{x/C_-}^{t} f_2(\tau)\frac{(t-\tau)}{t_1} - 2)\exp[-\eta_2\tau]\,d\tau]$$

$$\times [H(t-2t_1-x/C_-) - H(t-t_1-x/C_-)]\} \qquad (4.39)$$

4.2.4 Evaluation of Garg's Approximations

To obtain exact inverses to the "weak" and the "strong" coupling problems, Garg [50] made some assumptions. Primarily these amounted tto neglecting the Laplace transform parameter p in comparison with D or its reciprocal depending upon whether D took on very large (strong coupling) or very small (weak coupling) values. The reasonableness of these assumptions was examined. As the range of values of the trans-

formed parameter p extends over the entire positive interval, it would appear improper to compare the parameter D, or its inverse, with p in terms of order of magnitude. However, if $C_+ = C_0 = C_-$, the solution given by (4.31) for strong coupling is correct. But, for that case, $\theta = 0$ and the solution reduces to the one for the case $D \to \infty$. This special case requires that the quantity

$$(C_1^2 - C_2^2)^2 + 4C_1 2^2 C_{21}^2$$

should vanish, i.e. $C_1 = C_2$ and $C_{12} = C_{21} = 0$. This in turn requires $a/\rho^{(1)} = b/\rho^{(2)}$ and $c = 0$, i.e. the only coupling in (4.6) and (4.7) is through the viscous coupling. Vanishing of c implies that the constitutive relations for the fluid and solid partial stresses are uncoupled.

For the case of weak coupling too, Garg used a linear approximation in D for roots of the characteristic equation; but for determination of the amplitudes, D was set equal to zero. If the same linearization is used for the amplitudes as well, the solution would be

$$\begin{aligned} A_1 &= -\bar{\phi}(p) J_1/F, & A_2 &= \bar{\phi}(p) J_2/F \\ B_1 &= \bar{\phi}(p) L_1/F, & B_2 &= \bar{\phi}(p) L_2/F \end{aligned} \tag{4.40}$$

where

$$J_1 = (C_{12}^2 \lambda_1 + D/\rho_0^{(1)}) - (p + \nu) Q_1 - \frac{C_1^2 + C_{12}^2}{C_-^2} D/\rho_0^{(1)}$$

$$J_2 = (C_{12}^2 \lambda_2 + D/\rho_0^{(1)}) - (p + \nu) Q_1 - \frac{C_1^2 + C_{12}^2}{C_+^2} D/\rho_0^{(1)}$$

$$L_1 = p + (p + \nu) Q_2 + (1 - \frac{C_1^2 + C_{12}^2}{C_-^2}) D/\rho_0^{(1)} - C_1^2 \lambda_1 - (C_1^2 + C_{12}^2) \lambda_2$$

$$L_2 = p + (p + \nu) Q_2 + (1 - \frac{C_1^2 + C_{12}^2}{C_+^2}) D/\rho_0^{(1)} - C_1^2 \lambda_2 - (C_1^2 + C_{12}^2) \lambda_1$$

$$F = [C_{12}^2 p + (C_1^2 + C_{12}^2) D/\rho_0^{(1)}] R_1 + C_{12}^2 R_2 \tag{4.41}$$

$$R_1 = (C_+^2 - C_0^2)/(C_+^2 C_-^2)$$

$$R_2 = [C_0^2(C_+^2 + C_-^2) - 2C_+^2 C_-^2]/[C_+^2 C_-^2 (C_+^2 - C_-^2)]$$

$$\lambda_{1,2} = \alpha_{1,2}^2/p$$

$$Q_1 = \frac{C_{12}^2 (C_1^2 + C_{12}^2)}{C_+^2 C_-^2}$$

$$Q_1 = \frac{C_1^2 (C_1^2 + C_{12}^2)}{C_+^2 C_-^2}$$

The amplitudes are dependent on p in a complicated fashion and an analytical inverse is not available. Of course, for $\nu \to 0$ the expressions are identical to those in [50]. To examine the applicability of Garg's solution, the amplitudes for two materials, i.e., the one used in [50] and a coarse sand with mechanical properties listed in Table 1 were evaluated. In the table, K, K_1, K_2 are, respectively, the bulk moduli of the porous solid, the nonporous solid and the fluid. μ' is the shear modulus of the nonporous solid. (4.40) gave for Garg's material

$$J_1 = -(0.2238\,p + 101.45)$$

$$J_2 = -(0.0044\,p + 1.455)$$

$$L_1 = -(0.1054\,p + 65.01)$$

$$L_2 = (0.1139\,p + 34.98)$$

$$F = (0.8906\,p + 5757.4)$$

and for coarse sand

$$J_1 = -(54.966\,p + 148004.4)$$

$$J_2 = -(0.283\,p + 752.9)$$

$$L_1 = -(1.4065\,p + 7386.2)$$

Table 1

Mechanical Properties Used in the Example

		$\rho_o^{(1)}$ (gm/cm^3)	$\rho_o^{(2)}$ (gm/cm^3)	f	μ_p (dyn/cm^2)	K (dyn/cm^2)	K_1 (dyn/cm^2)	K_2 (dyn/cm^2)	D (gm/cm^{3}sec)
Weak Coupling	Garg et al.	2.1812	0.18	0.18	9.9×10^{10}	1.18×10^{11}	3.6×10^{11}	2.2×10^{10}	21.89
	Coarse Sand	1.59	0.33	0.33	7.544×10^{8}	1.635×10^{8}	1.53×10^{11}	2.12×10^{8}	21.78
Strong Coupling	Garg et al.	2.1812	0.18	0.18	9.9×10^{10}	1.18×10^{11}	3.6×10^{11}	2.2×10^{10}	21.89×10^{6}
	Fine Sand	1.48	0.44	0.44	9.79×10^{8}	2.12×10^{9}	7.07×10^{10}	6.23×10^{9}	96.8×10^{6}

k/μ (cm^{3}sec/gm)	C_- (cm/sec)	C_o (cm/sec)	C_+ (cm/sec)	C_1 (cm/sec)	C_2 (cm/sec)	C_{12} (cm/sec)	C_{21} (cm/sec)
0.148×10^{-2}	0.12979×10^{6}	0.35485×10^{6}	0.35812×10^{6}	0.35531×10^{6}	0.13730×10^{6}	0.65221×10^{5}	0.22704×10^{6}
0.5×10^{-2}	0.45027×10^{4}	0.37523×10^{5}	0.40969×10^{5}	0.40966×10^{5}	0.46072×10^{4}	0.29668×10^{4}	0.65123×10^{4}
0.148×10^{-8}	0.12979×10^{6}	0.35485×10^{6}	0.35812×10^{6}	0.35531×10^{6}	0.13730×10^{6}	0.65221×10^{5}	0.22704×10^{6}
0.2×10^{-8}	0.38241×10^{5}	0.89762×10^{5}	0.94413×10^{5}	0.68877×10^{5}	0.75048×10^{5}	0.44911×10^{5}	0.82367×10^{5}

$$L_2 = (53.276\,p + 139865.6)$$

$$F = (1.897\,p + 5757.4)$$

The above expressions show that the contribution of the terms containing p is negligible in comparison with the constant terms unless p takes on extremely large values. We note further that for both the materials, the contribution J_2 of the second wave in the solid to the total response is relatively small. For the coarse sand the contribution L_1 of the first wave in the fluid is also relatively small.

Garg's approximate solution was hardly distinguishable from the numerical inverse of the exact transformed solution. It seems appropriate to conclude that Garg's approximate solution for weak coupling is acceptable for a short time range after sudden application of uniform velocity at the end of the column. For the case of strong coupling, it appears reasonable to set

$$\gamma = \frac{p}{C_0}(1-\delta) \tag{4.42}$$

for sufficiently large values of D. (4.42) can be rewritten as

$$C_0^2\gamma^2 - p^2 = p^2(\delta^2 - 2\delta) \tag{4.43}$$

and results in

$$C_+^2\gamma^2 - p^2 = p^2\left[\left(\frac{C_+^2}{C_0^2} - 1\right) + \frac{C_+^2}{C_0^2}(\delta^2 - 2\delta)\right] \tag{4.44}$$

$$C_-^2\gamma^2 - p^2 = p^2\left[\left(\frac{C_-^2}{C_0^2} - 1\right) + \frac{C_-^2}{C_0^2}(\delta^2 - 2\delta)\right] \tag{4.45}$$

Substituting these relations into (4.10),

$$-2\nu p^3 = p^4\left(\frac{C_+^2}{C_0^2} - 1\right)\left(\frac{C_-^2}{C_0^2} - 1\right) - 2\delta\left[\frac{C_-^2}{C_0^2}\left(\frac{C_+^2}{c_0^2} - 1\right) + \frac{C_+^2}{C_0^2}\left(\frac{C_-^2}{C_0^2} - 1\right)\right] + O(\delta^2) \tag{4.46}$$

where $O(\delta^2)$ represents terms of second order in δ. Thus, a first order approximation to δ is:

$$\delta = -\frac{p}{2\beta}\left(\frac{C_+^2}{C_0^2} - 1\right) \tag{4.47}$$

where

$$\beta = \nu - p\Delta \tag{4.48}$$

and

$$\Delta = \frac{C_-^2}{C_0^2}\left(\frac{C_+^2}{C_0^2} - 1\right) + \frac{C_+^2}{C_0^2}\left(\frac{C_-^2}{C_0^2} - 1\right)$$

For the above result to match Garg's [50], it is necessary to assume $\beta = \nu$, i.e., to neglect the terms which contain p. (4.48) gave

$$\beta = 131.6\times10^6 + 0.879785\,p$$

and for a fine sand

$$\beta = 285.41\times10^6 + 1.184847\,p$$

Garg's linearization of δ and the further approximation to obtain an analytical solution were seen to yield results of acceptable accuracy and form a proper basis for developments of solutions for other boundary conditions.

4.2.5 Wave Propagation in a Fluid-Saturated Soil Layer

During the present research, the concepts described above were extended to a finite soil column (elastic soil layer) and to independently specified boundary conditions for the two constituents. The solution process consisted of constructing singular fields which incorporate all discontinuities of the velocity fields and their first and second derivatives. This additive decomposition left twice continuously differentiable fields which satisfy coupled hyperbolic second order differential equations with continuous forcing terms. The results of the analysis were compared with numerical inversion of

the Laplace transform solutions and also with numerical solutions obtained by using the finite element method. Details of this research are documented in items 1.15 and 2.8 in Appendix B.

4.3 SEMI-DISCRETE SOLUTION

In order to separate the error contribution of the spatial and the temporal approximations, an eigenfunction approach to solution of spatially discretized equations of motion was developed. This was expected to provide a benchmark for evaluation of fully discretized time domain solution procedures. The studies showed the presence of a high frequency spurious oscillatory component related to the spatial mesh size. With refinement of the mesh, the lowest eigenvalues of the Laplace transform solution were found to converge. A Ritz vector type approach in which the base vectors are related to the excitation could possibly improve the accuracy of the solution.

The procedure employed consisted of a finite element discretization of the coupled equations of motion to get the matrix equations

$$\begin{bmatrix} M_{ss} & M_{sf} \\ M_{sf}^T & M_{ff} \end{bmatrix} \begin{Bmatrix} \ddot{u} \\ \ddot{w} \end{Bmatrix} + \begin{bmatrix} C_{ss} & 0 \\ 0 & C_{ff} \end{bmatrix} \begin{Bmatrix} \dot{u} \\ \dot{w} \end{Bmatrix} + \begin{bmatrix} K_{ss} & K_{sf} \\ K_{sf}^T & K_{ff} \end{bmatrix} \begin{Bmatrix} u \\ w \end{Bmatrix} = \begin{Bmatrix} R_s \\ R_f \end{Bmatrix} \tag{4.49}$$

Here u, w are the soil displacement and the displacement of the fluid relative to the soil respectively. C_{ss} represents solid damping. M, K and C are, respectively, the mass, stiffness and damping with the subscripts ss, ff and sf indicating the respective solid, fluid and coupling components. The solid damping was introduced by Ghaboussi [53] as a linear combination of the stiffness and mass matrices, (Rayleigh damping), in the following form;

$$C_{ss} = a_1(M_{ss} - f^2 M_{ff}) + a_2(K_{ss} - \alpha^2 K_{ff}) \tag{4.50}$$

where a_1, a_2 are constants. (4.49) can be expressed compactly as;

$$[M]\{\ddot{U}\} + [C]\{U\} + [K]\{U\} = \{R\} \tag{4.51}$$

where

$$\{U\} = \begin{Bmatrix} u \\ w \end{Bmatrix}$$

and [M], [C], [K] are, respectively, the system mass, damping and stiffness matrices. Dropping the square brackets for convenience, these equations after Laplace transformation become:

$$(s^2M + sC + K)q = F \tag{4.52}$$

where

$$\left.\begin{aligned} q &= \bar{U} = \bar{U}(s) \\ F &= F(s) = \bar{R} + sMU_0 + M\dot{U}_0 + CU_0 \end{aligned}\right| \tag{4.53}$$

and U_0, $\dot{U}_0$ are the initial conditions for nodal point displacement and velocities. (4.52) is a system of quadratic equations. To linearize the system, let

$$\dot{q} = sq \tag{4.54}$$

Premultiplying by M, and rearranging,

$$M\dot{q} - sMq = 0 \tag{4.55}$$

Hence (4.52) can be written as

$$-(K + sC)q - sM\dot{q} = -F \tag{4.56}$$

Combining (4.55) and (4.56):

$$\left(\begin{bmatrix} M & 0 \\ 0 & -K \end{bmatrix} - s \begin{bmatrix} 0 & M \\ M & C \end{bmatrix} \right) \begin{Bmatrix} \dot{q} \\ q \end{Bmatrix} = - \begin{Bmatrix} 0 \\ F \end{Bmatrix} \tag{4.57}$$

or,

$$[A - sB]\dot{q} = -f \tag{4.58}$$

where:

$$A = \begin{bmatrix} M & 0 \\ 0 & -K \end{bmatrix} \qquad B = \begin{bmatrix} 0 & M \\ M & C \end{bmatrix}$$

$$\bar{q} = \begin{Bmatrix} \dot{q} \\ q \end{Bmatrix} \qquad \bar{f} = \begin{Bmatrix} 0 \\ F \end{Bmatrix}$$

(4.58) is a system of linear equations. A and B are symmetric matrices. The prescribed boundary conditions on displacements, velocities etc. were enforced following Wilson's method. To obtain a solution to these equations, the vector $\bar{q}$ was expressed as a linear combination of a set of independent vectors Q_n, $n = 1,2,\ldots m$, in the following form:

$$\bar{q} = \sum_{n=1}^{m} a_n Q_n = [Q]\{a\} \tag{4.59}$$

where a_n are coefficients and Q_n is the n^{th} column of the matrix [Q]. The eigenvectors of the problem

$$[A - sB]y = 0 \qquad ; n = 1,2,\ldots m \tag{4.60}$$

were taken to be the independent vectors. The eigenvalues s_n were determined as the roots of the polynomial equation

$$|A - sB| = 0 \tag{4.61}$$

(4.58) and (4.59) give

$$(A - sB)Qa = -\bar{f} \tag{4.62}$$

Premultiplying both sides by Q^T

$$A^*a - sB^*a = -Q^T\bar{f} \tag{4.63}$$

where $A^* = Q^TAQ$ and $B^* = Q^TBQ$ are diagonal matrices due to orthogonality of Q with respect to A and B. The n^{th} equation is

$$A_n^*a_n - sB_n^*a_n = -Q_n^T\bar{f} \tag{4.64}$$

where

$$A_n^* = Q_n^T A Q_n = s_n Q_n^T B Q_n = s_n B_n^* \tag{4.65}$$

Substitution of (4.65) into (4.64) gave

$$s_n B_n^* a_n - s B_n^* a_n = -Q_n^T \bar{f} \tag{4.66}$$

Hence

$$a_n = \frac{-Q_n^T \bar{f}}{(s_n - s) B_n^*} \tag{4.67}$$

Substitution of (4.67) in (4.59) gave the solution in the Laplace transform space:

$$\bar{q} = \sum_{n=1}^{m} \frac{Q_n^T \bar{f}}{(s - s_n) B_n^*} Q_n \tag{4.68}$$

This series was inverted, term by term, to get the required results in the form of nodal displacements and velocities as functions of time. These functions were evaluated for specified values of the time variable to determine the solutions as well as secondary quantities of interest e.g., the stress in the material.

Items 1.8 and 4.2 in Appendix B contain details of the procedures as well as examples for validation of the computer codes.

4.4 FINITE ELEMENT SOLUTIONS

4.4.1 Variational Formulation

Variational formulations of the linearized version of the theory and its extension to include material nonlinearity were developed to construct a basis for alternate finite element approaches to the problem. Ghaboussi [53] had developed a variational formulation of Biot's theory but for the purpose of finite element analysis he used the Galerkin procedure. Also, this variational formulation did not allow for the boundary conditions properly nor did it allow for interelement discontinuities inherent in finite

element methods.

In order to systematically develop variational principles, the equations of motion were written in a form that they would constitute a self-adjoint system in an appropriate linear vector space. This procedure was based on previous work by Gurtin [71,72], Mikhlin [98] and Sandhu and his co-workers [135-138]. The self-adjoint system of equations for the problem is:

$$A(u) = f \qquad \text{on} \quad R \times [0, \infty) \tag{4.69}$$

Here A is a matrix of operators. Explicitly

$$A = \begin{vmatrix} \rho & \rho^{(2)} & 0 & -L & 0 & 0 \\ \rho^{(2)} & \rho^{(2)}/f+1^{\alpha}(1/k) & -t^{\alpha}\frac{\partial}{\partial m} & 0 & 0 & 0 \\ 0 & t^{\alpha}\frac{\partial}{\partial m} & 0 & 0 & 0 & -t^{\alpha} \\ L & 0 & 0 & 0 & -t^{\alpha} & 0 \\ 0 & 0 & 0 & -t^{\alpha} & p & t^{\alpha}\alpha M\delta_{ij} \\ 0 & 0 & -t^{\alpha} & 0 & t^{\alpha}\alpha M\delta_{kl} & t^{\alpha}M \end{vmatrix} \tag{4.70}$$

where

$$L = \frac{1}{2} t^{\alpha}(\delta_{lm}\frac{\partial}{\partial k} + \delta_{km}\frac{\partial}{\partial l} \tag{4.71}$$

and

$$p = t^{\alpha}(E_{ijkl} + \alpha^2 M \delta_{ij}\delta_{kl}) \tag{4.72}$$

Also in (4.69),

$$u = \begin{vmatrix} u_m \\ w_m \\ \pi \\ \tau_{ij} \\ e_{kl} \\ \xi \end{vmatrix} \qquad \text{and} \qquad f = \begin{vmatrix} F_m \\ G_m \\ 0 \\ 0 \\ 0 \\ 0 \end{vmatrix} \tag{4.73}$$

Elements of the operator matrix A satisfy self-adjointness with respect to the bilinear mapping

$$\langle f, g \rangle = \int_R f^* g \, dR \tag{4.74}$$

i.e., they satisfy the relation

$$\sum_{j=1}^{n} \langle u_j, A_{ij} u_j \rangle_R = \langle u_i, \sum_{j=1}^{n} A_{ij} u_j \rangle_R + D_{\partial R}(u_i, u_j), \quad i = 1, 2, \ldots n \tag{4.75}$$

where $D_{\partial R}(u_i, u_j)$ denotes quantities associated with the boundary ∂R of the region of interest R. Consistent boundary conditions for (4.69) are

$$\begin{aligned}
&-t^e u_i n_j = -t^e u_i n_j \quad \text{on} \quad S_1 \times [0, \infty) \\
&-t^e w_i n_i = -t^e w_i n_i \quad \text{on} \quad S_2 \times [0, \infty) \\
&t^e \pi n_i = t^e \hat{\pi} n_i \quad \text{on} \quad S_3 \times [0, \infty) \\
&t^e \tau_{ij} n_j = t^e T_i \quad \text{on} \quad S_4 \times [0, \infty)
\end{aligned} \tag{4.76}$$

Consistent form of the internal jump discontinuities is

$$\begin{aligned}
&-t^e (u_i n_j)^+ = -t^e (g_1)_i n_j \quad \text{on} \quad S_{11} \times [0, \infty) \\
&-t^e (w_i n_i)^+ = -t^e g_2 \quad \text{on} \quad S_{21} \times [0, \infty) \\
&t^e (\pi n_i)^+ = t^e g_3 n_i \quad \text{on} \quad S_{31} \times [0, \infty) \\
&t^e (\tau_{ij} n_j)^+ = t^e g_4 n_i \quad \text{on} \quad S_{41} \times [0, \infty)
\end{aligned} \tag{4.77}$$

Boundary operators C_{ij}, $i, j = 1, 2, \ldots n$ are said to be consistent with the matrix of field operators if in (4.75)

$$D_{\partial R}(u_i, u_j) = \langle u_i, \sum_{j=1}^{n} C_{ij} u_j \rangle_{\partial R} - \sum_{j=1}^{n} \langle u_j, C_{ji} u_i \rangle_{\partial R} \tag{4.78}$$

Here, surfaces S_{11}, S_{21}, S_{31} and S_{41} are embedded in the interior of R Operators in the self-adjoint operator matrix in (4.70) have the following relationships

$$\langle t^e u_{i,j}, \tau_{ij} \rangle_R = -\langle t^e u_i, \tau_{ij,j} \rangle_R$$

$$+ \langle t^* u_i n_j, \tau_{ij} \rangle_{S_1} + \langle t^* u_i, \tau_{ij} n_j \rangle_{S_4}$$

$$+ \langle t^* (u_i n_j)', \tau_{ij} \rangle_{S_{11}} + \langle t^* u_i, (\tau_{ij} n_j)' \rangle_{S_{41}} \tag{4.79}$$

$$\langle t^* w_{i,i}, \pi \rangle_R = - \langle t^* w_{i,i}, \pi \rangle_R$$

$$+ \langle t^* w_i n_i, \pi \rangle_{S_2} + \langle t^* w_i, \pi n_i \rangle_{S_3}$$

$$+ \langle t^* (w_i n_i)', \pi \rangle_{S_{21}} + \langle t^* w_i, (\pi n_i)' \rangle_{S_{31}} \tag{4.80}$$

Here we assume that $\langle \, , \, \rangle_R$ is the sum of quantities evaluated over the subregions of R such that all the surfaces S_1, S_2, S_3, S_4 are contained in the union of the boundaries of these subregions. For the coupled system (4.69) the governing function is defined as;

$$\Omega(u) = \langle \rho u_i, u_i \rangle_R + 2\langle \rho^{(2)} w_i, u_i \rangle_R - \langle t^* \tau_{ij,j}, u_i \rangle_R + \langle (\frac{\rho^{(2)}}{f} + 1^* \frac{1}{k}) w_i, w_i \rangle_R$$

$$- \langle t^* \pi_{,i}, w_i \rangle_R + \langle t^* w_{i,i}, \pi \rangle_R - 2\langle t^* \xi, \pi \rangle_R + \langle t^* u_{i,j}, \tau_{ij} \rangle_R$$

$$- 2\langle t^* e_{ij}, \tau_{ij} \rangle_R + \langle t^* (E_{ijkl} + \alpha^2 M \delta_{ij} \delta_{kl}) e_{kl}, e_{ij} \rangle_R$$

$$+ 2\langle t^* \alpha M \delta_{ij} e_{ij}, \xi \rangle_R + \langle t^* M \xi, \xi \rangle_R - 2\langle u_i, F_i \rangle_R - 2\langle w_i, G_i \rangle_R$$

$$- \langle \tau_{ij}, t^* (u_i - 2u_i) n_j \rangle_{S_1} - \langle \pi, t^* (w_i - 2w_i) n_i \rangle_{S_2}$$

$$+ \langle w_i, t^* (\pi - 2\pi) n_i \rangle_{S_3} + \langle u_i, t^* (\tau_{ij} n_j - 2T_i) \rangle_{S_4}$$

$$- \langle \tau_{ij}, t^* ((u_i n_j)' - 2(g_1)_i n_j) \rangle_{S_{11}} - \langle \pi, t^* ((w_i n_i) - 2g_2) \rangle_{S_{21}}$$

$$+ \langle w_i, t^* ((\pi n_i)' - 2g_3 n_i) \rangle_{S_{31}} + \langle u_i, t^* ((\tau_{ij} n_j)' - 2g_4 n_i) \rangle_{S_{41}} \tag{4.81}$$

The Gateaux differential of this function along $v = \{\bar{u}_i, \bar{w}_i, \bar{\pi}, \bar{\tau}_{ij}, \bar{e}_{ij}, \bar{\xi}\}$ is;

$$\Delta_v \Omega(u) = \langle \bar{u}_i, \rho u_i + \rho^{(2)} w_i - t^* \tau_{ij,j} - 2F_i \rangle_R$$

$$+ \langle u_i, \rho \bar{u}_i + \rho^{(2)} \bar{w}_i - t^* \bar{\tau}_{ij,j} \rangle_R$$

$$+ \langle w_i, \rho^{(2)} u_i + (\frac{\rho^{(2)}}{f} + 1^* \frac{1}{k}) w_i - t^* \pi \text{sib}, i - 2G_i \rangle_R$$

$$
\begin{aligned}
&+ \langle w_i, \rho^{(2)}\ddot{\bar{u}}_i + (\frac{\rho^{(2)}}{f} + 1^{\circ}\frac{1}{k})\bar{w}_i - t^{\circ}\bar{\pi}_{,i} \rangle_R \\
&+ \langle \bar{\pi}, t^{\circ}w_{i,i} - t^{\circ}\xi \rangle_R + \langle \pi, t^{\circ}\bar{w}_{i,i} - t^{\circ}\bar{\xi} \rangle_R \\
&+ \langle \bar{\tau}_{ij}, t^{\circ}u_{i,j} - t^{\circ}e_{ij} \rangle_R + \langle \tau_{ij}, t^{\circ}\bar{u}_{i,j} - t^{\circ}\bar{e}_{ij} \rangle_R \\
&+ \langle \bar{e}_{ij}, -t^{\circ}\tau_{ij} + t^{\circ}(E_{ijkl} + \alpha^2 M\delta_{ij}\delta_{kl})e_{kl} + \alpha M\delta_{ij}\xi \rangle_R \\
&+ \langle e_{ij}, -t^{\circ}\bar{\tau}_{ij} + t^{\circ}(E_{ijkl} + \alpha^2 M\delta_{ij}\delta_{kl})\bar{e}_{kl} + \alpha M\delta_{ij}\bar{\xi} \rangle_R \\
&+ \langle \xi, -t^{\circ}\pi + t^{\circ}\alpha M\delta_{kl}e_{kl} + t^{\circ}M\xi \rangle_R \\
&+ \langle \xi, -t^{\circ}\bar{\pi} + t^{\circ}\alpha M\delta_{kl}\bar{e}_{kl} + t^{\circ}M\bar{\xi} \rangle_R \\
&- \langle \bar{\tau}_{ij}, t^{\circ}(u_i n_j - 2\hat{u}_i n_j) \rangle_{S_1} - \langle \tau_{ij}, t^{\circ}\bar{u}_i n_j \rangle_{S_1} \\
&- \langle \bar{\pi}, t^{\circ}(w_i n_i - 2\hat{w}_i n_i) \rangle_{S_2} - \langle \pi, t^{\circ}\bar{w}_i n_i \rangle_{S_2} \\
&- \langle \bar{w}_i, t^{\circ}(\pi n_i - 2\hat{\pi} n_i) \rangle_{S_3} - \langle w_i, t^{\circ}\bar{\pi} n_i \rangle_{S_3} \\
&- \langle \bar{u}_i, t^{\circ}(\tau_{ij} n_j - 2\hat{T}_i) \rangle_{S_4} - \langle u_i, t^{\circ}\tau_{ij} n_j \rangle_{S_4} \\
&- \langle \bar{\tau}_{ij}, t^{\circ}((u_i n_j)' - 2(g_1)_i n_j) \rangle_{S_{1i}} - \langle \tau_{ij}, t^{\circ}(\bar{u}_i n_j)' \rangle_{S_{1i}} \\
&- \langle \bar{\pi}, t^{\circ}((w_i n_i)' - 2g_2) \rangle_{S_{2i}} - \langle \pi, t^{\circ}(\bar{w}_i n_i)' \rangle_{S_{2i}} \\
&- \langle \bar{w}_i, t^{\circ}((\pi n_i)' - 2g_3 n_i) \rangle_{S_{3i}} - \langle w_i, t^{\circ}(\bar{\pi} n_i)' \rangle_{S_{3i}} \\
&- \langle \bar{u}_i, t^{\circ}((\bar{\tau}_{ij} n_j)' - 2(g_4) n_j) \rangle_{S_{4i}} - \langle u_i, t^{\circ}(\bar{\tau}_{ij} n_j)' \rangle_{S_{4i}} \qquad (4.82)
\end{aligned}
$$

Using (4.79) and (4.80) the Gateaux differential is seen to vanish if and only if all the field equations along with the boundary conditions and the jump discontinuities are satisfied. (4.79) and (4.80) relate pairs of operators in the operator matrix A and may be used to eliminate either of the elements in each pair from the function $\Omega(u)$ in (4.81). Eight alternate forms can be obtained by using either or both relations. Elimination of an operator A_{ij} from the function implies that state variable u_j need not be in the domain M_{ij} of A_{ij}. This results in relaxating the requirement of smoothness of u_j

thereby extending the space of admissible states. In the context of the finite element method, it is clear that the extension of the admissible space provides greater freedom in selection of approximation functions.

If the admissible state is constrained to satisfy some field equation and/or boundary conditions, certain specialized forms of the variational principle are realized. This procedure is used to reduce the number of free variables in the governing function. Also, certain assumptions in the spatial or temporal variation of some of the variables lead to approximate theories. In the context of direct methods of approximation the constarints assumed in the specialization must be satisfied by admissible states.

As an example, for the extended functional obtained by using (4.79) and (4.80) to eliminate $\tau_{ij,1}$ and $\pi_{,1}$ from (4.81), specialization to satisfy $(4.69)_3$ and $(4.69)_4$ i.e, satisfying identically the kinematic relationships gives

$$\begin{aligned}\Omega_1 = {} & <\rho u_i, u_i>_R + 2<\rho^{(2)} w_i, u_i>_R + <(\frac{\rho^{(2)}}{f} + 1^*\frac{1}{k})w_i, w_i>_R \\ & + <t^*(E_{ijkl} + \alpha^2 M\delta_{ij}\delta_{kl})e_{kl}, e_{ij}>_R + 2<t^*\alpha M\delta_{ij}e_{ij}, \xi>_R \\ & + <t^*M\xi, \xi>_R - 2<u_i, F_i>_R - 2<w_i, G_i>_R \\ & - 2<\tau_{ij}, t^*(u_i - \hat{u}_i)n_j>_{S_1} - 2<\pi, t^*(w_i - \hat{w}_i)n_i>_{S_2} \\ & - 2<w_i, t^*\hat{\pi}n_i>_{S_3} - 2<u_i, t^*\hat{T}_i>_{S_4} \\ & - 2<\tau_{ij}, t^*((u_i n_j)' - (g_1)_i n_j)>_{S_{1i}} - 2<\pi, t^*((w_i n_i)' - g_2)>_{S_{2i}} \\ & - 2<w_i, t^* g_3 n_i>_{S_{3i}} - 2<u_i, t^* g_4 n_i>_{S_{4i}} \end{aligned} \tag{4.83}$$

If the field variables over the domain are continuous, the jump discontinuity terms drop out giving the specialization;

$$\begin{aligned}\Omega_2 = {} & <\rho u_i, u_i>_R + 2<\rho^{(2)} w_i, u_i>_R + <(\frac{\rho^{(2)}}{f} + 1^*\frac{1}{k})w_i, w_i>_R \\ & + <t^*(E_{ijkl} + \alpha^2 M\delta_{ij}\delta_{kl})e_{kl}, e_{ij}>_R + 2<t^*\alpha M\delta_{ij}e_{ij}, \xi>_R \end{aligned}$$

$$+ \langle t^{*}M\xi, \xi \rangle_{R} - 2\langle u_i, F_i \rangle_{R} - 2\langle w_i, G_i \rangle_{R}$$

$$- 2\langle \tau_{ij}, t^{*}(u_i - \hat{u}_i)n_j \rangle_{S_1} - 2\langle \pi, t^{*}(w_i - \hat{w}_i)n_i \rangle_{S_2}$$

$$- 2\langle w_i, t^{*}\hat{\pi}n_i \rangle_{S_3} - 2\langle u_i, t^{*}\hat{T}_i \rangle_{S_4} \qquad (4.84)$$

Further specialization of (4.84) to the case where displacement boundary conditions are identically satisfied yields the function governing the two field formulation proposed by Ghaboussi [53] except that in the present formulation the boundary terms are consistent.

Figure 7 diagramatically depicts the possible extensions of the general variational principle based on the direct formulation. Figure 8 shows the same for the complementary formulation. In either case, only the specializations listed in the report (item 1.7 in Appendix B) are shown. Evidently, other extended forms could be used as starting points for specialization.

Details of this effort are contained in items 1.7 and 3.2 in Appendix B. For nonlinear problems, a quasilinearized form of the nonlinear equations was used to develop a variational formulation (item 1.13 in Appendix B).

4.4.2 Two- and Three-Field Formulations

In the two-field formulations of Biot's theory the soil displacement and the displacement of fluid relative to the soil were used as the two field variables. The pore pressures were determined through a constitutive relationship using volumetric strain of the soil and the change in fluid content. During the course of the present research, it was felt that this approach may not yield sufficiently accurate estimates of the pore pressures because of the need for numerical evaluation of the derivatives. A three-field formulation introducing the pore-pressure as the third field variable was derived as a specialization from the general variational principle. Assuming the boundary conditions

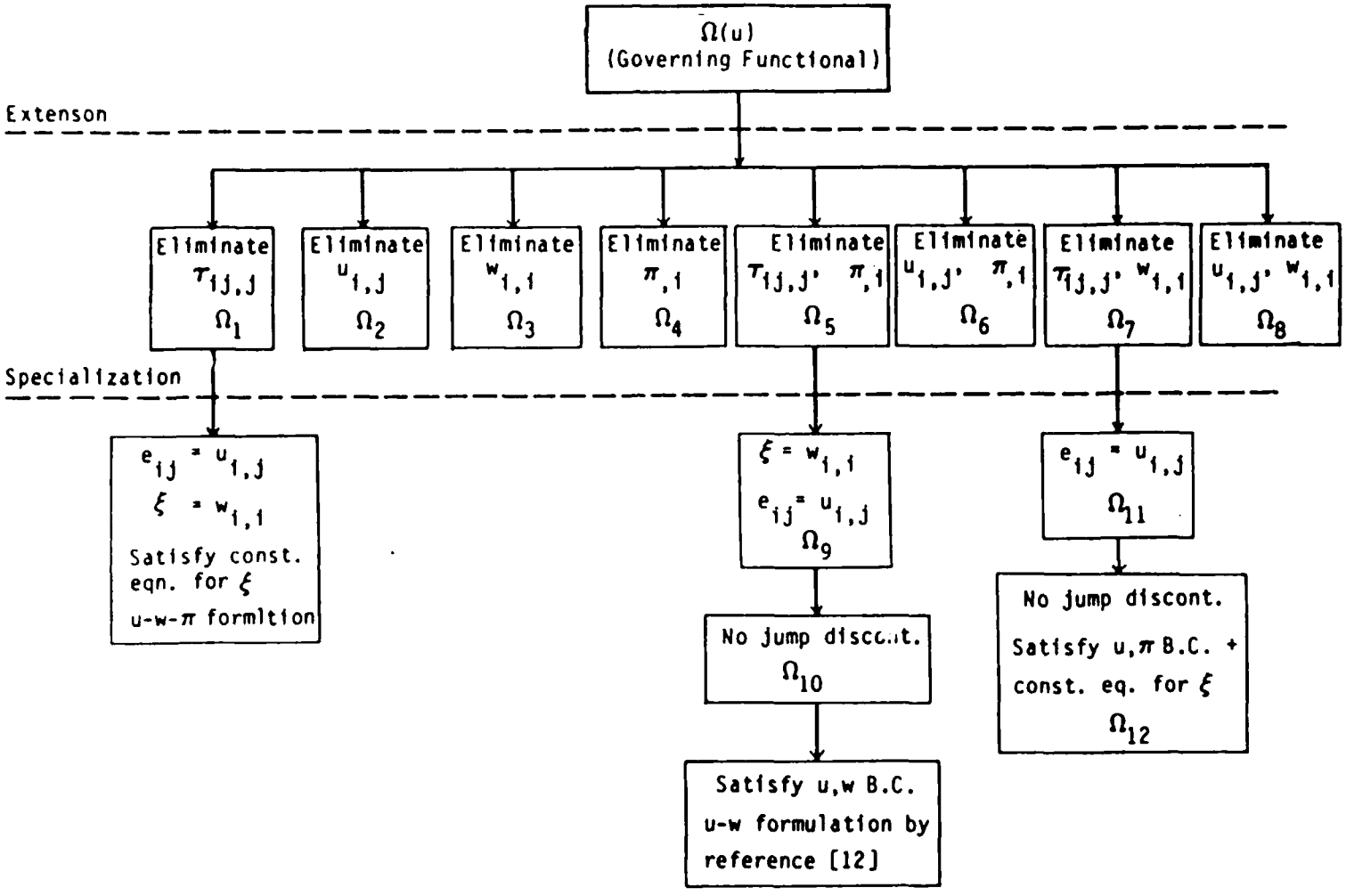

Figure 7: Family of Variational Principles by Direct Formulation

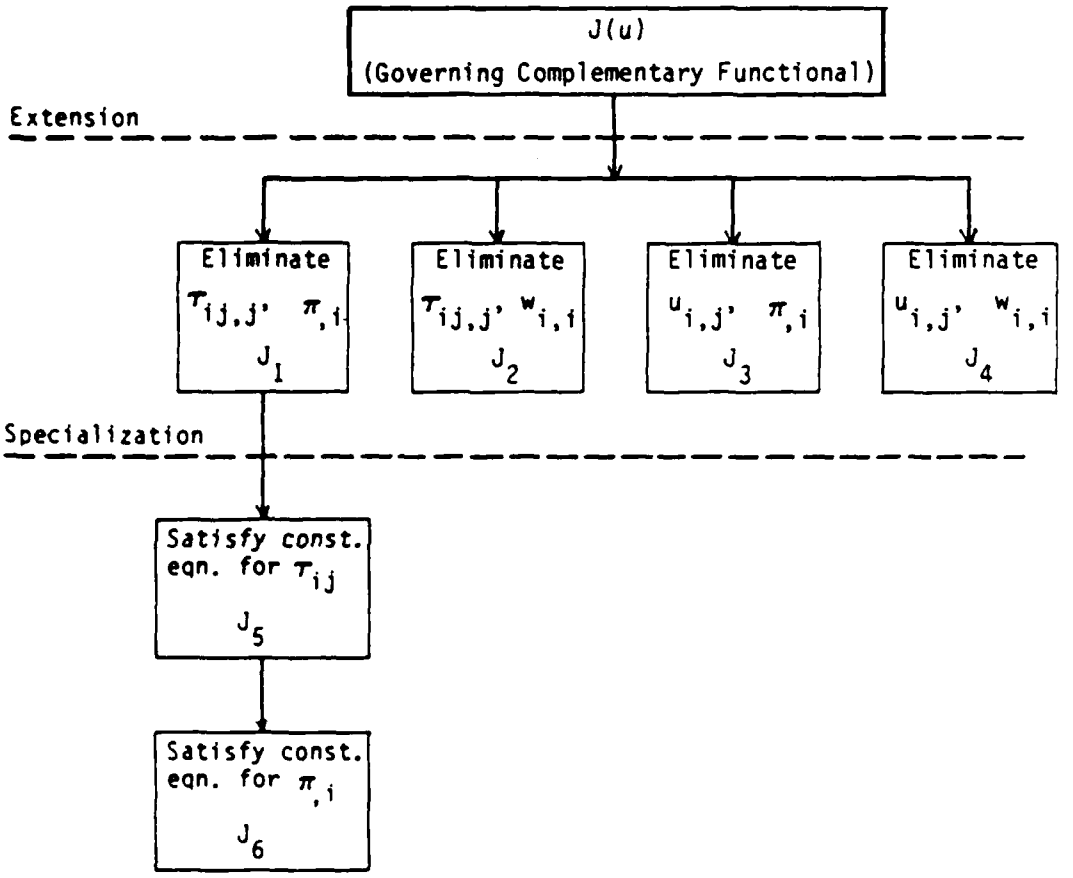

Figure 8: Family of Complementary Variational Principles

on S_1 and S_3 are identically satisfied, the governing function for this was:

$$\Omega = <\rho u_i, u_i>_R + 2<\rho^{(2)} w_i, u_i>_R + <(\rho^{(2)}/f + 1^* \frac{i}{k}) w_i, w_i>_R$$
$$-2<t^* \pi_{,i}, w_i>_R + <t^* E_{ijkl} e_{kl}, e_{ij}>_R + 2<t^* \alpha \delta_{ij} e_{ij}, \pi>_R$$
$$- <t^* \frac{\pi}{M}, \pi>_R - 2<u_i, F_i>_R - 2<w_i, G_i>_R$$
$$+2<\pi, t^* \hat{w}_i n_i>_{S_2} - 2<u_i, t^* \hat{T}>_{S_4} \qquad (4.85)$$

This formulation was implemented in a finite element computer code to obtain continuous pore pressure distributions. The three-field formulation also allowed direct specification of the fluid pressures on the boundaries, which is not possible with the two-field formulations, where this boundary condition could only be applied as a linear constraint in terms of soil displacement and relative fluid displacement. The studies showed that though the numerical difference in the results from the two- and three-field formulations was only slight, the three-field formulation was much more expensive. However, it has the distinct advantage of being able to prescribe boundary values for pore presssures. Items 1.10, 3.4 and 4.1 of Appendix B contain details of the formulation and a study of its effectiveness.

4.4.3 Spatial Discretization

Most succesful schemes for approximate solution of the coupled problem of quasi-static soil deformation and fluid flow have been based on the use of higher order interpolation for the displacements and a lower order for the pore water pressures. These elements are expensive to use in terms of computer time. Elements based on the use of the same order of interpolation had been found to give unreliable results just after loading and would be suspect for use in dynamic problems. Incompatible interelement boundaries have been used to combine the economy of lower order elements and

yet retain higher order local interpolation. These elements satisfy the patch test for completeness for certain element geometries. Ghaboussi's four point incompatible element [52,53] was implemented in a computer program for consolidation analysis to compare its performance with that of higher order elements for efficiency and accuracy. Details of this study are contained in item 1.3 of appendix B. These studies were useful in the selection of the strategy appropriate to the problem of dynamic analysis of liquid-filled soils. The comparative study showed that the incompatible element gave results almost identical to those obtained using the higher order elements based on biquadratic interpolation for displacements, but was significantly more economical. This made Ghaboussi's element a good candidate for extension to nonlinear, three-dimensional and dynamic problems.

Three different finite element strategies were used to cover the cases of one- and two-dimensional wave propagation. Both bilinear and biquadratic interpolation schemes were implemented along with Ghaboussi's incompatible element and cubic Hermite polynomials for one-dimensional wave propagation. These interpolation schemes were implemented in a dynamic analysis computer program and used to solve one-dimensional wave propagation problems for which exact solutions were available. The code was used to solve one-dimensional wave propagation in a single material. Both the steady state and the transient cases were considered. Garg's [50] theoretical solutions for the case of weak as well as strong couplings were used as benchmarks. Application of the computer code to all these problems showed excellent agreement between the numerical and the theoretical solutions. The code could not be tested for two-dimensional wave propagation because of lack of exact solutions for that case. Reports listed as items 1.3, 1.15 and 2.3 of Appendix B describe some of this work.

4.4.4 Singularity Elements

Conventional finite element procedures cannot adequately model pore pressures near loaded free-draining boundaries because of the singularity in the pore pressure that exists immediately after the load is applied. Special finite elements, developed by Lee [89], to allow for line singularities were used to simulate propagation of waves in saturated soil. These elements use interpolating functions of the type

$$1 - ax - (1-a)x^n$$

where the index n is sufficiently large and coefficient a is chosen to be

$$a = 1 - \exp(-mt)$$

and were found to be satisfactory for proper representation of singularity at the wave front. These elements have the property that for $t = 0$, $a = 0$ and, therefore, the interpolating function is $1 - x^n$ and as t increases the function approaches $1 - x$. This element reproduces the line singularity occuring in one-dimensional consolidation problem immediately after loading and the singularity at a wave front. The interpolating scheme would approach $1 - x$ as time t increases. This research is described in items 1.1 and 3.1 in Appendix B.

4.4.5 Time Domain Integration

The results for one-dimensional analysis, for which exact solutions are available, showed that the conventional time-domain integration procedures found to be quite effective for single material problems, were also acceptable for the coupled problem of dynamics of saturated soils. A popular scheme is Wilson's β, γ, θ single step method. For two-dimensional cases, no exact solutions are available. For this reason, all the code verification had to be done on one-dimensional wave propagation problems. The requirements for an acceptable time step integration scheme were that the results should be insensitive to the choice of time-domain integration selected by the user and that with reduction of the size of the time step the approximate solution should con-

verge.

A modification to Wilson's method was introduced in order to specify velocity boundary conditions. Finite element discretization of the spatial domain leads to:

$$M\ddot{U} + C\dot{U} + KU = R \tag{4.86}$$

where M, K and C are the mass, stiffness and damping matrices, respectively, and R is the load vector at time t_n In (4.86), the square brackets and curly braces have been dropped for convenience, as in (4.52). In Wilson's scheme the displacements and velocities at time $(t+\theta\Delta t)$ are expressed in terms of U, $\dot{U}$ and U at time t_n as

$$U_{n+\theta} = U_n + \theta\Delta t\dot{U}_n + (1/2-\beta)(\theta\Delta t)^2\ddot{U}_n + \beta(\theta\Delta t)^2\ddot{U}_{n+\theta} \tag{4.87}$$

$$\dot{U}n+\theta = U_n + (1-\gamma)(\theta\Delta t)\ddot{U}_{n+\theta} \tag{4.88}$$

in which β and γ are Newmark's coefficients. Substituting (4.87) and (4.88) into (4.86) yields

$$KU^*_{n+\theta} = R^*_{n+\theta} \tag{4.89}$$

where

$$K^* = K + \frac{1}{\beta(\theta\Delta t)^2}M + \frac{1}{\beta(\theta\Delta t)}C$$

$$R^*_{n+\theta} = R_{n+\theta} + \frac{1}{\beta(\theta\Delta t)^2}Ma_{n+\theta} + \frac{1}{\beta(\theta\Delta t)}Cb_{n+\theta} \tag{4.90}$$

$$a_{n+\theta} = U_n + (\theta\Delta t)\dot{U}_n + (1/2-\beta)(\theta\Delta t)^2\ddot{U}_n$$

$$b_{n+\theta} = U_n + (1-\beta/\gamma)(\theta\Delta t)^2\ddot{U}_n$$

Assuming cubic variation of nodal point displacement over the time step (t_n, t_{n+1}) in terms of displacement, velocity and acceleration at time t_n, the values of these quantities at time $(t_n+\Delta t)$ are

$$U_{n+1} = \frac{1}{\theta^3}U_{n+\theta} + \left|1-\frac{1}{\theta^3}\right|U_n + \left|1-\frac{1}{\theta^2}\right|\Delta tU_n + \frac{1}{2}\left(1-\frac{1}{\theta}\right)(\Delta t)^2\ddot{U}_n$$

$$\dot{U}_{n+1} = \frac{\gamma}{\beta\theta^3\Delta t^2}(U_{n+\theta} - U_n) + \left(1 - \frac{\gamma}{\beta\theta^2}\right)\dot{U}_n + \left(1 - \frac{\gamma}{2\beta\theta}\right)\Delta t\ddot{U}_n \tag{4.91}$$

$$\ddot{U}_{n+1} = \frac{1}{\beta\theta^3\delta t^2}(U_{n+\theta} - U_n) - \frac{1}{\beta\theta^2\Delta t}\dot{U}_n + \left(1 - \frac{1}{2\beta\theta}\right)\ddot{U}_n$$

In a given problem, when velocities are prescribed at certain points, the corresponding accelerations and displacements are also known. In developing the modified scheme, all features of Wilson's method were sought to be retained. This enabled application of the scheme directly without elimination of known degrees-of-freedom which is quite cumbersome in dynamic problems. Let subscripts a, b denote the unknown and specified quantities, respectively. Then for the stage $(n+\theta)$ at time $t_n + \theta\Delta t$, (4.86) can be rewritten in partitioned form as

$$\begin{bmatrix} M_{aa} & M_{ab} \\ M_{ba} & M_{bb} \end{bmatrix} \begin{Bmatrix} \ddot{u}_a \\ \ddot{u}_b \end{Bmatrix}_{(n+\theta)} + \begin{bmatrix} C_{aa} & C_{ab} \\ C_{ba} & C_{bb} \end{bmatrix} \begin{Bmatrix} \dot{u}_a \\ \dot{u}_b \end{Bmatrix}_{(n+\theta)} + \begin{bmatrix} K_{aa} & K_{ab} \\ K_{ba} & K_{bb} \end{bmatrix} \begin{Bmatrix} u_a \\ u_b \end{Bmatrix}_{(n+\theta)} = \begin{Bmatrix} R_a \\ R_b \end{Bmatrix}_{(n+\theta)} \tag{4.92}$$

Rearrangement of terms in (4.92) gives

$$[K]\begin{Bmatrix} u_a \\ u_b \end{Bmatrix}_{(n+\theta)} = \begin{Bmatrix} R_a \\ R_b \end{Bmatrix}_{(n+\theta)} - [M]\begin{Bmatrix} \ddot{u}_a \\ 0 \end{Bmatrix}_{(n+\theta)} - [M]\begin{Bmatrix} 0 \\ \ddot{u}_b \end{Bmatrix}_{(n+\theta)} - [C]\begin{Bmatrix} \dot{u}_a \\ 0 \end{Bmatrix}_{(n+\theta)} - [C]\begin{Bmatrix} 0 \\ \dot{u}_b \end{Bmatrix}_{(n+\theta)} \tag{4.93}$$

From (4.87)

$$\ddot{u}_{n+\theta} = \frac{1}{\beta(\theta\Delta t)^2}[u_{n+\theta} - u_n - \theta\Delta t\,\dot{u}_n - (1/2 - \beta)(\theta\Delta t)^2\ddot{u}_n] \tag{4.94}$$

Substituting (4.94) in (4.88)

$$\dot{u}_{n+\theta} = \frac{\gamma}{\beta(\theta\Delta t)}[u_{n+\theta} - u_n - \theta\Delta t(1 - \beta/\gamma)\dot{u}_n - (1/2 - \beta/\gamma)(\theta\Delta t)^2\ddot{u}_n] \tag{4.95}$$

Rewriting (4.94) and (4.95) for the unknown quantities u_a and $\dot{u}_a$

$$\begin{Bmatrix} \ddot{u}_a \\ 0 \end{Bmatrix}_{(n+\theta)} = \frac{1}{\beta(\theta\Delta t)^2}\left(\begin{Bmatrix} u_a \\ 0 \end{Bmatrix}_{(n+\theta)} - \begin{Bmatrix} u_a \\ 0 \end{Bmatrix}_n - (\theta\Delta t)\begin{Bmatrix} \dot{u}_a \\ 0 \end{Bmatrix}_n - (1/2 - \beta)(\theta\Delta t)^2\begin{Bmatrix} \ddot{u}_a \\ 0 \end{Bmatrix}_n\right) \tag{4.96}$$

$$\begin{Bmatrix} \dot{u}_a \\ 0 \end{Bmatrix}_{(n+\theta)} = \frac{\gamma}{\beta(\theta\Delta t)}\left(\begin{Bmatrix} u_a \\ 0 \end{Bmatrix}_{(n+\theta)} - \begin{Bmatrix} u_a \\ 0 \end{Bmatrix}_n - (\theta\Delta t)(1 - \beta/\gamma)\begin{Bmatrix} u_a \\ 0 \end{Bmatrix}_n - (1/2 - \beta/\gamma)(\theta\Delta t)^2\begin{Bmatrix} \ddot{u}_a \\ 0 \end{Bmatrix}_n\right) \tag{4.97}$$

Substituting (4.96) and (4.97) into (4.93) gives

$$\begin{bmatrix} K^*_{aa} & K^*_{ab} \\ K^*_{ba} & K^*_{bb} \end{bmatrix} \begin{Bmatrix} u_a \\ u_b \end{Bmatrix}_{(n+\theta)} = \begin{Bmatrix} R^*_a \\ R^*_b \end{Bmatrix} \tag{4.98}$$

where

$$K^*_{aa} = K_{aa} + \frac{1}{\beta(\theta\Delta t)^2} M_{aa} + \frac{\gamma}{\beta(\theta\Delta t)} C_{aa} \tag{4.99}$$

$$K^*_{ab} = K_{ab} + \frac{1}{\beta(\theta\Delta t)^2} M_{ab} + \frac{\gamma}{\beta(\theta\Delta t)} C_{ab} \tag{4.100}$$

$$K^*_{ba} = K_{ba} + \frac{1}{\beta(\theta\Delta t)^2} M_{ba} + \frac{\gamma}{\beta(\theta\Delta t)} C_{ba} \tag{4.101}$$

$$K^*_{bb} = K_{bb} + \frac{1}{\beta(\theta\Delta t)^2} M_{bb} + \frac{\gamma}{\beta(\theta\Delta t)} C_{bb} \tag{4.102}$$

$$\begin{aligned} \begin{Bmatrix} R^*_a \\ R^*_b \end{Bmatrix} = \begin{Bmatrix} R_a \\ R_b \end{Bmatrix}_{(n+\theta)} & [M] \frac{1}{\beta(\theta\Delta t)^2} \left(\begin{Bmatrix} u_a \\ 0 \end{Bmatrix}_n + \begin{Bmatrix} 0 \\ u_b \end{Bmatrix}_{n+\theta} + (\theta\Delta t) \begin{Bmatrix} \dot{u}_a \\ 0 \end{Bmatrix}_n + (1/2-\beta)(\theta\Delta t)^2 \begin{Bmatrix} \ddot{u}_a \\ 0 \end{Bmatrix}_n \right) \\ & + [C] \frac{\gamma}{\beta(\theta\Delta t)} \left(\begin{Bmatrix} u_a \\ 0 \end{Bmatrix}_n + \begin{Bmatrix} 0 \\ u_b \end{Bmatrix}_{n+\theta} + (\theta\Delta t)(1-\beta/\gamma) \begin{Bmatrix} \dot{u}_a \\ 0 \end{Bmatrix}_n + (1/2-\beta/\gamma)(\theta\Delta t)^2 \begin{Bmatrix} \ddot{u}_a \\ 0 \end{Bmatrix}_n \right) \\ & - [M] \begin{Bmatrix} 0 \\ \ddot{u}_b \end{Bmatrix}_{n+\theta} - [C] \begin{Bmatrix} 0 \\ \dot{u}_b \end{Bmatrix}_{n+\theta} \end{aligned} \tag{4.103}$$

Wilson's method of allowing for prescribed displacement boundary condition was used to rewrite (4.98) as

$$\begin{bmatrix} K^*_{aa} & 0 \\ 0 & I \end{bmatrix} \begin{Bmatrix} u_a \\ u_b \end{Bmatrix}_{(n+\theta)} = \begin{Bmatrix} R^{**}_a \\ \dot{u}_b \end{Bmatrix}_{(n+\theta)} \tag{4.104}$$

where

$$R^{**}_a = R^*_a - K^*_{ab} \hat{u}_{b(n+\theta)} \tag{4.105}$$

and $\hat{u}_b$ are the prescribed values of u_b I denotes the identity matrix. The first set of equations in (4.104) is the first set of (4.98) modified for the known u_b and the second set of equations are trivial equations introduced to avoid reordering of elements of the displacement vector.

The procedure discussed above was used to solve the problem of wave propagation in a finite soil column of length (L = 50cm.) shown in Figure 9. The excitation was applied at the top (x = 0). The base of the soil column was assumed to be rigid and impervious. The material properties were chosen to be the same as used by Garg [50], i.e.,

$$n^{(1)} = 0.82, \quad n^{(2)} = 0.18, \quad \rho^{(1)} = 2.1812 \text{ g/cm}^3, \quad \rho^{(2)} = 0.18 \text{ g/cm}^3$$

$$K_1 = 0.36 \times 10^{12}, \; K = 0.118 \times 10^{12}, \; K_2 = 0.22 \times 10^{11}, \; G = 0.99 \times 10^{11} \quad \text{(all in dynes/cm}^2\text{)}$$

These are related to Biot's constants and yield

$$E = 0.2321 \times 10^{12} \text{ dynes/cm}^2, \quad \nu = 0.171, \quad \alpha = 0.6722, \quad M = 0.1047 \times 10^{12} \text{ dynes/cm}^2$$

Two example problems with different boundary conditions, Figure 10, one following Garg [50] and the other suggested by Morland (item 1.15. in Appendix B) were solved using the numerical inversion of the Laplace transform solution and the direct finite element procedure. Mathematically, the boundary conditions are:

Example 1:

$$\left.\begin{aligned} v^{(1)}(0,t) &= H(t) \\ v^{(2)}(0,t) &= H(t) \end{aligned}\right| \qquad (4.106)$$

where H(t) is the Heaviside function. Corresponding velocity transformations are

$$\left.\begin{aligned} \bar{v}^{(1)}(0,p) &= 1/p \\ \bar{v}^{(2)}(0,p) &= 1/p \end{aligned}\right| \qquad (4.107)$$

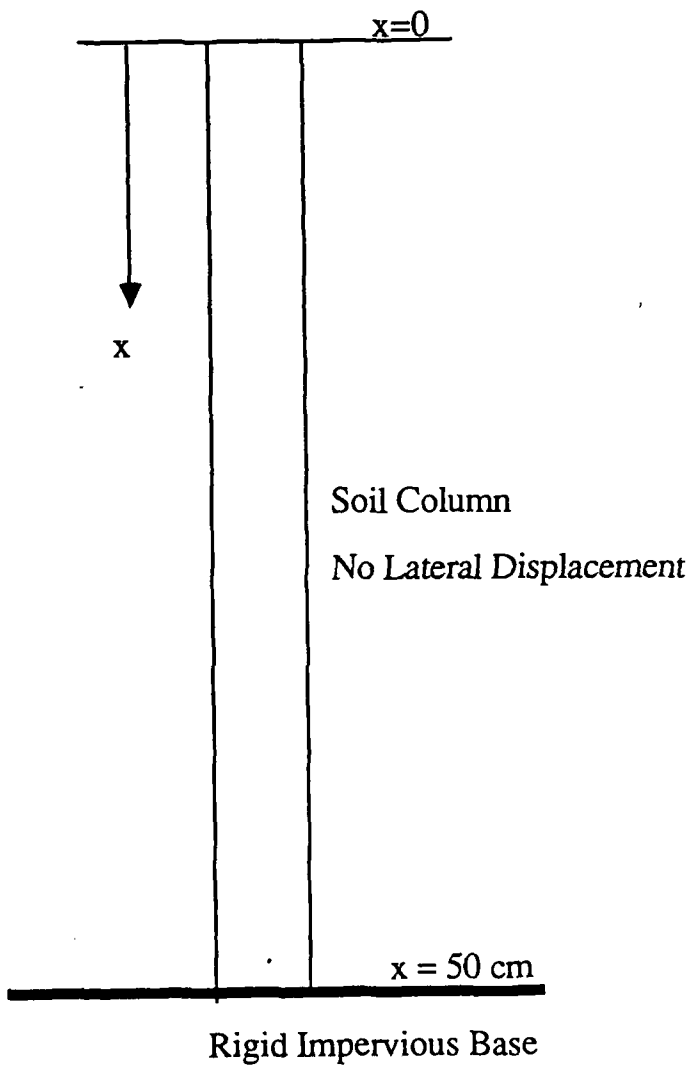

Figure 9: Representative Soil Column

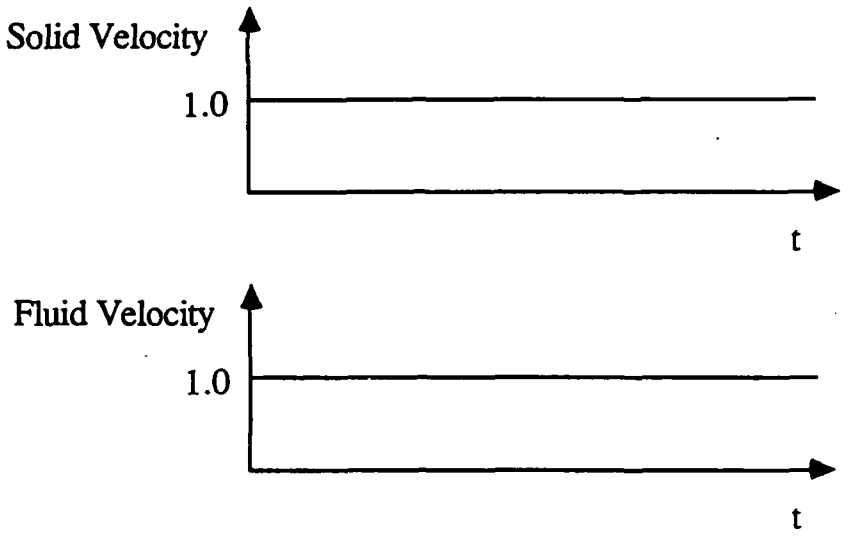

Example 1

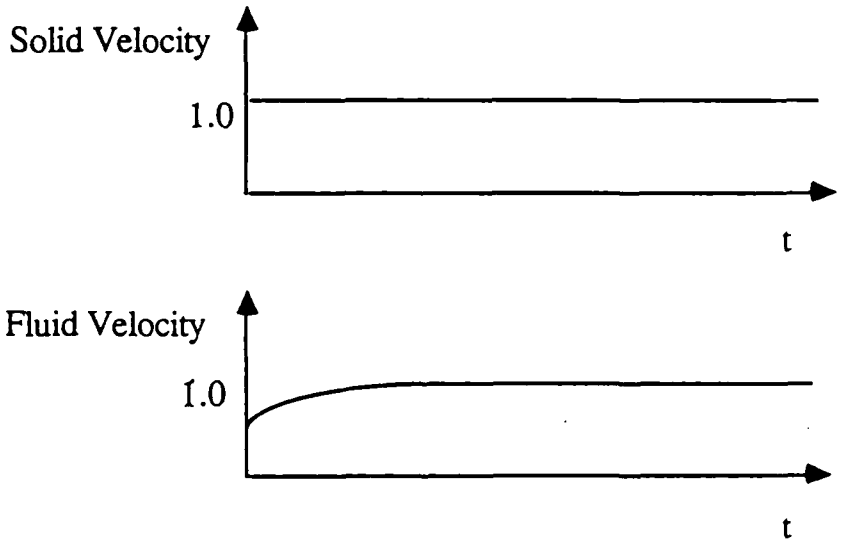

Example 2

Figure 10: Types of Excitation Applied on the Soil Column

Example 2:

$$\left.\begin{aligned} v^{(1)}(0,t) &= H(t) \\ v^{(2)}(0,t) &= [1-0.2\,e^{-t/T}]H(t) \end{aligned}\right| \qquad (4.108)$$

$t=(L/C_0)=140.9\ \mu$sec was taken as a normalizing factor. In this example, the fluid velocity specified at the boundary was different from the specified solid velocity and increased gradually from a value of 0.8 at $t=0$ to unity over the time scale. The velocity transformations are given by

$$\left.\begin{aligned} \bar{v}^{(1)}(0,p) &= 1/p \\ \bar{v}^{(2)}(0,p) &= 1/p-0.2/(p+1) \end{aligned}\right| \qquad (4.109)$$

Two values of the drag parameter:

$$D = 0.219\times 10^{2} \qquad g/cm^3\text{–sec}$$

$$D = 0.219\times 10^{8} \qquad g/cm^3\text{–sec}$$

representing the so-called low drag (free relative motion between constituents) and high drag (negligible relative motion) were used. The corresponding values for the ratio K/μ used in the finite element analysis were 0.148×10^{-2} and 0.148×10^{-8}, respectively.

Numerical inversion of the Laplace transform solution to the problem was carried out using 5000 terms in Dubner's [41] formula

$$f(t) = (1/\tau)e^{r\tau}\sum_{k=0}^{\infty}{}' \mathrm{Re}[f(r+k\pi i/2\tau)\cos(k\pi t/2\tau)] \qquad 0\leqslant t\leqslant\tau \qquad (4.110)$$

where prime signifies that only half of $k=0$ term is included in the sum. Dubner [41] showed that the error could be made small for $0\leqslant t\leqslant\tau$ by choosing $r\tau$ sufficiently large, where r is a real number. The value of $r\tau$ was set equal to 5.017. The velocity histories at four locations, namely 10 cm and 30 cm from the free surface,

were recorded over a total time period of 986.4 μsec at intervals of 14 μsec. This allowed for six reflections of the faster C_+ wave and two reflections of the slower C_- wave. The CPU time on the IBM 3081 mainframe was 70 min.

The finite element solution was a uniform spatial mesh for Example 1 but for Example 2 modelled the boundary layer by a fine mesh of elements near the top surface including a singularity element adjacent to the surface. Thus in Example 1 the spatial discretization consisted of 100 linear elements and 986 time steps of size 1 μsec in the time domain. In Example 2, 100 elements Of 0.005 cm length were employed near the top surface and 100 elements of 0.495 cm for the remainder of the column. The temporal integration involved 141 steps of 0.01 μsec and 985 steps of 1 μsec.

The velocity histories for low drag and high drag for Example 1 are shown in Figure 11 to Figure 14 and Figure 15 to Figure 18, respectively. For Example 2, Figure 19 to Figure 22 illustrate the low drag effects and Figure 23 to Figure 26 the high drag. In both examples, excellent agreement of numerical results is seen. In example 2, a refined mesh consisting only of linear elements was not able to reproduce the sharp wave fronts and large oscillations were encountered. This was overcome by the use of singularity element near the top boundary. The shape functions for this element were of the type $(1-\zeta^{\beta})$ and ζ^{β} over (0,1). The index β was taken to be 100.

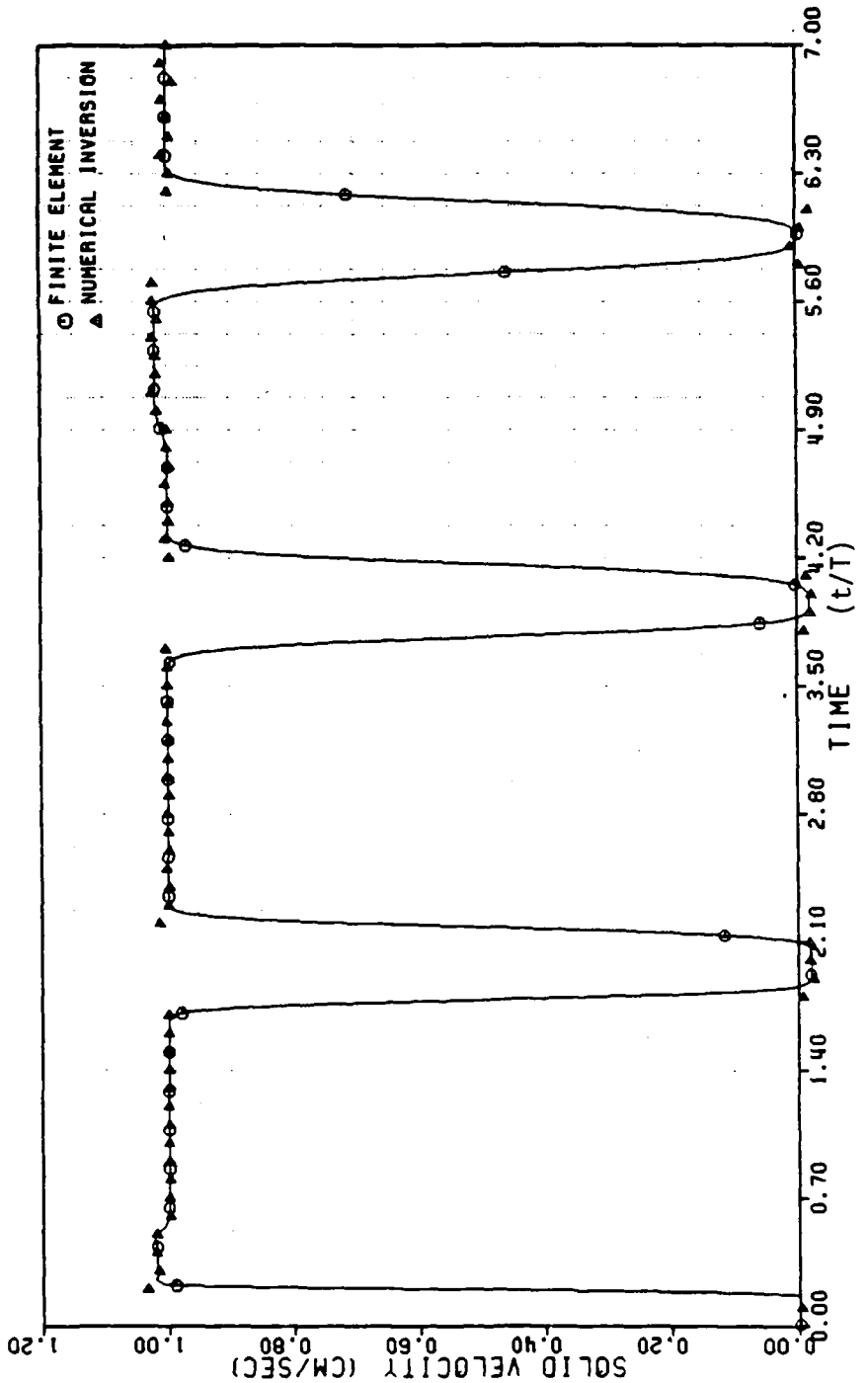

Figure 11: Example 1: Solid Velocity History at 10 cm. (Low Drag)

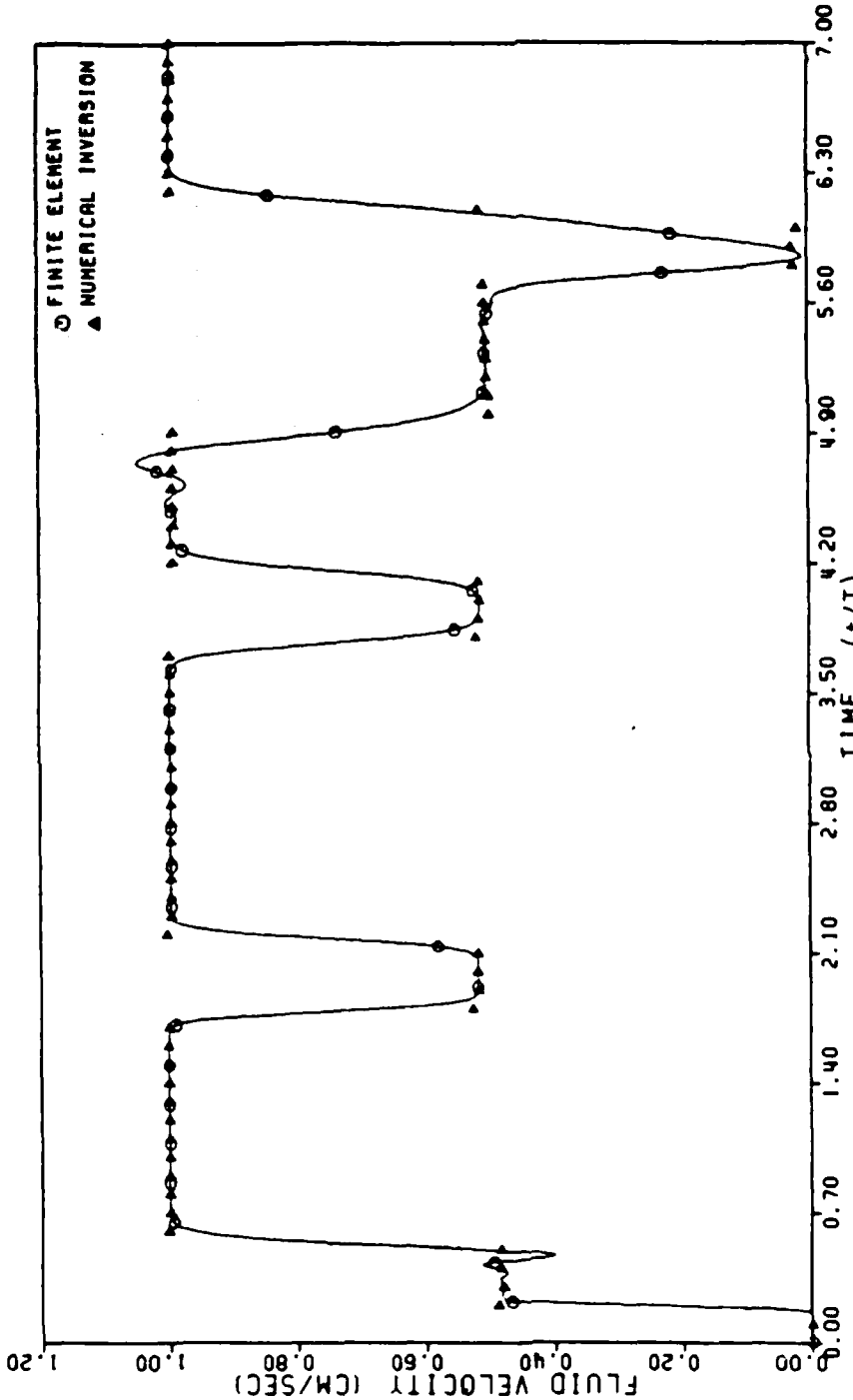

Figure 12: Example 1: Fluid Velocity History at 10 cm. (Low Drag)

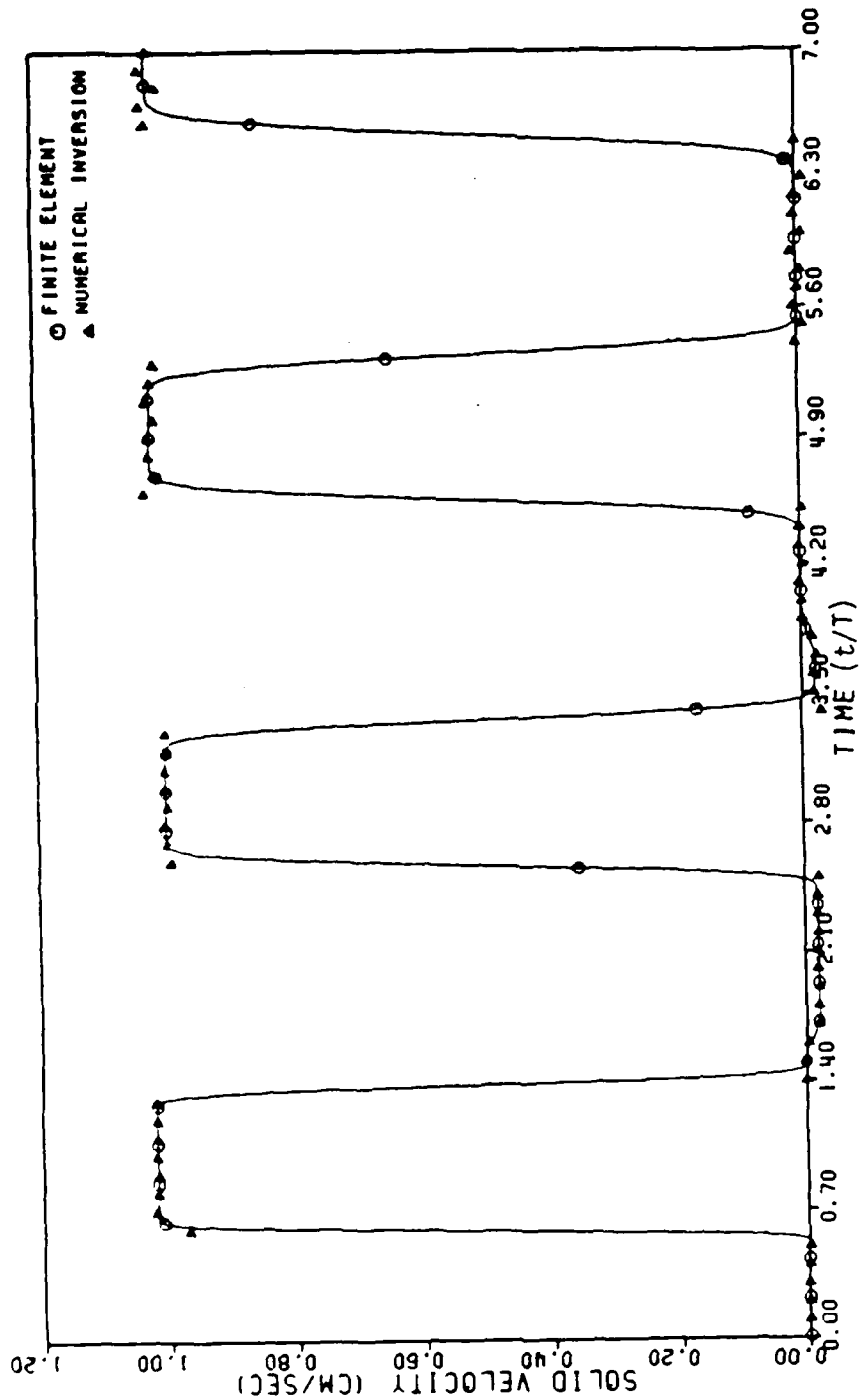

Figure 13: Example 1: Solid Velocity History at 30 cm. (Low Drag)

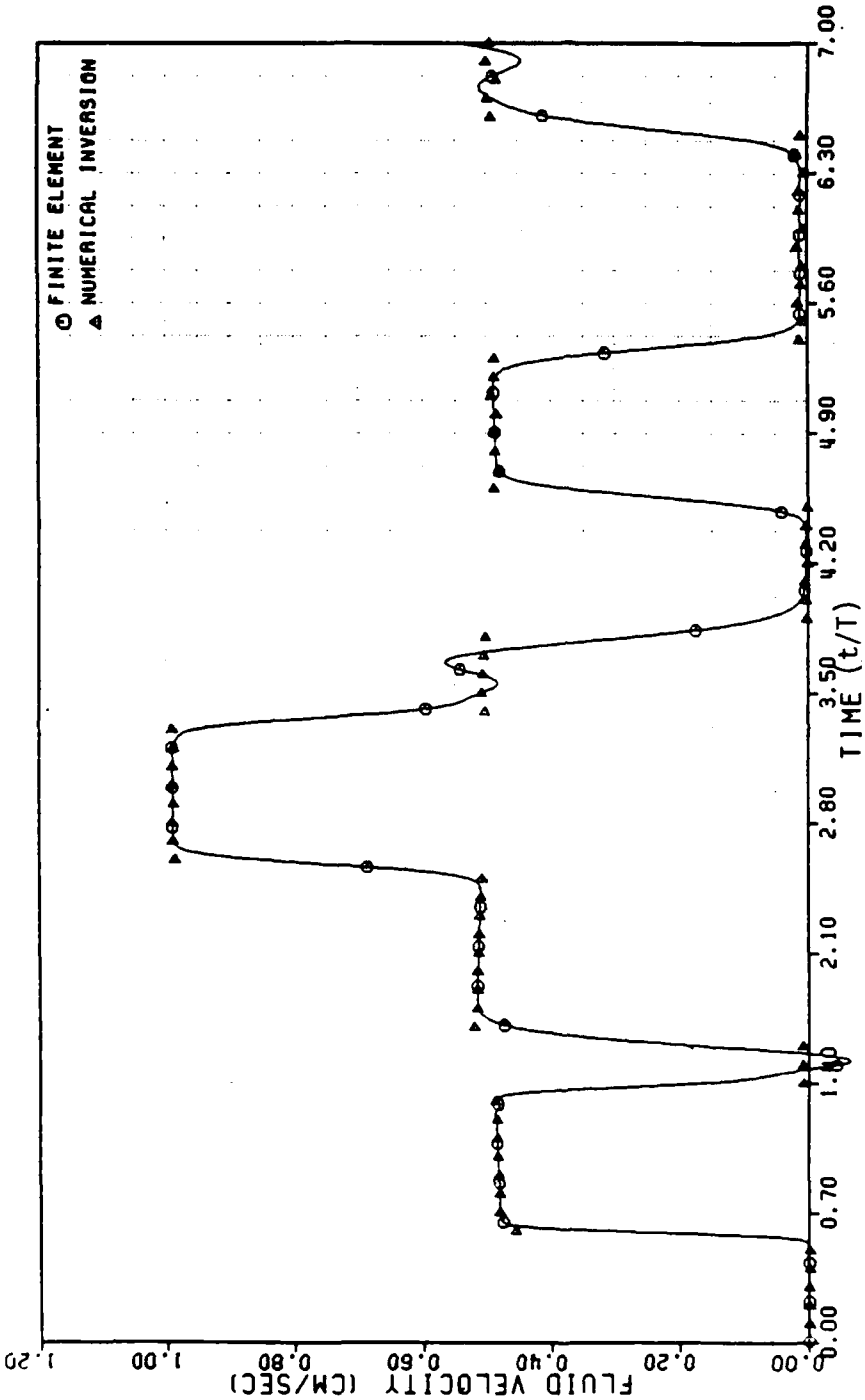

Figure 14: Example 1: Fluid Velocity History at 30 cm. (Low Drag)

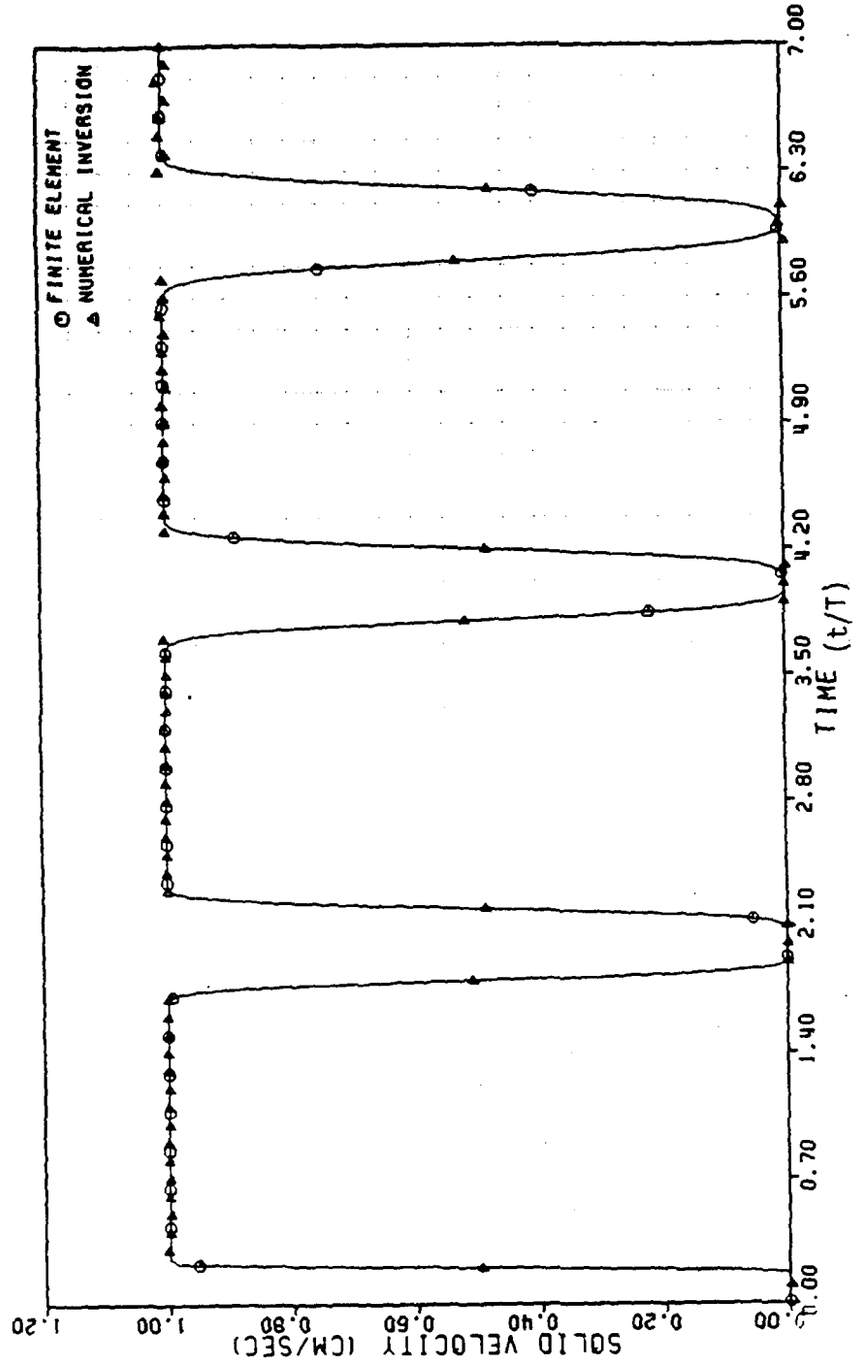

Figure 15: Example 1: Solid Velocity History at 10 cm. (High Drag)

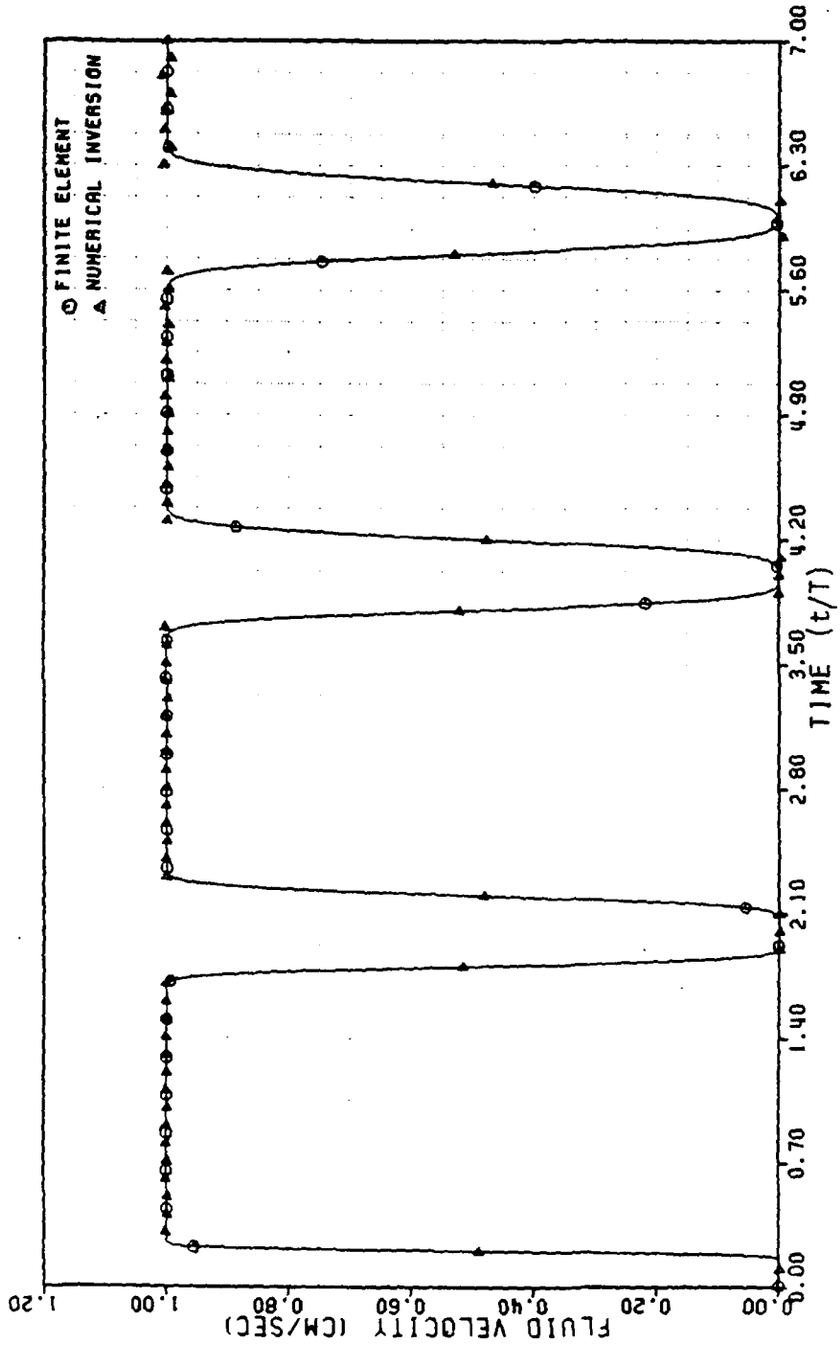

Figure 16: Example 1: Fluid Velocity History at 10 cm. (High Drag)

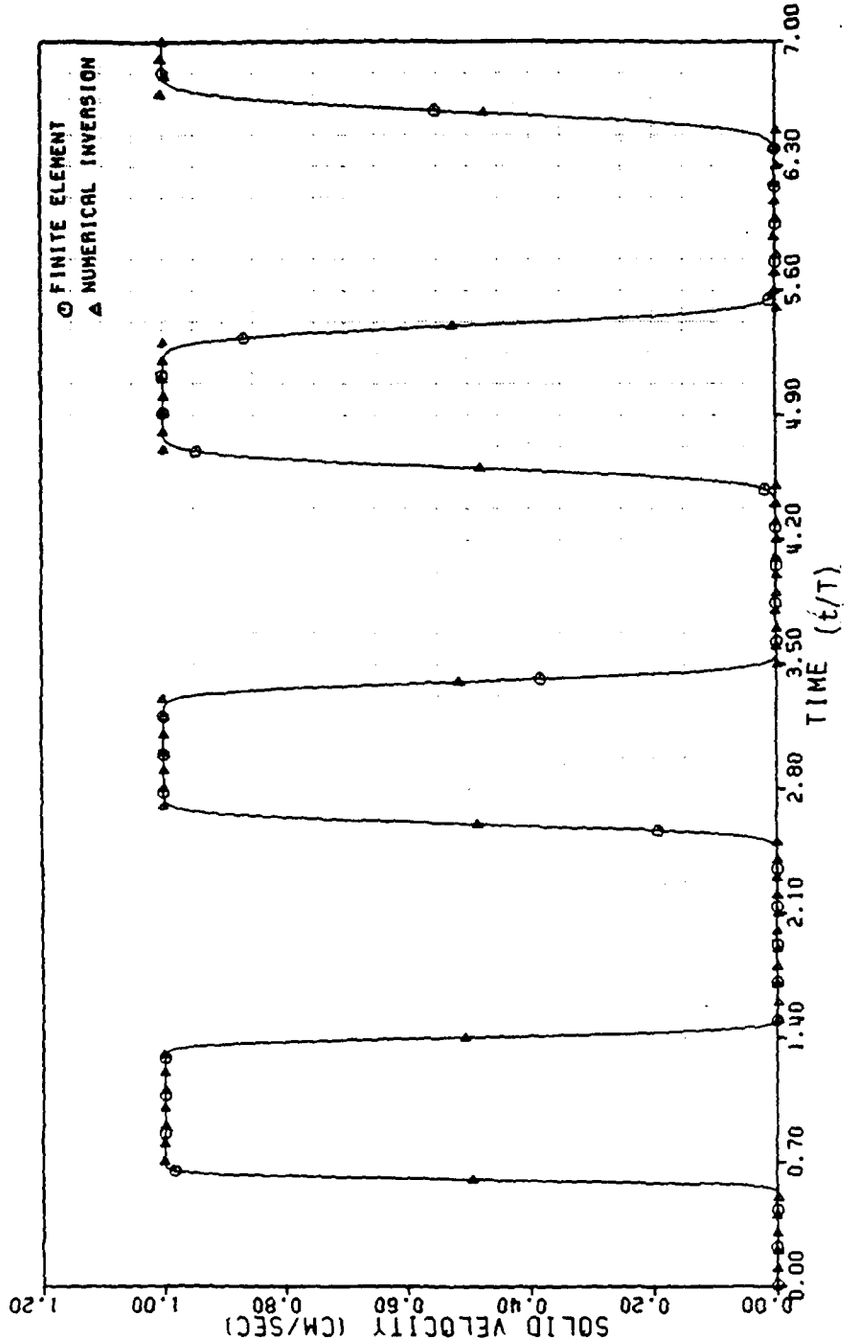

Figure 17: Example 1: Solid Velocity History at 30 cm. (High Drag)

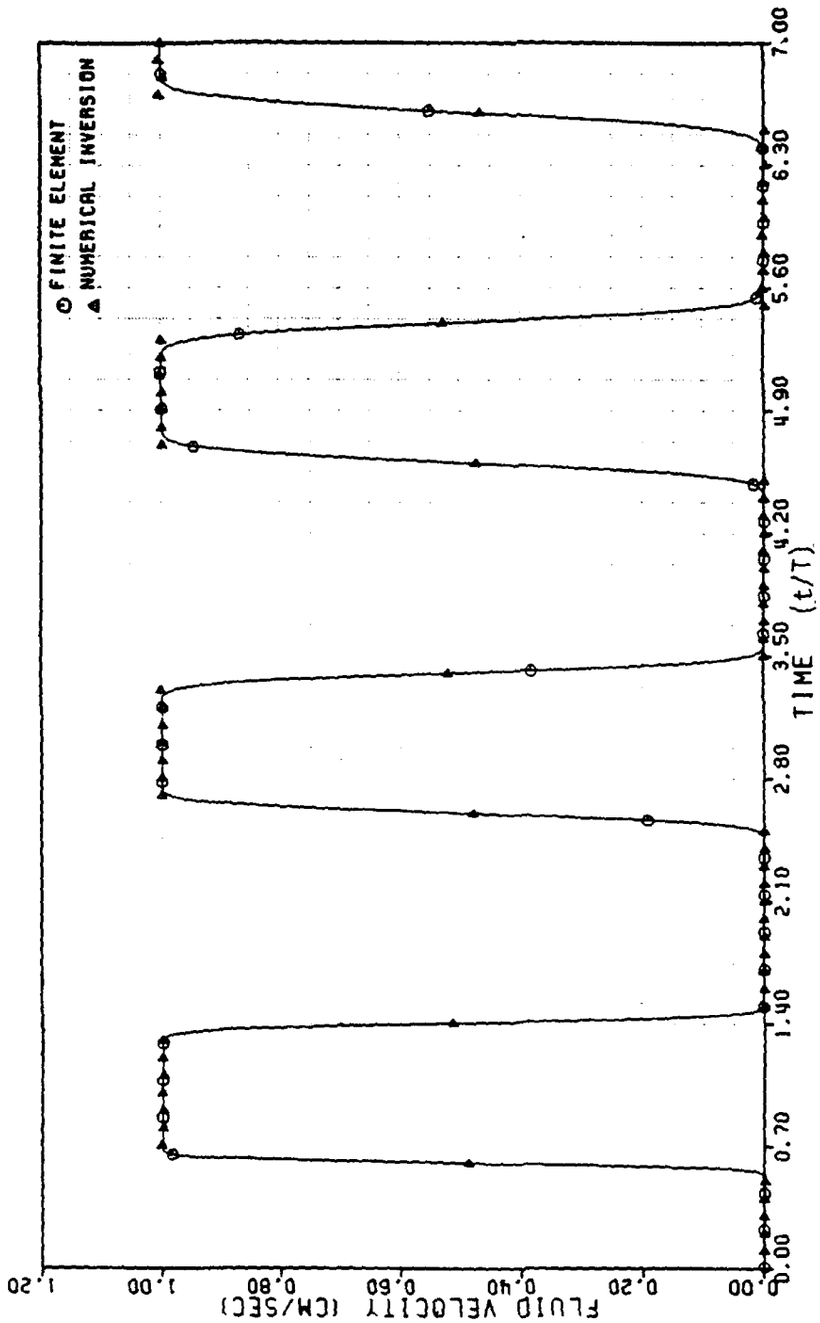

Figure 18: Example 1: Fluid Velocity History at 30 cm. (High Drag)

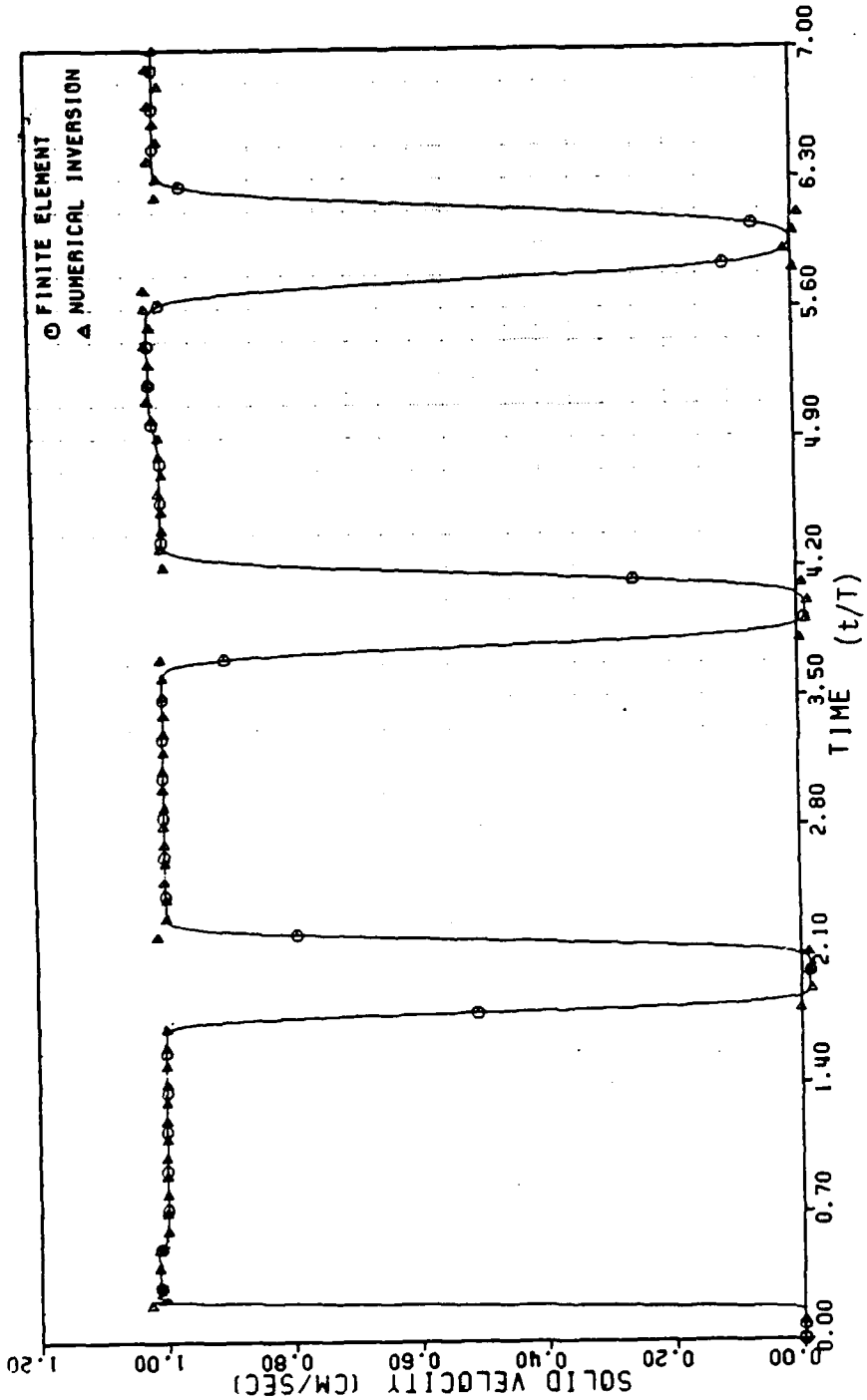

Figure 19: Example 2: Solid Velocity History at 10 cm. (Low Drag)

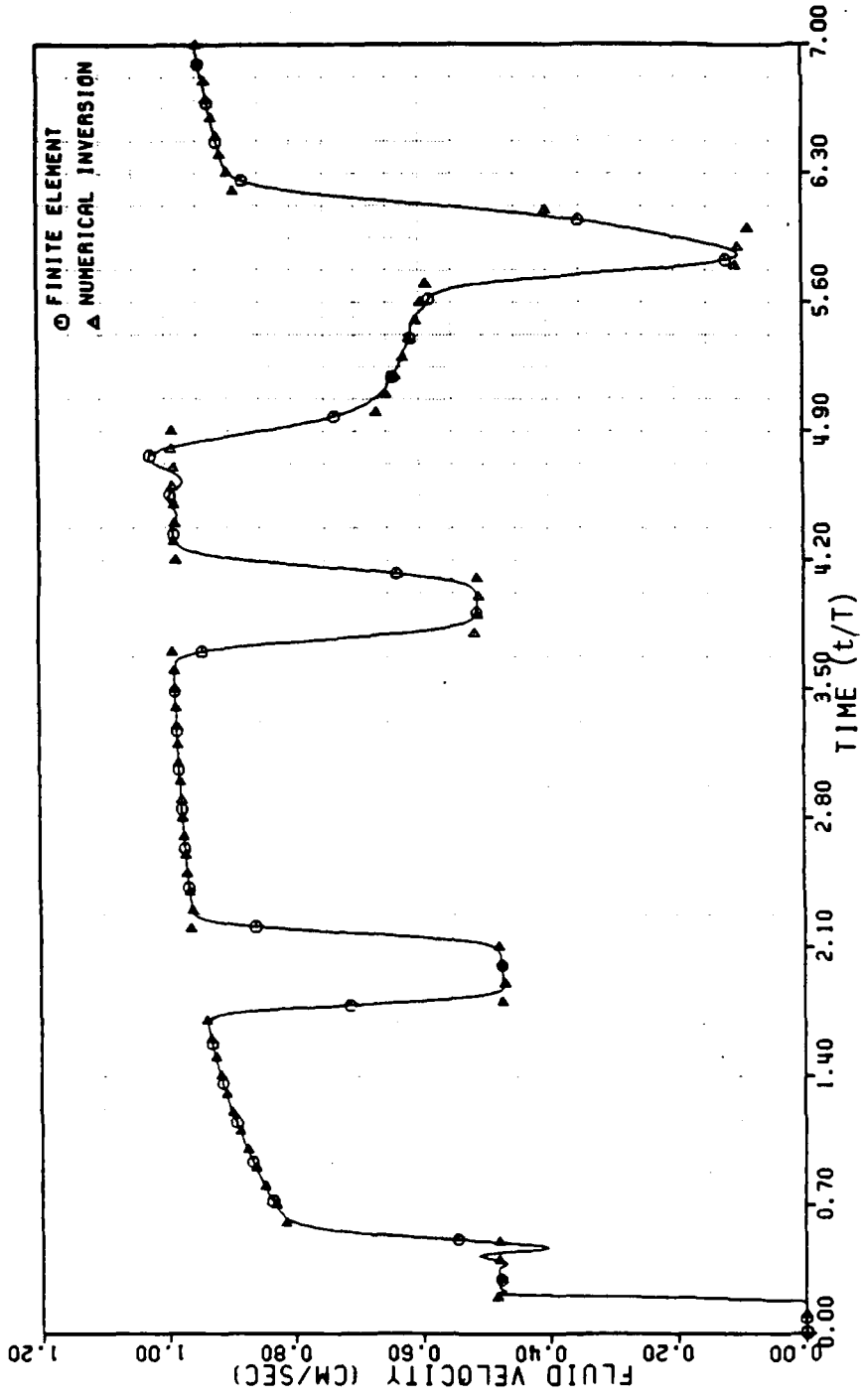

Figure 20: Example 2: Fluid Velocity History at 10 cm. (Low Drag)

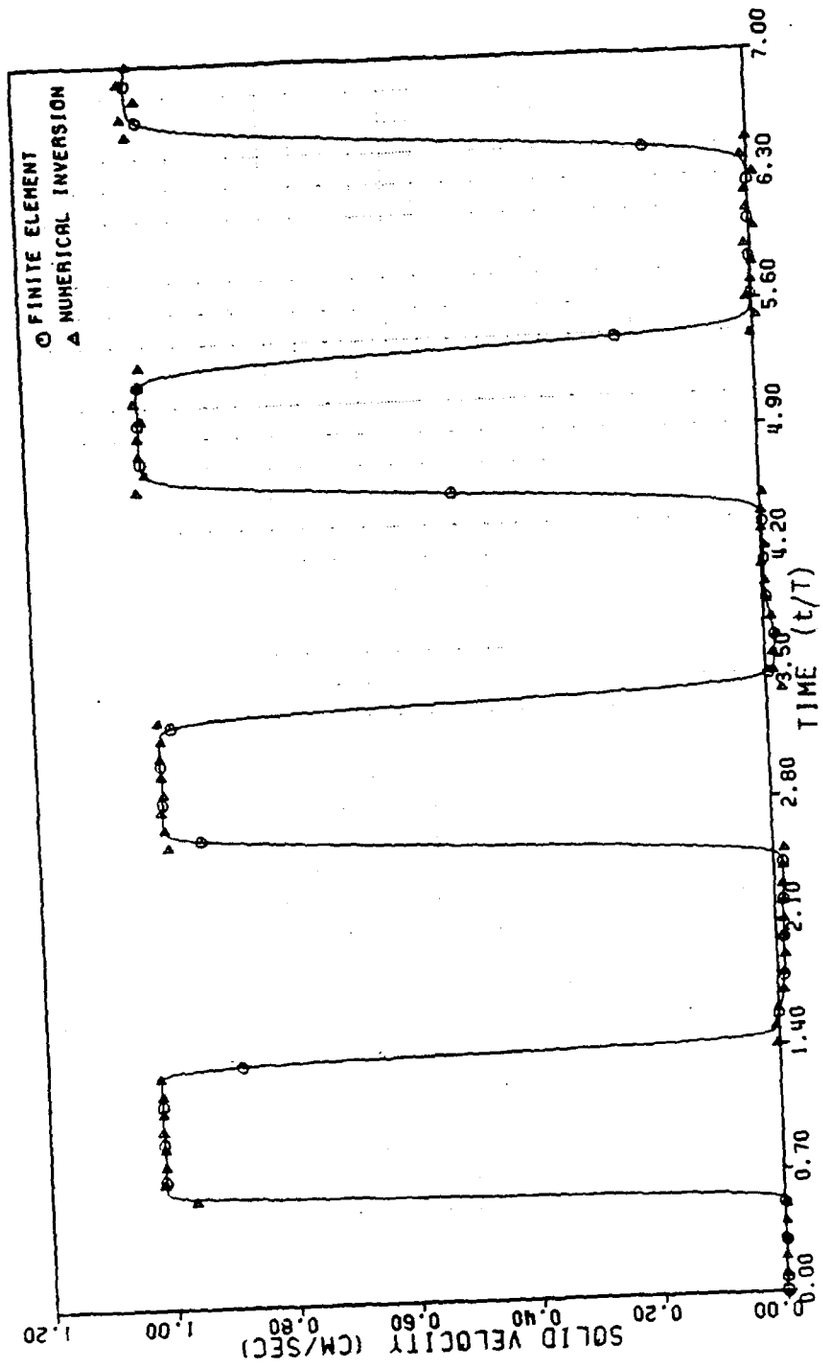

Figure 21: Example 2: Solid Velocity History at 30 cm. (Low Drag)

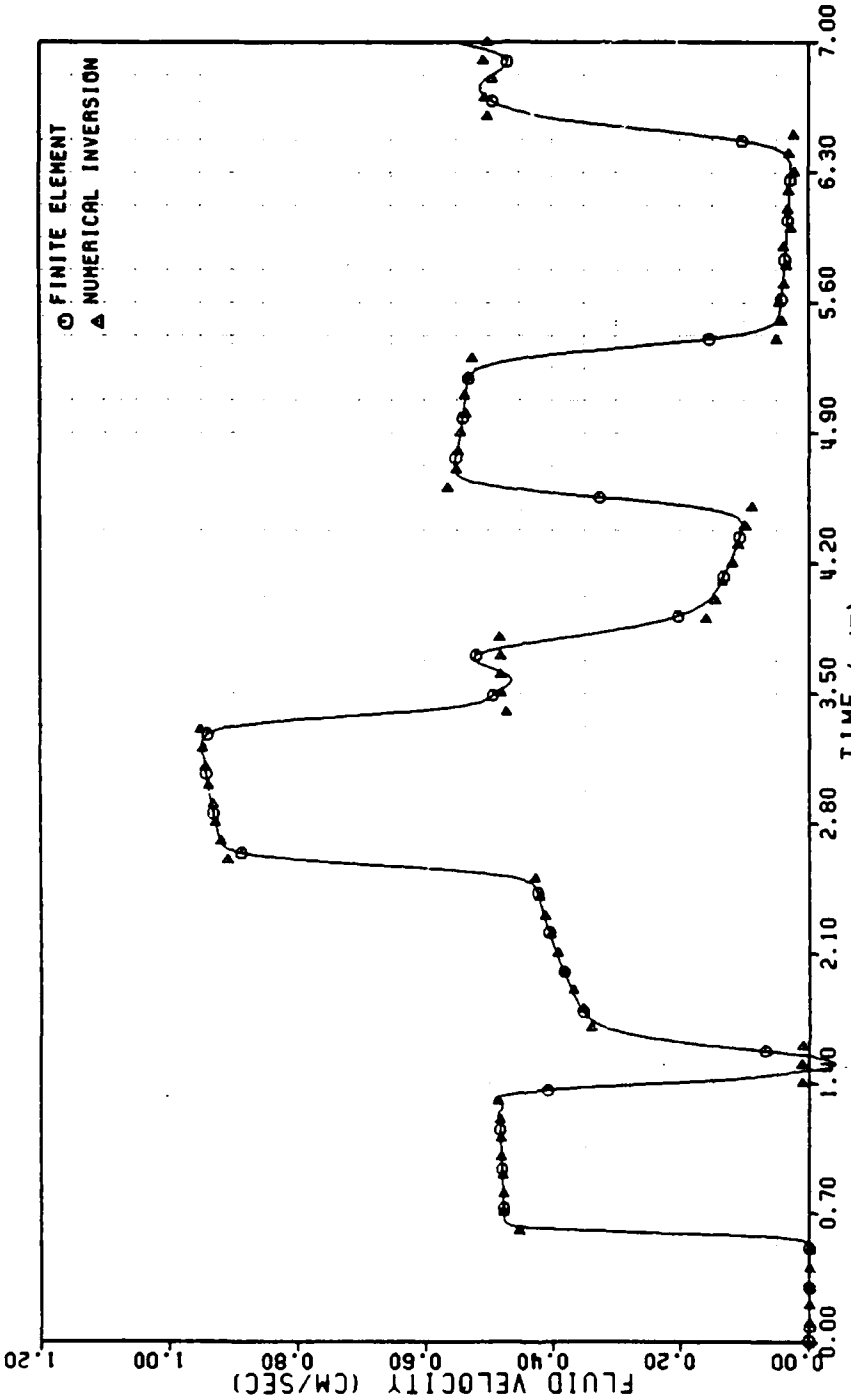

Figure 22: Example 2: Fluid Velocity History at 30 cm. (Low Drag)

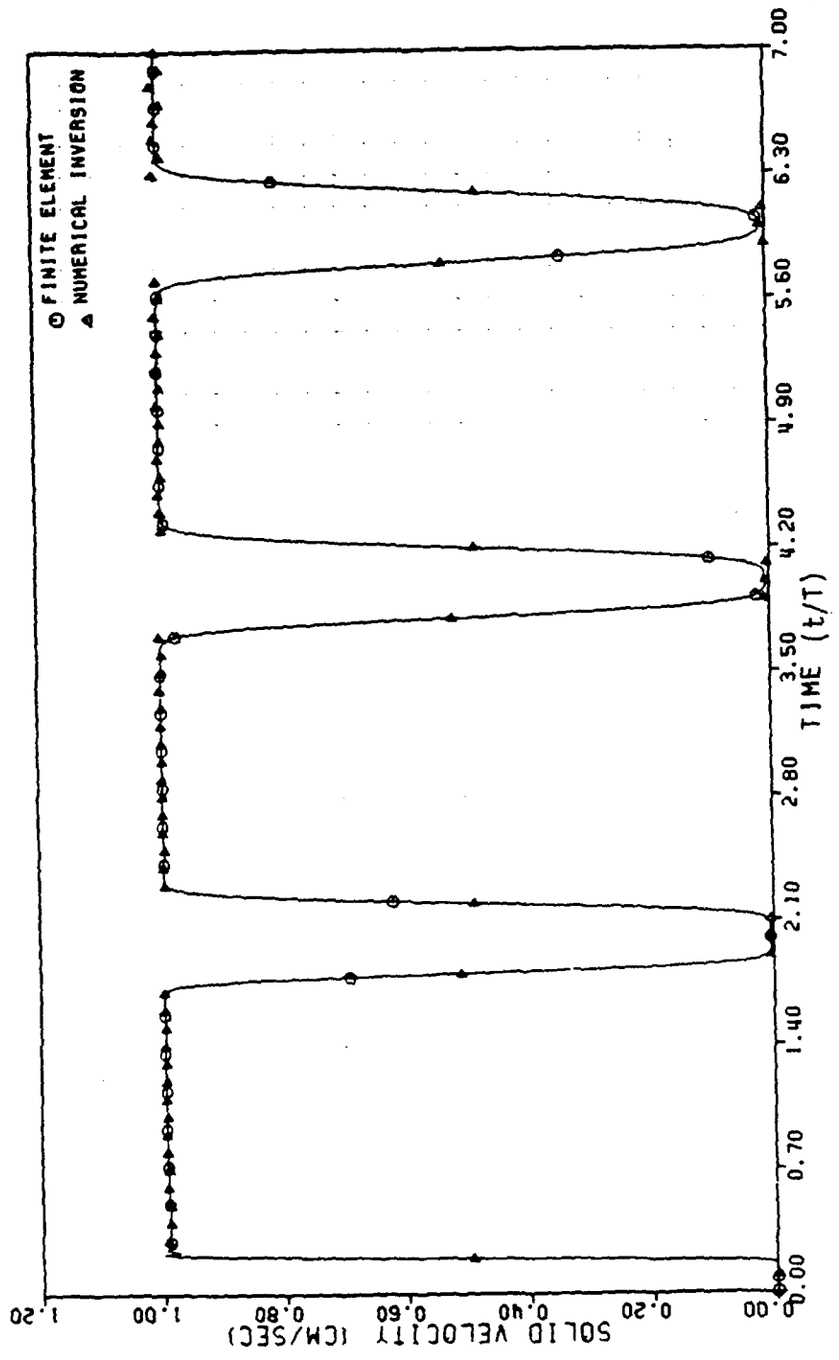

Figure 23: Example 2: Solid Velocity History at 10 cm. (High Drag)

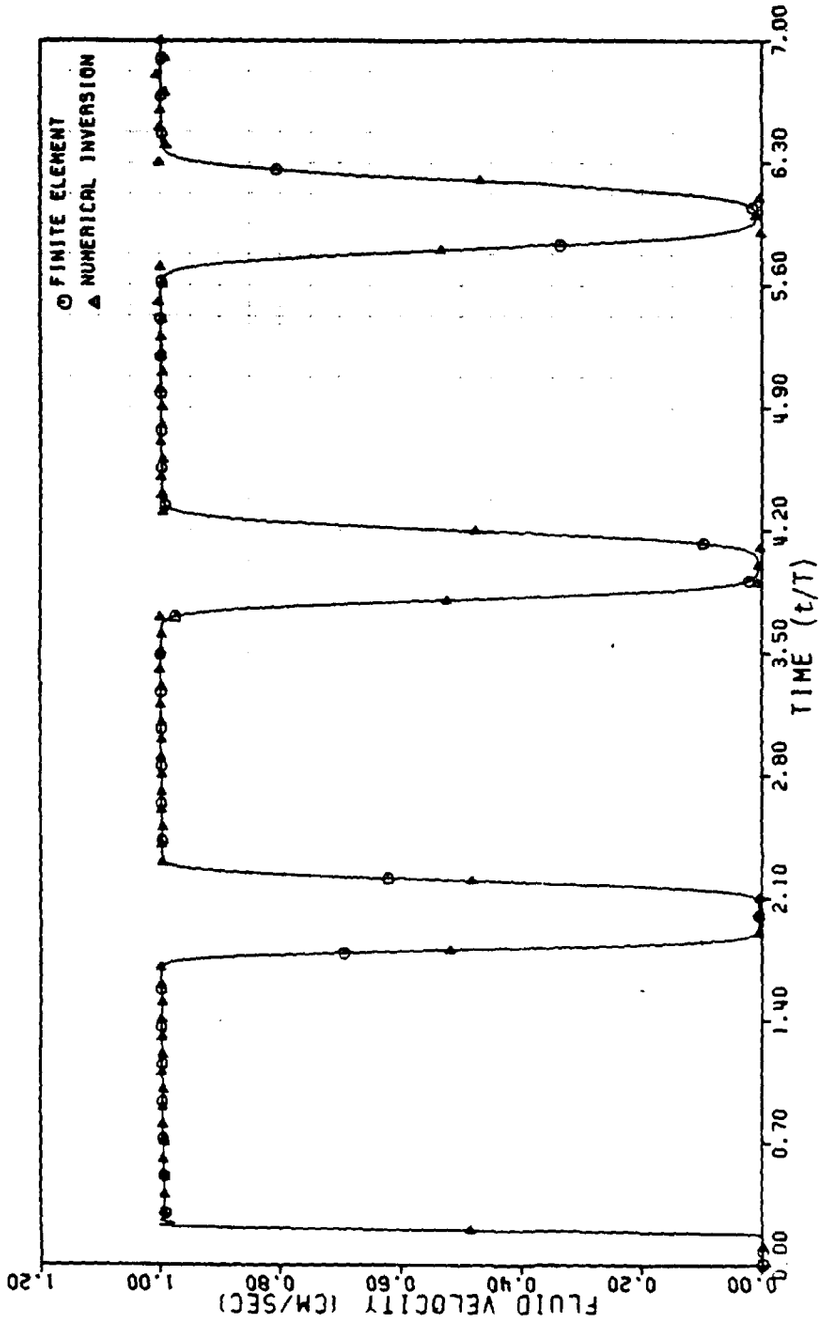

Figure 24: Example 2: Fluid Velocity History at 10 cm. (High Drag)

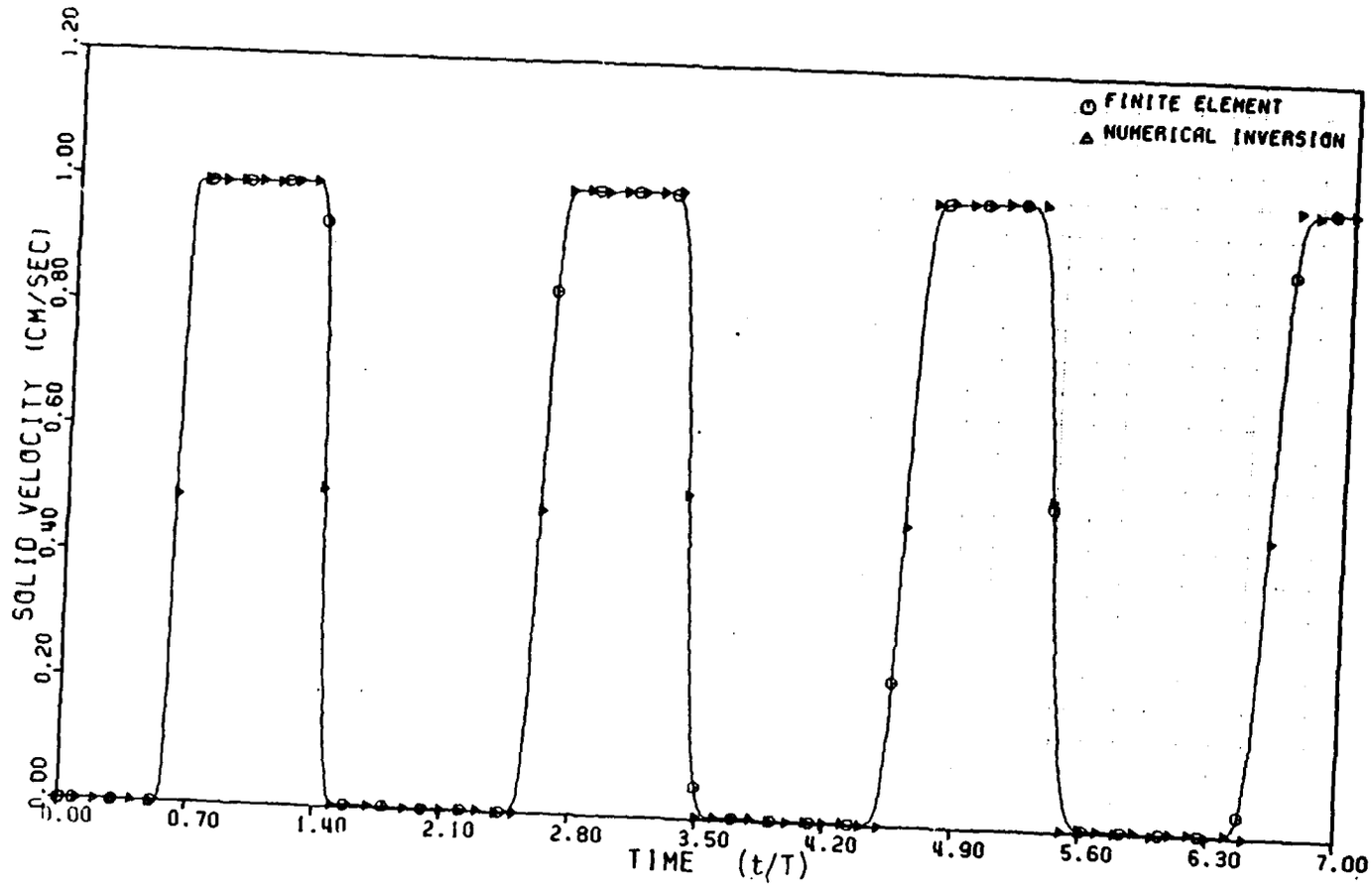

Figure 25: **Example 2: Solid Velocity History at 30 cm. (High Drag)**

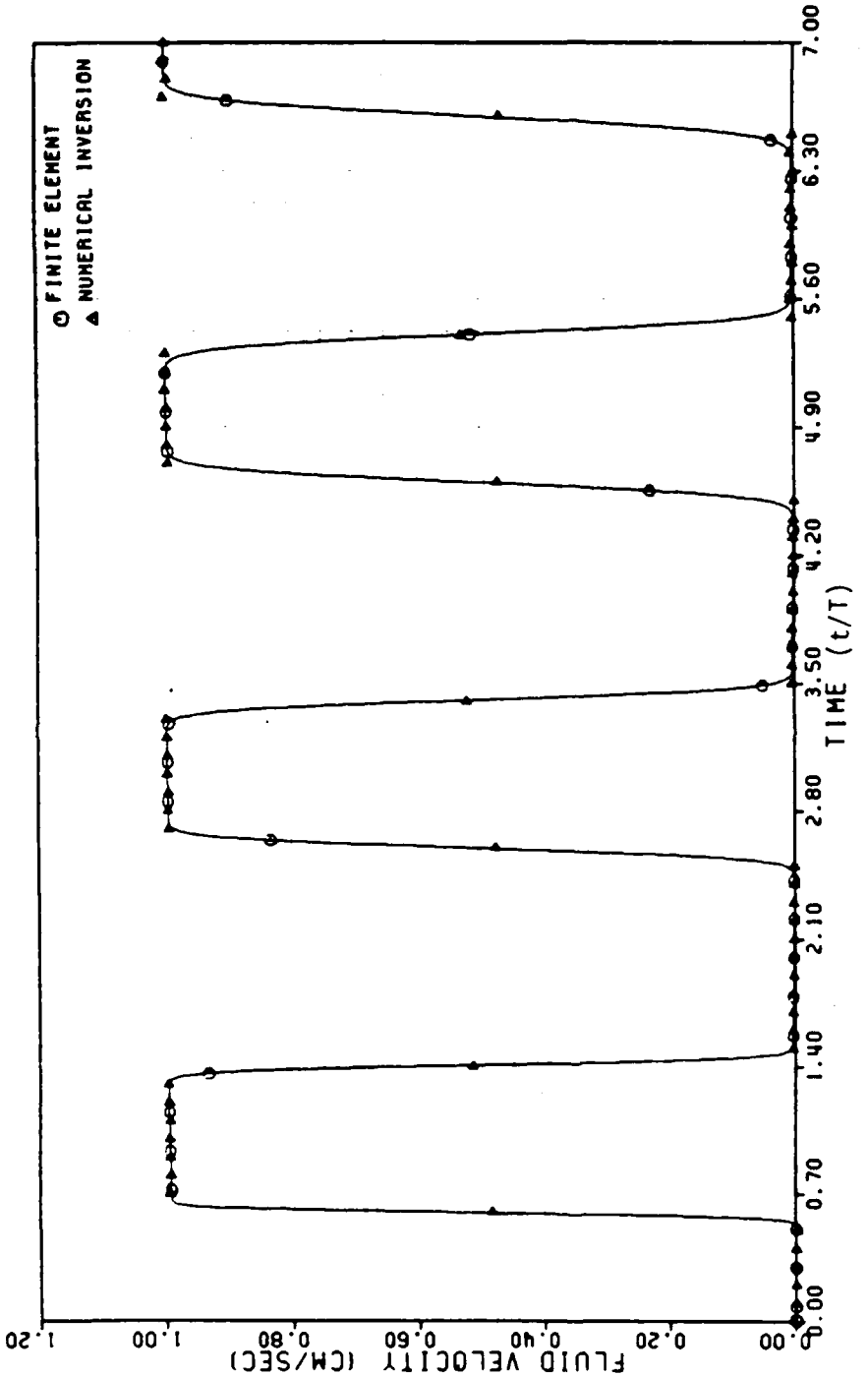

Figure 26: Example 2: Fluid Velocity History at 30 cm. (High Drag)

4.4.6 Nonlinear Problems

For nonlinear problems, an incremental approach was necessary. The equations governing this case along with a variational formulation of the problem were developed (item 1.13 of Appendix B). Only material nonlinearity was considered.

At any instant of time t, the equilibrium forces acting on the discretized system can be represented by

$$\begin{bmatrix} M_{ss} & M_{sf} \\ M_{ss} & M_{sf} \end{bmatrix} \begin{Bmatrix} \ddot{u} \\ \ddot{w} \end{Bmatrix} + \begin{bmatrix} 0 & 0 \\ 0 & C_{ff} \end{bmatrix} \begin{Bmatrix} \dot{u} \\ \dot{w} \end{Bmatrix} + \begin{bmatrix} K_{ss} & 0 \\ 0 & 0 \end{bmatrix} \begin{Bmatrix} u \\ w \end{Bmatrix} + \begin{bmatrix} K_{ss} & K_{sf} \\ K_{ss} & K_{sf} \end{bmatrix} \begin{Bmatrix} u \\ w \end{Bmatrix} = \begin{Bmatrix} F_s \\ F_s \end{Bmatrix} + \begin{Bmatrix} P_s \\ P_s \end{Bmatrix} \tag{4.111}$$

Alternatively, one might write

$$F_I(t) + F_D(t) + F_S^{\bullet}(t) + F_S^{\bullet\bullet}(t) = P(t) \tag{4.112}$$

where F_I, F_D are, respectively, the inertial and the damping force vector. $F_S^{\bullet}$ represents the internal resisting force related to the solid deformation only and $F_S^{\bullet\bullet}$ is the internal resisting force arising out of deformation of the fluid and coupling between the two phases, P denotes the applied load vector. A short time Δt later, the equation would be

$$F_I(t + \Delta t) + F_D(t + \Delta t) + F_S^{\bullet}(t + \Delta t) + F_S^{\bullet\bullet}(t + \Delta t) = P(t + \Delta t) \tag{4.113}$$

Subtracting (4.112) from (4.113),

$$F_I(t + \Delta t) - F_I(t) + F_D(t + \Delta t) - F_D(t) + F_S^{\bullet}(t + \Delta t) - F_S^{\bullet}(t)$$

$$+ F_S^{\bullet\bullet}(t + \Delta t) - F_S^{\bullet\bullet}(t) = P(t + \Delta t) - P(t) \tag{4.114}$$

Noting

$$F_I(t + \Delta t) = M(t + \Delta t)\ddot{u}(t + \Delta t), \tag{4.115}$$

expanding $M(t + \Delta t)$ and $\ddot{u}(t + \Delta t)$ in terms of Taylor's series, and retaining only the first order terms in Δt gives

$$F_I(t + \Delta t) = M(t)\ddot{u}(t) + M(t)\,\Delta\ddot{u}(t) + \Delta M(t)\ddot{u}(t) \tag{4.116}$$

Similarly, the quantities

$$F_D(t+\Delta t) = C(t+\Delta t)\dot{u}(t)$$

$$F_S^*(t+\Delta t) = K^*(t+\Delta t)u(t+\Delta t) \tag{4.117}$$

$$F_S^{**}(t+\Delta t) = K^{**}(t+\Delta t)u(t+\Delta t)$$

can be approximated as

$$F_D(t+\Delta t) = C(t)\dot{u}(t) + C(t)\Delta\dot{u}(t) + \Delta C(t)\dot{u}(t)$$

$$F_S^*(t+\Delta t) = K^*(t)u(t) + K^*(t)\Delta u(t) + \Delta K^*(t)u(t) \tag{4.118}$$

$$F_S^{**}(t+\Delta t) = K^{**}(t)u(t) + K^{**}(t)\Delta u(t) + \Delta K^{**}u(t)$$

Use of (4.116) and (4.118) in (4.114) yields

$$M(t)\Delta\ddot{u}(t) + \Delta M(t)\ddot{u}(t) + C(t)\Delta\dot{u}(t) + \Delta C(t)\dot{u}(t) + K^*(t)\Delta u(t) + \Delta K^*(t)u(t)$$
$$+ K^{**}\Delta u(t) + \Delta K^*u(t) = P(t+\Delta t) - M(t)\ddot{u}(t) + C(t)\dot{u}(t)$$
$$- K^*(t)u(t) + K^{**}(t)u(t) \tag{4.119}$$

This represents a general form of incremental equations. If mass, damping and stiffness quantities at time t are known, (4.119) can be solved for $\Delta u(t)$ by step-forward integration scheme, which also yields $\Delta\dot{u}(t)$ and $\Delta\ddot{u}(t)$. In doing so, the quantities themselves are dependent on the solution $\Delta u(t)$ and hence an iterative scheme to reduce the cumulative error is necessary.

The theory was specialized to the case of nonlinearity only in the soil/stress relations. This case was implemented in two finite element programs. In the code NAOWP (Nonlinear Analysis of Wave Propagation) elastic-perfectly plastic and bilinear stress-strain relations were used. The other code named DANS (Dynamic Analysis of Nonlinear Soils) incorporated a more general model of elastic-plastic work-hardening proposed by Singh [160]. A modular structure was used so that a variety of models could be selected. Local iteration was employed within each time step and convergence assured

before going on to the next step. NAOWP was designed to model one-dimensional wave propagation. Linear variation over the spatial elements was assumed. In DANS (item 1.19 of Appendix B), bilinear and biquadratic isoparametric elements were implemented for two-dimensional wave propagation analyses. Since no exact solutions for nonlinear wave propagation in fluid-saturated soils were available, the codes were verified against exact solutions for single material wave propagation. Exact solutions for bilinear solids subjected to dynamic excitation have been developed by Belytschko [10] and for an elastic-perfectly plastic solid by Wood [173]. Figure 27 describes the discretization for a soil column as well as the suddenly applied loading for the three cases tested. Figure 28 shows the stress history for case 3 plotted against the exact solution by Belytschko. Figure 29 shows the stress pulse of short duration used by Wood [173] along with the elastic-perfectly plastic soil column. Figure 30 to Figure 34 show the stress profiles at time equal to 4, 8, 12, 16 and 20 plotted against the exact solution by Wood [173] for different levels of mesh refinement. Item 1.13 of Appendix B contains details of the approach as well as illustrative applications of the two computer programs to wave propagation through a saturated soil layer.

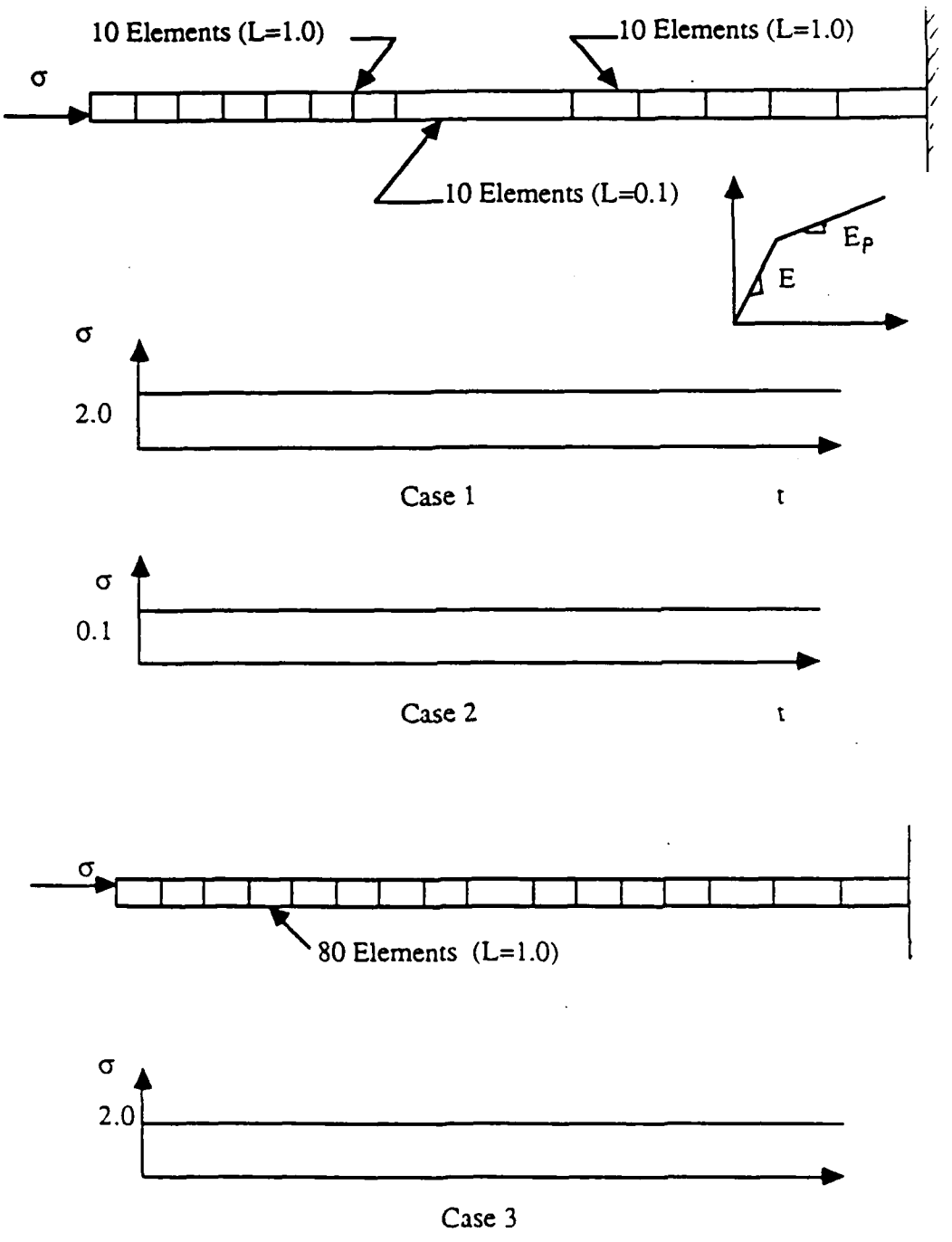

Figure 27: Discretization of the Soil Column

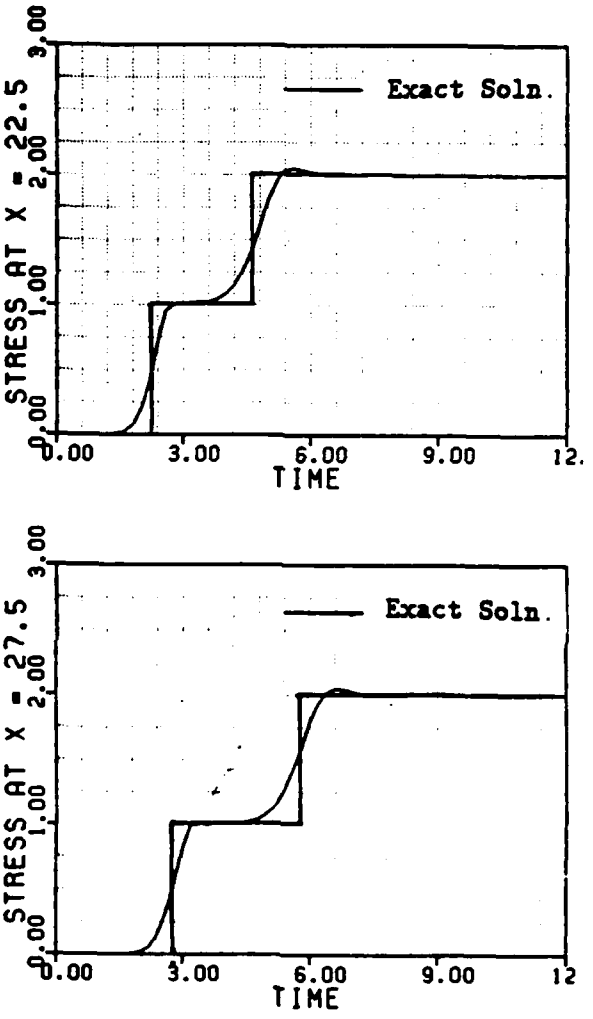

Figure 28: Sress History for Case 3.

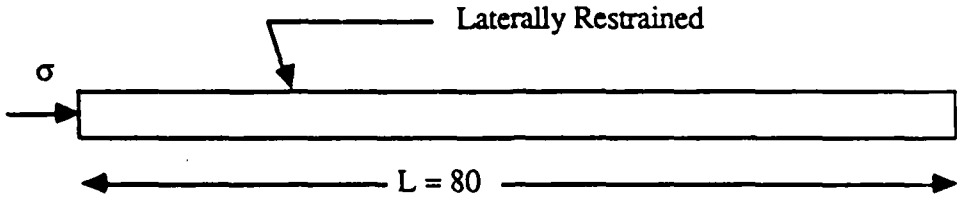

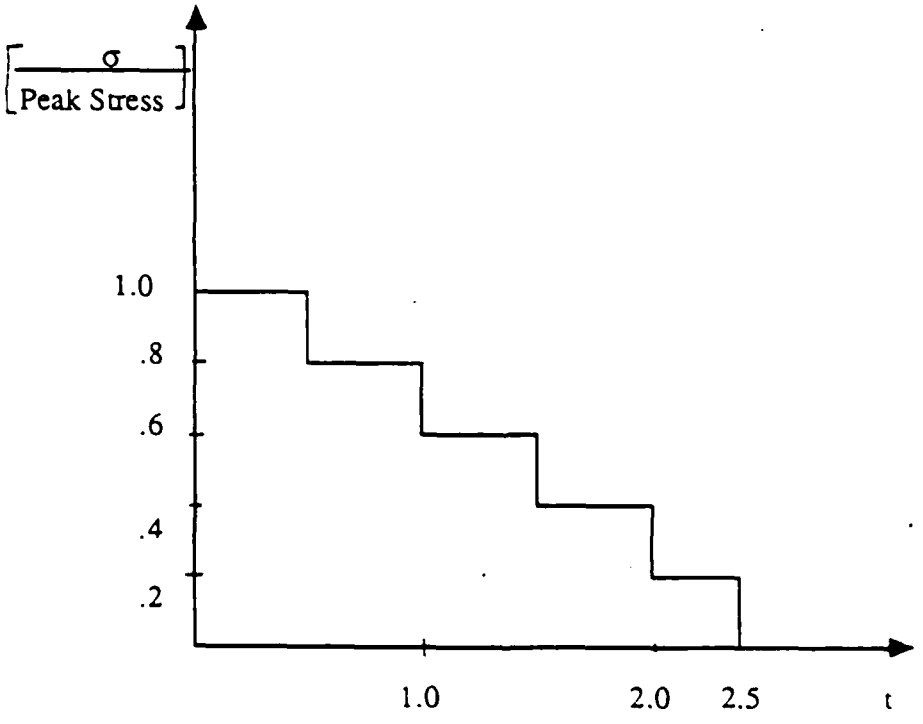

Figure 29: Solid Column Under Stress Pulse of Short Duration

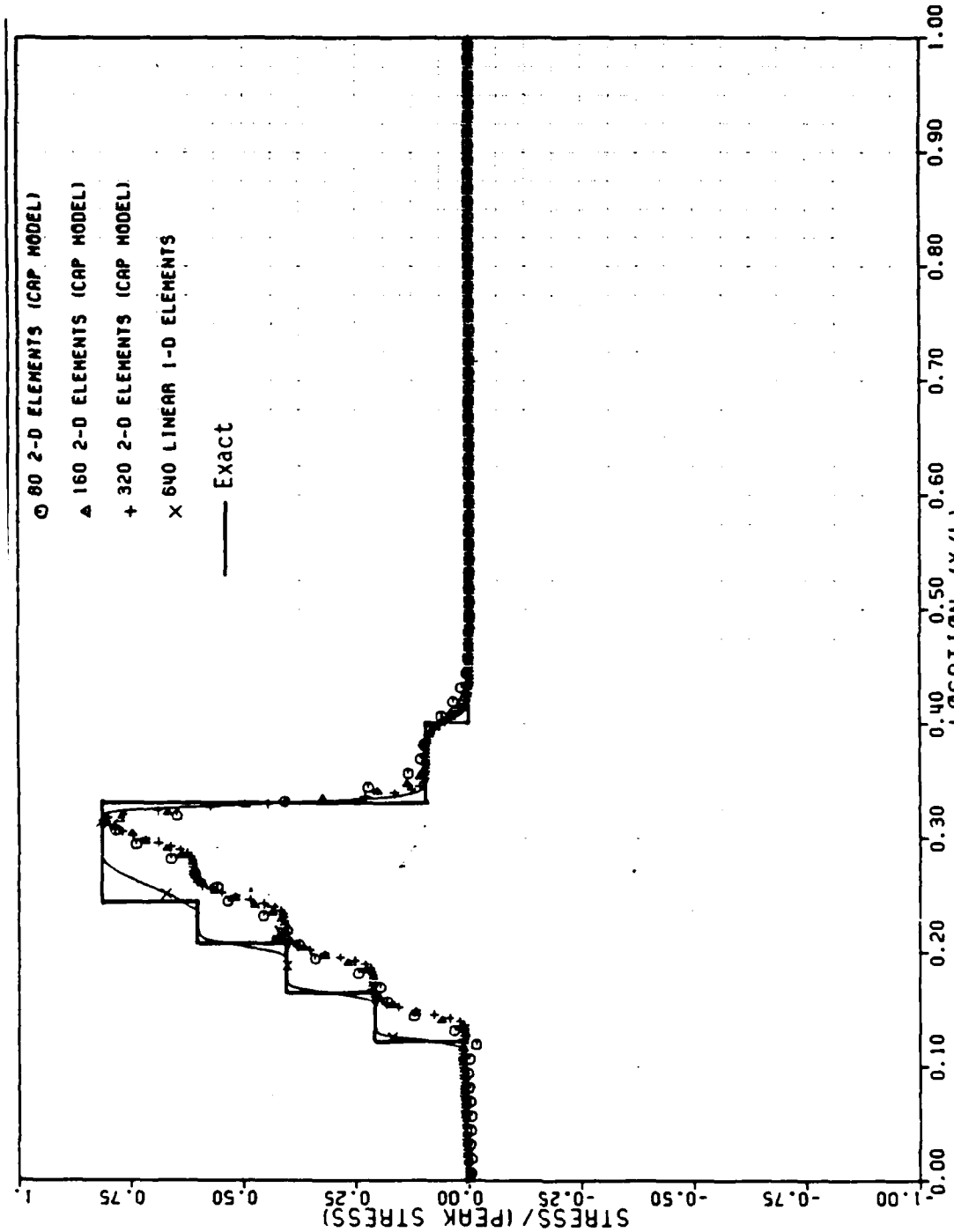

Figure 30: Stress Profile at t = 4.

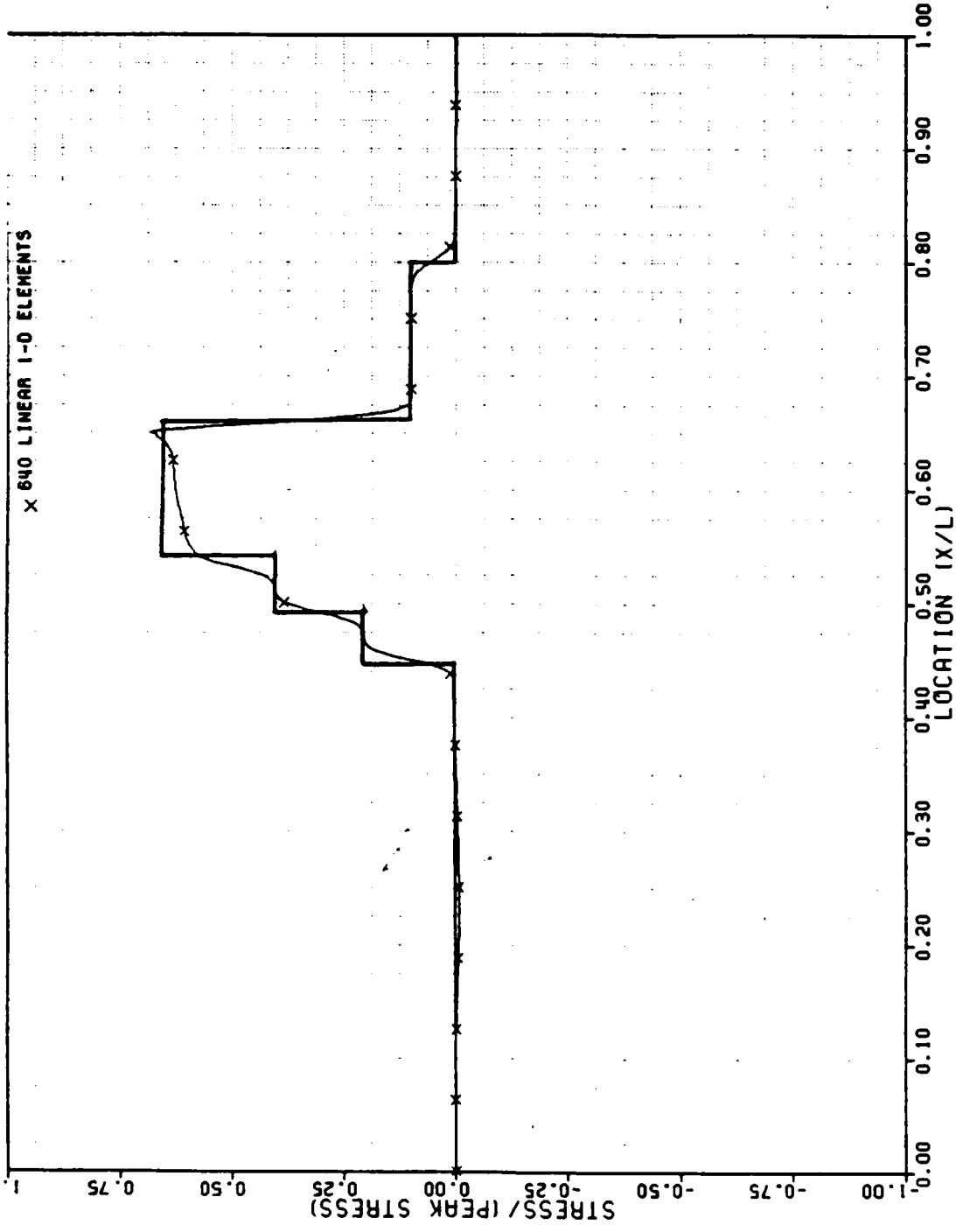

Figure 31: Stress Profile at t = 8.

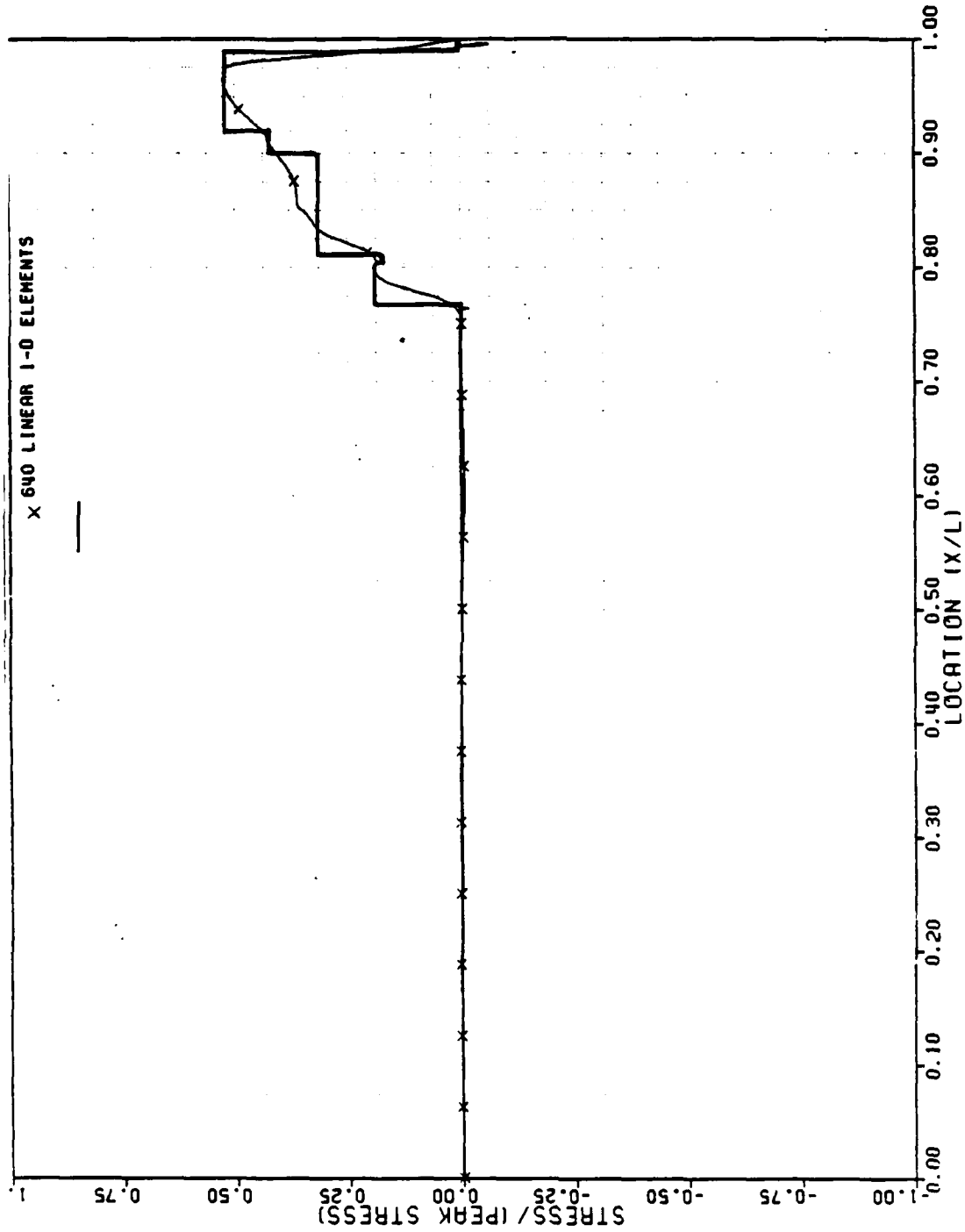

Figure 32: Stress Profile at t = 12.

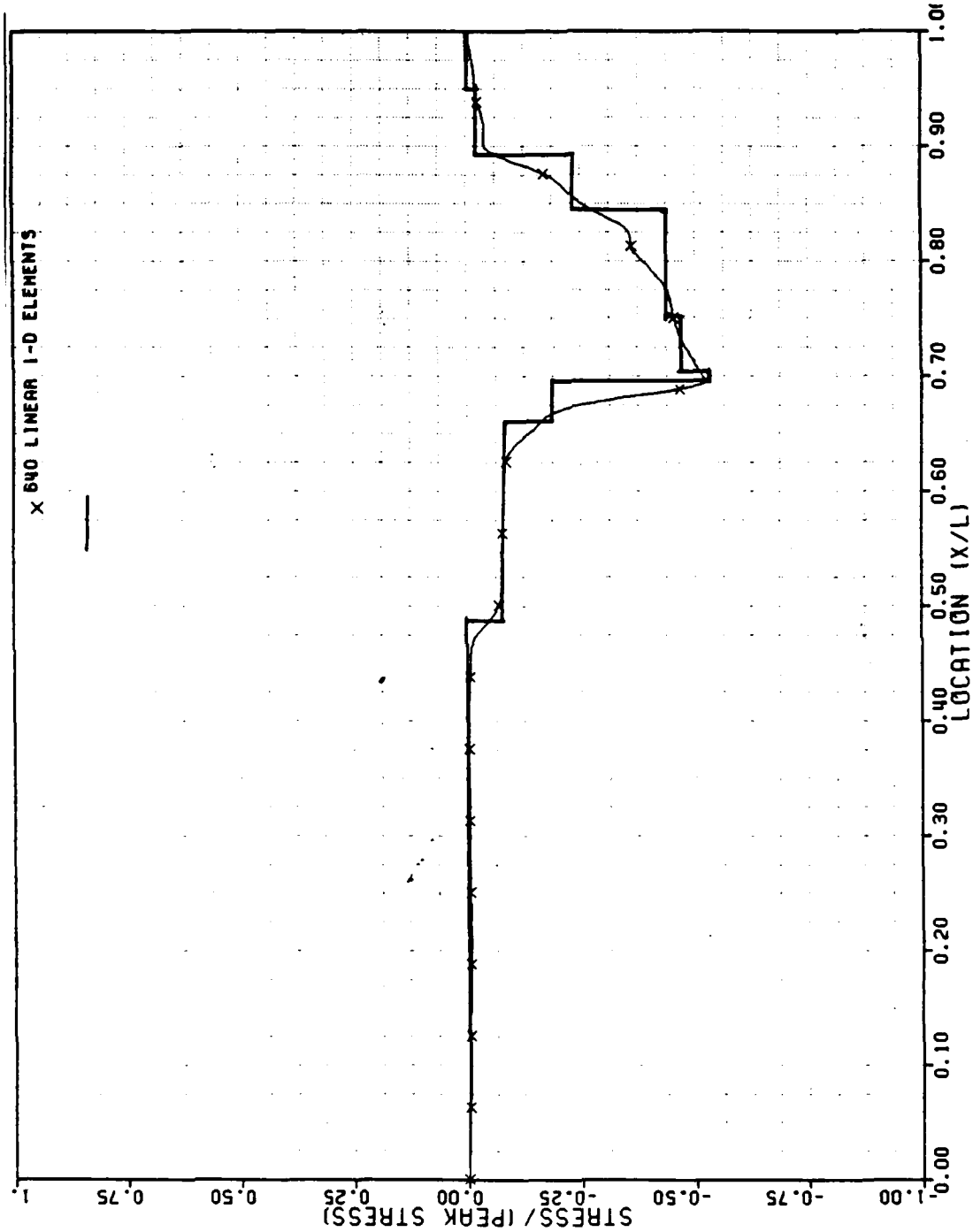

Figure 33: Stress Profile at t = 16.

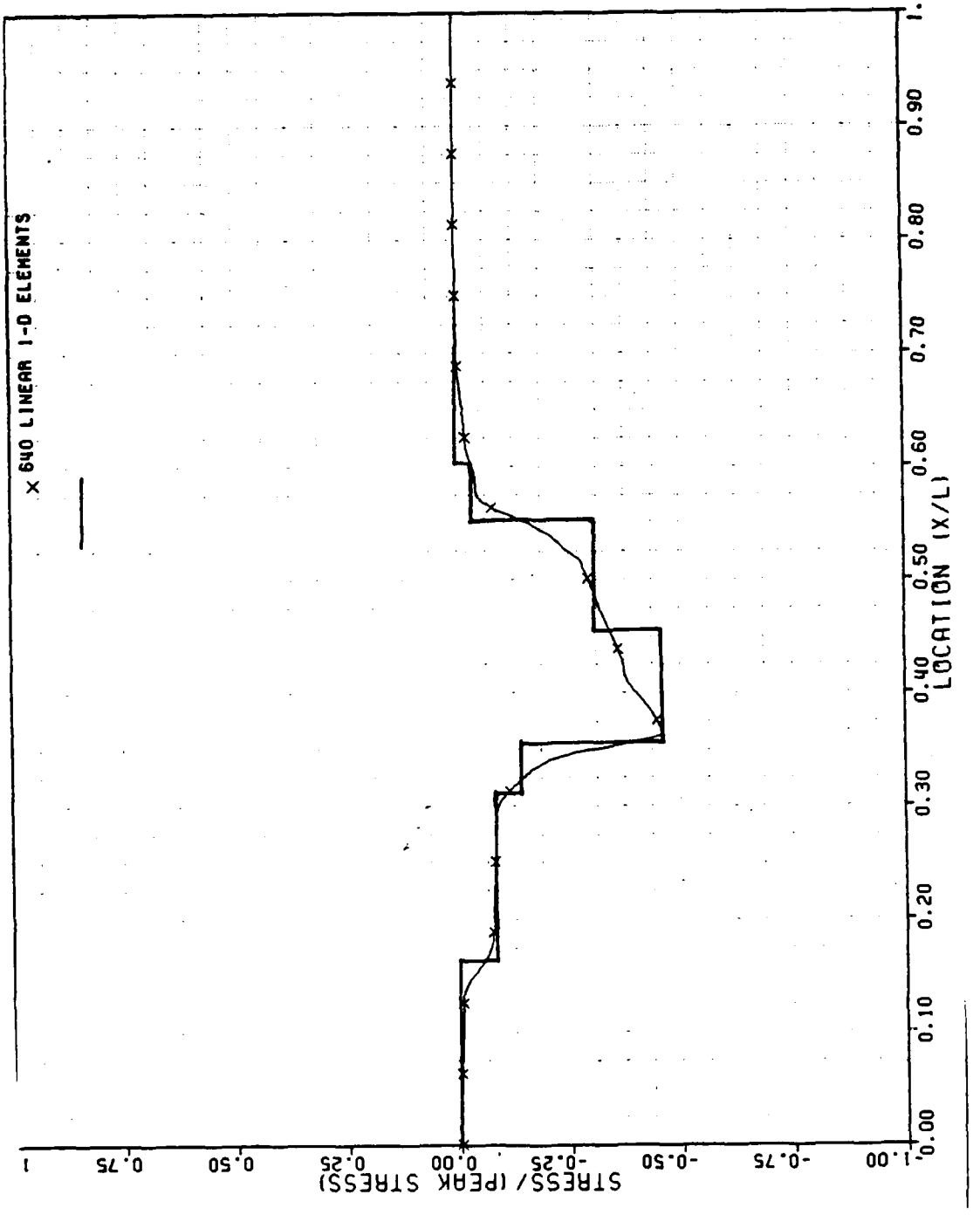

Figure 34: Stress Profile at t = 20.

Section V

LABORATORY INVESTIGATIONS

5.1 INTRODUCTION

Historically, laboratory studies of material behavior of saturated sands under cyclic stress conditions have played an important role in the determination of liquefaction potential. Numerous investigators have tried to model and predict the potential and probability of liquefaction occurring in soils. Various test apparatus have been designed or modified in an attempt to provide an accurate representation of the stress state generated in-situ by ground motion. A number of experimental devices including the cyclic triaxial, cyclic simple shear, torsional shear and shaking table have been developed. A wide diversity of data have been generated with the use of a dynamic (or pseudo-dynamic) excitation loading pattern. Detailed reviews of these experimental programs and design methods based upon them, can be found in several state-of-the-art reports. In particular, those by Seed [155-158], Finn [44], Casagrande [31] and the National Research Council [109] should be noted.

The laboratory method used in this study to load the sand samples was a shaking table. It is well known that the variety of small scale apparatus currently in use in the laboratory introduce non-uniform stress and strain fields in the sample being tested (eg. [31,127,94,174]). Since the onset of liquefaction is clearly a local phenomenon, it is certain that a measure of the liquefaction resistance of a saturated sand would be affected by these stress and strain concentrations. The result of stress concentration induced liquefaction would be an underprediction of the true liquefaction resis-

tance. Therefore, although the shaking table is not as widely used as the other laboratory devices identified above, because it does more closely simulate actual field conditions, several previous investigators have used it as the basis for liquefaction studies. Among the many reports available on experimental programs are several in which shaking table tests were conducted specifically for the purpose of studying liquefaction including the programs of Finn [45], O-Hara [115], DeAlba [38], Seed [158] and Sasaki [139].

In an experimental program performed on samples of saturated sand in 1971, Finn [45] demonstrated the usefulness of the shaking table for conducting liquefaction studies. They observed that the shaking table offered several advantages over cyclic triaxial and simple shear devices. Chief among these advantages were: embedded instrumentation having a negligible effect on sample response can be used; the distribution of pore pressures over time can be monitored; the uniform accelerations developed in the plane strain specimens more closely corresponds to actual field conditions.

O-Hara [115] conducted shaking table tests on two different uniform sands. In addition, he performed cyclic triaxial and cyclic simple shear tests on the same material. He observed that sand samples tested on his shaking table typically showed an increased resistance to initial liquefaction when compared with the behavior of the same materials when tested in either of the two small scale devices.

The shaking table tests reported by DeAlba [38] performed on specimens of Monterey No. 0 sand. The samples were 4 inches high by 90 by 42 inches at the base tapering to 74 by 30 inches at the top. This shape was chosen so that a rubber membrane could easily be placed over the specimen and then pressurized to simulate a buried soil element. The size was chosen to provide free field conditions in the central portion of the specimen. The membrane under which the sample was confined allowed

the specimen to deform during the application of the cyclic load. Additional surcharge was applied to the specimen in the form of a reaction mass which was composed of steel shot placed in a bag on the top surface of the sand sample. Pore pressures were measured at several locations.

The results of further tests conducted on the Berkeley apparatus were presented by Seed [158] in an experimental program designed to study the effects of seismic history on a sand deposit. In these tests, Seed et.al. observed a dramatic increase in the number of cycles required to induce liquefaction in samples which previously had been subjected to cyclic motions significant enough to raise the pore pressure but not enough by themselves to cause liquefaction. Seed et.al. attribute the observed increase in cyclic strength to grain rearrangement. They pointed out that there is substantial evidence that these higher values of liquefaction resistance are more representative of the actual performance of natural sand deposits which have been subjected to past cyclic motions.

Sasaki [139] conducted a series of shaking table tests on sand samples. The sample size they chose was much larger than had been used in any previous programs (12 meters long by 3 meters high by 2 meters wide) and it is therefore more likely that true free field conditions existed in their samples. The samples were formed by pluviation through air similar to the procedure employed by Seed [158]. Saturation was reportedly accomplished by displacing the air through the infiltration of water from the bottom of the sample. The sand surface was unconfined. Instrumentation consisted of embedded pressure transducers and accelerometers. Measurements of cyclically induced increases in pore pressure were made at a total of 35 locations within the sample in both the free field and in the vicinity of an embedded concrete box intended to simulate a roadway. It should be noted that the increased pore pressure was an order of magnitude greater immediately beneath the roadway than it was in the free

field. Clearly the rate of pore pressure increase during shaking is very sensitive to the presence of local irregularities, in this case rigid inclusions.

In order to minimize these local effects on an experimentally obtained estimate of liquefaction potential, the test apparatus described in the following sections was employed. Herein we give a summary. Details are given in items 1.9, 2.6 and 4.3 of Appendix B.

5.2 EXPERIMENTAL FACILITIES

5.2.1 Introduction

The facilities used in the laboratory investigation of the liquefaction phenomenon were designed for the purpose of providing reproducible results in which the stress and strain conditions at the sample boundaries were well understood and could be reconstructed accurately in a numerical model. They consisted of a unidirectional shaking table to which was attached a test box with a capacity if approximately one cu. ft. of soil. The instrumentation employed to monitor the sample behavior consisted of accelerometers and pressure transducers.

5.2.2 Shaking table

A shaking table with a capacity of 2500 lbs. located in the Soil Dynamics laboratory at the Ohio State University was designed for the liquefaction testing program. Table motion was provided by an MTS system capable of producing peak accelerations of approximately $\pm$ 2 g. These high acceleration levels were achieved when the original 3 gpm pump was replaced by a 10 gpm pump purchased with contract funds. In order to make best use of the increased capacity of the pump, the existing single 10 gpm servovalve was replaced by dual 10 gpm servovalves in conjunction with two accumulators. The accumulators significantly improved the system performance during

conditions of peak fluid flow. The input signal could be either periodic or an externally programmed random acceleration time history. A schematic diagram of the liquefaction testing system is shown in Figure 35.

5.2.3 Test Box

The test chamber which was bolted to the shaking table was designed so that:

- The length to height ratio of the samples would be such that a free field plane strain condition existed in a substantial portion of the specimen.
- Moveable inner walls which would provide the required lateral support to the sample during construction, could be withdrawn at the start of the cyclic test so that the sample could deform under plane strain conditions.
- Normal stresses on the horizontal faces of the sample could be chosen independently of the stresses on the top face, thereby allowing for tests to be constructed on samples without requiring that K be = 1.

A diagram of the test chamber is shown in Figure 36.

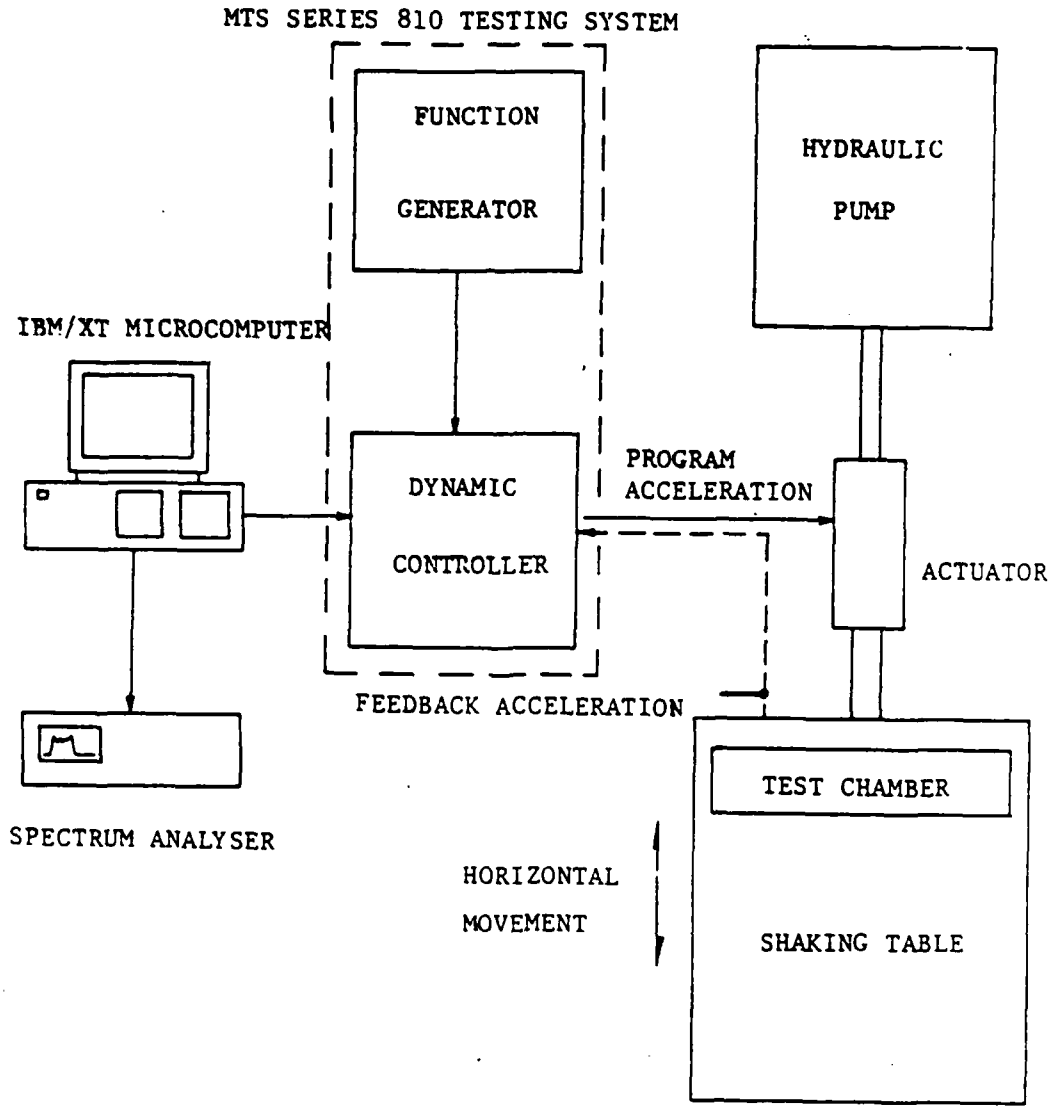

Figure 35: Large Scale Liquefaction Testing System

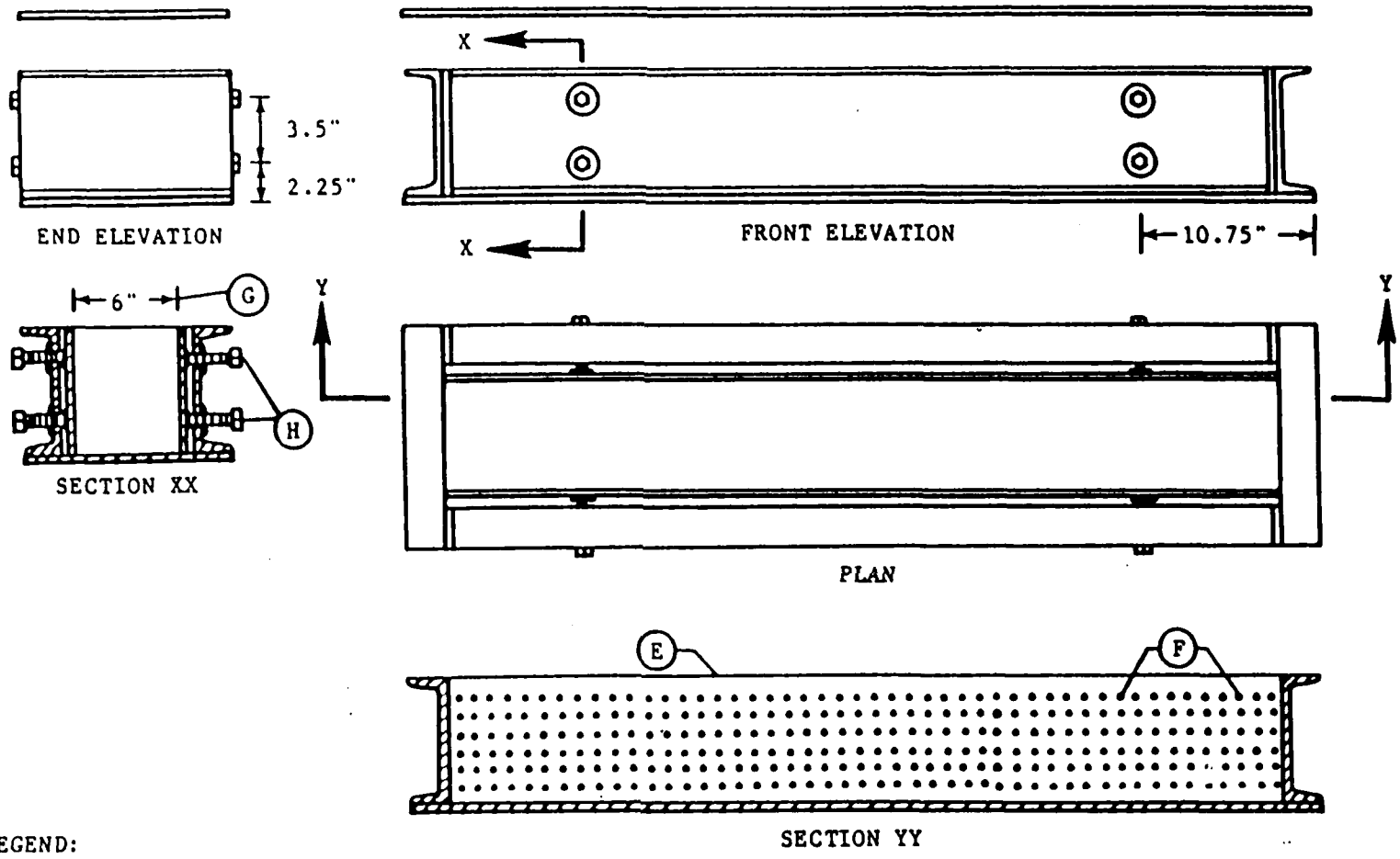

LEGEND:

E: MOVEABLE INNER WALLS
F: HOLES FOR TRANSMITTING PRESSURE
G: MINIMUM SAMPLE WIDTH
H: ADJUSTING BOLTS FOR INNER WALLS

Figure 36: Sample Test Chamber

5.2.4 Rubber Membrane

The rubber membrane surrounding the sample was made to the exact dimensions of the sample test chamber with the inner walls in their unretracted position. It was constructed so that different horizontal and vertical pressures could be applied to the sample. The membrane had to be thin and flexible so that the confining pressures would be transmitted uniformly, but strong enough to withstand the working pressures used. A fiber reinforced (nylon on nitrile) synthetic rubber sheet with a thickness of .025 cm met these requirements and was to make the membranes. The lower membrane, to which the horizontal pressure was applied, was in the shape of a rectangular box, supporting the bottom and four sides of the sample. The top membrane was a rectangular sheet placed on top of the sample after construction. With the lid of the test box in place, the top membrane acted as a gasket, sealing the confining fluid around the sides from the fluid on the top of the specimen.

5.2.5 Instrumentation

Two types of instrumentation were employed in the laboratory investigation. Pore water pressure measurements were made using transducers attached to hypodermic needles. This allowed for direct measurement of the pore water pressure within the interior of the sample while causing minimal disturbance to the specimen. Small $\pm$ 5 g accelerometers were placed near the top of the sample and at the sample base to record table (input) motion as well as the response at the top of the sample. A typical instrumentation configuration is shown in Figure 37.

5.2.6 Test Material

Uniform Ottawa sand was used in all tests conducted during the experimental program. The minimum and maximum densities were determined to be 14.03 KN/cc and 15.99 KN/cc respectively. The grain size distribution for the test sand is shown in Figure 38.

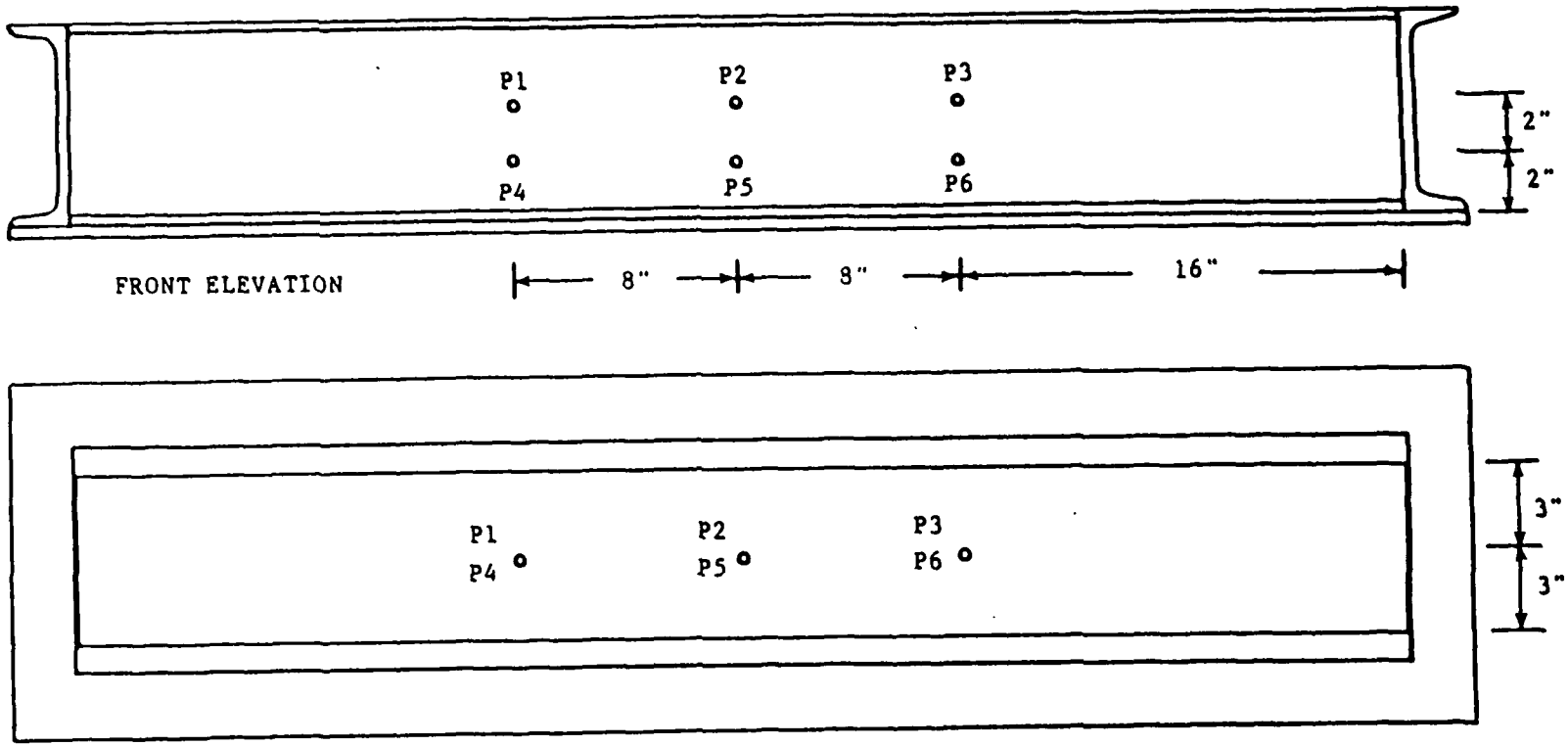

LEGEND:

P1...P6: PRESSURE TRANSDUCERS

Figure 37: Relative Positions of Pore Pressure Transducers

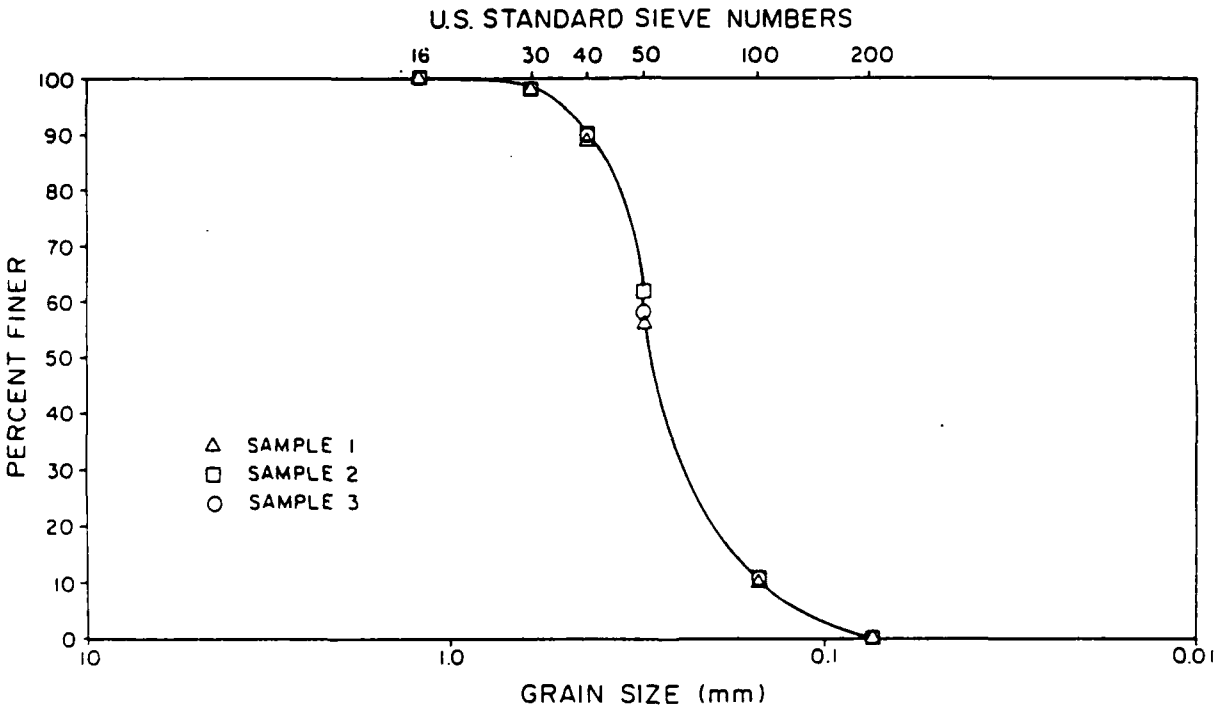

Figure 38: Ottawa Sand Gradation

5.3 TESTING PROCEDURES

5.3.1 Sample saturation

It is important for the proper measure of pore-pressure rise as a function of shaking that the sample be completely saturated. The procedure chosen for saturating the test specimens was to boil the sample in deaired water under a vacuum for not less than 30 minutes. Each sample was constructed in the test chamber by pluviation through water. This method was chosen because it has been our experience that preparing specimens this way will consistently yield saturated, uniform samples at a desired density. In order to increase the liquefaction potential, the samples tested in the OSU studies were deposited in a loose state, with relative densities ranging from 23% to 54%. To be sure full saturation was achieved, Skempton's pore water pressure parameter (B) was determined prior to testing. According to Black and Lee [22], values of B equal to 1.0 signify full saturation of samples of low relative density. A value for B greater than 0.95 signifies an acceptable degree of saturation for sand samples having high degrees of relative density. Considering the relative densities used in this study, a B value greater than or equal to 0.98 was considered indicative of full saturation.

5.3.2 Sample Confinement

Since the top of the specimen could be pressurized independently of the sides, any ratio of vertical to horizontal stress could have been used. Two different different ratios were tested. The response of samples consolidated under isotropic conditions were the majority of the tests performed in order to make comparisons with other experimental data practical. Several samples were liquefied after being consolidated anisotropically (K = 0.6).

5.3.3 Input Motions

Two types of input motions were used in this study. The first, a harmonic input of 10 Hz was chosen to allow for comparison between published liquefaction data which are predominantly periodic. The second, a random amplitude acceleration time history was included in the program to more closely simulate the type of motion actually experienced during a seismic or a blast induced disturbance.

5.3.4 Harmonic motion

A nominal 10 Hz table motion was used in all harmonic tests. The 10 Hz frequency was chosen because it was high enough that significant acceleration levels (> 2 g) could be achieved within the stroke range of the actuator and yet was well below the natural frequency of the unstrained sample, thus permitting an assumption of uniform accelerations throughout the height of the sample. As can be seen in Figure 39, acceleration time histories recorded at the top of the specimen confirmed that the ratio of sample to table accelerations was, in fact, approximately equal to 1.0 with a phase shift consistent with a wave speed of about 1000 in/sec.

De Alba [38] had constructed their sand samples using a reaction mass which had been placed on top of the sample. In an attempt to explain experimentally the difference between DeAlba's and our results, our test conditions as described above were modified. The modification consisted of a reaction mass similar to that used by DeAlba being added to the test specimen.

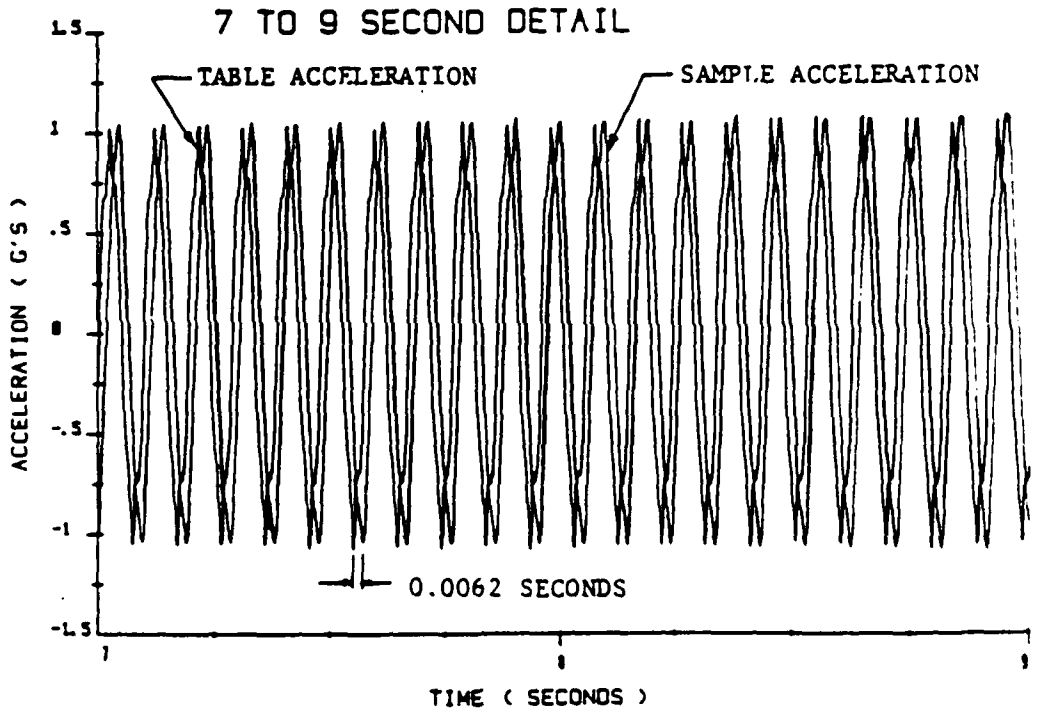

Figure 39: Comparison of Table and Sample Acceleration Time Histories for Harmonic Excitation

5.3.5 Random Motion

A standard method of illustrating the frequency content of an acceleration time history is by means of a Fourier amplitude spectrum. The Fourier spectrum is an indication of the final energy in the excitation as a function of frequency. In the context of the liquefaction tests, the peaks of the spectrum represent frequencies at which relatively large amounts of energy were supplied to the shaking table/sand system. The Fourier amplitude spectrum for the input excitation is presented in Figure 40. The spectra show the dominant frequencies of the pink noise input to be between 6 to 15 Hz. This frequency range was selected to symmetrically bracket the harmonic liquefaction potential data. The input motions were derived from data generated on an IBM/PC XT microcomputer and show an essentially constant amplitude in the desired frequency range. Three different time histories, each with essentially the same spectral content, were used as inputs to the shaking table.

5.3.6 RESULTS

The studies presented in this chapter were conducted to provide a better understanding of the liquefaction phenomenon through large scale liquefaction potential testing, and to provide data from carefully controlled experiments which would be suitable for use in model verification. Herein, a summary covering principal findings is given. Details are available in items 1.11, 1.16, 1.18, 4.3 and 4.4 of Appendix B.

The results of the harmonic input liquefaction tests performed on isotropically consolidated samples during this study are presented in Figure 41. The data are given in terms of number of cycles of shaking required for the sample reach the liquefied state versus the cyclic stress level. This type of presentation has been used by other investigators [88,96,107,145], and is presented here to facilitate a comparison between data collected in this study with those presented by DeAlba [38]. In Figure 41, it can

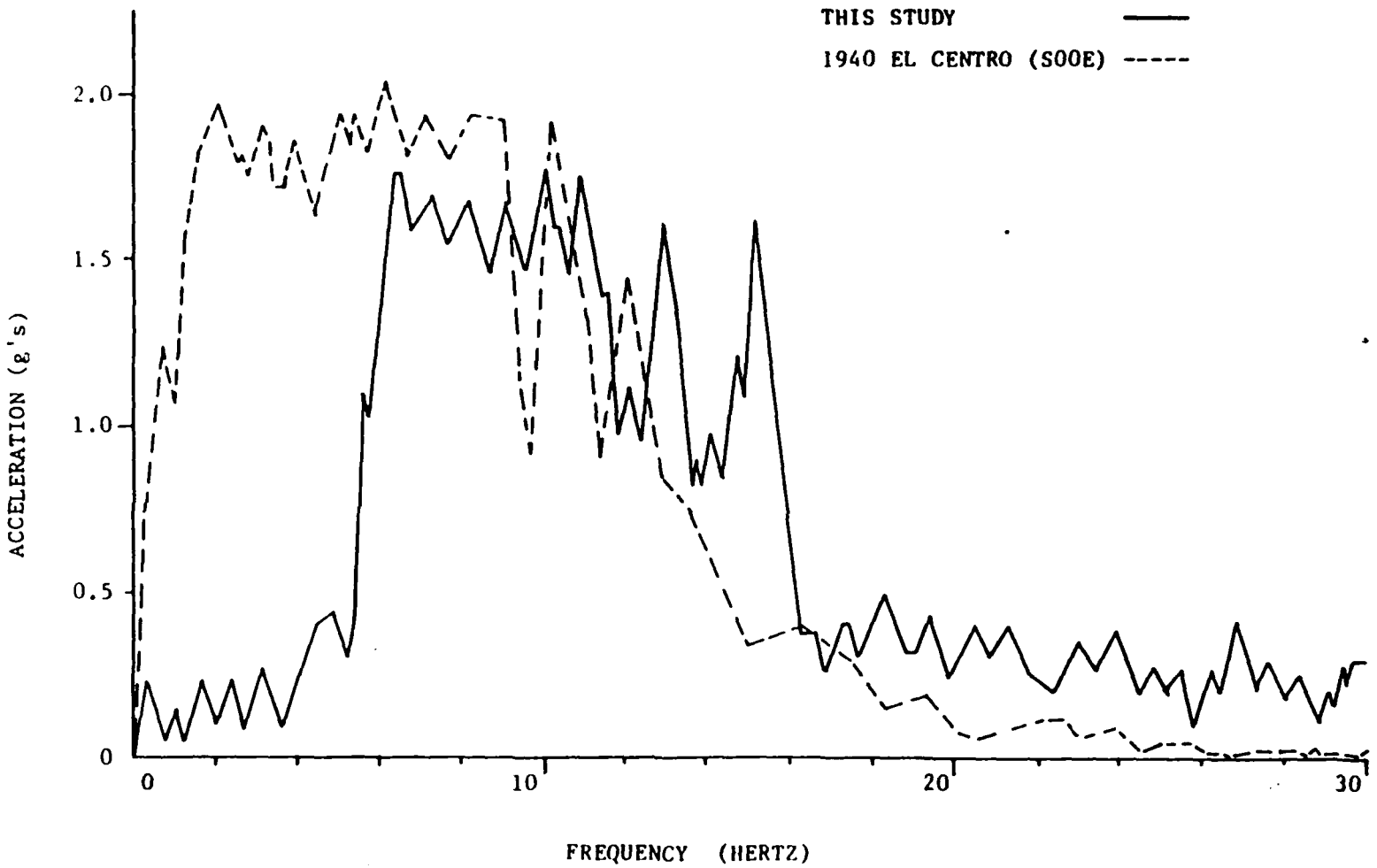

Figure 40: Fourier Spectrum of Random Amplitude Acceleration

be seen the samples tested on The Ohio State University facility were consistently less susceptible to liquefaction and predictions based upon our results would result in much less conservative estimates of liquefaction potential.

When the results of the anisotropic tests are presented in the same format as the isotropic test data, using the mean normal stress to represent the effective confinement, the curve defining the number of cycles to liquefaction plots very close to the curve of the isotropic results as can be seen in Figure 42.

As shown in Figure 43, little effect on the liquefaction potential was seen experimentally when a reaction mass similar to the type used by DeAlba et.al. was placed on top of the sample. This result would indicate that the presence or absence of a reaction mass (regardless of its height) had little effect on the liquefaction potential of the sand sample.

The results of the different tests conducted using random motions are presented in Figure 44. It can be seen from this figure that although there is general qualitative agreement regarding the observed liquefaction potential among the different types of random dynamic loadings applied, precise quantitative agreement was not observed.

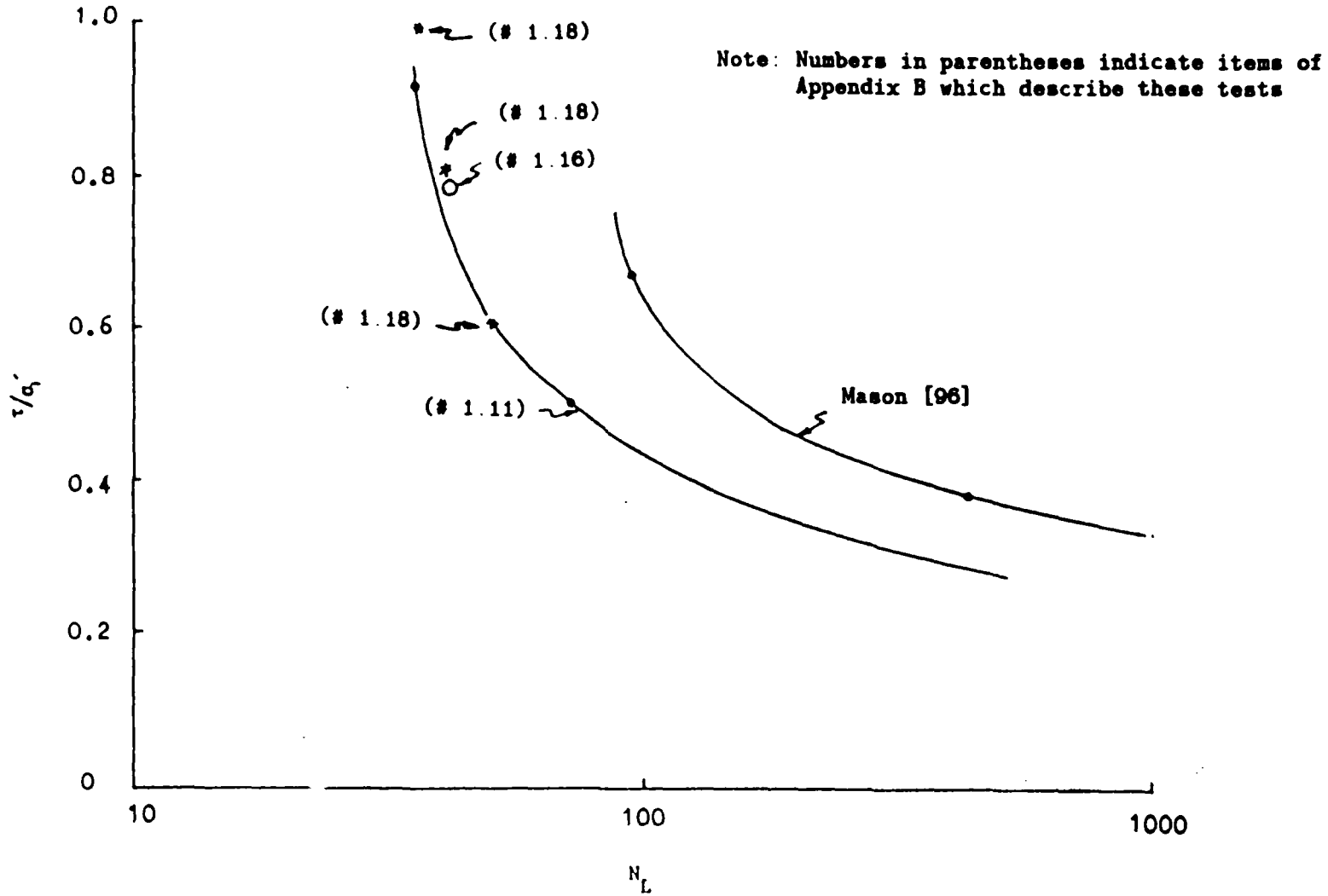

Figure 41: Liquefaction Test Results for Harmonic Excitation

Note: Numbers in parentheses indicate items of Appendix B which describe these tests

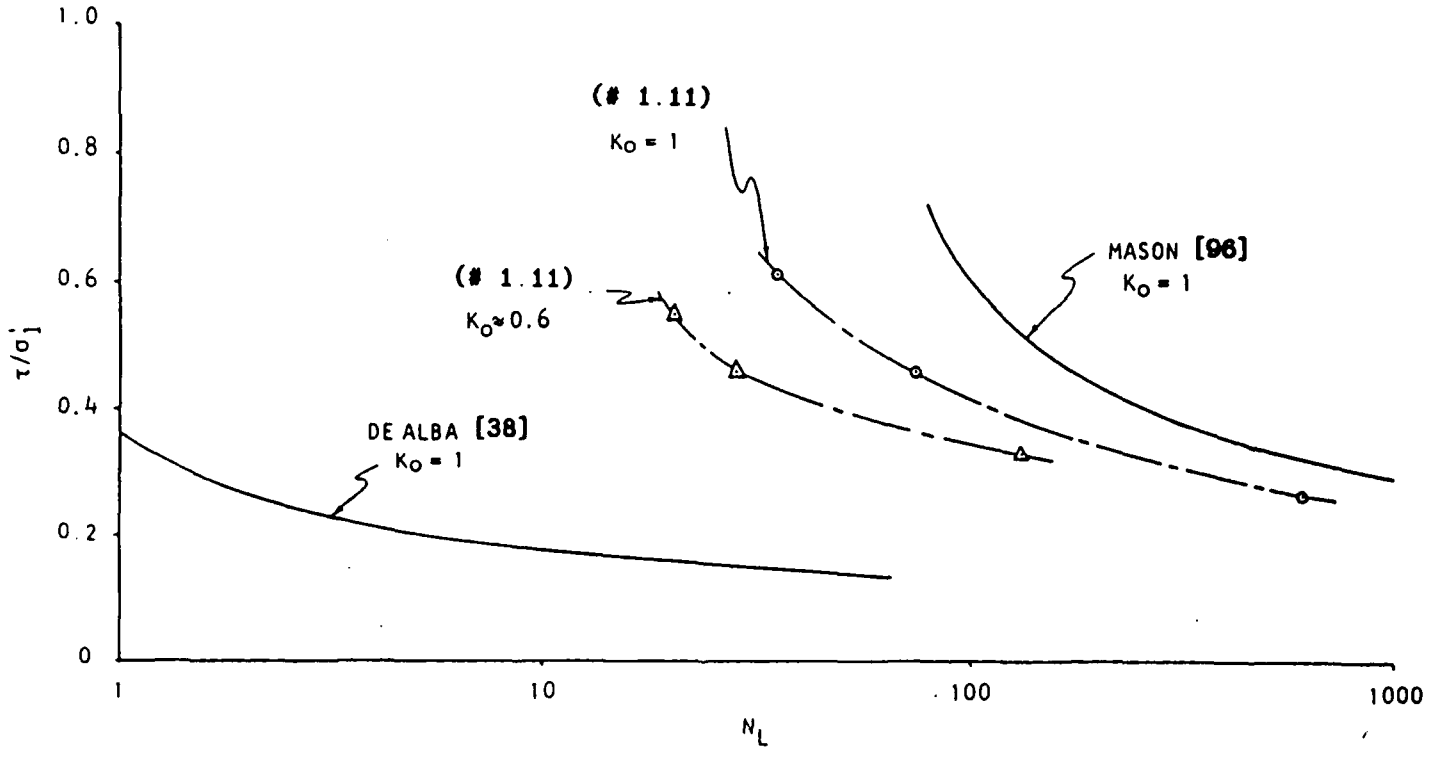

Figure 42: Liquefaction Test Results for Anisotropically Consolidated Samples

Note: Numbers in parentheses indicate items of Appendix B which describe these tests

o TESTS WITH REACTION MASS

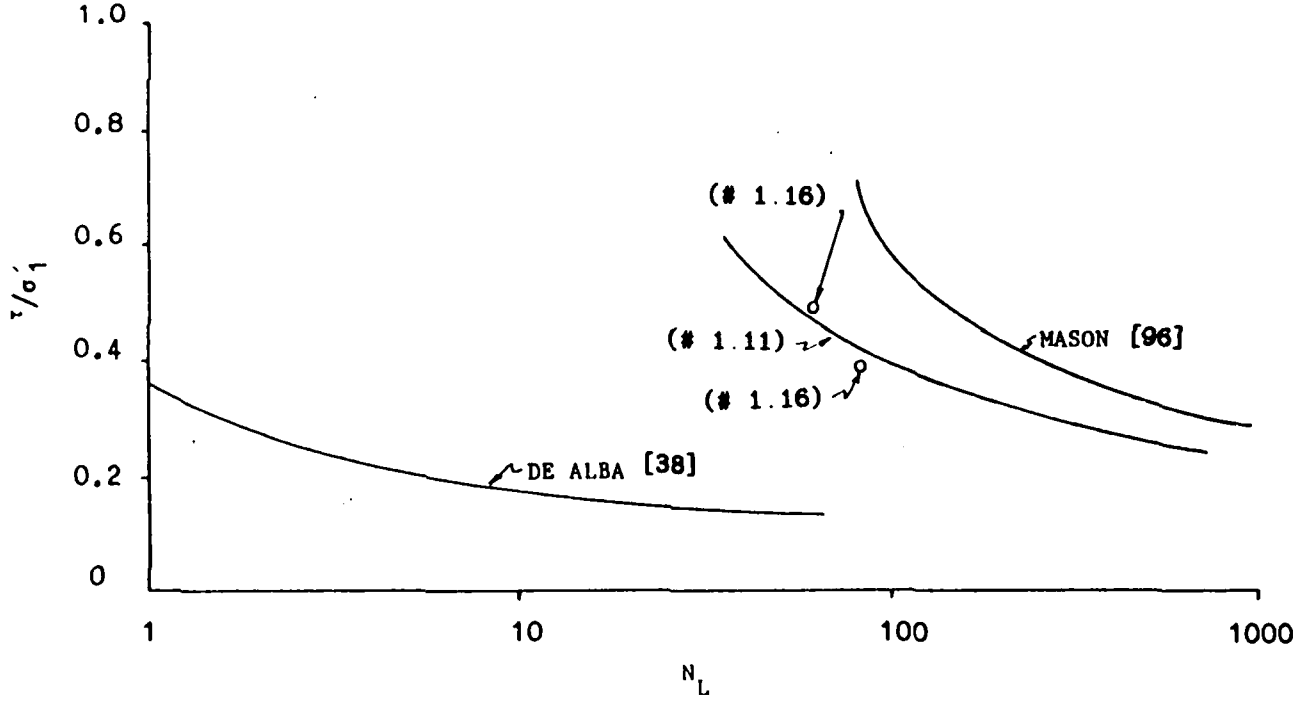

Figure 43: Liquefaction Test Results Obtained with a Reaction Mass on the Sample

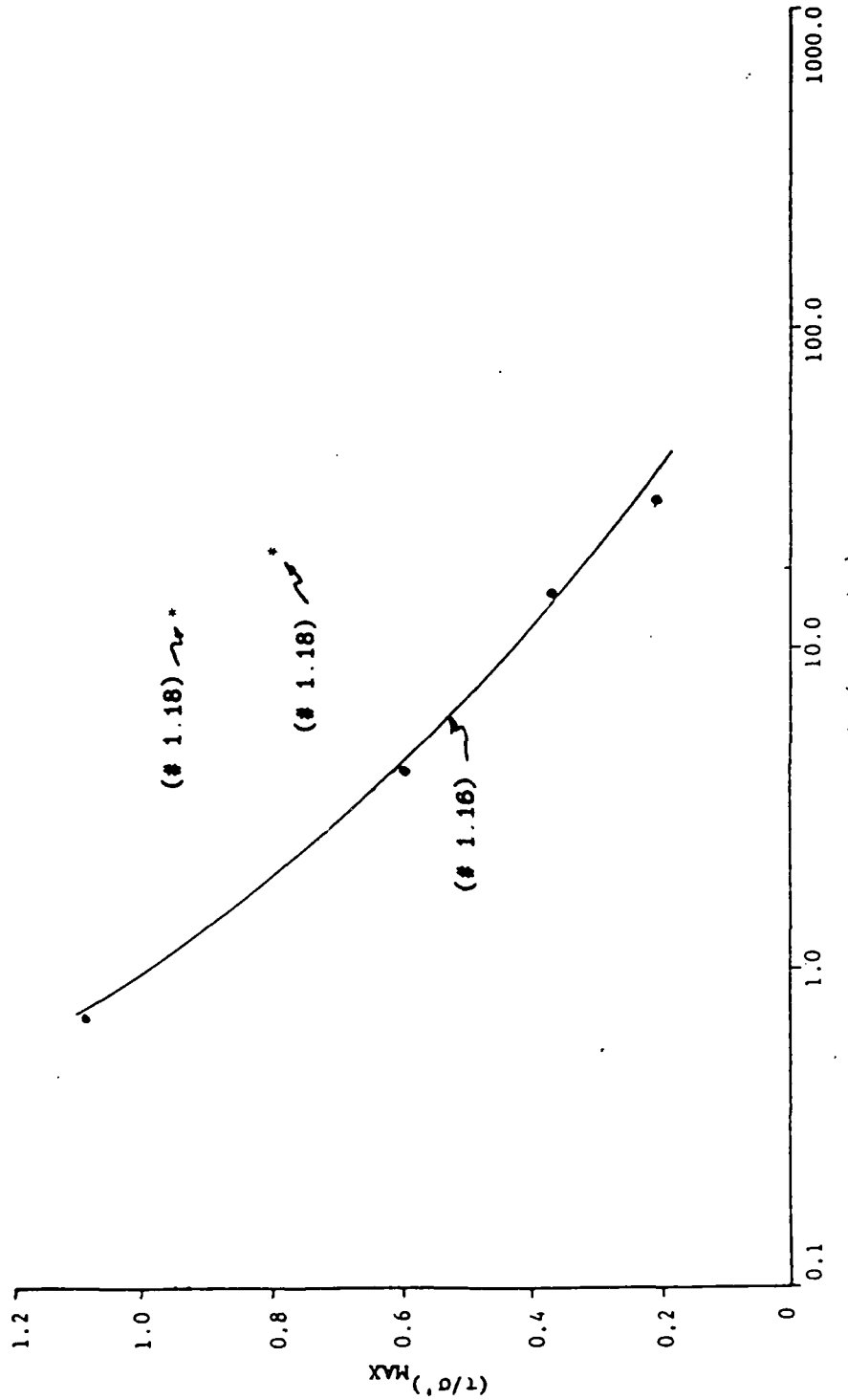

Figure 44: Liquefaction Test Results for Random Amplitude Excitation

5.4 DISCUSSION

The motivation for the test program conducted at The Ohio State University has been the generation of data to be used in the development and verification of mathematical models. This purpose was different from any of the previous laboratory programs in that the chief goal of those programs was to develop empirical relationships which would, for a limited range of field conditions, allow seismic designs to be made. Therefore, in the current study, although the sample boundary conditions applied were designed to simulate stresses in the field as closely as was practical, it was imperative that the design of the test apparatus allow for boundary conditions which could be clearly defined, that the material constants be thoroughly described, and the density of the sample be as uniform as practically possible.

Over the duration of the project, several experimental programs have been conducted. The results of these programs have shown that the test apparatus used was capable of operating successfully and providing consistent results. The relatively small offsets between the points identifying the onset of liquefaction as plotted in Figure 41 can be explained by observing that similar samples were often of slightly different relative densities. It was also shown experimentally that tests conducted with the same testing apparatus continued to provide consistent results even with the addition of a reaction mass of the type reported by DeAlba [38]. Therefore, the boundary conditions imposed on the top of the sand sample by this reaction mass cannot be the explanation as to why the testing apparatus used in this study gave much different results for liquefaction potential when compared with the results presented by De Alba [38]. Other boundary conditions must have existed in their samples which we have not been able to reproduce with the apparatus used in this study. It is likely that the precise method used by DeAlba [38] to attach the steel shot filled bag to the top of the sample chamber caused localized stress concentrations at the sand-shot interface. These small

zones of high stress intensity would then be expected to generate locally high pore pressures resulting in premature liquefaction.

Although some soil structure rearrangement is certainly likely during cyclic loading, we find it difficult to attribute the eightfold strength increases observed by Seed [158] solely to the change in structure which might result from the shaking of a homogeneous sample, particularly while maintaining the same density. What is more likely is that the pre-liquefaction shaking and subsequent drainage of a specimen resulted in the formation of a more uniform sample. Wolfe [172] has shown in earlier tests conducted on cubical specimens which were loaded cyclically to liquefaction and then allowed to drain, that a much smaller strength increase is observed, one that is consistent with the observed increase in relative density which follows shaking and subsequent reconsolidation.

Three different band limited white (or pink) noise excitations provided the shear stress on a number of isotropically consolidated samples. From published reports available to the authors, it is believed that these were the first such tests conducted on large scale samples. All acceleration time histories contained the same dominant frequencies (6 to 15 Hz). If, however, the time to liquefaction is plotted versus maximum shear maximum shear stress ratio, different curves for the different input motions emerge. Therefore, it appears that the use of the maximum shear stress within the soil sample during cyclic loading is not by itself an appropriate method with which to characterize the effects of ground shaking on liquefaction potential.

Several potential causes of the differences between the liquefaction data obtained in this study and the data reported by DeAlba [38] can be identified. It is apparent that liquefaction is essentially a local phenomenon, i.e. local irregularities greatly affect the initiation of liquefaction. Therefore, non-uniformity in the material itself, or in the load applied should be investigated.

5.4.1 Non-uniformity of sand samples

An experimental program conducted by Mulilis [107] showed the importance of the method of sample formation on the liquefaction resistance of a specimen. The samples prepared by DeAlba [38] were made by pluviation through air and subsequent saturation, whereas all the specimens prepared in the present study were saturated by boiling under a vacuum then deposited entirely under water at a constant drop height. The data presented by Mulilis [107] clearly show that samples made by these two methods demonstrate different cyclic strengths. They attributed the strength differences observed to significantly different soil structures. A review of their findings shows that although the wet pluviation technique we used can be expected to result in higher cyclic strengths than does dry pluviation, it is not likely that the structural differences obtained alone can explain the magnitude of the difference we have observed between the two sets of results. Castro [32] attributes the cyclic behavior of sands to changes in the void spaces at the local level. Marcuson [95] in reporting the results of an experimental program designed specifically to study the effects of sample uniformity on liquefaction resistance, observed markedly increased cyclic strengths in highly uniform samples. Furthermore, Gilbert [56] has recently shown that samples prepared by pluviation through water are more uniform than samples prepared by the popular method of moist tamping.

5.4.2 Nonuniformities due to testing

Wood [173] observed that pore pressures measured at the ends of the triaxial or simple shear sample are unlikely to be useful unless tests are done slowly enough to guarantee pore pressure equalization throughout the sample. In all tests conducted during this study, measurements of pore pressure rise were made within the sample itself not at a sample boundary. Furthermore pore pressures were measured at more than one

location in the sample during every test. A comparison of the pore pressure time histories made during the test indicates that at any instant in time a uniform pressure existed throughout the central portion of the sample. As shown in Figure 44, this time dependent but spatially independent pore pressure was typically observed throughout the duration of the test.

5.4.3 Membrane penetration

Lade [87] and Hernandez studied the effects of membrane penetration on the undrained response of sands in triaxial compression. They observed that the existence of membrane penetration in samples being subjected to cyclic loading results in in increase in sample volume as the pore pressures in the sample rise during shaking. This volume change, if not accounted for, would result in an overestimation of the liquefaction resistance since the test was in reality a partially drained test. Lade and Hernandez cite data which indicate that membrane peneteration is negligible for sands with grain sizes below 0.1 to 0.2 mm, or for effective stresses below 1.0 kg/sq cm. The grain size distribution for the Ottawa sand used in this study was given in Figure 38. This figure shows that the sand used roughly corresponds to sands falling in the range where the membrane effects would be condidered negligible. Also effective stresses on the sample were typically on the order of 1.0 kg/sq.cm. Nevertheless, due to the large sample surface covered by the membrane, it was felt to be important for the amount of membrane penetration to be measured accurately in order to assess what effect, if any, membrane penetration had on our liquefaction measurements.

The penetration of the membrane into the sample was measured after the sample was pressurized to the test conditions and before the internal supporting walls were retracted. The test chamber was attached to a volume change measuring device. With the isotropic confining pressure constant on the saturated sand sample, the back pressure

was incrementally raised to simulate generation of an increase in pore water pressure during actual dynamic testing. Membrane penetration could be measured as movement of the membrane out from between the sand grains and recorded in the form of volume change on a manometer. The amount of membrane penetration measured was consistently less than 1.75×10^{-4} percent of the sample volume. This amount of penetration was considered negligible.

5.4.4 Nonuniformity of the confining pressure at the sample boundaries

Since in the shaking table configuration used, the confining water must be accelerated along with the sample, there was some concern that the mass of the water, which was arbitrarily chosen, could be affecting the distribution of pressures on the vertical faces of the sample. Early measurements of the pressure in the confining fluid had failed to show any variation during shaking, but it was felt that additional testing was warranted. Therefore, in a specific attempt to determine experimentally the effect of the volume of confining water on the uniformity of the confining pressure and therefore on liquefaction potential, plates were inserted into the space occupied by the confining fluid. The effect was to reduce the volume of water by more than 50%. No effect on liquefaction potential was observed.

The results of a test program in which saturated sand specimens were subjected to harmonic as well as random time histories of base accelerations have been presented. The data show that loose sands can be liquefied in the laboratory and that the resistance to liquefaction is strongly dependent upon the sample boundary conditions. The test apparatus employed in the program described herein minimized stress irregularities at sample boundaries and should therefore be seen to be an improvement over other laboratory methods for determining liquefaction potential.

Section VI

DISCUSSION

6.1 OBJECTIVE OF THE RESEARCH PROGRAM

The objective of the research program was to critically examine the theoretical basis of the equations governing the behavior of saturated soils under dynamic loading in order to identify/develop appropriate theory which would properly allow for soil-water interaction and be thermodynamically consistent. The work would involve implementation of the theory or theories in appropriate solution procedures. A program of laboratory investigation was included to constitute a reliable database for verification of the theoretical findings.

6.2 ACCOMPLISHMENTS

6.2.1 Review of Theories

The existing theories have been carefully reviewed. Limitations of the theories and their differences have been carefully listed and discussed. The main findings of the research program have been discussed at length in the text of this report and in the publications listed in Appendix B. A brief summary of the conclusions is given below.

The commonly used "engineering approach" to study of liquefaction, though it has been successfully utilized for the study of many case histories, cannot be directly extended to multi-dimensional situations. Even for simple one-dimensional cases, it requires considerable "judgement" on the part of the engineer in addition to tedious laboratory investigations on the dynamic behavior of the soil.

Biot's theory uses some ad hoc assumptions. These include the existence of an energy function for the mixture and the existence of an inertial coupling introduced through a kinetic energy expression involving product of the velocities of the soil and the pore-water. There are questions regarding the existence and the nature of this coupling. Definitely, under certain circumstances (e.g., small pore size) a portion of the fluid could be moving effectively with the soil. This coupling would only constitute a different partitioning of the total mass into one that moves with the soil velocity and the remainder which moves relaive to the soil. However, the introduction of a "coupled mass" appears to be entirely artificial and without any physical basis. Theories of mixtures have been developed starting from different assumptions. Truesdell assumed the additivity of the total energy of the constituents and proposed artificial definitions for the stresses to obtain an identity of form between the equations of balance for the mixture as a whole and those for the individual constituents. It is apparent that the mixture does not have an existence as a continuum in motion and, therefore, the question of writing equations of motion for it should not arise much less the effort to give them the same form as the equations for each constituent. Truesdell's "third postulate" which states that the motion of the mixture is governed by the same equations as is a single body, is unnecessary and irrelevant. Green's theory, on the other hand, assumes the additivity of stresses and fluxes. However, Green as well as Crochet, introduced energy functions for the mixture. Their work does not necessarily require the notion of a mixture as a continuum in motion. Bowen's contention that Green's theory is a special case of Truesdell's for vanishing relative velocities is clearly incorrect because Green's theory is no less general than Truesdell's. There are differences in the meanings attached to different terms even though the form of the equations is the same. It appears that balance equations ought to be written for each constituent allowing for interaction. Introduction of thermodynamic quantities associated with a mix-

ture as a continuum in motion is incorrect. These quantities, in relation to the mixture, must arise as a consequence of the quantities associated with individual constituents and need not have any physical interpretation.

Truesdell and some others wrote the equations of balance directly considering the motion of the constituents of the mixture across an elementary fixed volume in space. The contents of this fixed volume change constantly. For this reason, some investigators have proposed writing constitutive equations for porosity. This would be unnecessary if the balance laws are written for the same set of soil particles as in Gibson's theory of nonlinear one-dimensional consolidation.

Constitutive relations are required for the diffusive resistance or the interaction force. Truesdell's theory of mechanical diffusion includes other theories as specializations. Green's theory is quite similar.

There is considerable confusion regarding the definition of partial stresses. Terzaghi's dual definition for effective stress cannot be accepted. The effective stress is different from partial stress in the soil. The latter includes dependence upon the kinematics of the fluid in addition to the dependence upon the kinematics of the soil whereas the effective stress is defined as the part of the soil stress which depends directly upon the strain in the soil skeleton. Biot's and Green's assumption of the existence of an energy function for the mixture would lead, in the linear case, to a symmetrical constitutive coupling between the soil and the water. However, because this assumption is questionable, this coupling, even if it exists, need not be symmetrical. This is in line with Morland's views.

6.2.2 A Dynamical Theory of Saturated Soils.

A theory of dynamics of saturated soils was developed. This theory is based upon the study of balance of a fixed set of particles of the soil contained in a reference volume in the initial configuration. This reference volume moves during the process and changes shape as well. The description of deformation and motion was accomplished through the use of convected coordinates as introduced by Novozhilov [112]. This eliminated the need for writing constitutive equations for porosity. It also enabled a clearer definition of the stresses acting on the representative volume. The theory may be regarded as an extension of Gibson's theory of one-dimensional consolidation to three-dimensions and inclusion of inertia effects.

6.2.3 Development of Solution Procedures.

Truesdell's as well as Green's theories, for the case of small motions coincide with Biot's for dynamics of saturated soils. The new dynamical theory of saturated soils would also coincide with Green's theory if the representative volume containing the fixed set of particles undergoes extremely small deformations. Very few solutions were available for the problem. Exact solutions had been developed by Biot and some other investigators for some simple problems. Numerical solutions had been attempted but they had, in general, not been verified against exact solutions and were suspect. In the present research effort, in order to study the effectiveness of various theories in modelling dynamic response of soil systems, it was necessary to systematically develop solution procedures. These included exact, semi-discrete, as well as numerical solutions to Biot's formulation of the problem of wave propagation in saturated soils and numerical solution of Seed's and Finn's theory. Solutions were also developed for the case of non-linear material behavior.

Exact solutions were developed for several cases of loading of an infinite column and of a finite layer of saturated soil. For the infinite column, these consisted of integration of Garg's fundamental solution. For the finite layer solutions were developed for the case of independent specification of velocities of the fluid and the soil at the boundary. In case of a sudden application of velocity, the singularity was separated from the smooth diffusion and the two solutions superposed for the linear theory. It was noticed that Garg had made some assumptions for the case of "weak coupling" and some others for the case of "strong coupling". The validity of these assumptions has been carefully examined and documented.

Semi-discrete solutions were developed using the Laplace Transform technique in conjunction with a finite element discretization. Effect of refinement of mesh upon the accuracy of the results was examined. The eigenvalue problem becomes extremely large with mesh refinement. This approach, though useful perhaps for benchmarking numerical time-domain solution procedures, was seen to be computationally too expensive.

In order to develop finite element solution procedures in a systematic manner, the equations of motion were written in self-adjoint form in an appropriate space. Variational formulations along with extensions and several interesting specializations were developed. Numerical solutions using spatial discretization by finite elements and numerical integration over the time-domain using interpolation schemes of suitable order, were developed and verified against some exact solutions. Several types of elements were used to obtain an optimal combination of accuracy and computational economy. For suddenly applied dynamic disturbances, it was found necessary to use "singularity" elements to properly reproduce the wave propagation.

For Biot's theory, the usual form is the two-field formulation in which the displacements of the constituents are chosen to be the field variables. A three-field formulation including the pore-water pressures as the additional field variable was written and finite element solution procedures developed for the same. It was found that this scheme gave practically the same results as the two field formulation for the problems in which the velocities were specified. However, the two-field formulation applies the specified fluid pressure condition (e.g. free-draining boundary) in an indirect manner. In the three field formulation this specification is direct.

Computer programs for two-dimensional wave programs were developed but could not be checked against exact solutions because no solutions for wave propagation in two- or three- dimensional saturated soil systems were available.

Wave propagation through nonlinear saturated soils was modelled in a finite element based computer program. No exact solutions for wave propagation in nonlinear saturated soils are available. The code was checked against two solution for wave propagation in a single nonlinear material continuum.

6.2.4 Laboratory Investigations.

Shaking table tests were conducted on saturated samples of a uniform Ottawa sand. The use of a shaking table combined with the large size of the samples minimized the effects of stress irregularities at sample boundaries and the method used to construct the samples minimized material non-uniformities. In the program described in this report both harmonic and random amplitude table acceleration time histories were utilized. A significant increase in the resistance to liquefaction, as compared with the results of other published experimental programs, was measured. Potential causes for the differences in test results were investigated. It was concluded that the test apparatus and the methods employed in the current program should be seen as an improvement over other experimental methods for determining liquefaction potential.

6.3 FUTURE WORK

Additional work on research in the general area of dynamics of saturated soils is needed. A major shortcoming of the available models is that they have not been carefully tested against actual experiments in the field or in the laboratory. The reason for this is that experiments simulating simple boundary conditions are difficult to set-up and most experiments that are convenient to carry out constitute very difficult boundary-value problems for which verified computer codes are difficult to come by. There is need to design test set-ups which are essentially one-dimensional wave propagation experiments so that the carefully verified solution procedures developed in the present research can be used to substantiate the theoretical concepts regarding behavior of saturated soils. On the other hand, there is need to develop analytical solutions to two- and three- dimensional linear as well as nonlinear problems so that the data from shake-table tests which are essentially two- dimensional, can be utilized to verify the theoretical models. Any of the models would need material properties as input data. There is need to define the nonlinear behavior of saturated sands very carefully and to relate it to the propertries of the single materials involved. There has been difficulty even in characterising dry sand behavior [110]. For saturated materials, the role of the pore-water pressures, the existence and the nature of the constitutive coupling and the existence or otherwise of the inertial coupling need to be studied. The relation between the mechanics of the particles and the behavior of the soil mass needs to be investigated. The soil in the field as well as the laboratory is never absolutely uniform. The spatial variation in material properties would be greater in the field than in the laboratory where the conditions can be controlled. The effect of the degree of randomness on the overall behavior of the soil is extremely important for realistic utilization of the results of the experiments in the laboratory for the situation in the field. Also, spatial variation in material properties could result in local

liquefaction leading to perhaps a "domino" effect in promoting catastrophic liquefaction in the soil mass in the field even though the soil might have been found to have high resistance to liquefaction in laboratory tests.

Section VII

LIST OF REFERENCES

1. Adkins, J.E., *Non-Linear Diffusion I. Diffusion and Flow of Mixtures of Fluids*, Phil. Trans., Roy. Soc., Ser. A., Vol. 255, 607-633, 1963.

2. Adkins, J.E., *Non-Linear Diffusion II. Constitutive Equations for Mixtures of Isotropic Fluids*, Phil. Trans., Roy. Soc., Ser. A., Vol. 255, 635-648, 1963.

3. Adkins, J.E., *Diffusion of Fluids Through Aelotropic Highly Elastic Solids*, Arch. Rat. Mech. Anal., Vol. 15, 225-234, 1964.

4. Aifantis, E.C., *On The Problem of Diffusion in Solids*, Acta Mechanica, Vol. 37, 265-296, 1980.

5. American Society of Civil Engineers, *Uplift in Masonry Dams*, Final Report, Sub-Committee on Uplift of Masonry Dams, Transactions, Amer. Soc. Civ. Engrs., Vol. 117, 1218-1252, 1952.

6. Atkin, R.J., *Constitutive Theory for a Mixture of an Isotropic Elastic Solid and a Non-Newtonian Fluid*, Z.A.M.P., Vol. 18, 803-825, 1967.

7. Atkin, R.J., and R.E. Craine, *Continuum Theories of Mixtures: Basic Theory and Historic Development*, Quar. J. App. Math., Vol. 29, Pt. 2, 209-244, 1976.

8. Ayoub, S.F., Analysis of Elastic-Plastic Continuum at Large Deformation Using Hybrid Description and Finite Element Method, Ph.D. dissertation, The Ohio State University, Columbus, Ohio, 1986.

9. Bedford, A., and D.S. Drumheller. *Recent Advances Theories of Immiscible and Structured Mixtures*, Int. J. Engrg. Sci., Vol. 21, 863-960, 1983.

10. Belytschko, T., H.J. Yen, and R. Mullen, *Mixed Methods for Time Integration*, Com. Meth. Appl. Mech. and Engg., 17/18, 259-275, 1979.

11. Biot, M.A., *General Theory of Three-Dimensional Consolidation*, Jour. App. Phy., Vol. 12, 155-164, 1941.

12. Biot, M.A., *Consolidation Settlement Under a Rectangular Load Distribution*, Jour. App. Phy., Vol. 12,426-430, 1941.

13. Biot, M.A., and F.M. Clingan, *Consolidation Settlement of a Soil with an Impervious Top Surface*, Jour. App. Phy., Vol. 12, 578-581, 1941.

14. Biot, M.A., *Theory of Elasticity and Consolidation for a Porous Anisotropic Solid*, Jour. App. Phy., Vol. 26, No. 2, 182-185, 1955.

15. Biot, M.A., *Theory of Deformation of a Porous Viscoelastic Anisotropic Solid*, Jour. App. Phy., Vol. 27, No. 5, 459-467, 1956.

16. Biot, M.A., and D.R. Willis, *The Elastic Coefficients of the Theory of Consolidation*, Jour. App. Mech., Amer. Soc. Mech. Engrs., 594-601, December 1957.

17. Biot, M.A., *Theory of Propagation of Elastic Waves in a Fluid-Saturated Porous Solid*, Parts I and II, Jour. Acous. Soc. Amer., Vol. 28, No. 2, 168-178, and 179-191, 1956.

18. Biot, M.A., *Mechanics of Deformation and Acoustic Propagation in Porous Media*, Jour. App. Phy., Vol. 33, No. 4, 1482-1498, 1962.

19. Biot, M.A., *Generalized Theory of Acoustic Propagation in Porous Dissipative Media*, Jour. Acous. Soc. Amer., Vol. 34, No. 9, 1254-1264, 1962.

20. Biot, M.A., *Theory of Stability and Consolidation of a Porous Medium Under Initial Stress"*, Jour. Math. Mech., Vol. 12, No. 4, 521-541, 1963.

21. Biot, M.A., *Theory of Finite Deformations of Porous Solids*, Indiana University Mathematics Journal, Vol. 21, No. 7, 597-620, 1972.

22. Black, K.D. and Lee, K.L., *Saturating Laboratory Samples by Back Pressure*, Journal of the Soil Mechanics and Foundations Division, ASCE, Vol. 99, No. SM1, January, 1973, pp. 75-93.

23. Bowen, R.M., *Towards a Thermodynamic and Mechanics of Mixtures*, Arch. Rat. Mech. Anal., Vol. 24, No. 5, 370-403, 1967.

24. Bowen, R.M., *Theory of Mixtures*, in Continuum Physics, Vol. III, Mixtures and EM Field Theories, Ed. A. C. Eringen, 1-127, Academic Press, N.Y., 1976.

25. Bowen, R.M., *Compressible Porous Media Models by Use of the Theory of Mixtures*, Int. Jour. Engrg. Sci., Vol. 20, No. 6, 697-735, 1982.

26. Carlson, R.W., *Permeability, Pore Pressure and Uplift in Gravity Dams*, Transactions, Amer. Soc. Civ. Engrs., Vol. 122, 587-613, 1957.

27. Carroll, M.M., *An Effective Stress Law for Anisotropic Elastic Deformation*, Jour. Geophy. Res., Vol. 84, 7510-7512, 1979.

28. Carroll, M.M., J.F. Schatz, and S.E. Yamada, *On Plastic Strain in Porous Materials*, Transactions, Amer. Soc. Mech. Engrs., Vol. 48, 976-978, 1981.

29. Carroll, M.M., and N. Katsube, *The Role of Terzaghi Effective Stress in Linearly Elastic Deformation"*, Amer. Soc. Mech. Engrs., Jour. of Energy Resource Tech., Vol. 105, 509-511, 1983.

30. Carter, J.P., J.C. Small, and J.R. Booker, *A Theory of Finite Elastic Consolidation*, Int. Jour. Solids Struct., Vol. 13, 467-478, 1977.

31. Casagrande, A. *Liquefaction and Cyclic Deformation of Sands: A Critical Review*, Harvard Soil Mechanics Series No. 88, January, 1976. Also in Proceedings, Fifth Pan-American Conference on Soil Mechanics and Foundation Engineering, Buenos Aires, 1975.

32. Castro, G., *Liquefaction and Cyclic Mobility of Saturated Sands*, Journal of the Geotechnical Engineering Division, ASCE, Vol. 101, No. GT6, June, 1975, pp. 551-569.

33. Chakraborty, S.K., and S. Dey, *The Propagation of Love Waves in Water-Saturated Soil Underlain by a Heterogeneous Elastic Medium*, Acta Mech., Vol. 44, 169-175, 1982.

34. Chao, B.T., W.T. Sha, and S.L. Soo, *Internal Coupling in Dynamic Equations of Components in a Mixture*, Int. J. of Multiphase Flow, Vol. 4, 219-223, 1978.

35. Coleman, B.D., and W. Noll, *The Thermodynamics of Elastic Materials with Heat Conduction and Viscosity*, Arch. Rat. Mech. Anal., Vol. 13. No. 3, 167-177, 1963.

36. Coleman, B.D., and V.J. Mizel, *Thermodynamics and Departures from Fourier's Law of Heat Conduction*, Arch. Rat. Mech. Anal., Vol. 13. No. 4, 245-261, 1963.

37. Crochet, M.J., and P.M. Naghdi, *On Constitutive Equations for Flow of Fluid Through an Elastic Solid*, Int. Jour. Engrg. Sci., Vol. 4, 383-401, 1966.

38. De Alba, P., C.K. Chan, and H.B. Seed, Determination of Soil Liquefaction Characteristics by Large-Scale Laboratory Tests, Shannon and Wilson, Inc. and Agbabian Associates, Report prepared for the U.S. Nuclear Regulatory Commission, September, 1976.

39. Demiray, H., *A Continuum Theory of Chemically Reacting Mixtures of Fluids and Solids", Int. Jour. Engrg. Sci., Vol.* 19, 253-268, 1981.

40. Deresiewicz, H., *The Effect of Boundaries on Wave Propagation in a Liquid Filled Porous Solid*, I. Reflection of Plane Waves at a Free Plane Boundary(Non-Dissipative Case), Bull. Seis. Soc. Amer., Vol. 50, 597-607, 1960; II. Love Waves in a Porous Layer, Bull. Seis. Soc. Amer., Vol. 51, 51-59, 1961; III. Reflection of Plane Waves at a Free Plane Boundary(General Case), Bull. Seis. Soc. Amer., Vol. 52, 575-625, 1962; IV. Surface Waves in a Half Space, Bull. Seis. Soc. Amer., Vol. 52, 627-638, 1962; V. (Co-author J.T.Rice), Transmission Across a Plane Interface, Bull. Seis. Soc. Amer., Vol. 54, 409-416, 1964; VI. Love Waves in A Double Surface Layer, Bull. Seis. Soc. Amer., Vol. 54, 417-423, 1964; VII. Surface Waves in a Half Space in the Presence of a Liquid Layer, Bull. Seis. Soc. Amer., Vol. 54, 425-430, 1964; VIII. (Co-author, B. Wolfe),Reflection of Plane Waves at an Irregular Boundary, Bull. Seis. Soc. Amer., Vol. 54, 1537-1561, 1964.

41. Dubner, H., and J. Abate, *Numerical Inversion of Laplace Transforms by Relating them to Finite Fourier Cosine Transform*, J. Assoc. Comp. Mach., 15, 1, 1968.

42. Finn, W.D.L., *Response of Saturated Sands to Earthquakes and Wave Induced Forces*, Int. Symp. Numer. Methods in Offshore Engrg., Swansea, Wales, January 1977.

43. Finn, W.D.L., *Soil Dynamics-Liquefaction of Sands*, Proceedings of the First International Microzonation Conference, Seattle, WA, Vol. 1, 1972, pp. 87-111.

44. Finn, W.D.L., *Liquefaction Potential: Developments Since 1976*, Proceedings of the International Conference on Recent Advances in Geotechnical Earthquake Engineering and Soil Dynamics, Vol II, St. Louis, MO, April-May, 1981, pp. 655-681.

45. Finn, W.D.L., Emery, J.J. and Gupta, Y.P., Soil Liquefaction Studies Using a Shake Table, Closed Loop, MTS Systems Corporation, Fall/Winter, 1971, pp. 14-18.

46. Fukuo, Y., *The Dynamic Theory of the Deformation of a Granular Solid Fully Saturated with a Liquid*, Bull. Disas. Prev. Res. Inst., Kyoto University, Japan, Vol. 18, Pt. 4, No. 146, 1-15, 1969.

47. Fung, Y.C., Foundations of Solid Mechanics, Prentice Hall, New Jersey, 1965.

48. Garg, S.K., *Wave Propagation Effects in Fluid-Saturated Porous Solids*, Jour. Geophy. Res., Vol. 76, No. 32, 7947-7962, 1971.

49. Garg, S.K., and A. Nur, *Effective Stress Laws for Fluid-Saturated Porous Rocks*, Jour. Geophy. Res., Vol. 78, 5911-5921, 1973.

50. Garg, S.K., A.H. Nayfeh, and A.J. Good, *Compressional Waves in Fluid Saturated Elastic Porous Media*, Jour. App. Phy., Vol.45, 1968-1974, 1974.

51. Garg, S.K., Personal Communication with R.S. Sandhu, 1986.

52. Ghaboussi, J., and E.L. Wilson, Flow of Compressible Fluid in Porous Elastic Media, Report No. UCSESM 71-12, Structural Engineering Laboratory, University of California, Berkeley, California, 1971.

53. Ghaboussi, J., and E.L. Wilson, *Variational Formulation of Dynamics of Fluid-Saturated Porous Elastic Solids*, Proceedings, Amer. Soc. Civ. Engrs., Vol. 98, Jour. Engrg. Mech. Div., No. EM4, 947-963, 1972.

54. Ghaboussi, J., and E.L. Wilson, *Seismic Analysis of Earth Dam-Reservoir System*, Proceedings, Amer. Soc. Civ. Engrs., Vol. 99, Jour. Soil Mech. Found. Div., No. SM10, 849-862, 1973.

55. Gibson, R.E., R.L. England, and M.J.L. Hussey, *The Theory of One-Dimensional Consolidation of Saturated Clays*, Geotechnique, Vol. 17, 261-273, 1967.

56. Gilbert, P.A. and W.F. Marcuson III, *Density Variation in Triaxial Specimens Subjected to Cyclic and Monotonic Loading*, Journal of the Geotechnical Engineering Division, ASCE, Vol. 114, No. 1, 1988.

57. Goodman, M.A., and S.C. Cowin, *A Continuum Theory of Granular Materials*, Arch. Rat. Mech. Anal., Vol. 44, 249- 266, 1972.

58. Gray, D.H., Coupled Flow Phenomena in Clay-Water Systems, Ph.D. Thesis, University of California, Berkeley, California, 1966.

59. Gray, D.H., *Thermo-osmotic and Thermo-elastic Coupling in Saturated Soils*, Highway Research Board, Special report No. 103, 1969.

60. Green, A.E., and J.E. Adkins, *A Contribution to the Theory of Nonlinear Diffusion*, Arch. Rat. Mech. Anal., Vol. 15, 235-246, 1964.

61. Green, A.E., and R.S. Rivlin, *On Cauchy's Equations of Motion*, Z. Angew. Math. Phy., Vol. 15, 290-292, 1964.

62. Green, A.E., and P.M. Naghdi, *A Dynamical Theory of Interacting Continua*, Int. Jour. Engrg. Sci., Vol. 3, 231-241, 1965.

63. Green, A.E., and T.R. Steel, *Constitutive Equations for Interacting Continua*, Int. Jour. Engrg. Sci., Vol. 4, 483-500 1966.

64. Green, A. E., and P.M. Naghdi, *A Theory of Mixtures*, Arch. Rat. Mech. Anal., Vol. 24, 243-263, 1967.

65. Green, A.E., and P.M. Naghdi, *A Note on Mixtures*, Int. Jour. Engrg. Sci., Vol. 6, 631-635, 1968.

66. Green, A.E., and P.M. Naghdi, *On Basic Equations for Mixtures*, Quar. Jour. Mech. App. Math., Vol. XXII, Pt. 4, 427-438, 1969.

67. Green, A.E., and P.M. Naghdi, *The Flow of a Fluid Through a Solid*, Acta Mechanica, Vol. 9, 329-340, 1970.

68. Guggenheim, E.A., Thermodynamics: An Advanced Treatment for Chemists and Physicists, Interscience, New York, 1949.

69. Gurtin, M.E., and G. De La Penha, *On the Thermodynamics of Mixtures I. Mixtures of Rigid Heat Conductors*, Arch. Rat. Mech. Anal., Vol. 36, 390-410, 1972.

70. Gurtin, M.E., M.L. Oliver, and W.D. Williams, *On Balance of Forces for Mixtures*, Quar. J. App. Math., Vol. 30, 527-530, 1973.

71. Gurtin, M.E., *Variational Principles in the Linear Theory of Viscoelasticity*, Arch. Rat. Mech. Anal., Vol. 13, 179-191, 1963.

72. Gurtin, M.E., *Variational Principles in Linear Elastodynamics*, Arch. Rat. Mech. Anal., Vol. 16, 234-254, 1964.

73. Haimson, B., Hydraulic Fracturing in Porous and Nonporous Rock and its Potential for Determination of In-Situ Stresses at Great Depths, Ph.D. Thesis, Univ. of Minnesota, Minneapolis - St. Paul, Minnesota, 1968.

74. Harza, L.F., *Significance of Pore Pressures in Hydraulic Structures*, Transactions, Amer. Soc. Civ. Engrs., Vol. 114, 193-284, 1949.(Discussion by D. McHenry).

75. Hiremath, M.S., Wave Propagation in Fluid-Saturated Solid, Ph.D. Thesis, The Ohio State University, Columbus, Ohio, 1987.

76. Hsieh, L., and C.H. Yew, *Wave Motions in a Fluid-Saturated Porous Medium*, Amer. Soc. Mech. Engrs., J. Appl. Mech., 873-878, December 1973.

77. Idriss, I.M., *Seismic Response of Horizontal Soil Layers*, Proceedings, Amer. Soc. Civ. Engrs., Vol. 94, Jour. Soil Mech. Found. Div., No. SM4, 1003-1031, 1968.

78. Idriss, I.M., H. Dezfulian, and H.B. Seed, Computer Programs for Evaluating the Seismic Response of Soil Deposits with Nonlinear Characteristics Using Equivalent Linear Procedures, Monograph, Geotechnical Engineering, Department of Civil Engineering, University of California, Berkeley, California, 1969.

79. Idriss, I.M., H.B. Seed, and H. Dezfulian, *Influence of Geometry and Material Properties on the Seismic Response of Soil Deposits*, Proceedings, 4th World Conference on Earthquake Engineering, Chile, 1979.

80. Idriss, I.M., and H.B. Seed, *Seismic Response of Soil Deposits*, Proceedings, Amer. Soc. Civ. Engrs., Vol. 96, Jour. Soil Mech. Found. Div., No. SM2, 631-638, 1970.

81. Keener, K.B., *Uplift Pressures on Concrete Dams*, Transactions, Amer. Soc. Civ. Engrs., Vol. 116,1218-1264, 1951.

82. Kelly, P.D., *A Reacting Continuum*, Int. J. Engrg. Sci., Vol. 2, 129-153, 1964.

83. Kenyon, D.E., *The Theory of an Incompressible Solid-Fluid Mixture*, Arch. Rat. Mech. Anal., Vol. 62, 131-147, 1976. Also, Corrigendum, Arch. Rat. Mech. Anal., Vol. 64, 385, 1977.

84. Kenyon, D.E., *Consolidation in Compressible Mixtures*, Jour. App. Mech., Amer. Soc. Mech. Engrs., Vol. 45, 727-732, 1978.

85. Kiefer, F.W., H.B. Seed, and I.M. Idriss, *Analysis of Earthquake Ground Motions at Japanese Sites*, Bull. Seis. Soc. Amer., 1970.

86. Krause, G., *Konsolidationstheorien im Rahmen der Mechanik der Gemische*, Die Bautechnik, 95-103, March 1977.

87. Lade, P.V. and S.B. Hernandez, *Membrane Penetration Effects in Undrained Tests*, Journal of the Geotechnical Engineering Division, ASCE, Vol. 103, No. GT2, February, 1977,pp. 109-125.

88. Lee, K.L., and H.B. Seed, *Cyclic Stress Conditions Causing Liquefaction of Sand*, Proceedings, Amer. Soc. Civ. Engrs., Vol. 93, Jour. Soil Mech. Found. Div., No. SM1, 47-70, 1967.

89. Lee, S.C., Special Finite Elements for Analysis of Soil Consolidation, M.S. Thesis, The Ohio State University, Columbus, Ohio, 1982.

90. Leliavsky, S., *Experiments in Effective Uplift Area in Gravity Dams*, Transactions, Amer. Soc. Civ. Engrs., Vol. 112, 444-487, 1947.

91. Leliavsky. S., Irrigation and Hydraulic Design, Vol. I, Chapman and Hall, 1955.

92. Lo, K.Y., *The Pore-Pressure Strain Relationship of Normally Consolidated Undisturbed Clays*, Parts I and II, Canadian Geotech. Jour., Vol. 6, 383-395, 1969.

93. Lubinski, A., *The Theory of Elasticity for Porous Bodies Displaying Strong Pore Structure*, Proc., 2nd U.S. National Cong. Appl. Mech., 247-256, 1954.

94. Lucks, A.S., J.T. Christian, G.E. Brandow, and K. Hoeg, *Stress Conditions in NGI Simple Shear Test*, Journal of the Soil Mechanics and Foundations Division, ASCE, Vol 98, January, 1972, pp. 155-160.

95. Marcuson, W.F., Personal Communication with W.E.Wolfe.

96. Mason, S.F., Large Scale Testing of Sand Liquefaction, M.S. Thesis, The Ohio State University, Columbus, Ohio, 1982.

97. Maxwell, J.C., *On the Displacement in a Case of Fluid Motion*, Proc. London Math. Soc., 693, 1869.

98. Mikhlin, S.G., The Problem of the Minimum of a Quadratic Functional, Holden-Day, San Francisco, 1965.

99. Mills, N., *On a Theory of Multi-Component Mixtures*, Quar. Jour. Mech. App. Maths., Vol. 20, 499-508, 1967.

100. Mokadam, R.G., *Thermodynamic Analysis of the d'arcy Law*, Jour. of App. Mech., Amer. Soc. Mech. Engrs., Vol.6, 208-212, 1961.

101. Mokadam, R.G., *Application of Thermodynamics of Irreversible Processes to Flow of Multicomponent Fluids Through Porous Solids*, Inzhenernyi-fizicheskii Zhurnal, Vol. VI, No. 6, 1963. (in Russian).

102. Mokadam, R.G., *Themodynamic Analysis of the Coefficient of Diffusion*, Inzhenernyi-fizicheski Zhurnal, Vol. IX, No. 2, 1966.(in Russian).

103. Morland, L.W., *A Simple Constitutive Theory for a Fluid-Saturated Saturated Porous Solid*, Jour. Geophy. Res., Vol. 77, 890-900, 1972.

104. Morland, L.W., *A Theory of Slow Fluid Flow Through a Porous Thermoelastic Matrix*, Geophy. Jour. Roy. Astro. Soc., Vol. 55, 393-410, 1978.

105. Morland, L.W., *Slow Viscous Flow Through a Deformable Matrix*, Geotechnical and Environmental Aspects of Geopressure Energy, Ed. S. Saxena, Engineering Foundation, New York, 363-366, 1980.

106. Morland, L.W., and A. Sawicki, *A Mixture Model for the Compaction of Saturated Sand*, 1983.

107. Mulilis, J.P., H.B. Seed, C.K. Chan, J.K. Mitchell, and K. Arulanandan, *Effects of Sample Preparation on Sand Liquefaction*, Journal of the Geotechnical Engineering Division, ASCE, Vol. 103, No. GT2, February, 1977,pp. 91-108.

108. Muller, I., *A Thermodynamic Theory of Mixtures of Fluids*, Arch. Rat. Mech. Anal., Vol. 28, 1-39, 1968.

109. National Academy of Science, Liquefaction of Soils During Earthquakes, Committee on Earthquake Engineering, National Academy Press, Washington D.C., 1985.

110. National Science Foundation, International Workshop on Constitutive Equations for Granular Non-Cohesive Soils, Case Western Reserve University, Ed. A. Seeda, July 22-24, 1987

111. Noll, W., *A Mathematical Theory of the Mechanical Behavior of Continuous Media*, Arch. Rat. Mech. Anal., Vol. 2, No. 3, 197-226, 1958.

112. Novozhilov, V.V., Theory of Elasticity, Available from U.S. Dept. of Commerce (Office of Technical Services), Translated from Russian, 1961.

113. Nur, A., and J.D. Byerlee, *An Exact Effective Stress Law for Elastic Deformation of Rock with Fluids*, Jour. Geophy. Res., Vol. 76, 6414-6419, 1971.

114. Oden, J.T., and J.N. Reddy, Variational Methods in Theoretical Mechanics, Springer-Verlag, New York, 1983.

115. O-Hara, S., The Results of Experiment on the Liquefaction of Saturated Sands with a Shaking Box: Comparison with Other Methods, Reprinted from Technology Reports of the Yamaguchi University, Vol. 1, No. 1, December, 1972.

116. Oliver, M.L., *On Balanced Interactions in Mixtures*, Arch. Rat. Mech. Anal., Vol. 49, 195-224, 1973.

117. Oliver, M.L., and W.D. Williams, *Formulation of Balance of Forces in Mixture Theories*, Quar. App. Math., Vol. 33, 81-86 1976.

118. Onsager, L., *Reciprocal Relations in Irreversible Processes, II*., Physical Review, Vol. 38, 2265-2279, 1931.

119. Pecker, C., and H. Deresiewicz, *Thermal Effects on Wave Propagation in Liquid-Filled Porous Media*, Acta Mechanica, Vol. 16, 45-64, 1973.

120. Polubarinova-Kochina, P.I., The Theory of Ground Water Movement, 1952, Translated from Russian by Roger De Wiest, J.M., Princeton Univ. Press, Princeton, 1962.

121. Prevost, J.H., *Mechanics of Continuous Porous Media*, Int. Jour. Engrg. Sci., Vol. 18, 787-800, 1980.

122. Prevost, J.H., *Nonlinear Transient Phenomena in Saturated Porous Media*, Comp. Methods Engrg. App. Mech., Vol. 20, 3-18 1982.

123. Prevost, J.H., *Two-surface versus Multi-surface Theories A Critical Assessment*, Int. Jour. Numer. Anal. Methods Engrg., Vol. 6, 323-337, 1982.

124. Rice, J.R., and M.P. Cleary, *Some Basic Stress Diffusion Solutions for Fluid-Saturated Elastic Porous Media with Compressible Constituents*, Rev. Geophy. Space Phy., Vol. 14, 227-241, 1976.

125. Riney, T.D., S.K. Garg, J.W. Kirsch, L.W. Morland, and C.R. Hastings, Stress Wave Effects in Inhomogeneous and Porous Earth Materials, Report 3SR-267, Systems, Science and Software, La Jolla, California, 1970.

126. Riney, T.D., S.K. Garg, J.W. Kirsch, C.R. Hastings, and K.G. Hamilton, Wave Propagation in Porous Geologic Composites, Report 3SR-648, Systems, Science, and Software, La Jolla, California, 1971.

127. Roscoe, K.H., *An Apparatus for the Application of Simple Shear to Soil Samples*, Proceedings of the Third International Conference on Soil Mechanics, Zurich, Volume 1, 1953, pp. 186- 191.

128. Ross, G.A., H.B. Seed, and R.R. Migliaccio, *Bridge Foundation Behavior in Alaska Earthquake*, Proceedings, Amer. Soc. Civ. Engrs., Vol. 95, Jour. Soil Mech. Found. Div., No. SM4, 1007-1036, 1969.

129. Sampaio, R., *An Approximate Theory of Mixtures with Diffusion*, Arch. Rat. Mech. Anal., Vol. 62, 99-116, 1976.

130. Sampaio, R., and W.O. Williams, *Thermodynamics of Diffusing Mixtures*, J. de Mecanique, Vol. 18, 19-45, 1979.

131. Sandhu, R.S., Fluid Flow in Saturated Porous Elastic Media, Ph.D. Thesis, University of California, Berkeley, California, 1968.

132. Sandhu, R.S., Finite Element Analysis of Soil Consolidation, Report OSURF-3570-76-3, Geotechnical Engineering Report No. 6, The Ohio State University, Columbus, Ohio, 1976.

133. Sandhu, R.S., and H. Liu, *Analysis of Consolidation of Viscoelastic Soils*, Numer. Methods in Geomechanics, Aachen, 1979, Ed. W. Wittke, Balkema, 1255-1263, 1979.

134. Sandhu, R.S., *Finite Element Analysis of Subsidence due to Fluid Withdrawal*, U.S.-Venezuela Forum on Land Subsidence Due to Fluid Withdrawal, Fountainhead, Oklahoma, 1982.

135. Sandhu, R.S., and Pister, K.S., *A Variational Principle for Linear Coupled Field Problems*, Int. J. Engg. Sc., Vol. 8, 989-999, 1970.

136. Sandhu, R.S., and Pister, K.S., *Variational Principles for Boundary Value and Initial-Boundary Value Problems*, Int. J. Solids Struct., Vol. 7, 639-654, 1971.

137. Sandhu, R.S., and Salaam, U., *Variational Formulation of Linear Problems with Non-homogeneous Boundary Conditions and Internal Discontinuities*, Comp. Methods App. Mech. Engg., Vol. 7, 75-91, 1975.

138. Sandhu, R.S., *Variational Principles for Finite Element Approximations*, in Finite Elements in Water Resources Engineering, Editors G.F. Pindar, C.A. Brebbia, Pentech Press, 1976.

139. Sasaki, Y. and E. Taniguchi, *Large Scale Shaking Table Tests on the Effectiveness of Gravel Drains for Liquefiable Sand Deposits*, Proceedings of the Conference on Soil Dynamics and Earthquake Engineering, Vol. 2, 1982, pp. 843-857.

140. Scheidegger, A.E., The Physics of Flow Through Porous Media, Macmillan, 1960; University of Toronto Press, 1974.

141. Schiffman, R.L., and A.A. Fungaroli, *Consolidation due to Tangential Loads*, Sixth Int. Conf. Soil Mech. Found. Engrg., 188-192, 1965.

142. Schiffman, R.L., A.T.F. Chen, and J.C. Jordan, *An Analysis of Consolidation Theories*, Proceedings, Amer. Soc. of Civ. Engrs., Vol. 95, Jour. Soil Mech. Found. Div., No. SM1, 285-312, 1965.

143. Schiffman, R.L., *The Stress Components of a Porous Medium*, Jour. Geophy. Res., Vol. 75, 4035-4038, 1970.

144. Schiffman, R.L., *Thermoelastic Theory of Consolidation*, Environmental and Geophysical Heat Transfer, Vol. 4, Heat Transfer Div., Amer. Soc. Mech. Engrs., 78-84, 1972.

145. Seed, H.B., and K.L. Lee, *Liquefaction of Saturated Sand During Cyclic Loading*, Proceedings, Amer. Soc. Civ. Engrs., Vol. 92, Jour. Soil. Mech. Found. Div., No. SM6, 105-134, 1966.

146. Seed, H.B., and I.M. Idriss, *Analysis of Soil Liquefaction: Niigata Earthquake*, Proceedings, Amer. Soc. Civ. Engrs., Vol. 93, Jour. Soil Mech. Found. Div., No. SM3, 83-108, 1967.

147. Seed, H.B., *Landslide During Earthquakes Due to Liquefaction. The Fourth Terzaghi Lecture*, Proceedings, Amer. Soc. of Civ. Engrs., Vol. 94, Jour. Soil Mech. Found. Div., No. SM5, 1053-1122, 1968.

148. Seed, H.B., and I.M. Idriss, *Influence of Soil Conditions on Ground Motion During Earthquakes*, Proceedings, Amer. Soc. of Civ. Engrs., Vol. 95, Jour. Soil Mech. Found. Engrg. Div., No. SM1, 99-137, 1969.

149. Seed, H.B., and K.L. Lee, *Pore Water Pressure in Earth Slopes Under Seismic Loading Conditions*, Proceedings, 4th World Conference on Earthquake Engineering, Chile, 1969.

150. Seed, H.B., and I.M. Idriss, *Analysis of Ground Motions at Union Bay, Seattle, During Earthquake on Distant Nuclear Blasts*, Bull., Seis. Soc. Amer., Vol. 60, No. 1, 1970.

151. Seed, H.B., I.M. Idriss, and H. Dezfulian, Relationships Between Soil Conditions and Building Damage in the Caracas Earthquake of July 29,1967, Report No. EERC 70-2, Earthquake Engineering Research Center, University of California, Berkeley, California, 1970.

152. Seed, H.B., and I.M. Idriss, *Influence of Soil Conditions on Building Damage Potential During Earthquakes*, Proceedings, Amer. Soc. Civ. Engrs., Vol. 97, Jour. Struct. Div., No. ST2, 639-663, 1971.

153. Seed, H.B., R.V. Whitman, H. Dezfulian, R. Dobry, and I.M. Idriss, *Soil Conditions and Building Damage in 1967 Caracas earthquake*, Proceedings, Amer. Soc. Civ. Engrs., Vol. 98, Jour. Soil Mech. Found. Division, No. SM8, 787-806, 1971.

154. Seed, H.B., K.L. Lee, I.M. Idriss and F. Makdisi, Analysis of the Slides in the San Fernando Dams During the Earthquake of Feb.9, 1971, Report EERC 73-2, Earthquake Engineering Research Center, University of California, Berkeley, California, 1973.

155. Seed, H.B., *Landslides During Earthquakes Due To Soil Liquefaction*, Journal of the Soil Mechanics and Foundations Division, ASCE, Vol. 94, No. SM5, September, 1968, pp. 1053-1122.

156. Seed, H.B., *Soil Liquefaction and Cyclic Mobility Evaluation for Level Ground During Earthquakes*, Journal of the Geotechnical Engineering Divison, ASCE, Vol. 105, No. GT2, February, 1979, pp. 201-225.

157. Seed, H.B., *Evaluation of Soil Liquefaction Effects of Level Ground During Earthquakes*, Proceedings, ASCE Annual Convention, Sept-Oct, 1981, pp.

158. Seed, H.B., Mori, K. and Chan, C.K., Influence of Seismic *History on Liquefaction of Sands*, Journal of the Geotechnical Engineering Division, ASCE, Vol. 103, No. GT4, April, 1977 pp. 257-270.

159. Shi, J.J., K.R. Rajagopal, and A.S. Wineman, *Applications of the Theory of Interacting Continua to the Diffusion of a Fluid Through a Nonlinear Elastic Media*, Int. Jour. Engrg. Sci., Vol. 19, 871-889, 1981.

160. Singh, R.D., Mechanical Characterization and Finite Element Analysis of Elastic-Plastic, Work-Hardening Soils, Ph.D. Dissertation, The Ohio State University, 1972.

161. Suklje, L., Rheological Aspects of Soil Mechanics, Interscience, 1969.

162. Terzaghi, K., Theoretical Soil Mechanics, John Wiley, New York, 1943.

163. Terzaghi, K., *Effective Area of Uplift*, Engineering News Record, June 1963; Also, Transactions, Amer. Soc. Test. Mat., 1945.

164. Truesdell, C., and R.A. Toupin, *The Classical Field Theories*, Handbuch der Physik, Vol. III/1, Ed. S. Flugge, Springer-Verlag, 1960.

165. Truesdell, C., *Mechanical Basis of Diffusion*, Jour. Chem. Phy., Vol. 37, No. 10, 2336-2344, 1962.

166. Truesdell, C., Rational Thermodynamics, McGraw-Hill, 1969.

167. Tsien, H.S., *On the Basic Equations of Soil Dynamics*, Problems of Continuum Mechanics, Muskhelishvili Anniversary Volume, Noordhoff, The Netherlands, 1961.

168. Verruijt, A., *Some Remarks on the Principle of Effective Stress*, IUTAM Conference on Deformation and Failure of Granular Materials, Delft, The Netherlands, 1982.

169. Verruijt, A., *The Theory of Consolidation*, in Fundamentals of Transport Phenomenon in Porous Media, NATO Advance Study Institute, Edited by J. Bear and M.Y. Corapcioglu, 1984.

170. Walsh, J.B., *The Effect of Crack on Compressibility of Rock*, J. Geophy. Res., Vol. 70, 381, 1965.

171. Westmann, R.A., Nonlinear Three Dimensional Theory of Consolidation, Unpublished Report, University of California at Los Angeles, California, 1967.

172. Williams, W.O., *On Stresses in Mixtures*, Arch. Rat. Mech. Anal., Vol.70, 251-260, 1979.

173. Wolfe, W.E., Cyclic Strength of Cubic Saturated Sand Samples, M.S. Thesis, University of California, Los Angeles, 1973.

174. Wood, D.M., *Laboratory Investigations of the Behavior of Soils under Cyclic Loading: a Review*, in, Soil Mechanics - Transient and Cyclic Loads, G.N. Pande and O.C. Zienkiewicz eds., John Wiley and Sons Ltd. pub, 1982,pp. 513-582.

175. Wright, D.F., P.A. Gilbert, and A.S. Saada, *Shear Devices for Determining Dynamic Soil Properties*, Proceedings of the ASCE Specialty Conference on Earthquake Engineering and Soil Dynamics, Pasadena, Vol. 2, 1978, pp. 1056-1075.

176. Zangar, C.B., Theory and Problems of Water Percolation, Engineering Monograph No. 8, U.S. Bureau of Reclamation, Denver, Colorado, 1953.

Appendix A

CONVECTED COORDINATES

This appendix contains a summary of some definitions, relations and formulae related to the use of convected coordinates in the mechanics of continua. The discussion follows Green [65] and Fung [47].

A.1 NOTATION

Indices, which may either be subscripts or superscripts, such as x^i, x_i, p^{ij}, q_{ijm} etc. are used to denote components of tensors of various orders. A single element ϕ having no indices constitutes a system of zero order. Systems of elements with one and two indices, are respectively, termed first order and second order.

The summation convention used throughout this report implies that the repetition of an index (whether superscript or subscript) in a term denotes summation with respect to that index over the range 1, 2, 3.

A.2 COORDINATE TRANSFORMATION

Let θ^i denote a set of independent variables, whose differentials are $d\theta^i$. The mapping of θ^i into another set of variables $\bar{\theta}^i$ by any arbitrary single-valued function of the form

$$\bar{\theta}^i = \bar{\theta}^i (\theta^1, \theta^2, \theta^3) \tag{A.1}$$

specifies a transformation of coordinates. Here we have used the same notation for the function and its value. The arbitrary functions are assumed to possess derivatives upto the order required. The inverse transformation is assumed to be single valued and written as:

$$\theta^i = \theta^i(\bar{\theta}^1, \bar{\theta}^2, \bar{\theta}^3) \tag{A.2}$$

The differentials $d\theta^i$ and $d\bar{\theta}^i$ are related by

$$d\bar{\theta}^i = \bar{C}^i_j d\theta^j$$

$$d\theta^i = C^i_j d\bar{\theta}^j \tag{A.3}$$

Evidently,

$$\bar{C}^i_j C^j_k = C^i_j \bar{C}^j_k = \delta^i_k \tag{A.4}$$

where δ^i_k is Kronecker's delta. For reversibility of transformation it is sufficient that [65]

$$C = |\bar{C}^i_j| \neq 0 \tag{A.5}$$

While the transformations of the differentials in (A.3) is linear, the transformations of variables in (A.1) and (A.2) are not necessarily linear. The coordinate transformation with the properties described above, along with the condition (A.4), are called the admissible transformations [47]. If C is positive everywhere, then a right-handed set of coordinates is transformed into another right-handed set and the transformation is proper. In this work, the transformations are assumed to be admissible and proper, unless otherwise stated.

A.3 CONTRAVARIANT AND COVARIANT VECTORS

A system of order zero has only a single component ϕ in the variables θ^i and a single component $\bar{\phi}$ in the variables $\bar{\theta}^i$. ϕ is scalar if $\bar{\phi} = \phi$ for all $\bar{\theta}^i$.

Let a system of order one have components A^i and $\bar{A}^i$, in the variables θ^i and $\bar{\theta}^i$, respectively. Then, if

$$\bar{A}^i = \bar{C}^i_j A^j = \frac{\partial \bar{\theta}^i}{\partial \theta^j} A^j \tag{A.6}$$

the functions $\bar{A}^i$ and A^j are contravariant components of a tensor of order one. A system is a covariant tensor of order one if the components B_i in the variables θ^i and $\bar{B}_i$ in the variables $\bar{\theta}^i$ are related by,

$$\bar{B}_i = C^j_i B_j = \frac{\partial \theta^j}{\partial \bar{\theta}^i} B_j \tag{A.7}$$

Contravariant tensor components are indicated by superscripts and covariant components by subscripts. Transformations of contravariant and covariant components of second order tensors are given by,

$$\bar{A}^{ij} = \bar{C}^i_m \bar{C}^j_n A^{mn} \tag{A.8}$$

and

$$\bar{B}_{ij} = C^m_i C^n_j B_{mn} \tag{A.9}$$

(A.3) shows that the differentials transform according to the law of contravariant tensors. The use of upper index is appropriate in that case. The variables θ^i themselves are, in general, neither contravariant nor covariant and the position of their index is only a matter of convenience.

A.4 CURVILINEAR COORDINATES

Consider the coordinates x^i or x_i referred to a right handed orthogonal system, Figure 45, of axes in a three-dimensional Euclidean space. Let an admissible transformation of the types discussed earlier to θ' coordinates be defined by

$$\theta' = \theta'(x_1, x_2, x_3) \tag{A.10}$$

Since for each set of values of x_i, there exists a unique set of values of θ', it is possible to represent the Euclidean space by the variables θ', instead of cartesian system x_i. The relations

$$\theta'(x_1, x_2, x_3) = \text{constant} \tag{A.11}$$

with $i = 1$ to 3, represent three families of coordinate surfaces and the point of intersection determines a point P in space. The conditions imposed on θ' ensure that such a point is uniquely defined. The intersections of the coordinate surfaces are coordinate curves and θ' are curvilinear coordinates.

A.5 BASE VECTORS AND METRIC TENSORS

Let $\mathbf{R}$ be the position vector of a point P, whose coordinates are x_i or x^i and let $d\mathbf{R}$ denote the infinitesimal vector PQ, where Q has the coordinates $x_i + dx_i$ or $x^i + dx^i$. Then (Figure 46)

$$\mathbf{R} = x_i e^i = x^i e_i \tag{A.12}$$

and

$$d\mathbf{R} = dx_i e^i = dx^i e_i \tag{A.13}$$

where e_i and e^i are unit vectors. If $ds = |d\mathbf{R}|$ is the length of vector PQ, then

$$(ds)^2 = d\mathbf{R} \cdot d\mathbf{R} = dx_i\, dx_i \tag{A.14}$$

If θ_i, θ' are one to one continuous mappings for the x_i, x^i systems,

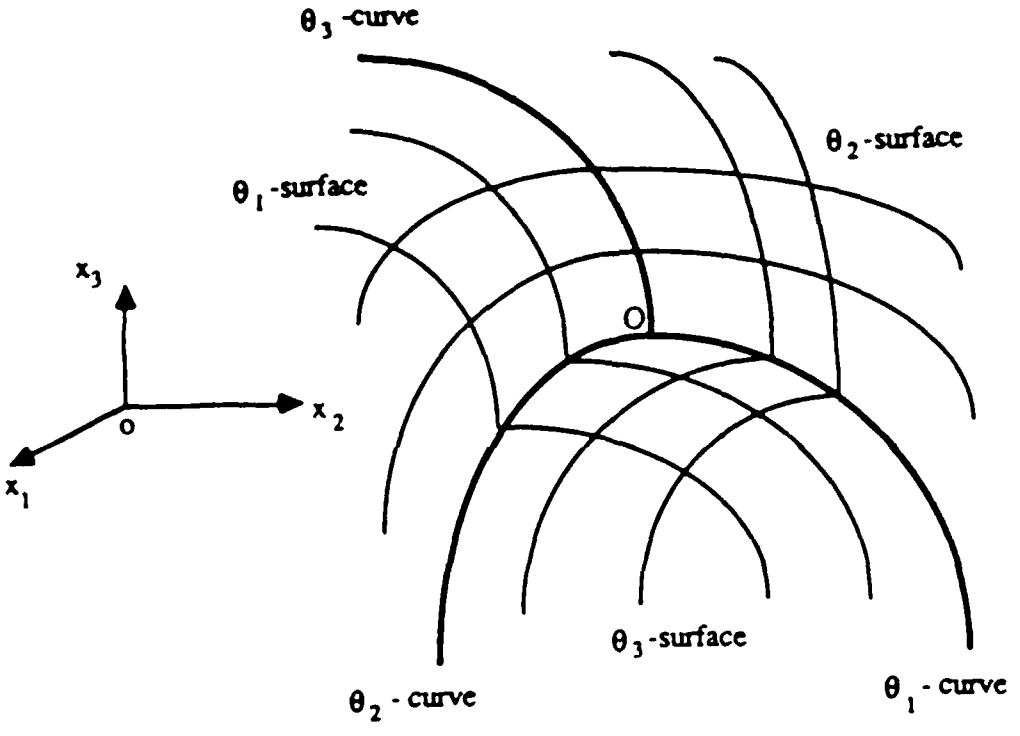

Figure 45: Coordinate Surfaces

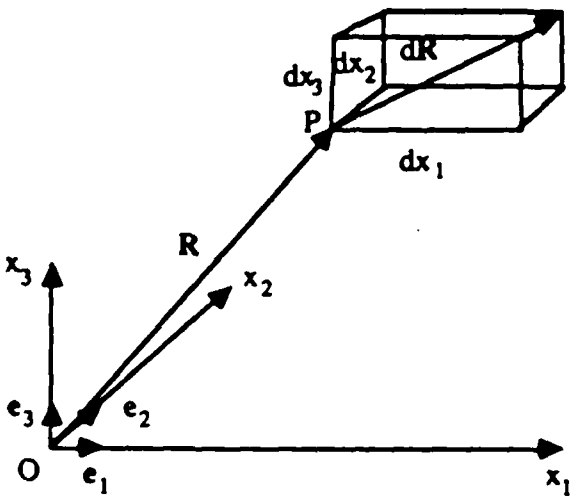

Figure 46: Position Vector and Its Differential

$$d\theta^i = \frac{\partial \theta^i}{\partial x^j} dx^j , \quad dx^i = \frac{\partial x^i}{\partial \theta^j} d\theta^j \tag{A.15}$$

$$d\theta_i = \frac{\partial x^j}{\partial \theta^i} dx_j , \quad dx_i = \frac{\partial \theta^j}{\partial x^i} d\theta_j \tag{A.16}$$

Consequently

$$d\mathbf{R} = dx_i \, e^i = \frac{\partial \theta^j}{\partial x^i} e^i \, d\theta_j = G^j d\theta_j \tag{A.17}$$

and also

$$d\mathbf{R} = dx^i e_i = \frac{\partial x^i}{\partial \theta^j} e_i \, d\theta^j = G_j d\theta^j \tag{A.18}$$

where

$$G_i = \frac{\partial x^j}{\partial \theta^i} e_j , \quad G^i = \frac{\partial \theta^i}{\partial x^j} e^j \tag{A.19}$$

The Kronecker delta and the permutation symbols are defined in rectangular cartesian coordinate system as

$$\delta^{ij} = \delta_{ij} = \delta^i_j = \delta^j_i = 0 \text{ for } i \neq j \ (=1 \text{ for } i = j) \tag{A.20}$$

$$e_{ijk} = e^{ijk} = \begin{cases} 0 \text{ (when two indices are equal)} \\ 1 \text{ (when i, j, k are in even permutation)} \\ -1 \text{ (when i, j, k are in odd permutation)} \end{cases} \tag{A.21}$$

Their counterparts in general coordinates θ^i are as follows:

$$G_{ij} = G_i . G_j = \frac{\partial x^m}{\partial \theta^i} \frac{\partial x^m}{\partial \theta^j} \tag{A.22}$$

$$G^{ij} = G^i . G^j = \frac{\partial \theta^i}{\partial x^m} \frac{\partial \theta^j}{\partial x^m} \tag{A.23}$$

$$G^i_j = G_j . G^i = \frac{\partial \theta^i}{\partial x^m} \frac{\partial x^m}{\partial \theta^j} = \delta^i_j \tag{A.24}$$

$$e_{ijk} = e_{ijk} \left| \frac{\partial x^m}{\partial \theta^n} \right| = e_{ijk} \sqrt{G} \tag{A.25}$$

$$e^{ijk} = e^{ijk} \left| \frac{\partial \theta^m}{\partial x^n} \right| = \frac{e^{ijk}}{\sqrt{G}} \tag{A.26}$$

where G is the determinant $|G_{ij}|$ and is positive for any proper coordinate system. The vectors G_i and G^i are connected by the relations

$$G^i = G^{ij} G_j \;\; ; \;\; G_i = G_{ij} G^j \tag{A.27}$$

G_{ij} is the Euclidean metric tensor of the coordinate system and G^{ij} is the associated metric tensor [47]. The magnitudes of these base vectors are,

$$|G_i| = \sqrt{G_i . G_i} = \sqrt{G_{ii}}$$

$$|G^i| = \sqrt{G^i . G^i} = \sqrt{G^{ii}} \tag{A.28}$$

where the index is not summed. The line element ds in (A.14) may now be written in the form

$$ds^2 = d\mathbf{R} . d\mathbf{R} = G_{ij} d\theta^i d\theta^j = G^{ij} d\theta_i d\theta_j = d\theta_i d\theta^j \tag{A.29}$$

A.6 PHYSICAL MEANING OF COVARIANT AND CONTRAVARIANT COMPONENTS OF A VECTOR

A vector w in terms of covariant and contravariant base vectors is

$$\mathbf{w} = w^i G_i = w_i G^i \tag{A.30}$$

where by (A.27),

$$w_i = G_{ij} w^j \quad w^i = G^{ij} w_j \tag{A.31}$$

According to (A.30), if $\mathbf{w}$ is represented by line vectors, then w^i are the components of $\mathbf{w}$ in the direction of the covariant base vectors $\mathbf{G}_i$, while w_i are the components of $\mathbf{w}$ in the direction of the contravariant base vectors $\mathbf{G}^i$ A two-dimensional illustration is shown in Figure 47. Some other results are

$$\mathbf{v} \cdot \mathbf{w} = G_{ij} v^i w^j = G^{ij} v_i w_j = v_i w^i = v^i w_i$$

$$|\mathbf{w}| = \sqrt{\mathbf{w} \cdot \mathbf{w}} = \sqrt{w_i w^i} \tag{A.32}$$

(A.30) can also be written as

$$\mathbf{w} = \frac{w^i \sqrt{G_{ii}}\, \mathbf{G}_i}{\sqrt{G_{ii}}} = \frac{w_i \sqrt{G^{ii}}\, \mathbf{G}^i}{\sqrt{G^{ii}}} \qquad \text{(no sum)} \tag{A.33}$$

$w^i \sqrt{G_{ii}}$ are components of $\mathbf{w}$ resolved in the direction of the unit vectors $\frac{\mathbf{G}_i}{\sqrt{G_{ii}}}$ which are tangent to the coordinate curves. A similar interpretation for $w_i \sqrt{G^{ii}}$ is possible. These components viz. $w^i \sqrt{G_{ii}}$ and $w_i \sqrt{G^{ii}}$ (i not summed) do not obey the tensor transformation laws and are not components of tensors.

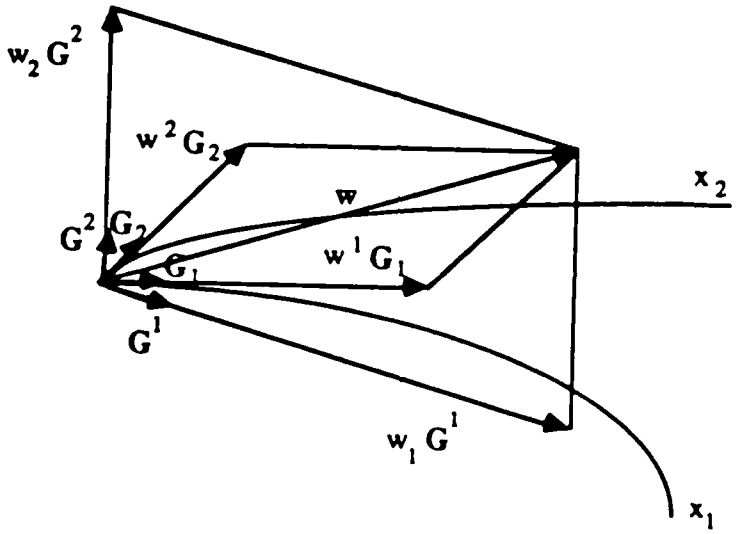

Figure 47: Covariant and Contravariant Components of a Vector

A.7 PARTIAL DERIVATIVES IN CARTESIAN COORDINATES

Consider $\bar{A}^i$, a contravariant tensor of order one, expressed as a function of coordinate system $\bar{x}_i$. The relationship with the description in the coordinate system x_i is given by (A.6) as:

$$\bar{A}^i(\bar{x}_1, \bar{x}_2, \bar{x}_3) = A^k(x_1, x_2, x_3)\frac{\partial \bar{x}^i}{\partial x^k} \tag{A.34}$$

Differentiating

$$\frac{\partial \bar{A}^i}{\partial \bar{x}^j} = A^k \frac{\partial^2 \bar{x}^i}{\partial \bar{x}^j \partial x^k} + \frac{\partial A^k}{\partial \bar{x}^j}\frac{\partial \bar{x}^i}{\partial x^k}$$

$$= A^k \frac{\partial^2 \bar{x}^i}{\partial x^m \partial x^k}\frac{\partial x^m}{\partial x^j} + \frac{\partial A^k}{\partial x^n}\frac{\partial x^n}{\partial \bar{x}^j}\frac{\partial \bar{x}^i}{\partial x^k} \tag{A.35}$$

If the two cartesian coordinate systems are related by an affine transformation, $\bar{x}_i = a_{ij}x_j + b_i$, a_{ij} and b_i being constants, $\frac{\partial^2 \bar{x}^i}{\partial x^j \partial x^k} = 0$ and $\frac{\partial \bar{x}^i}{\partial x^j} = a_{ij}$. Hence

$$\frac{\partial \bar{A}^i}{\partial \bar{x}^j} = \frac{\partial \bar{x}^i}{\partial x^k}\frac{\partial x^n}{\partial \bar{x}^j}\frac{\partial A^k}{\partial x^n} \tag{A.36}$$

(A.36) implies that for cartesian systems, related by an affine transformation, the partial derivative $\frac{\partial A^k}{\partial x^n}$ follows the transformation law for a mixed tensor of order two. The second order term in (A.35) does not vanish in curvilinear coordinates and thus the partial derivative of the tensor does not yield a higher order tensor.

A.8 COVARIANT DIFFERENTIATION

If $\mathbf{R}$ is taken to be a scalar function of the general coordinates viz.

$$\mathbf{R} = \mathbf{R}(\theta_1, \theta_2, \theta_3) \tag{A.37}$$

then

$$\mathbf{G}_i = \mathbf{R}_{,i} = \frac{\partial \mathbf{R}}{\partial \theta^i} \tag{A.38}$$

The differentiation of base vectors $\mathbf{G}_i$ yields

$$\mathbf{G}_{i,j} = \frac{\partial^2 \mathbf{R}}{\partial \theta^i \partial \theta^j} = \mathbf{R}_{,ij} = \mathbf{R}_{,ji} \tag{A.39}$$

Recalling (A.19) and noting that $\mathbf{e}_i$ form a set of constant base vectors,

$$\mathbf{G}_{i,j} = \frac{\partial^2 x^r}{\partial \theta^i \partial \theta^j} \mathbf{e}_r \tag{A.40}$$

which, upon use of (A.19), becomes

$$\mathbf{G}_{i,j} = \Gamma_{ij\alpha} \mathbf{G}^\alpha = \Gamma^r_{ij} \mathbf{G}_r \tag{A.41}$$

where

$$\Gamma_{ij\alpha} = \frac{\partial^2 x^r}{\partial \theta^i \partial \theta^j} \frac{\partial x^r}{\partial \theta^\alpha} \tag{A.42}$$

and

$$\Gamma^r_{ij} = G^{r\alpha} \Gamma_{ij\alpha} \tag{A.43}$$

(A.22) and (A.42) give

$$\Gamma_{ij\alpha} = \frac{1}{2} [G_{i\alpha,j} G_{j\alpha,i} - G_{ij\alpha}] \tag{A.44}$$

Similarly, (A.29) implies

$$\mathbf{G}^i_{,j} = -\Gamma^i_{jr} \mathbf{G}^r \tag{A.45}$$

The symbols $\Gamma_{ij\alpha}$ and Γ^r_{ij} are Christoffel symbols of the first and second kind, respectively. If $\mathbf{w}$ is a vector

$$\frac{\partial \mathbf{w}}{\partial \bar{\theta}^i} = \frac{\partial \mathbf{w}}{\partial \theta^r}\frac{\partial \theta^r}{\partial \bar{\theta}^i} = C_i^r \frac{\partial \mathbf{w}}{\partial \theta^r} = C_i^r \mathbf{w}_{,r} \tag{A.46}$$

so that $\mathbf{w}_{,r}$ transform according to the covariant transformation. Also, from (A.30),

$$\begin{aligned}\mathbf{w}_{,i} &= w^r_{,i}\mathbf{G}_r + w^r \mathbf{G}_{r,i} \\ &= w_{r,i}\mathbf{G}^r + w_r \mathbf{G}^r{}_{,i}\end{aligned} \tag{A.47}$$

Using (A.41) and (A.45)

$$\mathbf{w}_{,i} = w^r|_i \mathbf{G}_r = w_r|_i \mathbf{G}^r \tag{A.48}$$

where

$$w^r|_i = w^r{}_{,i} + \Gamma^r_{si} w^s \tag{A.49}$$

$$w_r|_i = w_{r,i} - \Gamma^s_{ri} w_s \tag{A.50}$$

The expressions $w^r|_i$ and $w_r|_i$ are the covariant derivatives of w^r and w_r, respectively, of the vector $\mathbf{w}$. Since $\mathbf{w}_{,i}$ transform according to covariant transformation, it follows from (A.48) that the covariant derivatives of a vector form a tensor of order two. Similarly, we can write expressions for derivatives of second order tensors in the following form,

$$\begin{aligned}A_{ij}|_r &= A_{ij,r} - \Gamma^m_{ir} A_{mj} - \Gamma^m_{jr} A_{im} \\ A^{ij}|_r &= A^{ij}_{\ ,r} + \Gamma^i_{rm} A^{mj} + \Gamma^j_{rm} A^{im}\end{aligned} \tag{A.51}$$

A.9 GEOMETRIC INTERPRETATION OF COVARIANT DERIVATIVES

Consider a vector field $\mathbf{w}$ associated with every point in space in the region under consideration. Let the vector $\mathbf{w}$ at a point P $(\theta^1, \theta^2, \theta^3)$ be

$$\mathbf{w}(P) = w^i(P)\mathbf{G}_i(P) \tag{A.52}$$

At a neighboring point Q $(\theta^1 + d\theta^1, \theta^2 + d\theta^2, \theta^3 + d\theta^3)$, the vector is

$$\mathbf{w}(Q) = \mathbf{w}(P) + d\mathbf{w}(P)$$

$$= [w^i(P) + dw^i(P)]\ [G_i(P) + dG_i(P)] \tag{A.53}$$

Taking the limit as $d\theta^i \to 0$, we get,

$$dw = [w^i + dw^i]\ [G_i + dG_i] - w^i G_i = w^i dG_i + dw^i G_i \tag{A.54}$$

and the derivative

$$\frac{\partial w}{\partial \theta^j} = w^i \frac{\partial G_i}{\partial \theta^j} + \frac{\partial w^i}{\partial \theta^j} G_i \tag{A.55}$$

Thus, the derivative of w consists of two parts viz. one due to the variation of the components of w^i as the coordinates θ^i are changed and the other arising from the change of the base vectors G_i as the position of the point θ^i is changed. Use of (A.41) in (A.55) gives

$$\frac{\partial w}{\partial \theta^j} = \frac{\partial w^r}{\partial \theta^j} G_r + w^i \Gamma^r_{ij} G_r$$

$$= [\frac{\partial w^r}{\partial \theta^j} + w^i \Gamma^r_{ij}]\ G_r$$

$$= w^r|_j G_r \tag{A.56}$$

Thus the contravariant derivative $w^r|_j$ represents the components of $\frac{\partial w}{\partial \theta^j}$ referred to the base vectors G_r.

A.10 GRADIENT, DIVERGENCE AND CURL IN CURVILINEAR COORDINATES

The gradient (grad ϕ), divergence (div F) and curl (curl A) where ϕ is a scalar and F, A are vectors are given by

$$\text{grad}\,\phi = \phi_{,r} G^r \tag{A.57}$$

$$\text{div}\,F = F^r|_r \tag{A.58}$$

$$\text{curl}\,A = \epsilon^{rst} A_s|_r G_t \tag{A.59}$$

These functions are invariant under general transformation of coordinates. More convenient forms are as follows:

$$\text{grad}\,\phi = \mathbf{G}^r \frac{\partial \phi}{\partial \theta^r} \tag{A.60}$$

$$\text{div}\,\mathbf{F} = \nabla . \mathbf{F} = \mathbf{G}^r . \frac{\partial [\mathbf{F}^s \mathbf{G}_s]}{\partial \theta^r}$$

$$= \mathbf{G}^r . \mathbf{G}_s \mathbf{F}^s|_r \tag{A.61}$$

$$= \mathbf{F}^r|_r$$

$$= [\frac{1}{\sqrt{G}}] (\sqrt{G}\,\mathbf{F}^r)_{,r} \tag{A.62}$$

$$\text{curl}\,\mathbf{A} = \nabla \times \mathbf{A} = \mathbf{G}^r \frac{\partial}{\partial \theta^r} \times \mathbf{A}_s \mathbf{G}^s$$

$$= \mathbf{G}^r \times \frac{\partial}{\partial \theta^r} (\mathbf{A}_s \mathbf{G}^s) \tag{A.63}$$

$$= \epsilon^{rst} \mathbf{A}_s|_r \mathbf{G}_t$$

If $\mathbf{w}$ is a vector defined throughout a volume V, which is bounded by a closed surface S and if $\mathbf{n}$ is a unit vector normal to the surface, then the usual form of Green's theorem is

$$\int_V \text{div}\mathbf{w}\, dV = \int_S \mathbf{w} . \mathbf{n}\, dS \tag{A.64}$$

Alternatively, in tensor notation,

$$\int_V \mathbf{w}^r|_r\, dV = \int_V \frac{1}{\sqrt{G}} (\sqrt{G}\,\mathbf{w}^r)_{,r}\, dV = \int_S \mathbf{w}^r \mathbf{n}_r\, dS \tag{A.65}$$

where

$$\mathbf{n} = \mathbf{n}_r \mathbf{G}^r \tag{A.66}$$

A.11 KINEMATICS AND KINETICS

A.11.1 Introductory

The particles of matter that occupy regions of Euclidean space form a body. A given body, B, may occupy different regions at different times. For convenience, we denote the configuration at time $\tau = 0$, as a reference configuration C_0. The fixed region of space C_0 is occupied by particles of the body. Now, if this material moves so that at a subsequent time $\tau = t$, it occupies a new region of space C, then the body is said to have undergone a motion. Mathematically, this can be represented by a series of coordinate transformations. In particular, the proper transformations assumed in this work ensure that the axioms of continuity and impenetrability are followed. As the continuum moves from one configuration to another, the matter in the neighborhood of each point is translated and rotated as a rigid body and is strained. Strain of an elemental volume is that part of the relative motion between neighboring particles that is not due to the rigid motion. In this section various measures of strain due to relative displacements are described with reference to a single material.

A.11.2 Geometric Relations

Consider a continuous three-dimensional body in the reference configuration C_0 at time $\tau = 0$. Let a system of coordinates a_i be so chosen that a point P of the body is described by P (a_1, a_2, a_3). At time $\tau = t$, let the body be in configuration C, having undergone a motion. The particle P, originally in C_0, now be at Q in C, with coordinates (x_1, x_2, x_3). The coordinate systems a_i and x_i may be curvilinear and need not be coincident. They both describe a Euclidean space, Figure 48.

The admissible transformations of the type described in Section A.2 are

$$x_i = x_i(a_1, a_2, a_3) \tag{A.67}$$

which has a unique inverse

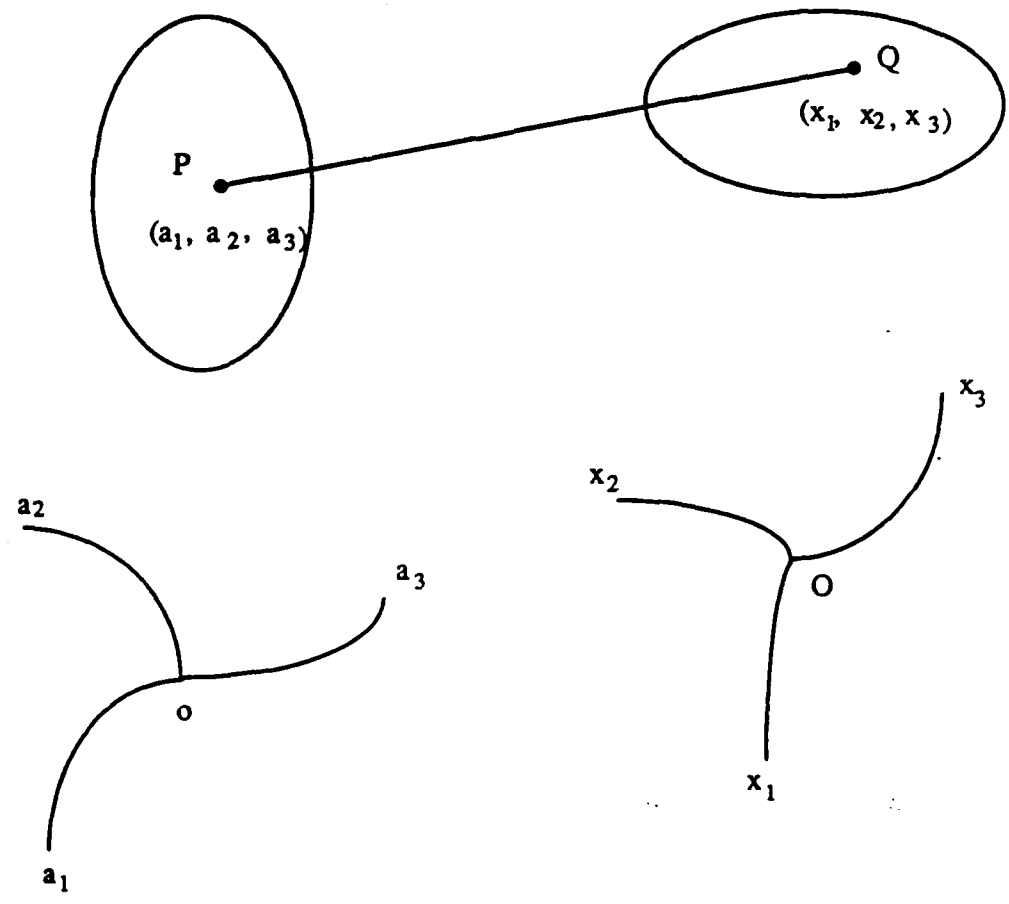

Figure 48: Deformation of a Body

$$a_i = a_i(x_1, x_2, x_3) \tag{A.68}$$

Consider an infinitesimal line element $P\bar{P}$ in the reference configuration C_o such that $\bar{P}$ is given by $\bar{P}(a_i + da_i)$. Then, ds_o, the length of $P\bar{P}$, is

$$ds_o^2 = a_{ij}\, da^i\, da^j \tag{A.69}$$

Here a_{ij} is the Euclidean metric for the coordinate system a_i. Let a corresponding line segment in the configuration C be $Q\bar{Q}$ and its length ds. Then

$$ds^2 = G_{ij}\, dx^i\, dx^j \tag{A.70}$$

where G_{ij} is the Euclidean metric tensor for the coordinate system x_i. Recalling (A.15), The change in length is:

$$ds^2 - ds_o^2 = [G_{mn} \frac{\partial x^m}{\partial a^i} \frac{\partial x^n}{\partial a^j} - a_{ij}]\, da^i\, da^j \tag{A.71}$$

or equivalently,

$$ds^2 - ds_o^2 = [G_{ij} - a_{mn} \frac{\partial a^m}{\partial x^i} \frac{\partial a^n}{\partial x^j}]\, dx^i\, dx^j \tag{A.72}$$

Defining strain tensors

$$E_{ij} = \frac{1}{2}[G_{mn} \frac{\partial x^m}{\partial a^i} \frac{\partial x^n}{\partial a^j} - a_{ij}] \tag{A.73}$$

$$e_{ij} = \frac{1}{2}[G_{ij} - a_{mn} \frac{\partial a^m}{\partial x^i} \frac{\partial a^n}{\partial x^j}] \tag{A.74}$$

we get

$$ds^2 - ds_o^2 = 2\, E_{ij}\, da^i\, da^j \tag{A.75}$$

or

$$ds^2 - ds_o^2 = 2\, e_{ij}\, dx^i\, dx^j \tag{A.76}$$

E_{ij} and e_{ij}, are, respectively, Green's strain tensor and Almansi strain tensor [47].

A.11.3 Description of Deformation

Generally, the initial and the deformed configurations are described with reference to a fixed rectangular cartesian frame.

However, an alternative introduced by Novozhilov [112] is to use a frame of reference which moves continuously with the body and deforms in such a way that the numerical values of the position coordinates of the particles of the body remain the same throughout the motion. This is convenient for finite deformation [47].

For fluid motion, the interest is centered not on the displacements of the particles or their velocities but the velocity distribution in the volume occupied by the fluid. The most convenient mathematical framework for this purpose is the Eulerian coordinates [112].

Consider a rectangular cartesian coordinate system a_i shown in Figure 49. The position vector of a typical point P_o in the reference configuration C_0 is

$$\mathbf{r} = a_i \mathbf{e}_i \tag{A.77}$$

where $\mathbf{e}_i$ are unit vectors along fixed axes. Let a typical point P_o in C_0 occupy position P in the new configuration C at time $\tau = (0 \leq \tau \leq t)$. The position vector of P referred to the same fixed axes is

$$\mathbf{R} = z_i \mathbf{e}_i \tag{A.78}$$

Components of the displacement vector are:

$$u_i = z_i - a_i \tag{A.79}$$

Also, the one to one correspondence between points in C and C_0 implies

$$z_i = z_i(a_1, a_2, a_3) \tag{A.80}$$

$$a_i = a_i(z_1, z_2, z_3) \tag{A.81}$$

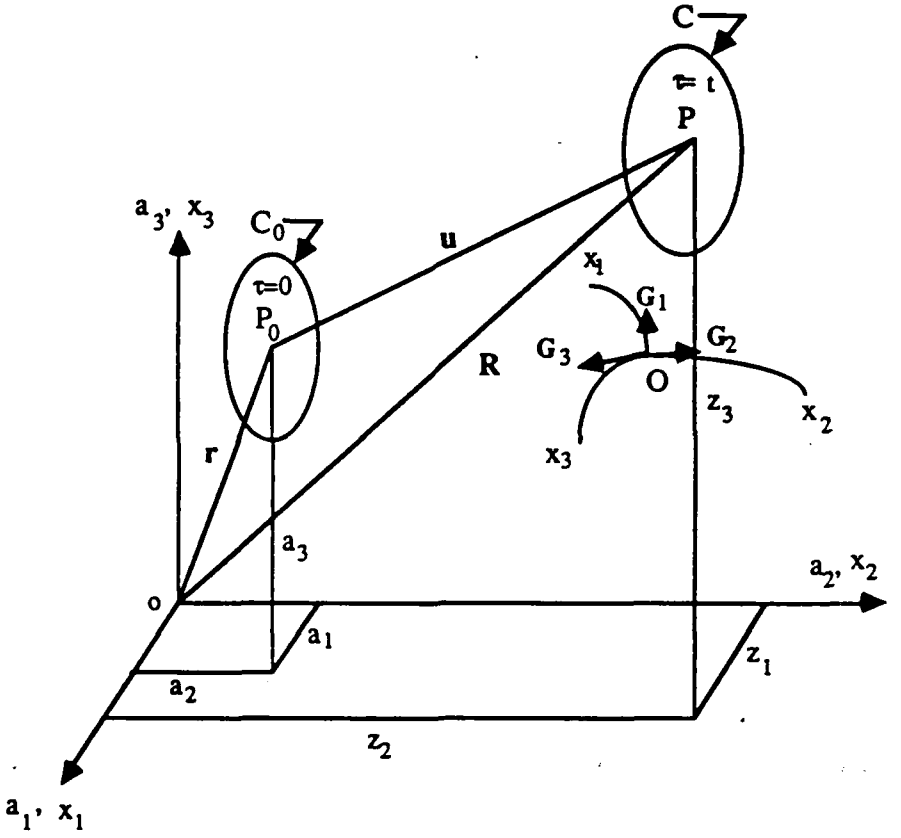

Figure 49: Convected Coordinate System

where a_i and z_i are admissible transformations. Here we do not differentiate between a function and its value. The difference will be clear in the context.

The velocity $\mathbf{v}$ of a particle referred to the fixed system of axes, is

$$\mathbf{v} = \dot{\mathbf{R}} = v_i \mathbf{e}_i \tag{A.82}$$

It follows from (A.79) that

$$v_i = \dot{z}_i = \dot{u}_i \tag{A.83}$$

Similarly, the acceleration $\mathbf{f}$ of a particle referred to the fixed system of axes is

$$\mathbf{f} = f_i \mathbf{e}_i = \dot{\mathbf{v}} = \ddot{\mathbf{R}} \tag{A.84}$$

and

$$f_i = \ddot{z}_i = \ddot{u}_i = \dot{v}_i \tag{A.85}$$

The initial state in C_o may also be described by a general curvilinear set of coordinates x_i so that,

$$a_i = a_i(x_1, x_2, x_3, \tau = 0) \tag{A.86}$$

where a_i is single-valued and continuously differentiable as many times as required. We may imagine this curvilinear system x_i to move continuously with the body as we pass from the reference state C_0 at $\tau = 0$ to the state C at $\tau = t$. The triplet of real numbers x_i are merely the labels that we assign to the positions corresponding to the material particles of the body in the reference configuration C_o. The values of x_i remain unchanged for the new position P in C. The coordinates x_i may be rectangular or curvilinear in C_o, but are curvilinear, in general, in C. Thus the coordinates of P with reference to the invariant convected coordinates are

$$z_i = z_i(x_1, x_2, x_3, \tau = t) \tag{A.87}$$

Using (A.15) and (A.86), we may define a contravariant vector dx^i, in C_o, as

$$dx^i = \frac{\partial x^i}{\partial a^j}\, da^j \qquad da^i = \frac{\partial a^i}{\partial x^j}\, dx^j \tag{A.88}$$

From (A.80) and (A.88)

$$dz^i = \frac{\partial z^i}{\partial a^j}\, da^j = \frac{\partial z^i}{\partial x^j}\, dx^j \tag{A.89}$$

and

$$dx^i = \frac{\partial x^i}{\partial z^j}\, dz^j \tag{A.90}$$

at a fixed time. The position vectors of P_o and P, respectively, take the form

$$\mathbf{r} = \mathbf{r}(x_1, x_2, x_3) \tag{A.91}$$

and

$$\mathbf{R} = \mathbf{R}(x_1, x_2, x_3, t) \tag{A.92}$$

The displacement vector is

$$\mathbf{u} = \mathbf{u}(x_1, x_2, x_3, t) \tag{A.93}$$

Noting that the convected frame x_i is rectangular in C_o, the base vectors g_i, g^j for the system x_i in the body at C_o are

$$g_i = r_{,i} = e_i \tag{A.94}$$

$$g_i \cdot g^j = e^i \cdot e^j = \delta^i_j \tag{A.95}$$

The metric tensors g_{ij}, g^{ij} are

$$g_{ij} = g_i \cdot g_j = \delta_{ij} \qquad g^{ij} = g^i \cdot g^j = \delta^{ij} \tag{A.96}$$

Similarly, the base vectors G_i, G^i and metric tensors G_{ij}, G^{ij} for the curvilinear system x_i in the body at time t are

$$G_i = R_{,i} \qquad G_i \cdot G^j = \delta^j_i \tag{A.97}$$

$$G_{ij} = G_i \cdot G_j = \frac{\partial z^r}{\partial x^i}\,\frac{\partial z^r}{\partial x^j} \tag{A.98}$$

$$G^{ij} = G^i \cdot G^j = \frac{\partial x^i}{\partial z^r}\,\frac{\partial x^j}{\partial z^r} \tag{A.99}$$

The strain tensor in convected coordinate system x_i is defined as

$$\gamma_{ij} = \frac{1}{2}(G_{ij} - g_{ij}) = \frac{1}{2}(G_{ij} - \delta_{ij}) \tag{A.100}$$

For line elements corresponding to the vectors $\mathbf{r}$ and $\mathbf{R}$ viz. ds_o and ds, respectively,

$$ds_o^2 = g_{ij}\,dx^i\,dx^j = \delta_{ij}\,dx^i\,dx^j \tag{A.101}$$

$$ds^2 = G_{ij}\,dx^i\,dx^j \tag{A.102}$$

and

$$ds^2 - ds_o^2 = 2\,\gamma_{ij}\,dx^i\,dx^j \tag{A.103}$$

γ_{ij} may be expressed in terms of the displacement vector $\mathbf{u}$ or its components with respect to the base vectors $\mathbf{g}_i$ (i.e. $\mathbf{e}_i$) or $\mathbf{G}_i$. We have

$$\mathbf{G}_i = \mathbf{R}_{,i} = \mathbf{r}_{,i} + \mathbf{u}_{,i} = \mathbf{e}_i + \mathbf{u}_{,i} = (g_{mi} + u_{m,i})\,\mathbf{e}_m = (\delta_{mi} + u_{m,i})\,\mathbf{e}_m \tag{A.104}$$

Hence,

$$\gamma_{ij} = \frac{1}{2}(\mathbf{g}_i \cdot \mathbf{u}_{,j} + \mathbf{g}_j \cdot \mathbf{u}_{,i} + \mathbf{u}_{,i} \cdot \mathbf{u}_{,j}) = \frac{1}{2}(\mathbf{G}_i \cdot \mathbf{u}_{,j} + \mathbf{G}_j \cdot \mathbf{u}_{,i} - \mathbf{u}_{,i} \cdot \mathbf{u}_{,j}) \tag{A.105}$$

The displacement vector $\mathbf{u}$ may be expressed in terms of base vectors of C_o and C. Thus,

$$\mathbf{u} = u_m\,\mathbf{e}_m$$

$$\mathbf{u}_{,i} = u_{,i}\,\mathbf{e}_m \tag{A.106}$$

and

$$\mathbf{u} = U_m\,\mathbf{G}^m = U^m\,\mathbf{G}_m$$

$$\mathbf{u}_{,i} = U_m|_i\,\mathbf{G}^m = U^m|_i\,\mathbf{G}_m \tag{A.107}$$

(A.106) and (A.105) give

$$\gamma_{ij} = \frac{1}{2}[u_{i,j} + u_{j,i} + u_{m,i}\,u_{m,j}] \tag{A.108}$$

Similarly, (A.107) along with (A.97) through (A.99) gives

$$\gamma_{ij} = \frac{1}{2}[U_i|_j + U_j|_i - U_m|_i\,U_m|_j] \tag{A.109}$$

A.11.4 Velocity and Acceleration in Convected Coordinates

When referred to the state C_p the expressions for velocity and acceleration vectors with respect to x_i coordinates are

$$\mathbf{v} = \dot{u}^i \mathbf{e}_i = \dot{u}_i \mathbf{e}^i = \dot{u}_i \mathbf{e}_i \tag{A.110}$$

$$\mathbf{f} = \ddot{u}^i \mathbf{e}_i = \ddot{u}_i \mathbf{e}^i = \ddot{u}_i \mathbf{e}_i \tag{A.111}$$

The vectors $\mathbf{v}$ and $\mathbf{f}$ can also be resolved in terms of the base vectors $\mathbf{G}_i, \mathbf{G}^i$ of the configuration C. Several alternative representations are possible. Thus,

$$\mathbf{v} = v^m \mathbf{G}_m = v_m \mathbf{G}^m \tag{A.112}$$

$$\mathbf{f} = f^m \mathbf{G}_m = f_m \mathbf{G}^m \tag{A.113}$$

(A.79) and (A.104) give

$$\mathbf{G}_m = z_{i,m} \mathbf{e}_i = \frac{\partial z^i}{\partial x^m} \mathbf{e}_i \tag{A.114}$$

and

$$\mathbf{G}^m = \frac{\partial x^m}{\partial z^i} \mathbf{e}^i \tag{A.115}$$

Hence,

$$\mathbf{v} = v^m \frac{\partial z^i}{\partial x^m} \mathbf{e}_i = v_m \frac{\partial x^m}{\partial z^i} \mathbf{e}^i \tag{A.116}$$

$$\mathbf{f} = f^m \frac{\partial z^i}{\partial x^m} \mathbf{e}_i = f_m \frac{\partial x^m}{\partial z^i} \mathbf{e}^i \tag{A.117}$$

Comparing (A.110) with (A.116) and (A.111) with (A.117),

$$v^m \frac{\partial z^i}{\partial x^m} = \dot{u}^i = \dot{u}_i \tag{A.118}$$

$$v_m \frac{\partial x^m}{\partial z^i} = \dot{u}_i = \dot{u}^i \tag{A.119}$$

$$f^m \frac{\partial z^i}{\partial x^m} = \ddot{u}^i = \ddot{u}_i \tag{A.120}$$

$$f_m \frac{\partial x^m}{\partial x^i} = \ddot{u}_i = \ddot{u}^i \tag{A.121}$$

A.11.5 Changes in Volume and Area

The convected coordinate system is rectangular cartesian in the initial state and curvilinear in the deformed state. Consider an elementary rectangular parallelopiped enclosed by the six surfaces viz.

$$x_i = \text{constant and } x_i + dx_i = \text{constant } (i=1 \text{ to } 3) \tag{A.122}$$

The vectors $e_i dx_i$ (no sum) form the sides of the parallepiped, the volume of which is given by,

$$dV_0 = dx_1 dx_2 dx_3 = dx^1 dx^2 dx^3 \tag{A.123}$$

After motion and deformation, the rectangular parallepiped is deformed into a parallopiped with sides defined by $G_i dx^i$ (no sum) $i = 1, 2, 3$. The new volume is

$$dV = |G_1 . (G_2 \times G_3)| dx^1 dx^2 dx^3 \tag{A.124}$$

but

$$|G_1 . (G_2 \times G_3)| = |z_{ij}| = |G_{ij}| = \sqrt{G} \tag{A.125}$$

Hence

$$dV = \sqrt{G}\, dx_1 dx_2 dx_3 = \sqrt{G}\, dV_0 \tag{A.126}$$

If dA_{10} denotes an elementary area in the reference configuration on the coordinate plane $x_1 = \text{constant}$, then

$$dA_{10} = |e_2 \times e_3| dx_2 dx_3 = dx_2 dx_3 = dx^2 dx^3 \tag{A.127}$$

After deformation, the originally plane area dA_{10} becomes a curved surface dA_1 with vectors $G_2 dx^2$ and $G_3 dx^3$ as its sides. The area

$$dA_1 = |G_2 \times G_3| dx^2 dx^3 \tag{A.128}$$

but

$$\mathbf{G}_2 \times \mathbf{G}_3 = \epsilon_{23t}\mathbf{G}^t = \sqrt{G}\,e_{23t}\mathbf{G}^t = \sqrt{G}\,\mathbf{G}^1 \tag{A.129}$$

The magnitude $|\mathbf{G}_2 \times \mathbf{G}_3|$ is

$$|\mathbf{G}_2 \times \mathbf{G}_3| = |\sqrt{G}\,\mathbf{G}^1| = \sqrt{G G^{11}} \tag{A.130}$$

Hence

$$dA_1 = \sqrt{G G^{11}}\,dx^2\,dx^3 \tag{A.131}$$

In general,

$$dA_i = \sqrt{G G^{ii}}\,dx^j\,dx^k \quad \text{(no sum on i and } i \neq j \neq k) \tag{A.132}$$

in which dA_i denote the areas in the deformed body which in the undeformed state has values dA_{i0} (i = 1 to 3).

A.11.6 Kinetics

This discussion follows [65]. Let the surfaces $x_i =$ constant at a point P in the deformed state C form a tetrahedron. The edges of the tetrahedron are formed by the coordinate curves PP_i of length ds_i and the curves P_1P_2, P_2P_3, P_3P_1, (Figure 50). Let the surfaces $x_i =$ constant of the tetrahedron have the areas dA_i. These may be represented vectorially by

$$\mathbf{G}^i \frac{dA_i}{\sqrt{G^{ii}}} \tag{A.133}$$

where $\dfrac{\mathbf{G}^i}{\sqrt{G^{ii}}}$ is the unit base vector. Also, the area of $P_1P_2P_3$ denoted by dA, is represented vectorially by $\mathbf{n}\,dA$, where $\mathbf{n}$ is the unit normal to the surface. Hence, since the area $P_1P_2P_3$ is vectorially equivalent to the areas dA_i

$$\mathbf{n}\,dA = \sum_{i=1}^{3} \frac{\mathbf{G}^i\,dA_i}{\sqrt{G^{ii}}} \tag{A.134}$$

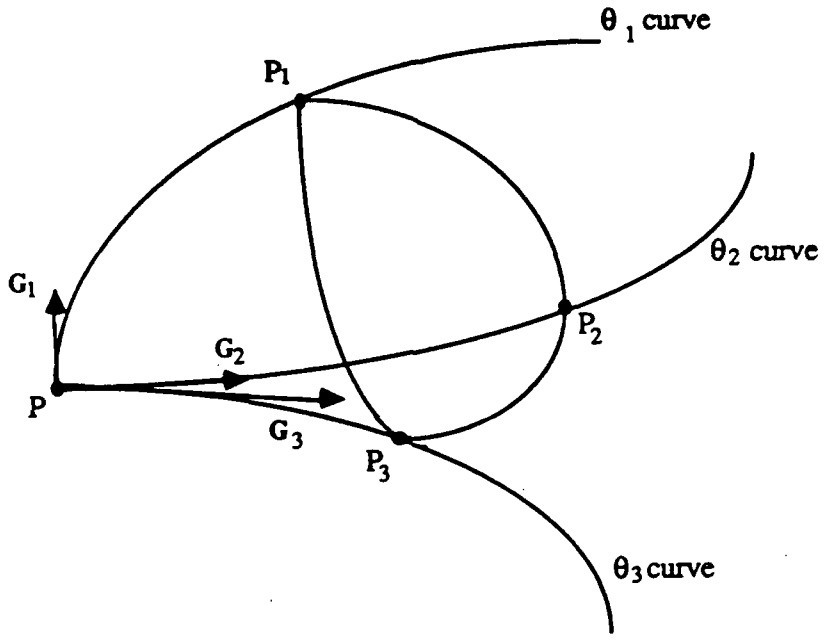

Figure 50: Infinitesimal Curvilinear Tetrahedron

so that if n_i are the covariant components with respect to the base vectors $\mathbf{G}^i$, it follows that,

$$n_i \mathbf{G}^i dA = \frac{\mathbf{G}^i dA_i}{\sqrt{G^{ii}}}$$

$$\text{or} \quad n_i \sqrt{G^{ii}} dA = dA_i \tag{A.135}$$

Let $\mathbf{t}$ denote the stress per unit area of the surface at a point P in the deformed body. Cauchy's equation of motion, following Green [65], is

$$\int_A \mathbf{t}\, dA + \int_V \rho(\mathbf{F} - \mathbf{f})\, dV = 0 \tag{A.136}$$

where V an the arbitrary volume in the body in the state C and is bounded by a closed surface A. Also, ρ is the density of the body in C. $\mathbf{F}$ and $\mathbf{f}$ are the body force and acceleration vectors, respectively. Applying the equation of motion to an infinitesimal tetrahedron $PP_1P_2P_3$ we have, in the limit, keeping the direction of $\mathbf{n}$, the normal to the area, fixed,

$$\mathbf{t}\, dA = \mathbf{t}_i\, dA_i \tag{A.137}$$

Note that dA_i are the areas of the surfaces of the tetrahedron under consideration and $\mathbf{t}_i$ are the stress vectors associated with these elemental areas. Volume forces and inertia terms acting on the tetrahedron do not appear in this equation since they are of higher order of smallness than the surface forces. (A.135) and (A.136) give

$$\mathbf{t} = \sum_{i=1}^{3} n_i \mathbf{t}_i \sqrt{G^{ii}} \tag{A.138}$$

The stress vector $\mathbf{t}$ is invariant under transformation of coordinates and n_i are components of covariant vector. It implies that $\mathbf{t}_i \sqrt{G^{ii}}$ is a contravariant type transformation and

$$\mathbf{t}_i \sqrt{G^{ii}} = \tau^{ij} \mathbf{G}_j = \tau^i_j \mathbf{G}^j \tag{A.139}$$

where τ^{ij} and τ^{i}_{j} are componenets of the associated contravariant and mixed tensors of second order, called stress vectors. (A.138) and (A.139) give

$$t = \frac{n_i T_i}{\sqrt{G}} = \tau^{ij} n_i G_j = \tau^{i}_{j} n_i G^j \tag{A.140}$$

where

$$T_i = t_i \sqrt{G G^{ii}} = \sqrt{G}\, \tau^{ij} G_j = \sqrt{G}\, \tau^{i}_{j} G^j \tag{A.141}$$

T_i is introduced for convenience. An element of area at a point x_r in the body C is $\sqrt{GG^{ii}}\, dx^j dx^k$ (i not summed and $i \neq j \neq k$) and the force across this element is,

$$t_i \sqrt{GG^{ii}}\, dx^j dx^k = T_i\, dx^j dx^k \tag{A.142}$$

The conditions at the boundary surface of the body, at which surface tractions are prescribed, require

$$t = P = P^i G_i = P_j G^j \tag{A.143}$$

(A.140) gives

$$\tau^{ij} n_i = P^j \tag{A.144}$$

and

$$\tau^{i}_{j} n_i = P_j \tag{A.145}$$

It is generally assumed that the geometry of the reference configuration is known a priori, it is often convenient to define the state of stress at a point by relating to its position in the initial configuration. The stress vector, t, is referred to a surface S at time t in body C and measured per unit area of S. The stress tensor τ^{ij} referred to x_i coordinates in C and is measured per unit area of these coordinate surfaces.

If ${}_0t_i$ is a stress vector across the x_i surface in C, but measured per unit area of the corresponding x_i surface in C_0, then use of (A.142), yields

$$T_i\, dx^j dx^k = {}_0t_i \sqrt{g\, g^{ii}}\, dx^j dx^k \tag{A.146}$$

If s^{ij} is the stress vector measured per unit area of the undeformed body, associated with a surface in the deformed body, whose unit normal in its undeformed position is ${}_0n$,

$$ {}_0t = s^{ij}\,{}_0n_i\,G_j = s^i_j\,{}_0n_i\,G^j \tag{A.147} $$

where ${}_0n = {}_0n_i\,g^i = {}_0n^i\,g_i$. (A.139) gives

$$ {}_0t_i\sqrt{g^{ii}} = {}_0t_i\sqrt{\delta^{ii}} = s^{ij}G_j \tag{A.148} $$

(A.148) and (A.146) give

$$ T_i = {}_0t_i\sqrt{g\,g^{ii}} = \sqrt{g}\,s^{ij}G_j = s^{ij}G_j \quad \text{as } \sqrt{g} = 1 \text{ for a cartesian frame} \tag{A.149} $$

where

$$ s^{ij} = \sqrt{G}\,\tau^{ij} \tag{A.150} $$

s^{ij} are componets of the second Piola-Kirchoff stress tensor [114]. (A.104) along with (A.141) and (A.149) gives

$$ T_i = \sqrt{G}\,\tau^{ij}(\delta_{mj} + u_{m,j})\,e_m = s^{ij}(\delta_{mj} + u_{m,j})\,e_m = \sqrt{G}\,P^i_m\,e_m = S^i_m\,e_m \tag{A.151} $$

The stresses $P^i_m = \tau^{ij}(\delta_{mj} + u_{m,j})$ are measured per unit area of x_i surfaces in C but are referred to the base vectors e_i in C_0. The stresses $S^i_m = s^{ij}(\delta_{mj} + u_{m,j})$ are measured per unit area of the x_i surfaces in C_0 and are referred to the base vectors e_i in C_0. These are not symmetric. The stress tensor defined by components S^i_m is called the first Piola-Kirchoff stress tensor.

Appendix B

PUBLICATIONS AND PRESENTATIONS

The research program has resulted in the following publications and presentations.

B.1 RESEARCH REPORTS

1.1. Ranbir S. Sandhu, Shyan-Cyun Lee, and Hwie Ing The, Special Finite Elements for Analysis of Soil Consolidation, Geotechnical Engineering Report No. 9, OSURF 715107-83-2, AFOSR Grant 83-0055, August 1983.

1.2. Ranbir S. Sandhu, Mechanical Behavior of Saturated Soils - A Review, Geotechnical Engineering Report No. 10, OSURF 715927-85-1, AFOSR Grant 83-0055, April 1985.

1.3. Ranbir S. Sandhu, Baher L. Aboustit, and Soon-Jo Hong, An Evaluation of Finite Element Models for Soil Consolidation, Geotechnical Engineering Report No. 11, OSURF 715107-84-2, AFOSR Grant 83-0055, April 1984.

1.4. Mahantesh S. Hiremath, and Ranbir S. Sandhu, A Computer Program for Dynamic Response of Layered Saturated Sands, Geotechnical Engineering Report No. 12, OSURF 715107-84-3, AFOSR Grant 83-0055, June 1984.

1.5. Ranbir S. Sandhu, Soon-Jo Hong, and Baher L. Aboustit, Response of Saturated Soils to Dynamic Loading, Geotechnical Engineering Report No. 13, OSURF 715107-84-4, AFOSR Grant 83-0055, June 1984.

1.6. Ranbir S. Sandhu, Baher L. Aboustit, Soon-Jo Hong, and Mahantesh S. Hiremath, A Computer Program for Consolidation and Dynamic Response Analysis of Fluid-Saturated Media, Geotechnical Engineering Report No. 14, OSURF 715107-84-5, AFOSR Grant 83-0055, June 1984.

1.7. Ranbir S. Sandhu, and Soon-Jo Hong, Variational Principles for Dynamics of Linear Elastic Fluid-Saturated Soils, Geotechnical Engineering Report No. 16, OSURF 715729-85-3, AFOSR Grant 83-0055, April 1985.

1.8. Ranbir S. Sandhu, William E. Wolfe, and Harpal S. Chohan, An Eigenfunction Procedure for Dynamic Response Analysis of Saturated Soils, Geotechnical Engineering Report No. 18, OSURF 717885-88-1, AFOSR Grant 83-0055, February 1988.

1.9. William E. Wolfe, Ranbir S. Sandhu, and Vincent E. Amato, Preliminary Tests on Liquefaction of Ottawa Sand, Geotechnical Engineering Report No. 19, OSURF 716894-86-2, AFOSR Grant 83-0055, January 1986.

1.10. Ranbir S. Sandhu, William E. Wolfe, and Hann-Ling Shaw, Analysis of Dynamic Response of saturated Soils using a Three-Field Formulation, Geotechnical Engineering Report No. 20, OSURF 716894-86-3, AFOSR Grant 83-0055, June 1986.

1.11. William E. Wolfe, Ranbir S. Sandhu, and Vincent E. Amato, Shaking Table Tests of Anisotropically Consolidated Ottawa Sand, Geotechnical Engineering Report No. 21, OSURF 716894-86-2, AFOSR Grant 83-0055, March 1986.

1.12. Ranbir S. Sandhu, and Mahantesh S. Hiremath, Finite Element Analysis of Wave Propagation in Saturated Soils, Geotechnical Engineering Report No. 22, OSURF 717885-87-6, AFOSR Grant 83-0055, March 1987.

1.13. Ranbir S. Sandhu, and Mahantesh S. Hiremath, Wave Propagation in Non-Linear Fluid-Saturated Porous Solids, Geotechnical Engineering Report No. 23, OSURF 717885-87-9, AFOSR Grant 83-0055, July 1987.

1.14. Ranbir S. Sandhu, William E. Wolfe, and Soon-Jo Hong, Wave Propagation in Fluid-Saturated Elastic Porous Solids, Geotechnical Engineering Report No. 24, OSURF 716894-86-4, AFOSR Grant 83-0055, July 1986.

1.15. Leslie W. Morland, Ranbir S. Sandhu, William E. Wolfe, and Mahantesh S. Hiremath, Wave Propagation in a Fluid-Saturated Elastic Layer, Geotechnical Engineering Report No. 25, OSURF 717885-87-5, AFOSR Grant 83-0055, January 1987.

1.16. William E. Wolfe, Ranbir S. Sandhu and Dennis L. Jasinski, The Effects of Band-Limited White Noise Excitation on Liquefaction Potential in Large-Scale Tests, Geotechnical Engineering Report No. 26, OSURF 717885-87-8, AFOSR Grant 83-0055, January 1987.

1.17. Ranbir S. Sandhu, William E. Wolfe, and Mahantesh S. Hiremath, Computer Program DALES (Dynamic Analysis of Linear Elastic Soils), Geotechnical Engineering Report No. 27, OSURF 717885-87-7, AFOSR Grant 83-0055, March 1987.

1.18. William E. Wolfe, Ranbir S. Sandhu, and Harpal S. Chohan, An Evaluation of the Liquefaction Potential of Ottawa Sand Using a Shaking Table, Geotechnical Engineering Report No. 29, OSURF 717885-88-3, AFOSR Grant 83-0055, February 1988.

1.19. Ranbir S. Sandhu, William E. Wolfe, Mahantesh S. Hiremath, and Harpal S. Chohan, Computer Program DANS (Dynamic Analysis of Nonlinear Soils), Geotechnical Engineering Report No. 30, OSURF 717885-88-2, AFOSR Grant 83-0055, February 1988.

B.2 CONFERENCE PROCEEDINGS

2.1. Ranbir S. Sandhu, *Constitutive Models for Saturated Sands*, in Proceedings Part 2, Symposium on Interaction of Non-Nuclear Munitions with Structures, Air Force Academy, Colorado Springs, May 1983.

2.2. Ranbir S. Sandhu, *Constitutive Equations for Fluid-Saturated Porous Solids*, Proceedings, Engineering Foundation Conference on Compressibility Phenomena in Subsidence, Henniker College, Henniker, New Hampshire, July 29 to August 3 1984.

2.3. Ranbir S. Sandhu, Baher L. Aboustit, and S. J. Hong, *Finite Element Analysis of Flow and Deformation in Saturated Soils*, Proccedings, Second Symposium on interaction of Non-Nuclear Munitions with Structures, Panama City, Florida, April 1985.

2.4. Ranbir S. Sandhu, S. J. Hong, and Baher L. Aboustit, *Analysis of Response of Saturated Soil Systems Subjected to Dynamic Loading*, Proccedings, Second Symposium on interaction of Non-Nuclear Munitions with Structures, Panama City, Florida, April 1985.

2.5. Mahantesh S. Hiremath, and Ranbir S. Sandhu, *Application of Theories of Mixtures to Behavior of Fluid-Saturated Deformable Porous Media*, Proccedings, Second Symposium on interaction of Non-Nuclear Munitions with Structures, Panama City, Florida, April 1985.

2.6. Raymond M. Kolonay, William E. Wolfe, and Ranbir S. Sandhu, *Laboratory Data Collection and Processing Using a Microcomputer*, Proceedings, First Canadian Conference on Computer Applications in Civil Engineering/Micro-Computers, Hamilton, Ontario, May 1986.

2.7. Soon-Jo Hong, and Ranbir S. Sandhu, *Some Analytical Solutions of Elastic Wave Propagation in Fluid-Saturated Porous Media*, Eleventh canadian Conference of Applied Mechanics, University of Alberta, Edmonton, Alberta, May 1987.

2.8. Leslie W. Morland, Ranbir S. Sandhu, and William E. Wolfe, *Uniaxial Wave Propagation Through Fluid-Saturated Elastic Soil Layer*, Sixth Int. Conf. Num. Methods in Geomech., Innsbruck, Austria, April 1988.

B.3 REFEREED JOURNAL ARTICLES

3.1. Ranbir S. Sandhu, Shyan-Chyun Lee, and Hwie-Ing The, *Special Finite Elements for Analysis of Soil Consolidation*, Int. Jour. of Num. Anal. Methods in Geomech., Vol. 9, pp. 125-147, 1985.

3.2. Ranbir S. Sandhu, and Soon-Jo Hong, *Dynamics of Fluid-Saturated Soils - Variational Formulation*, Int. Jour. of Num. Anal. Methods in Geomech., Vol. 11, pp. 241-255, 1987.

3.3. Mahantesh S. Hiremath, Ranbir S. Sandhu, Leslie W. Morland, and William E. Wolfe, *Analysis of One-Dimensional Wave Propagation in a Fluid-Saturated Soil Column*, Int. Jour. of Num. Anal. Methods in Geomech., Vol. 12, pp. 121-140, 1988.

3.4. R. S. Sandhu, H. L. Shaw, and S. J. Hong, *A Three Field Finite Element Procedure for Analysis of Elastic Wave Propagation Through Fluid-Saturated Soils*, Accepted for Publication in the Int. Jour. Soil Dynamics and Earthquake Engg.

3.5. S. J. Hong, R. S. Sandhu, and W. E. Wolfe, *On Garg's Solution of Biot's Equations of Wave Propagation in a One-Dimensional Fluid-Saturated Elastic Porous Solid*, Accepted for Publication in Int. Jour. Num. and Anal. Methods in Geomech.

B.4 DISSERTATIONS AND THESES

4.1. Hann-Ling Shaw, Finite Element Analysis of Dynamic Response of Saturated Soils Using a Three-Field Formulation, M.S. Thesis, The Ohio State University, Columbus, Ohio, 1986.

4.2. Harpal S. Chohan, An Eigenfunction Procedure for Dynamic Response Analysis of Saturated Soils, M.S. Thesis, The Ohio State University, Columbus, Ohio, 1986.

4.3. Vincent E. Amato, Shaking Table Tests to Determine Liquefaction Potential of Anisotropically Consolidated Saturated Ottawa Sand, M.S. Thesis, The Ohio State University, Columbus, Ohio, 1986.

4.4. Dennis L. Jasinski, The effects of Band-Limited White Noise Excitation on Liquefaction Potential in Large-Scale Tests, M.S. Thesis, The Ohio State University, Columbus, Ohio, 1986.

4.5. Mahantesh S. Hiremath, A Dynamical Theory of Wave Propagation in Fluid-Saturated Solids, Ph.D., 1987.

B.5 OTHER PRESENTATIONS

In addition to the publications and presentations listed above, the principal investigator and his co-workers presented results of the research at the following conferences:

5.1. Ranbir S. Sandhu, *Application of Theories of Mixtures to Saturated Soils*, Engineering Foundation Conference on "Compressibility Phenomena in Subsidence", Henniker College, Henniker, New Hampshire, July 29 to August 3 1984.

5.2. Ranbir S. Sandhu, *Finite Element Analysis of Flow Through Deformable Porous Media*, Society of Engineering Science, 21st Annual Meeting, 15-17 October 1984, Virginia Polytechnic and State University, Blacksburg, Virginia.

Also Mr. Amato presented a paper on the experimental work at a seminar in Lexington, Kentucky on October 11, 1985. Dr. R.S. Sandhu was invited by the university of Rhode Island, Dept. of Civil Engineering, to present a guest lecture in November 1985, on Finite Element Analysis of Dynamics of Saturated Soils.

A summary of results of the research was made available in letter form to the National Research Council, Committee on Earthquake Engineering, Panel on Liquefaction. This panel planned to hold a workshop at MIT during March 1985 and seminars were conducted later in the year. Dr. Sandhu attended the National Research Council seminar on State-of-the-Art in Soil Liquefaction. A written contribution to the seminar report was submitted to Dr. Robert V. Whitman along with copies of the contribution to members of the Earthquake Engineering Committe of the National Reserach Council and the participants and observers at the workshop. Dr. Wolfe attended a symposium organized by the AFOSR at MIT on September 14 and 15, 1987.